University of Strathclyde
Energy Systems Research Unit

Aiding Renewable Energy Integration through Complimentary Demand-Supply Matching

By Francesca Jane Born
in fulfilment of the requirements for the degree of Doctor of Philosophy
20001

Acknowledgements

This thesis is dedicated to Claudine who wanted it more than I did, and that kept me going.

Though many people help influence my work, I would particularly like to thank those who made it possible. Thanks to Professor Joe Clarke for his guidance and to Cameron Johnstone for his encouragement and support. Gratitude to the rest of the ESRU team for they're input, especially to Nicola who assured me immensely in taking my work on. I would also like to acknowledge the feedback received from Scottish Power, ManWeb, Highland Regional Council, Glasgow City Council and Buro Happold.

Thanks to my mum for being my rock, my dad for providing the competition, Katy for being there, and Christine for accompanying me along a long and otherwise lonely journey.

I am indebted to Robin, for teaching my how to program, think, read and write, for understanding the mood swings and for supporting me emotionally and financially through it all.

Contents Page

List of Figures

Figure **page**

Chapter 5

List of Tables

Abstract

Sustainable development, in terms of energy production and use is dependent on renewable energy (RE) and energy efficient technologies. Information technology is vital in managing a large resource such as energy, and could play a key role in the dissemination of RE technologies. The purpose of the research presented was to determine the body of information and analysis techniques required to support RE deployment decisions.

Matching the demand for and supply of energy is the basis of this work, as it enables the identification of strategies for integrating renewables into the generation portfolio. The two criteria in matching are the relative magnitudes and temporal characteristics of supply and demand. Renewable technologies utilise intermittent sources of energy and therefore have inherently intermittent supply profiles. Matching is carried out using time series profiled data, for both demand and supply.

Numerous methods exist for obtaining demand profiles and ideally each of the methods can be consolidates to produce an information rich database.

Supply profiles can be measured or modelled. Modelling is significantly easier and less expensive than measuring and has the added advantage that location parameters can be adjusted to optimise matching strategies prior to installation.

Given sets of demand and supply profiles, optimal combinations can be defined by the similarities in trends and particularly in coincident peaks. The match between demand and supply can be improved by deploying demand management measures, either to reduce the demand or to alter the profile. Furthermore storage technologies and conventional generation can be used to improve the match from the supply side.

This thesis examines the issues of renewable energy demand and supply matching. The theories presented have been encapsulated in the development of a software tool specifically aimed to aid strategic decisions regarding renewable technology integration.

Chapter 1: Introduction

The focus of the work presented in this thesis is concerned with facilitating the analysis of renewable integration strategies through scenario based planning. This chapter briefly presents the material covered.

Chapter 2 presents a review of renewable energy (RE). The significance of sustainable development is discussed and the Kyoto protocol is used to show the world-wide commitment to sustainability. The current performance of renewable technologies is reviewed and future applications discussed. RE integration strategies are broadly classified as large and small-scale and the barriers and merits of each are presented.

Chapter 3 examines the role of information technology in the dissemination of renewable technologies. An argument is presented for the development of a framework in which computing power can be utilized to assist the market penetration of these technologies. The individual components of an energy information system are described and the need for further work in the field of matching supply and demand is discussed.

Chapter 4 reviews the different means and suitability of various techniques employed to obtain demand profiles including measuring, statistical methods and simulation. The concept of pooling all of the methods together is described as aggregated profiling which provides a framework in which each method can be deployed, depending on data availability. The framework enables demand scenario building.

Chapter 5 examines techniques to obtain renewable energy supply profiles to further the analysis of RE integration. Profiles may be obtained through measurement or simulation and a case is made for the simulation approach. Models are developed to

predict supply profiles for photovoltaic, wind and flat plate collector systems, based on manufacturers' specifications.
Chapter 6 discusses how demand and supply profiles can be analysed in order to optimise the match between them. This follows an analysis of statistical match indicators, and search algorithms are developed based on statistical methods and on the analysis of frequency components in time-series profiles.

Chapter 7 examines the effects of auxiliary systems on the matching of supply and demand profiles. Models are developed to predict the effects of battery storage systems and back-up generation on the match between supply and demand. Again the models are based on manufacturers specifications. Tariff analysis is incorporated to enable the economic evaluation of saving resulting from RE generation. A mathematical definition for a potential match metric is described.

Chapter 8 presents a software development, which encompasses the theories of previous chapters. The methodologies and mathematical models presented are realised in this program. This chapter describes the program from the user perspective and explains the goals behind the interface. Some of the software-engineering principles used in the system design are explained, together with certain choices made regarding the development approach, language and platform. Applications and users for the program are considered, and validation procedures are described

Chapter 9 presents two case studies used to demonstrate the applicability and functionality of the matching tool developed. The first presents the tool's use on a single building investigation and the second examines its use for a community-scale renewable integration project.

Chapter 10 reviews the work carried out and highlights the main issues covered. This is followed by recommendations for future research in this field.

Chapter 2: Sustainable Energy Prospects

2.1 Sustainability

The Fifth Environmental Action Programme established EU legislation with respect to the concept of sustainable development. The programme defined sustainable development as "*that which meets the needs of the present without compromising the ability of future generations to meet their own needs*"(The Fifth Environmental Action Programme, 2000). The policy objectives underlying this definition for energy were to ensure the compatibility between economic growth and efficient and secure energy supplies, together with a clean environment. Environmentally polluting by-products are produced with conventional energy generation, which additionally depends on finite energy sources that are gradually being depleted. However, energy is essential for socio-economic progress both in developing and industrialised countries and the demand for energy will increase with the global population, currently growing at a rate of 250,000 people per day (Elani et al., 1996).

In 1988, the director of the National Aeronautics & Space Administration, Goddard Institute for Space Studies testified before the American Congress, that human induced global warming was detectable in the climate record. Sceptics argued that the data was unclear and inconclusive. The predicted consequences of global warming included; world-wide floods; droughts; rising sea levels; category five hurricanes and typhoons. These effects were firmly debated. The one issue which was almost unanimously agreed was that deep reductions in carbon emissions could not be made economically without the use of green technologies (Hileman, 1997), (Leggett, 1996), (Lovejoy, 1996).

Green technologies denote energy efficiency and renewable energy technologies. Reductions in energy consumption are achieved through the application of energy

efficient technologies. For example, the efficiency of an energy system, such as a building, could be increased via a number of proven energy efficient measures; improved insulation; advanced glazing; energy control systems and high efficiency motors and pumps. Renewable energy sources are energy sources which can not be depleted through their utilisation, examples include solar; wind; hydro; biomass; ocean thermal and ocean wave energy.

On December 10 1997, 160 nations reached an agreement in Kyoto, Japan aimed at limiting emissions of carbon dioxide and other "greenhouse gases". The Kyoto Protocol calls for the industrialised nations to reduce their average national emissions over the period 2008-2012, to at least five percent below the 1990 levels. The Protocol permits some industrialised nations to modestly increase their emissions and makes special provisions for the members of the former Soviet Bloc. None of the developing countries, including those with large and growing emissions such as India and China, is required to limit its emissions. Figure 2.1 illustrates the pledged reductions of selected countries (Milloy, 1997).

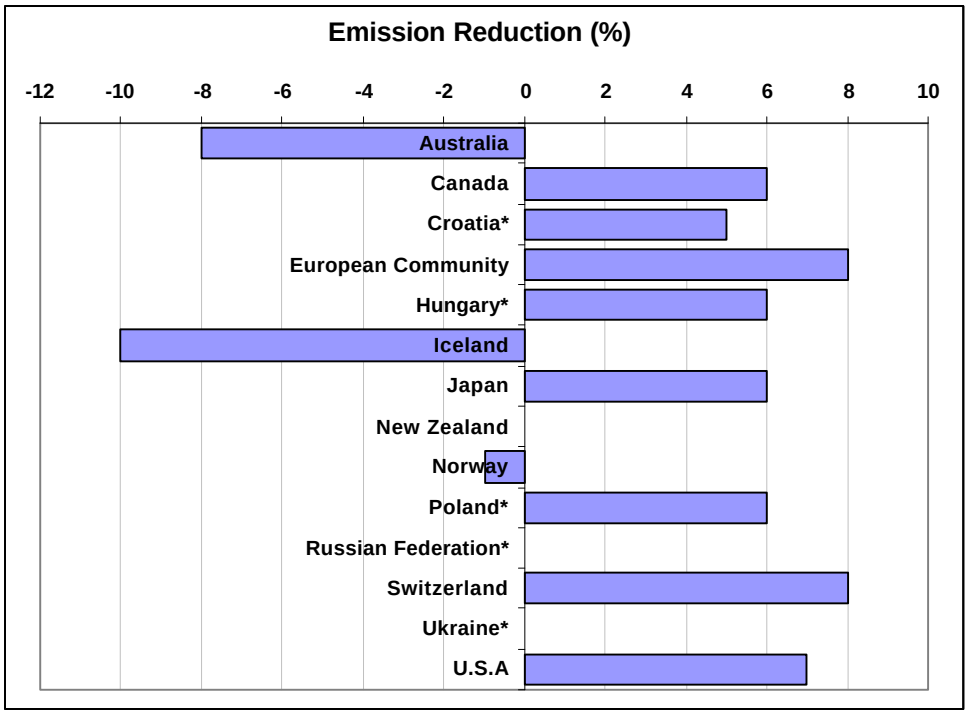

Figure 2.1: Pledged emissions reductions of selected countries (Milloy, 1997)

The agreement provides for a great deal of flexibility in how these targets are to be achieved. This flexibility encompasses emissions trading, whereby a country may gain emission credits for projects carried out to reduce emissions in developing countries.

The Kyoto Protocol is intended to signal to governments and businesses that limits will be placed on future emissions of greenhouse gases and that now is the time to begin implementing and developing the necessary technologies (Kopp et al., 1998). In order for the Kyoto Protocol to be successful, a continuous process of design innovation must be initiated to create a sustainable global energy system for the 21st Century (Lashof, 1998).

2.2 The Success of Renewables

Figures relating to the performance of renewable technologies are published in the Renewable Energy Manual (Renewable Energy Manual, 2000). The world market for renewable energy production systems, excluding hydroelectricity, was estimated to be about $1 billion in the past decade. In 1996, the worlds cumulative installed wind capacity was approaching 5 GW, with the largest capacity increases installed in Germany, India and the United Kingdom. Photovoltaic sales world-wide more than quadrupled in 10 years, while installation costs halved. The developed commercial geothermal energy resources are estimated at 9,927 MW world-wide. The annual average biomass fuel consumption totalled almost 59,080 MW over the period 1985-1990 (world-wide). In Europe, over 27 million tons of municipal solid waste are used to generate electricity and for heating in Europe. These figures demonstrate that the deployment of renewable technologies is beginning to make an impact on a world-wide scale.

In the U.S., renewable energy has generally been viewed positively and has been supported for almost 30 years. Figure 2.2 illustrates the U.S. energy consumption percentages by energy source in 1995. The total renewable contribution, excluding hydroelectricity is represented by the white portion of the pie chart (illustrated in the secondary plot) amounted to approximately 3.7%.

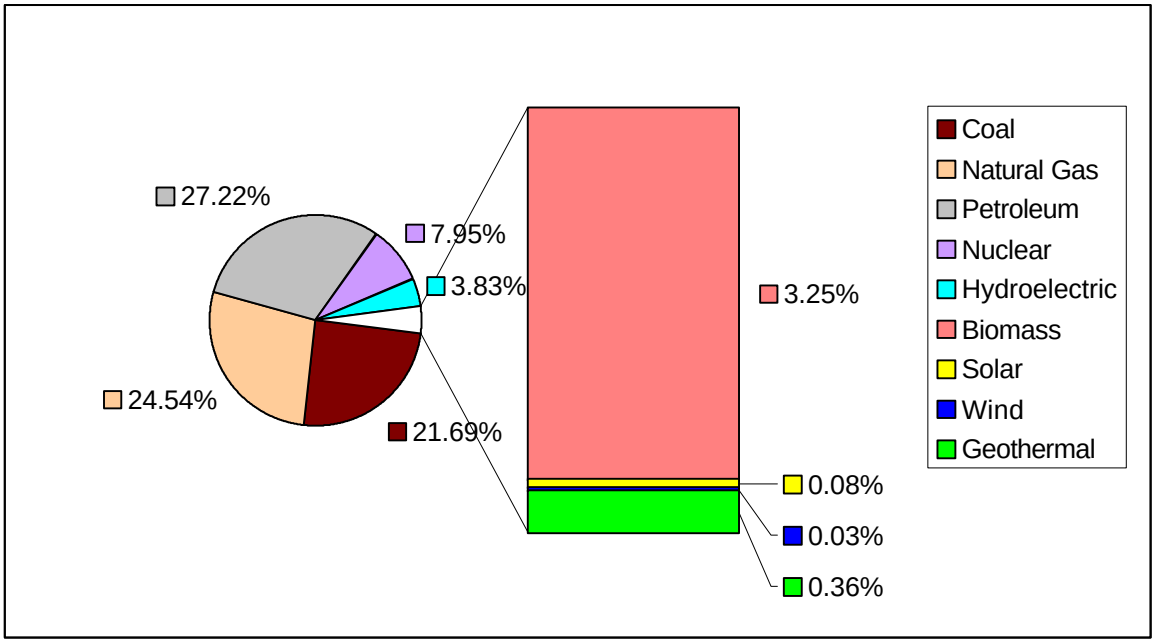

Figure 2.2: U.S. energy consumption by energy source, 1995 (Renewable Energy Manual, 2000)

It was predicted that wind, solar power and other renewable energy sources would make a significant contribution to U.S. energy by the year 2000. A project on renewable energy policy in the U.S., published work that expressed doubts over the ability of renewable technologies surviving in a competitive electricity market (Miller and Serchuk, 1996). These doubts proved to be well founded and renewable technologies failed to emerge as a prominent component of the U.S. energy infrastructure. Butraw et al. (Burtraw et al., 1999) explained the failure of (non-hydroelectric) renewables to emerge more prominently was primarily due to the unrelated decline in the cost of conventional energy generation. Renewable technologies have had to compete in an environment where changes in the regulation, technology and market structure of fossil fuels have led to a dramatic improvement in the environmental performance and cost of conventional generation. Although renewable technologies failed to attract vast

investment or benefit from economic scales in production, the cost of renewable electricity generation has reduced considerably.

The U.K. Government set a target to achieve 1500 MW of new renewable generating capacity by the year 2000 (Department of Trade and Industry, 1999). Legislation was introduced to drive the construction and operation of generation facilities fuelled by particular types of renewable fuels. This legislation, known as the Non-Fossil Fuel Obligation (NFFO), was initially set up in England and Wales and later by similar arrangements were formed in Scotland and Northern Ireland. The NFFO was designed to bridge the gap between technically proven and commercially viable technologies. In 1990, the idea that renewables could generate at competitive prices with conventional plants was not considered plausible. However, by 1996 the price gap closed dramatically (Thomas, 1996). The NFFO was succeeded by the Electricity Order 1998 (Statutory Instruments, 1998) for Non-Fossil Fuel Sources in England and Wales and Order 1999 (Statutory Instruments, 1999), for Scotland. These orders enforce public electricity suppliers to achieve specified aggregate amounts of generating capacity, from non-fossil fuel generating stations. Figures 2.3 and 2.4 illustrate the projected summative capacities to be added to the current portfolio of renewable energy in England and Wales and Scotland respectively. These figures illustrate that significant increases are expected. The specified non-fossil fuel generating stations include:

- Biomass generating stations fuelled by crops grown purposely to provide a source of energy and/or forestry waste.
- Hydro generating stations driven by any form of water power other than tidal or wave power.
- Waste to energy generating stations operating on fuel derived from municipal or industrial waste.
- Wind generating stations with generating capacities exceeding 1 MW.
- Small wind generating stations with capacities not exceeding 1 MW.
- Wave generating stations driven by any form of tidal or wave power.

- Landfill gas generating stations fuelled wholly by gas derived from landfill sites.

To date there have been five Non-Fossil Fuel Obligation Orders made in England and Wales, two equivalent Orders in Northern Ireland and three in Scotland. Together the Orders total 3.5GW (Declared Net Capacity) of new capacity and should contribute to around 5 per cent of UK electricity needs being met from renewables by 2003. These figures and the projections for the future look promising. However, the achievements from the early NFFO Orders currently total 650MW of successfully commissioned electricity plant. The goal for the year 2000 has not been attained, mainly due to a failure in obtaining the necessary planning permission or finance (Department of Trade and Industry, 1999).

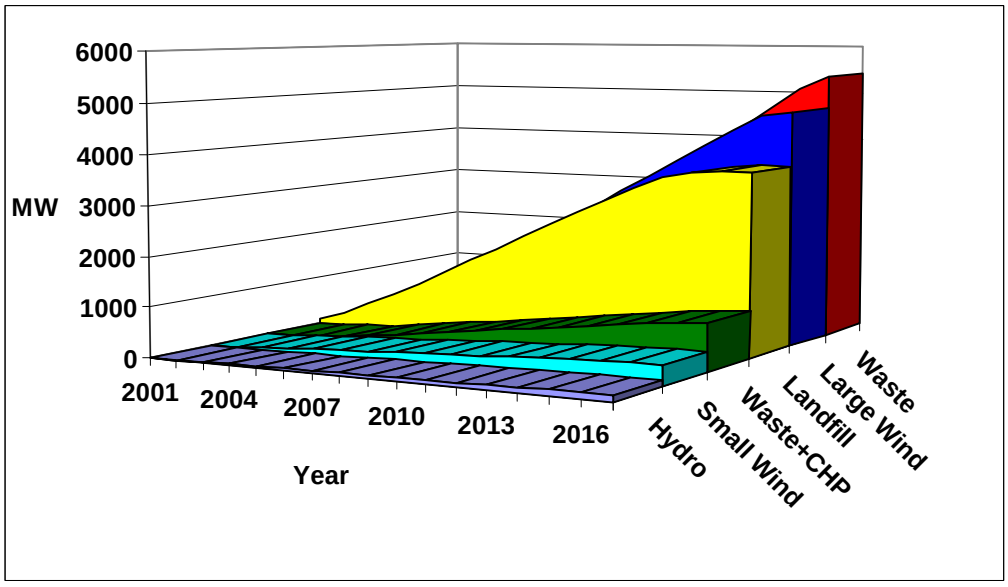

Figure 2.3: Aggregate renewable energy requirements for England and Wales (Statutory Instruments, 1998)

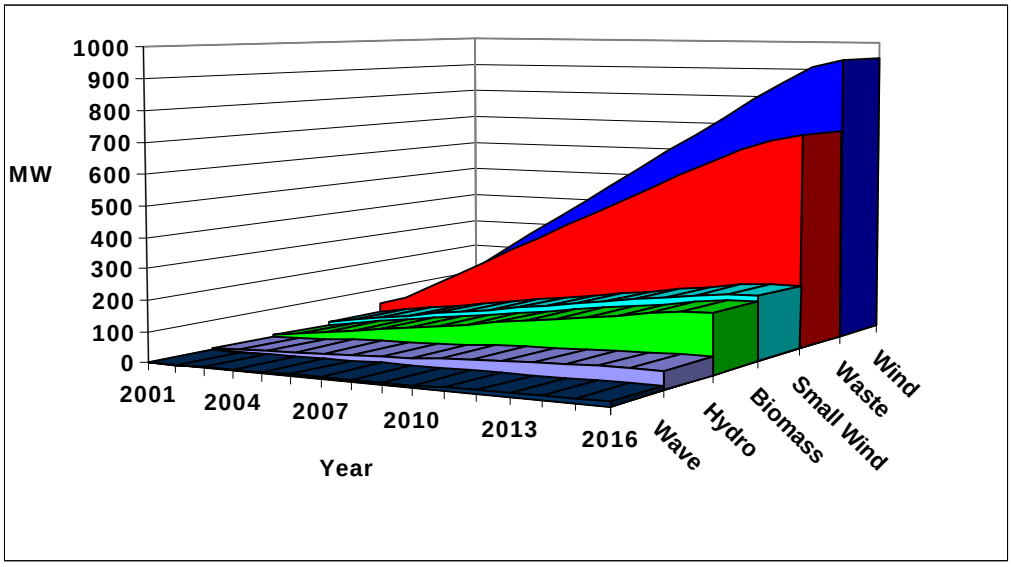

Figure 2.4: Aggregate renewable energy requirements for Scotland (Statutory Instruments, 1999)

2.3 The Future for Renewable Energy

In 1996, the global prospects for renewable energy were reviewed by the World Energy Council (Jefferson, 1996). It was reported that the current renewable contribution to global primary energy supply was 18%, with emerging technologies (modern biomass, solar, wind, geothermal, small hydro, ocean/tidal) accounting for only 2%. The review concluded that the process of developing renewable technologies needed to be accelerated as "*action postponed is liable to be opportunity lost*".

Although renewable energy use has increased throughout the world, it is estimated that developing countries (excluding Eastern Europe and the former Soviet Union) generate only 0.3 % of their electricity from renewables. Approximately 2 billion people still have no access to electricity, the majority of which are in developing countries that

possess large potentials of renewable resources. In developed countries, renewable power was originally used for rural electrification as this was less expensive than extending a grid infrastructure. As many developing countries lack electricity grids, renewable technologies may be the most economic means of supplying power. Additionally, as the capacity of renewable plant is typically smaller than that of conventional plant, they are better suited to small load centers and can be progressively matched to incremental changes in load growth (Renewable Energy Manual, 2000).

In developed countries, electricity grid infrastructures supply the vast majority of loads. Although remote locations present application areas for renewables, these are predominantly niche markets, which will not provide the emission reductions required by the Kyoto protocol.

To ensure sustainability renewable technologies need to be deployed on a large scale. This can be achieved through large-scale generating stations such as wind farms, hydro schemes and industrial scale solar hydrogen plants such as the Neunburg vorm Wald demonstration project (Szyszka, 1996). The major barriers relating to large-scale projects are environmental and land constraints. Land constraints, resulting in the failure to obtain planning permission have been part of the reason for the UK's failure to meet the renewable targets set for the year 2000 (Department of Trade and Industry, 1999). The land-intensity of renewable technologies has been described as their "*Achilles' heel*"(Gipe, 1996). Another restriction is the limited number of potential sites, as the viability of large-scale projects is dependent on an abundance of the renewable source. A large percentage of the potential sites with large-scale hydro generation in North America and Europe have already been developed (Baird, 1993). Furthermore, large-scale sources such as tidal barrages and offshore wind and wave power are likely to be situated remotely from load centers. Exploitation of these will require major investment in the reinforcement and expansion of the transmission grid. Much of the UK renewable energy resource is inaccessible at present. For example, the largest wind and wave resources are in north-west Scotland, but there is little or no

transmission infrastructure to supply potential consumers (Morgan, 1999). The final obstacle for large-scale renewable plant is the associated capital expenditure required, this being the other reason the UK failed to meet its renewable targets (Department of Trade and Industry, 1999).

The challenge of sustainability with regard to energy is becoming clear. The need for green technologies has been established and the commitment for their world-wide deployment is beginning to manifest. However, the barriers, which need to be overcome, before the renewable energy contribution becomes significant, are numerous. The world requires large-scale RE deployment, however, this seams to equate to large-scale investment and large-scale land use, both difficult hurdles to overcome. The work presented here is based on the suggestion that the solution to these issues is to down-scale.

Large-scale deployment of renewables is not confined to large-scale projects. The alternative is to deploy small independent systems on a large-scale. Such systems are ideally suited to building integration. Applications for building integrated systems are vast, with new buildings presenting clear opportunities for integration. The built environment consumes up to 50% of total delivered energy (Johnstone, 1993) and the potential for building integrated renewables to make a significant contribution to sustainability is considerable. There is also the additional advantage that by generating energy at the point of use, as is the case for building integrated energy systems, the energy losses due to transmission are avoided. Furthermore, the cost of increasing supply capacity can be displaced by the introduction of embedded capacity, depending on the scale of the embedded project.

Examples of small-scale renewable systems are listed below:

- Photovoltaics are ideally suited to building integration as roof or building façade installations (Ishikawa, 1996), (Wakamatu and Nitta, 1996). Incorporating heat

recovery with PV systems improves their efficiency and enables the recovered heat to be deployed in meeting a buildings thermal demands (Clarke et al., 1996). A successful example of PV integration is the photovoltaic rooftop project in Gelsenkirchen, Germany (Beneman et al., 1996). A Japanese study found that 5% of the gross electricity demand could realistically be supplied by PV residences (Kosuke, 1996).

- Solar flat plate collectors can be used to meet the energy demand for domestic hot water (Fuentes et al., 1996).

- Small-scale wind installations such as the ducted wind turbine (Webster, 1979) are designed for roof integration in high rise buildings. Alternatively, small autonomous wind turbines could be used for agricultural purposes or to meet the demands of small villages.

- The use of district heating and cooling and combined heat and power for a group of buildings or on a city-wide basis is well established (Kainlauri, 1996), (Copeland, 1998).

- Fuel cells present another example of a technology suited to small-scale applications, where site restrictions are virtually non-existent (Hart, 2000).

Small-scale renewable systems deployed on a large scale present a vast opportunity for developed nations. The deployment of such systems however, is not without technical difficulties.

2.4 Small Scale Renewable Energy Generation Issues

Small-scale renewable technologies are possible sources of power for embedded generation, i.e. generation capacity installed at the distribution network. However, typical electricity networks were not designed to support embedded generation.

In 1919, independent generators were connected directly to distribution networks serving local areas. The construction of the 132 kV National Grid allowed larger, more efficient generating stations to be used, with electricity transmitted to remote loads. After nationalisation in 1948, the 275 kV or 400 kV super-grid provided the means to transmit electricity from very large central power stations to distribution networks. The distribution systems were designed to accept bulk power at grid supply points and distribute power to customers. The direction of power flows in the distribution system was from higher to lower voltage levels (Jenkins, 1995). Figure 2.5 illustrates a simplified schematic of the network structure.

The network becomes considerably altered by the addition of embedded generation. The penetration of renewables would transform currently passive networks, responsible for supplying loads, into active networks where the relative magnitudes of generation and load, determine the direction of power flows. This situation is depicted schematically in figure 2.6.

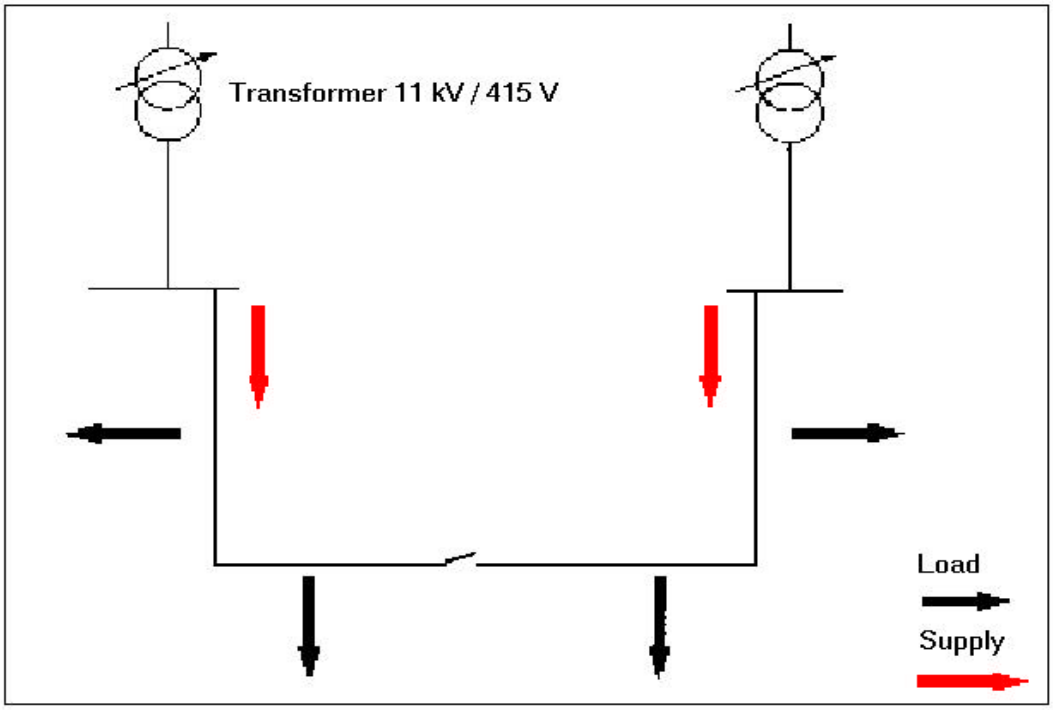

Figure 2.5: Schematic of a conventional passive distribution network (Jenkins, 1995)

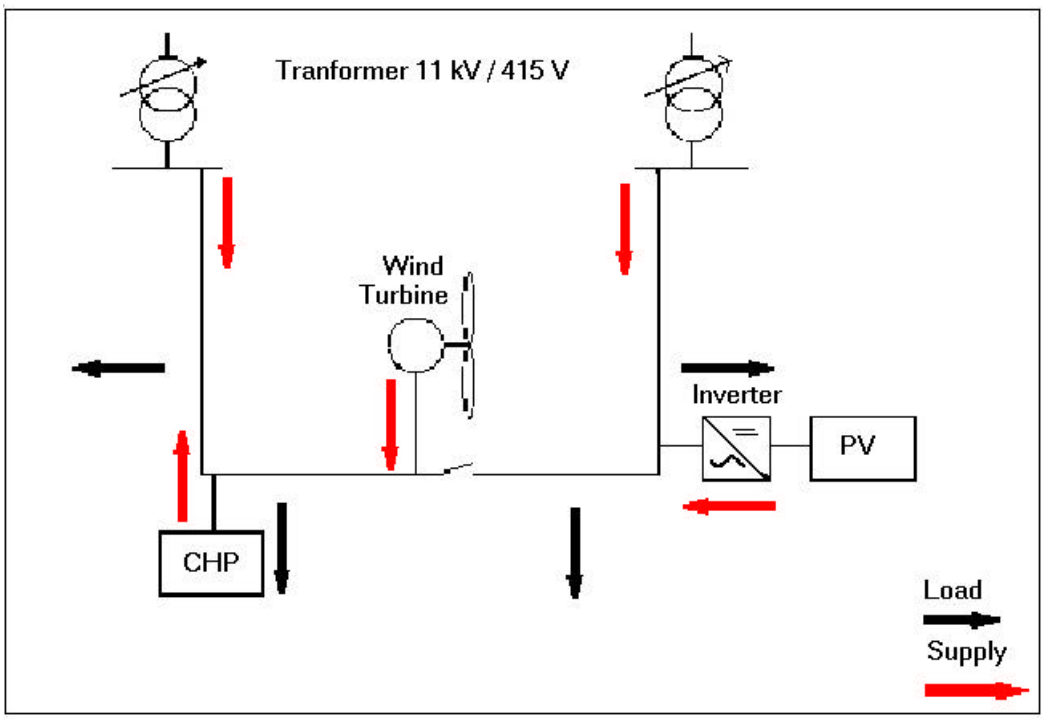

Figure 2.6: Schematic of a distribution network with embedded generation (Jenkins, 1995)

The intermittent nature of renewables and varying load profiles result in highly unpredictable power flows. Direct grid connection of a significant amount of intermittent power can jeopardise grid stability because of the abrupt variations in power generation (Jenkins, 1996). Changes in power flows can result in either increased or decreased network losses, depending on the magnitudes of loads and generation (Ciante and Barra, 1996). In addition to potentially decreasing system losses, embedded generators can help to free network capacity and delay system reinforcement (Salman, 1996). The potential benefits of embedding are largely dependent on the capacity of a distribution network, which will consequentially limit the size of a renewable project (Rodgers, 1996). Power Quality is also affected by embedded generation, with voltage disturbances and the harmonic distortion of voltage waveforms being the main causes for concern (Jenkins, 1995), (Thomas, 1996). In addition to the technical issues surrounding embedded generation, there are also financial and legal aspects concerning connection (McTague, 1996).

Demand forecasting is used to predict the electricity demands for the succeeding generation period. Utilities require planned hourly generation schedules together with demand forecasts, to formulate the necessary operational plans. These plans are used to decide on technicalities such as; unit commitment; spinning reserve; control reserves; fuel schedules and maintenance outages (Oldbach, 1994). Over predictions of demand and the inability to account for the renewable contribution to supply, result in wasted electricity.

2.5 Summary

Energy sustainability is dependent on renewable and energy efficiency technologies. The Kyoto protocol illustrated that international nations are aware and committed to deploying these technologies. The performance of renewable technologies have made considerable advances in recent years, despite having to compete in environments which favoured traditional fossil-fuel technologies. The U.K., like other countries has pledged to secure considerable amounts of additional renewable energy generating capacity. Optimistic projections have been made before, but goals not attained. The land intensity of large scale generating stations limits the potential applications for such developments. This barrier can be surmounted by significant penetration of small-scale systems. Such systems are ideally suited to building integration and the existing building stock present presents endless opportunities for the deployment of such technologies. However, a number of issues require to be considered if technologies are to be embedded in the distribution networks. A vital issue is to ensure personnel involved in demand forecasting and unit dispatch, are well informed of changes in generation and demand. Renewable energy deployment on any scale requires decisions to be made, which in turn depend on information. The work presented in this dissertation is concerned with providing the means to make informed decisions in renewable energy strategies.

2.6 References

1. Baird Stuart, Energy Facts: Hydro-electric Power, 1993, URL:http://www.iclei.org/efacts/hydroele.htm
2. Beneman Joachim and Chehab Oussama, Pilkington Solar International for PV Applications in Buildings, WREC 1996
3. Burtraw Dallas, Darmstadter Joel, Palmer Karen and McVeigh James, Renewable Energy : Winner, Looser or Innocent Victim? URL: http://www.repp.org/articles/mcveigh/index_mcveigh.html
4. Clarke J.A., Hand J.W., Johnstone C.M., Kelly N., Strachan P.A., Photovoltaic-Integrated Building Facades, WREC 1996
5. Coiante D. and Barra L., Renewable Energy Capability to Save Carbon Emissions, Solar Energy Vol.57, No. 6, pp. 485-491, 1996.
6. Copeland Peter, Study of 3 MW CHP Installation at Dundee University, Developments in Combined Heat and Power into the Millennium, May1998
7. Department of Trade and Industry, New and Renewable Energy Prospects for the 21st Century, 2000 URL:http://www.dti.gov.uk/renew/condoc
8. Elani U.A., Alawaji S.H., Hasnain S.M., The Role of Renewable Energy in Energy Management and Conservation, WREC 1996
9. Fuentes Manuel, Dicher Alan and Roaf Susan, The Oxford Solar House, WREC 1996
10. Gipe Paul, Overview of World-wide Wind Generation, WREC 1996
11. Hart David, Domestic Power and the Deregulated Market, Fuel Cells Bulletin, No 8, 2000, URL: http://www.energypartners.org/media%20papers/fc_bulletin.htm
12. Hileman Bette, Global Climate Change, News Focus, November 17, 1997 C&EN Washington, URL: http://pubs.acs.org/hotartcl/cenear/971117/global.html
13. Ishikawa Osamu, A Photovoltaic System Doubling as a Roofing Material for Houses, WREC 1996
14. Jefferson Michael, Global Prospects for Renewable Energy, WREC 1996
15. Jenkins N., Embedded Generation Part 2, Power Engineering Journal, October 1996

16. Jenkins N., Embedded Generation, Power Engineering Journal, June 1995
17. Johnstone S. Greener Buildings – the environmental impact of property, MacMillan Press, Basingstoke, 1993.
18. Kainlauri Eino O., Environmental Impovements Resulting from the Use of Renewable Energy Sources and Nonpolluting Fuels and Technologies with District Heating and Cooling, ASHRAE Transactions: Symposia, 3/5/1996, pp. 468-471
19. Kopp Raymond J., Morgenstern Richard D. and Toman Michael A., The Kyoto Protocol: Unresolved Issues, 1998, URL: http://www.weathervane.rff.org/features/feature026.html
20. Kosuke Kurokawa, An Overview of System Technology in Japan, WREC 1996
21. Lashof Daniel, How Workable is the Kyoto Protocol? The Kyoto Protocol Is a Vital First Step Toward Climate Protection, 1998, URL: http://www.weathervane.rff.org/pop/pop5/lashof.html
22. Leggett Jeremy, The Emerging Global-Warming Market Driver in the Energy Sector: A Status Report, WREC 1996.
23. Lovejoy Derek, The Necessity of Solar Energy, WREC 1996
24. McTague David, Embedded Generation: ESB Distribution Network Considerations, The Institution of Electrical Engineers, 1996
25. Miller A.S. and Serchuk A.H., Renewable Energy in Competitive Electricity Markets, WREC 1996
26. Milloy Steven J., Kyoto Protocol to the United Nations Framework Convention on Climate Change, 1997, URL: http://www.junkscience.com/news/accord.htm
27. Morgan R, Renewable Energy, The Institution of Electrical Engineers, PAB(S)515, 26 February 1999, Ref: 122/350, URL:http://www.iee.org.uk/PAB/Submisns/s515.htm
28. Oldbach Rolf, Embedded Electricity Generation, Msc Thesis, Strathclyde University,1994
29. Price W. R., Current Operating Problems Associated with Non-Utility Generation, IEE Transactions on Power Systems, Vol4, No 4

30. Rogers W. J. S., Impact of Embedded Generation on Design, Operation and Protection of Distribution Networks, IEE Colloquium, October 1996
31. Salman S.K., The Impact of Embedded Generation on Voltage Regulation and Losses of Distribution Networks, IEE Colloquium, October 1996
32. Statutory Instrument 1998 No. 2353 ,The Electricity (Non-Fossil Fuel Sources) (England and Wales) Order 1998
33. Statutory Instrument 1999 No. 439 (S. 24), The Electricity (Non-Fossil Fuel Sources) (Scotland) Order 1999
34. Szyszka Axel, Review of the Neunburg vorm Wald Solar Hydrogen Demonstation Project, Power Engineering Journal, October 1996
35. The Fifth Environmental Action Programme, 2000, URL:http://kola.dcu.ie/~environ/fifth.htm
36. The Renewable Energy Manual, 2000, URL:http://www.eia.doe.gov/solar.renewables/renwable.energy.annual/contents.html
37. Thomas Christopher G., Renewable Generation: The British Experience, WREC 1996
38. Thomas P.G., A REC's Experience of Embedded Generation within its Networks, The Institution of Electrical Engineers 1996
39. Wakamatu Seij and Nitta Yoshiteru, PVTEC Photovoltaic Activity and its Integration to Buildings, WREC 1996
40. Webster G.W., Devices for Utilising the Power of the Wind, United States Patent 4152556, May 1979

Chapter 3: Supporting Energy Decisions

Managing energy effectively encompasses two scales of decision making. Large-scale decisions are those made by utilities in ensuring the demand for energy is met. Small-scale decisions are those made by building owners and energy managers to ensure their own energy systems are optimised. The small scale has a direct effect on the larger scale, as trends of consumption are altered. Decisions are made based on information. There is an abundance of energy information available, however a framework in which to use this information is comparatively lacking.

3.1 Large Scale Decisions

The following sections describe two examples in which energy information is used within the utility infrastructure. The first examines the field of demand forecasting and summarises some of the methods used to meet forecasting objectives. The second example explores the relatively new field of demand side management.

3.1.1 Demand Forecasting

Demand forecasting is used to ensure unanticipated demands are met and that the demands placed on the system are matched to the resources delivered by generators therefore maintaining system balance (Central Maine Power Company, 2000), (Eto and Moezzi, 1993). Demand forecasting is performed for both short and long term periods, were the resulting predictions are used in different planning activities.

Short-term load forecasts are defined for periods up to one-week. The forecasts comprise load profiles, used by utilities for scheduling dispatch, system maintenance, economical allocation of resources and in making other immediate operating decisions. A 1985 research report from the British Power Company, showed that one million

pounds could be saved from accurate short-term load forecasting (Energico, 1997). Similarly, the American Department of Primary Industry estimated a saving of over two billion dollars (Energico, 1997).

Medium and long-term load forecasts are used to predict demands for periods up to two-years and several years, respectively. Medium term forecasts are used in planning maintenance and evaluating the necessity for additional capacity. Long-term forecasts are also used in assessing additional capacity, as well as assessing the fuel mix of additional generation (California Energy Commission, 1996). Accurate long term forecasting is essential due to the economics and construction times involved in incorporating additional generation and transmission facilities. Both medium and long term forecasts require temporal and spatial demand forecasts, as well as price forecasts.

Various approaches are used in determining future load profiles in the short term. The 'equivalent day' load forecasting methodology, described in the NEMMCO operating procedures (NEMMCO Operating Procedures, 2000) forecasts estimates of regional loads. The algorithm used is based on trained neural networks which learn patterns from past data to predict future trends. Neural networks have also been employed in a study to predict the loads on the island of Crete, in Greece (Bitzer et al., 1997). Historic load data was used to train the neural networks and resultant forecasts were tested against actual load data. This study found a number of problems in utilising the neural network approach, primarily due to insufficiencies in historical load data. Changes in demand patterns that cannot be attributed to control operations or measurement faults or temperature-related effects lead to erroneous forecasting.

Hybrid Forecasting models, employing a variety of forecasting techniques have also been investigated. One technique (Padhy et al., 1997) employs artificial intelligence to filter historical data in order to establish influencing factors and then uses statistical relationships to develop forecasts. Classification of profiles is frequently used in forecasting, Shrestha and Lie (Shrestha and Lie, 1993) presented a forecasting

procedure that classes profiles by considering the load profile as fuzzy in nature and uses this fuzzy description as input to a neural network. Balachandra and Chandru (Balachandra and Chandru, 1999) proposed the use of representative load curves to portray the dynamics of demand variations. A representative load curve is assigned to a group of load curves, which exhibit similar demand patterns. The classification of load curves is achieved using statistical techniques. Ozveren et all (Ozvern at al., 1997) published a methodology, which automated the classification of large-scale sets of electric demand using the fuzzy membership function. This function, in conjunction with mean and standard deviations of half-hourly loads, permits the identification of similarities between varying load profiles.

The methodology employed by NEMMCO (NEMMCO Operating Procedures, 2000) for long term forecasting is based on a time series analysis. This method is used to examine systematic and recurrent relationships in historical load data. The time series is decomposed into four main components: trend, seasonal, cyclic and irregular. Statistical methods are used to describe the behaviour of each component, in the succeeding period and decisions based on the resultant trends are used to construct the forecast. The trend component represents the gradual shifting of the time series, which is usually due to factors such as changes in population and changes in technology. The cyclical component is any regular pattern of sequences of points, above and below, the trend line lasting more than one year. Generally, it is believed that this component represents multiyear cyclical movements in the economy. The seasonal variations in demand are represented by regular patterns of variability within one-year periods. The residual of the time series, with trend, cyclical and seasonal components removed, represents the random variability of the time series. This irregular component can be attributable to short term, unanticipated and nonrecurring factors and is not predictable.

A Japanese study (Kermanshahi et al., 1997) proposed the use of a recurrent neural network, accounting for past and present economic conditions as well as electrical demand. The system requires historical demand data in addition to data, which is

responsible for demand variations. The demand influencing parameters include; economic parameters (e.g. Gross National Product, oil and electricity prices); society parameters (e.g. population, number of households, number of air conditioning systems); temperature data and environmental parameters (e.g. quantities of CO_2).

Demand forecasting objectives are to ensure planning activities are based on the realistic predictions of future requirements of the entire supply network. The various methods used in predicting future consumption trends are predominantly based on the extrapolation of past trends.

3.1.2 Demand Side Management

Environmental concern has induced electric utilities to consider a variety of options in securing energy requirements, including large-scale renewable generation schemes and Demand Side Management (DSM) programmes. Supply-side functions, such as the planning, construction, operation and maintenance of generation facilities were the traditional pursuits of utilities. DSM is a relatively new strategy concerned with employing measures to alter the system load curve. The primary objectives of DSM is to alter the system load curve to reduce variability and net demand, as large variations in demand limit the efficiency of the supply infrastructure. The Energy Information Administration (Energy Information Administration, 2000) reported the four fundamental methods used in altering the load curve as:

- Load shedding, which refers to any measure used to reduce net energy consumption both during peak and off-peak periods (e.g. energy efficiency programs).
- Peak clipping, which is used to reduce load during periods of peak power consumption (e.g. load management programs, interruptible load tariffs, time-of-use rates)
- Load shaping, which alters the load curve using methods similar to peak clipping when those activities are not limited to peak load periods.

- Load building, which is designed to increase consumption, particularly in off-peak periods which is known as ‘valley filling’ and can be achieved through the introduction of new electric technologies and processes, such as storage heating systems which are powered up during times of low demand.

Sporadic peaks in a system demand profile represent periods of peak demand and are problematic to utilities (US Department of Energy, 1995). In order to generate sufficient power during these short periods, operational plant is required to run at full load or additional peaking plant is required to be brought on-line. Neither of these options are favourable; regularly cycling plant operation to full load reduces both plant life and efficiency and peaking plant tends to be the most expensive to operate. Additionally, transmission and distribution systems have to be sized to accommodate these high but short-term loads, thereby substantially increasing the costs of these systems. There have been various attempts at smoothing out electrical demand through peak clipping, lopping or shaving. Demand side bidding, spot pricing and increased charging are designed to encourage customers to reduce loads during these peak periods. These techniques have resulted in demand redistribution, but not necessarily in a reduction of energy demand (Starbac et al., 1996).

Many DSM programs are viewed as resources, because they capture cost-effective energy savings that would otherwise not be achieved. Utilities compare the benefits and costs of DSM with the cost of additional generation. Savings and load reductions cannot actually be measured by metering and therefore must be approximated, using statistical analysis of energy usage and/or other estimation techniques. Estimating the value of DSM activities has received considerable attention in recent years. Bush and Eto (Bush and Eto, 1996) described the investment in DSM as an avoided cost due to the substantial costs that would be incurred through increases in supply capacity. It is argued that DSM could contain the growth of demand thereby deferring or even cancelling the need to expand capacity. This is particularly significant when transmission and distribution capacity expenditure is avoided, as this is substantially

higher than that of generation capacity. Another study focused on estimating the value of supply reliability (Willis and Garrod, 1997) where the value of DSM is questioned. In the event, of a loss of supply, utilities are required compensate customers. The authors suggest that, as DSM tends to be reflected in a reduction in the base load, as opposed to a differential reduction in peak loads and therefore can not be used to offset an increase in supply and reliability. Billinton and Lakanpal (Billinton and Lakanpal, 1996) used a 'reliability cost / reliability worth' approach to analyse the impact of DSM on reliability. The approach attempts to optimise the reliability level, by evaluating the cost of reliability incurred by the utility and the value of reliability perceived by the customer. The study illustrated that the optimal planning reserve margin varied depending on the type of DSM activity. Load reduction activities reduced planning reserve margin, whereas load shifting and building activities had little or no effect.

Renewable technologies, embedded at the distribution level, can be considered as a demand side opportunity as opposed to an additional supply capacity. The problems of integrating generation capacity at this level were discussed previously. However, integration with the distribution system is not technically necessary. Without connection to the distribution system, a source of supply forsakes its distribution capability and therefore does not represent supply capacity. Nevertheless, the power absorbed by the local load would represent a reduced demand to the utility, therefore classifying renewable technologies deployed in this way, as demand-side measures. Woodworth (Woodworth, 1996), suggested that reverse power flows, i.e. power exported to the distribution system, were uneconomic for co-generators, due to the cost of complying with regulations. Additionally, exported power sold through the electricity pool would be required to compete with the bidding prices of large-scale generation. A benefit-cost analysis of PV as a demand side measure (Byrne et al., 1996), demonstrated that, evaluated as a demand-side technology, PV was far more viable than was previously considered. The study was carried out in the U.S., where peak demands occur on hot summer days due to high utilisation of air-conditioning equipment and such days also correspond with abundant levels of solar isolation. The

peak in PV output, however, occurs prior to the peak in demand, by including modest storage facilities these peaks can be brought into phase with one another and thereby offer significant peak shaving benefits to utilities. The benefit-cost approach includes both the energy value (i.e. the systems ability to save energy) and the capacity value (i.e. the reduction in peak demand), in addition to other factors such as modularity and fossil fuel price protection. Modularity refers to the ability of matching incremental increases in load with equivalent capacity increments. Fossil fuel price protection refers to the security offered by renewable technologies against fuel price volatility and future environmental legislation. The potential of such a demand side measure is illustrated if the U.S. commercial-building sector is considered. This sector alone is responsible for the addition of 50 square kilometres of roof space each year, an area suitable for a potential of 3000–5000 megawatts of PV power (NREL, 2000).

3.1.3 The Information Framework

All of the techniques used in forecasting (both short and long-term) demands are based on historical load data. However, trends in historical load data may not identify the characteristics resulting from the deployment of new technologies. Demand side management activities are concerned with altering the system load curve. Energy efficient measures will reduce consumption but may also alter the shape of the load profile. Integrated renewable technologies will provide a source of energy used to meet some of the demand and therefore eliminate portions of the demand profile. Forecasting methods based on historical trends are inherently flawed if they do not account for the measures taken to change the consumption patterns of the past. This presents an example of how the same information is being used to meet different objectives and the lack of an energy information framework could compromise the overall objective to meet energy needs efficiently and effectively.

3.2 The Flow of Information

Figure 3.1 describes the information systems required in aiding energy-related decisions. Some form of tracking system is a prerequisite to decision making as it provides the necessary information on which informed decisions can be made. Having identified an area of action, a useful tool for energy strategy investigations would comprise a supply and demand matching facility to analyse the effects of both passive and active technologies in meeting demands. Detailed building appraisal systems could quantify the effects of certain decisions related to implementing technologies within the built environment. Where embedded generation schemes designed to export power to the distribution network are being investigated a component to assess the impact on grid stability and power quality is required. Finally, the predicted consequences of the decisions made need to be incorporated in demand forecasting methodologies. Within the described framework, the accuracy of predictions can be validated through comparisons with actual monitored trends.

The information framework described is applicable to all decision-makers concerned with energy, and sustainable energy decisions need to incorporate the green technologies of energy efficiency and renewable energy. In a survey of the financial perspective of renewable technologies (Langniss, 1996) it was found that supporting the dissemination of renewable energy technologies meant supporting people as opposed to technologies. The survey found local authorities to be the ideal framework for overall optimisation of the whole local-energy-system under economical and ecological aspects. In many countries including the U.K., permission to proceed with a renewable project is decided at the level of regional or local authorities. Municipalities require relevant energy information in order to promote renewable energy (Clarke and Grant, 1996).

An energy tracking system enables energy managers and utilities to prioritise measures to alter energy consumption through the various means available, including employing

renewables in a demand side management role. Tracking the resultant changes to consumption patterns would facilitate the prediction of how certain DSM activities affect the system load curve. Tracking spatial aspects of energy supply such as renewable source potentials, planning restrictions and the availability of a supply network infrastructure would prevent wasted efforts in planning unrealistic options.

Where renewable integration is identified as a possibility, unconstrained by land use, network and source availability, strategic investigations based on complimentary supply-demand matching could be initiated. The renewable technology (ies) identified could potentially be deployed in one of the following ways:

- To supply power to a single building integrated within the building envelope.
- To provide a small community with its power requirements through a dedicated network.
- To provide additional supply capacity by exporting power to the grid.

Analysing potential strategies for RE integration requires an insight into the relative magnitudes of supply and demand. However, as renewable sources are intermittent, magnitude matching alone can become meaningless, for example if the annual solar resource for a given area was found to be exactly that required to meet a street lighting load. The temporal match between supply and demand is critical in renewable energy. Every unsuccessful installation of renewables hinders their progress, as they are seen to be futile and expensive. Therefore, temporal matching is essential in the assessment of RE supplies.

Once a suitable supply and demand match is identified, a detailed analysis of building energy requirements should be initiated to further optimise the energy system. Where a renewable supply has been found to be suitable to meet the needs of numerous buildings, building simulation could be employed to investigate passive technology deployment to enhance the match between supply and demand. This level of

optimisation can be taken even further, where single buildings are subject to investigation and detailed building appraisal can determine whether the selected technology will have an adverse effect on building aspects such as comfort. Building appraisal tools have the additional capability of predicting the demands of sites where no information on consumption is available which effectively amounts to a virtual tracking system.

Where a renewable grid export approach is to be evaluated the impact on stability and power quality needs to be assessed. This enables utilities to ensure adverse affects from embedding renewables into the supply network are minimised.

Finally, the changes in consumption patterns resulting from RE deployment need to be accounted for in demand forecasting to ensure the prediction of future grid requirements are accurate. Accurate forecasts prevent the energy wastage associated with conventional generation used to meet forecast demands, which are being met via alternative means.

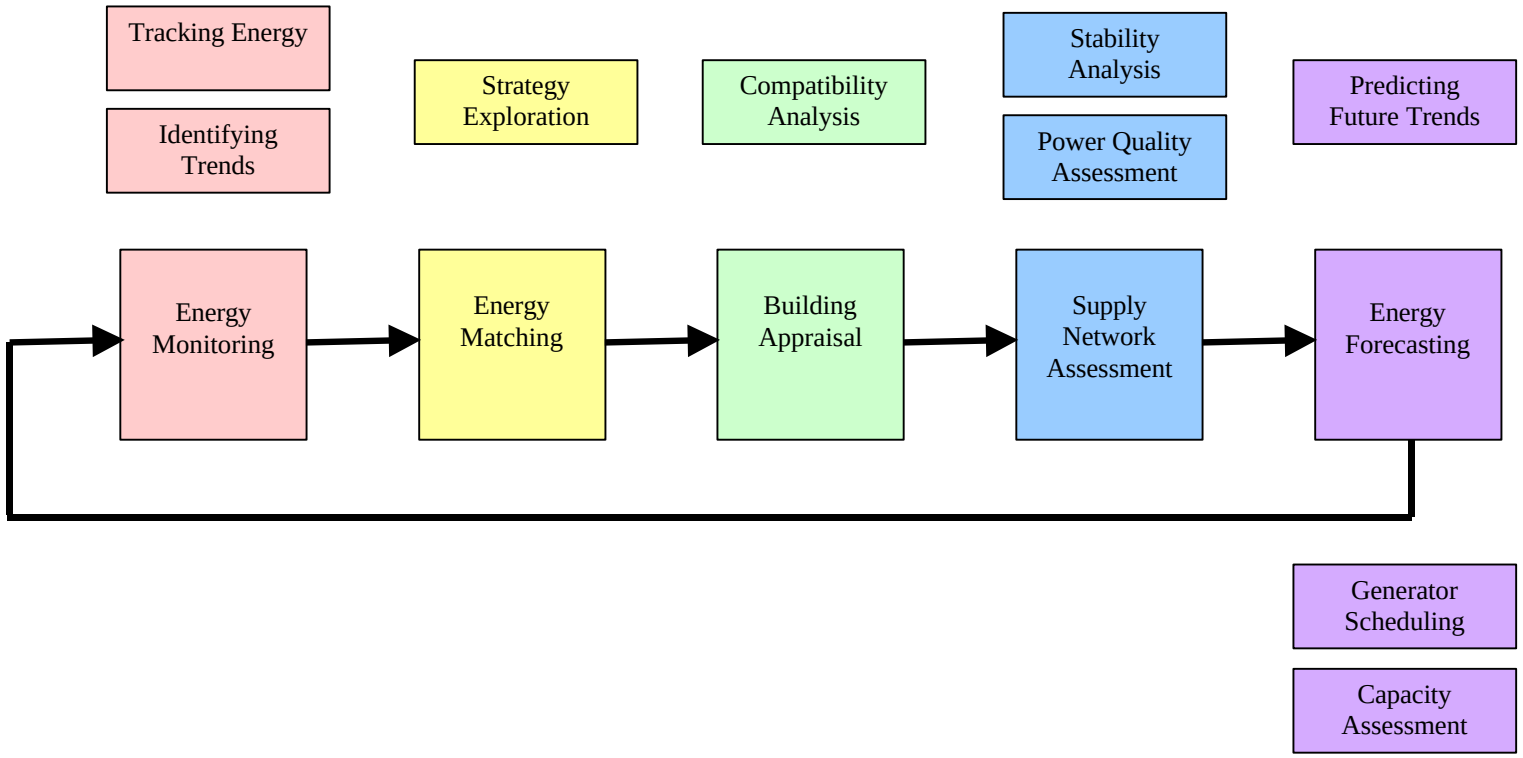

Figure 3.1: Components required in the energy information framework

3.3 Information Systems

Computer power has been largely responsible for the advances in renewable technologies and will be equally instrumental in their dissemination. The use of computer systems has had a direct effect on renewable energy technologies by advancing design and improving efficiencies (Osborne, 2000). Examples include improving the conversion efficiency of photovoltaic cells, increasing the aerodynamic performance of wind turbines and the development of power electronic devices to allow variable-rotor-speed operation of wind turbines, which reduce structural loads and improve power quality.

The dissemination of renewables is ideally suited to the framework described in the previous section and activities in the various components have resulted in a range of decision support tools:

A variety of energy tracking and decision support systems are currently available (e.g. QuickPlan (quickplan.htm), Entrack (Clarke et al., 1996)). These software tools enable users to monitor energy consumption in order to detect inefficiencies and faulty control systems, and evaluate the effects of building retrofits. They also provide spatial information related to enable renewable energy resource estimation by site, as well as environmental and socio-economic impact assessment. The EEP system (Jones et al., 1996) enables sustainable planning via emissions tracking and enables users to assess progress towards agreed reductions in emissions.

Specialised simulation tools are available for the analysis of renewable systems. Examples include solar ventilation air heating; biomass heating; wind energy; small hydro and photovoltaics (e.g. RETScreen (ENREN-f), IRES-KB (Castro et al., 1996)). Such programs facilitate the pre-feasibility analysis of renewable technologies and aid the procedure of evaluating the optimum technology for a given site by the evaluating supply potentials. Evaluating the role of renewables as a demand side measure requires

supply and demand matching. A comprehensive analysis of photovoltaic system modelling (Wolfe, 1985), identified that load behaviour was as critical to successful system design, as the PV array characteristics and the solar radiation levels. Iniyan et al (Iniyan et al., 2000) developed an optimal renewable energy mathematical model to investigate future renewable energy allocation in energy planning. In this work, possible RE options were considered which meet the energy demand of a variety of end uses. The model aimed to minimise the cost/efficiency ratio of a number of different technologies and therefore identify the best RE distribution pattern. Factors taken into account in this method include the social acceptance, potential and reliability of renewable technologies. However, the technique is based on annual demands and neglects variations in energy use patterns. The matching procedure described by Ramakumar et al. (Ramakumar et al., 1992) employs a knowledge-based approach in the design of integrated renewable energy systems. The procedure uses seasonal data sets to characterise each season by a set of available RE resources and load requirements. By systematically attempting to satisfy each of the seasonal demands with the cheapest supplies available, seasonal supply systems are constructed, from which an annual design is proposed. The work is primarily concerned with finding the most economic supply technologies to satisfy a number of prioritised demands. Again the high levels of variability involved in both demand and supply profiles are neglected in a seasonal approach. Profile variability is critical in any supply and demand matching exercise, as net supply and demand totals give no indication as to whether demands are satisfied at the time when they are required. The design of a RE system should ensure that times of RE availability coincide with periods of consumption.

The simulation of building demands is standard practice for energy consultants and architects involved in the appraisal of energy efficiency technologies. A range of software design tools are available, encompassing simple appraisal tools (e.g. ASEAM (ENREN-a), Energy 10 (ENREN-b)) and sophisticated packages (e.g. DOE-2 (ENREN-d), Esp-r (ENREN-c)). These tools are employed to evaluate a variety of energy dependent design measures, with the more advanced packages including features to

assess comfort, daylight and analyse different control systems. Furthermore, some of the building simulation tools incorporate renewable energy technology modelling, allowing building integrated system analysis (e.g. Esp-r (ENREN-c), TRYNSYS (ENREN-g)).

Packages are available to analyse power quality issues (Timko et al., 2000) and some of the methods employed in demand forecasting have already been described.

3.4 Summary

The framework envisaged for energy information management has been described and the individual components within that framework can be seen to be largely in place, with the exception of supply and demand matching tools. The work presented in the subsequent chapters examines the requirements of such a tool in detail. Figure 3.2 illustrates the complexity of design decisions required to integrate renewable technologies at the building level. The stages involved can be summarised as follows:

- The evaluation of the various demand systems and options for manipulating their profiles.
- The appraisal of technically feasible RE configurations.
- The optimisation between supply and demand systems through profile matching.
- The analysis of auxiliary systems in the context of enhancing the supply-demand match

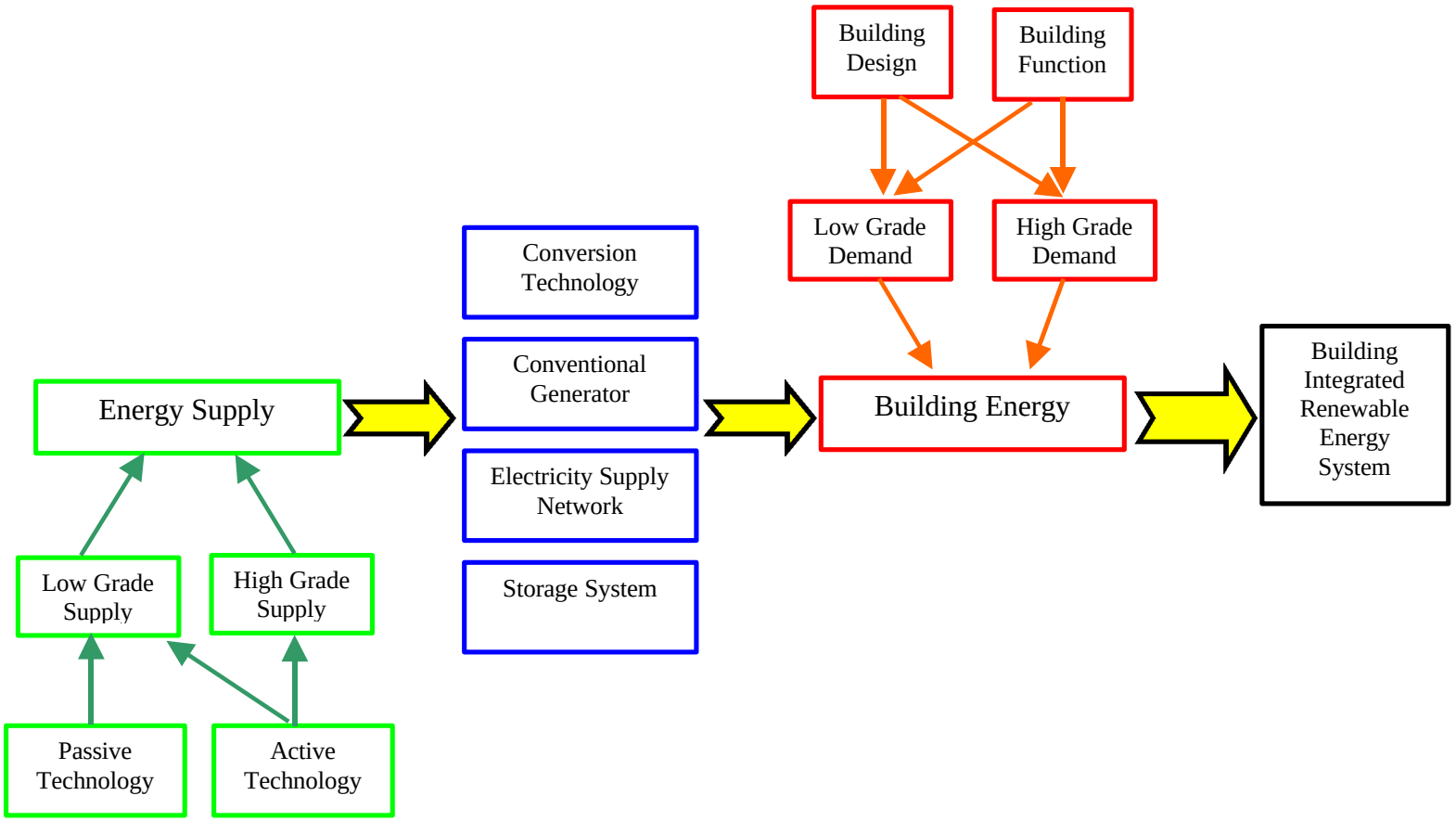

Figure 3.2: Design decisions required to integrate renewables at the building level

3.5 References

1. Central Maine Power Company, Chapter 321 Methodology Report #1, 2000 URL:http://www.cmpco.com/competition/cep/profiles/methodology1.pdf
2. Eto J. and Moezzi M., Analysis of PG&E's Residential End-Use Metered Data to Improve Electricity Demand Forecasts — Final Report , December 1993, URL:http://eetd.lbl.gov/EA/EMP/reports/34431.html
3. Balachandra P. and Chandru V., Modelling electricity demand with representative load curves, Energy 24, 1999, pp. 219-230.
4. Billinton R. and Lakanpal D., Impacts of Demand-side Management on Reliability Cost / Reliability Worth Analysis, IEE Proceedings on Generation, Transmission and Distribution, Vol. 143, No. 3, pp. 225-231, May 1996
5. Bitzer B., Papazoglou T. M., Rosser F., Intelligent Load Forecasting for the Electrical Power System on Crete, Proceedings 33rd Universities Power Engineering Conference (UPEC), pp.891-894, 1997
6. Bush J. F. and Eto J., Estimation of Avoided Costs for Electric Utility Demand Side Planning, Energy Sources, 1996, pp.473-499, URL:
7. Byrne J., Letendre S., Govindarajalu C., Wang Y., Evaluating the economics of Photovoltaics in a Demand-Side Management Role, Energy Policy, Vol. 24, No. 2, pp. 177-185, 1996
8. California Energy Commission, 1996 Electricity Report, 1996, URL:http://www.energy.ca.gov/ER96/FINALER96.PDF
9. Castro M.A., Caprio J., Peire J. and Rodriguez J.A., Renewable-Energy Integration Assessment Through a Dedicated Computer Program, Solar Energy Vol. 57, No.6, pp471-484, 1996
10. Clarke J.A. and Grant A. D., Planning Support Tools for the Integration of Renewable Energy at the Regional Level, WREC 1996
11. Clarke J.A., Evans M., Grant A. D., Karatolis A., Mumaw G., The Role of Information Technology in Urban Energy Policy Formation, 1996

12. Energy Efficiency and Renewable Energy Network (EREN-a), US Department of Energy, ASEAM, 2000, URL:http://www.eren.doe.gov/buildings/tools_directory/software/aseam.htm
13. Energy Efficiency and Renewable Energy Network (EREN-b), US Department of Energy, Energy-10, 2000, URL:http://www.eren.doe.gov/buildings/tools_directory/software/energy10.htm
14. Energy Efficiency and Renewable Energy Network (EREN-c), US Department of Energy, ESP-r, 2000, URL:http://www.eren.doe.gov/buildings/tools_directory/software/esp-r.htm
15. Energy Efficiency and Renewable Energy Network (EREN-d), US Department of Energy, DOE-2, 2000, URL:http://www.eren.doe.gov/buildings/tools_directory/software/doe-2.htm
16. Energy Efficiency and Renewable Energy Network (EREN-e), US Department of Energy, QuickPlan, 2000, URL:http://www.eren.doe.gov/buildings/tools_directory/software/quickplan.htm
17. Energy Efficiency and Renewable Energy Network (EREN-f), US Department of Energy, RETScreen, 2000, URL:http://www.eren.doe.gov/buildings/tools_directory/software/retscreen.htm
18. Energy Efficiency and Renewable Energy Network (EREN-g), US Department of Energy, TRNSYS, 2000, URL:http://www.eren.doe.gov/buildings/tools_directory/software/trynsys.htm
19. Energy Information Administration, U.S. Electric Utility Demand-Side Management: Trends and Analysis, 2000, URL:http://www.eia.doe.gov/cneaf/pubs_html/feat_dsm/contents.html
20. Iniyan S., Sumathy K., Suganthi L., A. A. Samuel, Sensitivity Analysis of Optimal Renewable Energy Mathematical Model on Demand Variations, Energy Conservation & Management, 41, pp.199-211, 2000
21. Jones P. J., Vaughan N. D., Sutcliffe A. and Lannon S., An Environmental Prediction Tool for Planning Sustainability in Cities, 4th Eurpean Conference on Architecture, 26-29 March 1996, Berlin Germany

22. Kermanshahi B., Akiyama Y., Yokoyama R., Asari M., Takahashi K.; Recurrent Neural Network for Forecasting Next 10 Years Loads of 9 Japanese Utilities, Proceedings 33rd Universities Power Engineering Conference (UPEC), 1997
23. Langniss Ole, Instruments to Foster Renewable Energy Investments in Europe: A Survey Under the Financial Point of View, WREC 1996
24. NEMMCO Operating Procedure: Load Forecasting, Document Number: SO_OP3710, March 2000, URL:http://www.nemmco.com.au/operating/systemops/so_op522v004.pdf
25. Newborough M. and Augood P., Demand-side Management Opportunities for the UK Domestic Sector, IEE Proceedings of Generation, Transmission and Distribution, Vol 146. No 3, May 1999
26. NREL, Photovoltaics and Commercial Buildings – A Natural Match, URL:http://www.nrel.gov/ncpv/pdfs/pv_com_bldgs.pdf, 2000
27. Osborne Dariane, The Relationship between the Increase in Computing Power and the Development and Adoption of Renewable Energy Technologies, 2000, www.??
28. Ozvern C.S., Fyall L., Birch A. P., A Fuzzy Clustering and Classification Technoique for Customer Profiling, Proceedings 33rd Universities Power Engineering Conference (UPEC), pp. 906-909, 1997
29. Padhy N. P., Paranjothi S. R., Ramachandran V., A Hybrid Fuzzy Neural Network-Expert System For Short Term Unit Comitment Problem, Microelectronics and Reliability 1997, Vol.37, No. 5, pp. 733 – 737.
30. Ramakumar R., Abouzahr I., Ashenayi K., A Knowledge-Based Approach to the Design of Integrated Renewable Energy Systems, IEE Transactions on Energy Conversion, Vol. 7, No. 4, December, 1992
31. Real-time Forecasting of Short-term Electricity Demand Source: Energico No 21, December 1997 URL:http://www.eidn.com.au/energyforecasting.htm
32. Roberts B. F., Load and Revenue Analysis and Forecasting for Restructured Electricity Markets, ESC Electric Utility Analysis Report 96-3, Economic Sciences Corporation, 1996, URL:http://www.econsci.com/euar9501.html

33. Shrestha and Lie T.T., Qualitative use of Forecast Variables in Hybrid Load Forecasting Techniques, IEE 2nd International Conference in Power System Control, Operation and Management, December 1993
34. Silverton C.L., Wallace A.R.; Application of Genetic Algorithms to Long-Term Generation Fuel Resource Management; Proceedings 33rd Universities Power Engineering Conference (UPEC), pp. 609-612, 1997
35. Strbac G., Farmer E.D., Cory B.J., Framework for the incorporation of demand-side in a competitive electricity market, IEE Proceedings on Generation, Transmission and Distribution, Vol. 143, No. 3, pp. 232-237, May 1996
36. Timko Kevin, Tang Le, Novosel Damir, Hakola Tapio, Kuisti Harri and Vu Khoi, PQ-Smart – A Simulation Tool for Power Quality Modelling and Analysis, URL:http://www.abb.com/global/seitp/seitp145.nsf/4d4b156f3e67c2f5c125682b0051f65f/3c5814bde30fc737c125697600335984!OpenDocument&ExpandSection=1#_Section1, 2000
37. US Department of Energy, Tapping Into the Sun, 1995, URL:http://www.nrel.gov/research/pv/tapsun.html
38. Willis K. G., Garrod G. D., Electricity Supply Reliability – Estimating the value of lost load, Energy Policy, Vol. 25, No.1, pp.97-103, 1997
39. Wolfe P. R., System Sizing – Further Advances Towards a Definitive Solution, Comission of the European Communities (Report), pp.64-70, 1985
40. Woodworth M., A Co-generators (CHP) Viewpoint, Conference of The Impact of Embedded Generation on the Distribution Networks, The Institution of Electrical Engineers, 1996

Chapter 4: Demand Profiles

4.1 Introduction

Demand profiles are the temporal description of load behaviour and an essential source of information on which energy decisions are made. This information exists in a variety of forms, pertaining to the way in which it is used. This chapter begins with a description of a variety of demand profiles, their origins and current uses and concludes with how the various pieces of information can be combined to provide a rich demand data source to aid energy decisions. Profiled demand data can be obtained directly through measurement, indirectly through the studies of load profiling and forecasting and virtually through building simulation. The merits of each technique are discussed and the concept of removing the distinction between methods to provide a composite data reserve is explored.

4.2 Direct Profiling: Measurement

In order to monitor cause and effect relationships in demand profiles, a number of parameters other than electrical consumption, require to be measured. This subsequently requires a range of data acquisition equipment including electrical loggers, whether data sensors, lighting intensity sensors and indoor temperature sensors (McDiarmid, 1996). Increasing the number of measured parameters also increases the associated costs and data processing requirements. Additionally, to obtain a true representation of electrical demand variations over time, the frequency of data acquisition is critical. At high sampling frequencies, individual appliance characteristics can be identified. The frequency of data acquisition will not only dictate the degree of detail obtained in a demand profile, but also the quantity of data processing and analysis required. As the sampling period is increased, the consumption data is summated and the individual load features are no longer identifiable. The graphs

illustrated in Figures 4.1 to 4.3 illustrate the effects of increased sampling rates on load profiling. The data described was received from Manweb and obtained for a residential premises over the period from 4:00 AM to 12:00 PM on the 6th July 1998. The same profile is illustrated at 10-second intervals, 5-minute intervals and half-hourly intervals in Figures 4.1- 4.3, respectively. In Figure 4.1, evidence of electrically heated appliances, with thermometer control can be readily observed by the rapid fluctuations in load behaviour. These fluctuations are as a result of repetitive cycles of drawing current for short time-periods before switching off. In Figure 4.2, evidence of this behaviour is removed as the sampling rate is increased to five minutes. Additionally, some of the peaks in the load profile are temporally displaced, due to the packaging of data into 5-minute intervals. In Figure 4.3, the original data has been summated into half-hour intervals and distinct characteristics of the true load behaviour are lost, leaving only evidence of occupancy and electrical appliance use. Finally, although each of the graphs presented can be integrated to produce the same consumption over the period, the peaks are decidedly different, with information regarding instantaneous power requirements becoming increasingly less accurate as sampling periods increase.

However, because electricity pool prices vary over time-scales of half-hours, much of the demand profile information available is in the form of metered and load research data typically defined at half-hour intervals.

4.2.1 Metering Technologies

In recent years, there have been rapid developments in both metering and the associated options for communication. The trend is towards modular systems of reduced costs, incorporating multi-functionality. Modularity refers to the separation of metering functionality into data collection and communication modules that can be installed by end-use customers, eliminating the need for site-visits and therefore facilitating the process of changing suppliers. Monitoring capabilities currently employed include the detection of outages, idle consumption in vacant buildings, meter tampering and energy

theft. Advanced features incorporate power quality monitoring and harmonic tracking. Customers and retailers are capable of changing the measurement parameters, allowing customers to select read periods and enabling alternative pricing options. Furthermore, system planning and design benefits derived from the detailed breakdown of customer loads include improvements in short-term load forecasting and the optimisation of supply system hardware. Additionally, load management strategies can be improved as energy management programs can be automated or remotely activated and compliance with interruptible load contracts can be verified.

One of the primary benefits of advanced metering is the increased accuracy in cost attribution. Load factors and power factors are, as integral to the cost of electricity, as consumption. Load factor has been defined as the ratio of average demand to peak demand. Interval metering ensures customers with varying load factors but similar cumulative consumptions are billed appropriately. High load factor customers, with uniform consumption profiles, cost less to serve than customers consuming the same quantity of kWh, at low load factors. Tariffs designed around peak demand and/or capacity charges could encourage customers to reduce their electricity bills through load shifting and peak demand reductions. In addition to load factor, power factor can also be measured and is the ratio of reactive power to apparent power. Reactive power is drawn by reactive loads and measured in kVA. Examples of reactive loads are electric motors and inductive heating devices. Today even domestic loads consisting of washing machines, water pumps, refrigerators and air conditioners, possess low power factors. The capacity of transmission and distribution systems is governed by current carrying capacity, in kVA. Consequently, increased demands for reactive power increase transmission and distribution currents resulting in increased losses. In extreme cases, large reactive power demands may cause instabilities in transmission and distribution system. As power factor is the ratio of reactive power to apparent power, and the apparent power incorporates portions of both real and reactive components, supplying low power factor loads requires a reduction in the proportion of real power. This condition is satisfied by operating generating plant at capacities lower than rated,

which consequently reduces operating efficiencies. The kWh tariff was designed around the Ferraris disk meter, which measures real power. The technology now exists to measure reactive power, enabling the introduction of a kVAh tariff, which would ensure consumers paid for both fuel and infrastructure costs. Such tariffs are under review by a number of electric utilities in countries where there is an acute shortage of power, coupled with the need to reduce transmission losses (Vithal and Kamat, 1999).

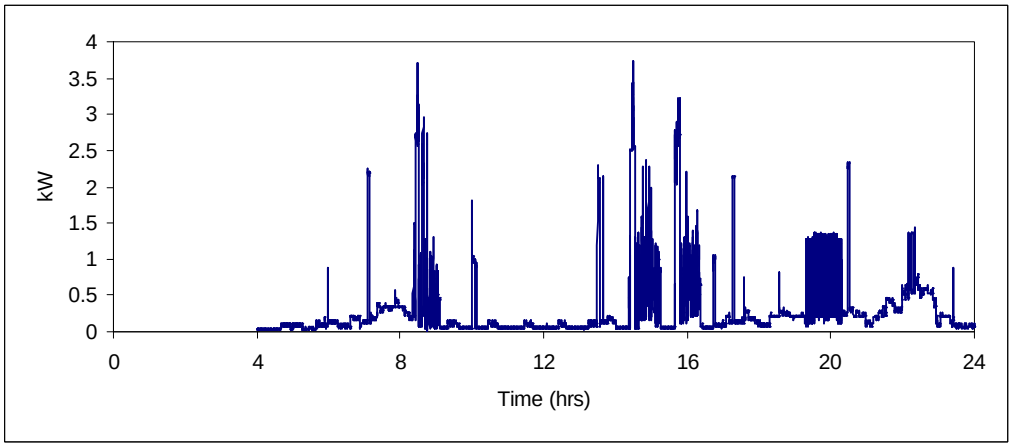

Figure 4.1: Domestic profile taken at 10-second intervals

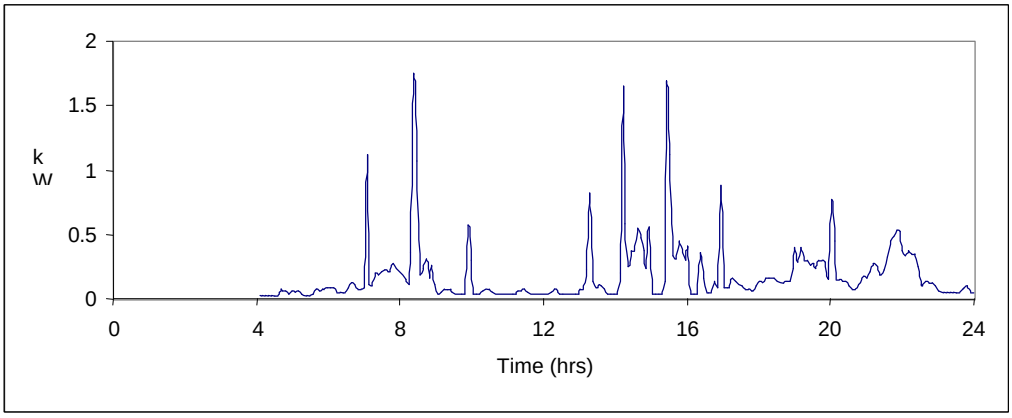

Figure 4.2: Domestic profile taken at 5-minute intervals

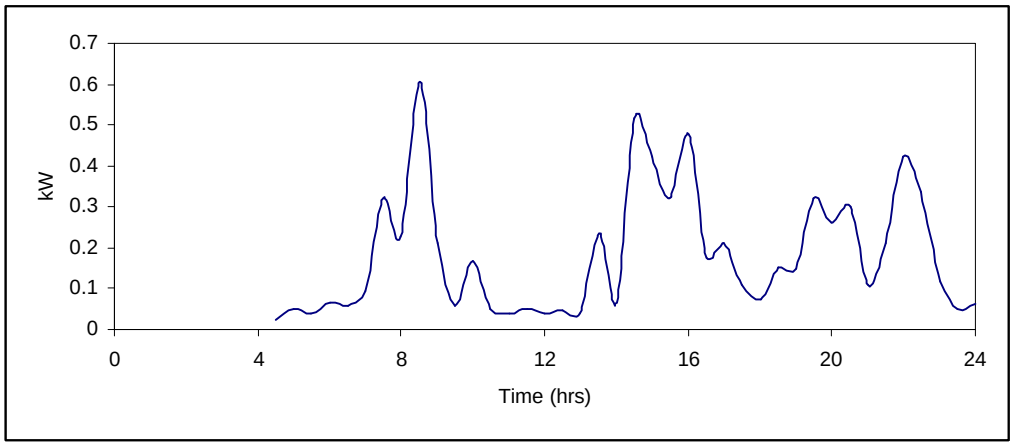

Figure 4.3: Domestic profile taken at 30-minute intervals

4.2.2 Metering Communications Options

In addition to advances in metering technologies, a number of communication options are available for transmitting data from customers to utilities and vice versa. The incorporation of these technologies eliminates the process and associated costs, of manual meter reading. The options available can be broadly classified as either wired or wireless.

Data transmission through wired hardware has the advantage that many of the physical networks are largely established. Power-Line Carrier (PLC) systems transmit data over existing electric networks. PLC applications are successfully being used in remote areas. However, limited bandwidths and slow data transmission render these systems unsuitable for bulk data transmission. A viable solution for applications requiring high-volume data exchange and two-way communication, is the use of direct telephone line connections over the Public Switched Telephone Network (PSTN). The PSTN connects meter reading devices and data processing units, with the duration of the connection limited and controlled by the network switch (George and Prins, 1998a). An alternative telephone network solution consists of 'solid state' meters that incorporate modems to facilitate remote meter reads. Relatively high costs associated with the installation of new telephone lines and fixed monthly charges for telephone services, has lead to the transmission of meter data, over lines already used for other services, such as fax or voice telephony. Another possible future wired-solution with long-term promise comprises broadband options such as coaxial cable and fiber optics, which offer a wide range of functionality, largely exceeding their potential use for meter reading. The hardware, however, is currently expensive and not widely available.

Wireless solutions include applications using digital mobile telephone networks, radio networks and satellites. The digital mobile telephone is becoming a popular medium through which to collect metering information. Provided the networks are available, digital mobile telephone connections can be installed quickly in areas where landline

telephone connections are not feasible. These networks are designed to handle large quantities of data and should be able to provide adequate bandwidth for services beyond simple meter reading. Mobile radio networks are currently widely deployed, but are unable to process the quantities of data, resulting from hourly meter readings. Fixed radio networks are typically the lowest cost alternative for densely populated regions. These networks consist of three types of radio networks; a Local Area Network (LAN); a Wide Area Network (WAN) and a System Controller Network. A Micro-cell Controller (MCC) stores processes and transmits the data to a System Controller Network through a WAN. The costs of fixed radio networks may prove lower than those associated with mobile radio solutions, as the complexities associated with mobility are avoided (George and Prins, 1998a). A further wireless metering communications system currently under development employs low-earth-orbiting satellites to achieve worldwide communications coverage. Some systems are already, partially operational and are reportedly being used to read electric meters at remote high-value customer sites for around $5 to $15 per meter reading (George and Prins, 1998a).

Internet applications can be adopted through either wired or wireless data transmission applications. The Transmission Control Protocol and Internet Protocol (TCP/IP) are sets of protocols developed to allow co-operating computers to share resources across a network (Davis, 2000a). TCP/IP is built on ‘connectionless’ technology, where information is transferred as a sequence of ‘datagrams’. Datagram are collections of data that are sent as single messages, through the network to a specified address individually. While datagrams are in transit, the network doesn't know that there is any connection between them. The TCP/IP protocols package and unpackage data to permit its transmission (Davis, 2000b). The Electric Power and Research Institute (EPRI) envisage the development of an ‘Energy Internet’ that would allow utilities and retailers to gather and transmit data to and from meters (George and Prins, 1998b). An Energy Network would allow utilities and retailers to manage customer loads, collect metering data and provide direct marketing and feedback on energy usage through an Internet

connection. However, there are currently some concerns regarding security and data integrity.

One concern with metering is the potential that consumers and energy service providers could be locked into a single technology that may quickly become obsolete. This can have very serious financial implications as was recently experienced by Motorola Inc. in the $5-billion Iridium project. Iridium operated a network of 66 low-earth orbiting satellites offering wireless telephone and paging services that enable customers to communicate from any location on earth. However, due to the decreasing prices of alternative technologies the terms of the projects loan could not be met and the project had to be abandoned (CNN America, 1999).

Utilities worldwide require mandatory interval metering for customers, whose consumption is around 500 kW or more. In the U.K., metering is obligatory for all customers above 100 kW (Allera and Horsburgh, 1998). Although interval metering is the most accurate means of acquiring demand profiles, the financial implications of metering installation and the resultant data processing costs, currently prevent ubiquitous metering deployment.

4.3 Indirect Profiling: Employing Trends

Where metering is not considered viable, load profiling is becoming generally accepted as the technique employed to support the implementation of retail choice. The UK electricity pool depends on load profiling for settlement purposes and has thereby established a means of estimating the demand profiles of a variety of customer types. Customers are classified by their consumption patterns, which have been assigned through an intensive research and monitoring program.

Generators sell produced power through a bidding system, whereby the generators that bid the lowest price per kW secure the specified capacity to feed power to the system on

that day. Suppliers buy electricity from the pool, which they sell onto customers. The pool price changes every half-hour and price fluctuations can often be dramatic, as the demand/supply balance changes. Customers are protected from the variations in pool price by having fixed price contracts with suppliers kW (Allera and Horsburgh, 1998).

Prior to June 1999, only customers with a maximum demand of 100 kW or more (just over 50,000 customers) had the option of choosing an alternative supplier. These customers all had metering systems, which recorded their half-hourly consumption, allowing the costs of supply to be recovered. Thereafter the competitive electricity supply market extended to all 26 million U.K. customers. A large scale half-hourly metering programme was not considered practical as the associated metering, installation and data processing costs were expected to be substantial. An estimated cost of £350 per installed meter indicated that the cost for full-scale deployment would exceed £8 billion (Dick, 1999). Both the Electricity Pool of England & Wales and Scottish Electricity Settlements Ltd concluded that, in general, load profiling would provide a satisfactory cost-effective approach (Braithwait and Sung, 1998).

A load profile describes the pattern of electricity demand for a customer or group of customers, distinguished by common characteristics over a given period. In the UK, load profiles are usually provided for a specific day or a representative day type. Statistical relationships are employed to identify the influence of temperature and time of sunset. The characteristics used to distinguish customers may include tariff rates, economic activity or the ratio of the load factor. The profiles indicate how customers use electricity differently. For example, typical domestic customers on the standard single rate take a high proportion of their total usage during the day and evening, while domestic customers on the two-rate Economy 7 tariff use proportionately more electricity at night.

For energy trading purposes, the accuracy of load profiles for a particular period is not of great significance. The importance is the load profiles' ability to give an acceptable

estimate of the cost of energy supply over the trading year. The inaccuracies that arise are typically due to sampling and modelling errors. Sampling errors refer to the inability of a sample load to exactly replicate the load characteristics of the relevant population. Modelling errors relate to the limitations imposed by the assumptions used to predict a particular load scenario.

The concept of load profiling is similar to that of setting rates, used by most regulated utilities worldwide. Rates are typically based on cost-of-service models that use customer class data, based on load shapes or, coincident peak demand to allocate costs. Retailers are more concerned with the aggregate load of all customers they serve, than with errors at the individual customer level. Where load profiles are used for scheduling purposes, the discrepancies between the aggregate forecast load profile and actual load represent an energy imbalance. Depending on the load profiling system employed, the aggregate estimated profile may be accurate, even when customer level profiles are not. A study examining the New England Electric System profiling method, found load profiling errors for energy that were less than ± 10 percent, whereas the errors for peak demand were of the order of ± 40 percent (George and Prins, 1998c).

Fundamentally, load profiling approaches may be classified as either static or dynamic. Static load profiles are predetermined, typically from historical load research data and do not vary with current conditions, such as weather. Dynamic load profiles use same-day information to estimate load profiles and are typically estimated using one of three approaches:

1) A technique known as dynamic metering employs metered data from a statistically representative sample of customers read remotely each day. The accuracy of this approach depends on homogeneity within groups of customers.

2) Dynamic modelling refers to a technique whereby statistical relationships between half-hourly demands and driving variables such as weather, daylight hours and day

type, are identified through regression analysis. The statistical model obtained is subsequently used in the calculation of half-hourly loads for each day, based on the current values of driving variables. The accuracy of this method is determined by the homogeneity within groups of customers, and by the accuracy of the regression. An alternative approach is to use historical demand data, which matches the current day characteristics based on the system load, weather conditions or calendar days.

3) Net system load calculations are employed to estimate aggregate loads. This approach subtracts the load from all customers with interval-metered data, from total system loads. The remainder, known as the net system load is used to represent the individual loads of each customer within the group. The accuracy of this method, is again, largely dependent on the degree of homogeneity within the group.

An important consideration in developing load profiles is the number of customer segments. The level of segmentation chosen may vary from the simplest option, where all customers in a system are assigned the same load profile, to highly detailed segmentation based on a variety of criteria that are correlated with usage patterns. The level of segmentation in a profiling system represents a trade-off between the cost of developing and administering the process and the accuracy of cost estimation for particular customers. The fewer the number of segments, the greater the likelihood of cost shifting among customers in a heterogeneous population. In California, where load profiles are currently segmented along traditional rate class lines, alternative methods are being considered, including segmentation by average consumption, climate zone, appliance mix and dwelling type (George and Prins, 1998b).

In the U.K., a contract for the provision of eight profile classes in conjunction with related profiling services, was submitted for competitive tender by the Pool and was awarded to the Load Research Group of the Electricity Association (Allera and Horsburgh, 1998). The EA had maintained a database of half-hourly electricity demands for a sample of electricity customers (domestic, commercial and industrial)

throughout the UK for a number of years. This national sample included approximately 2,500 under 100kW customers and was used as the foundation for profiling where each customer was assigned to a relevant Profile Class.

A linear regression technique is used to determine statistical relationships between the demand data for each half-hour with temperature and sunset time, the two most significant factors influencing demand variations within the day and between seasons. These regression equations are calculated for specific day and season types, and recalculated annually for each Profile Class, based on updated sample demands. The resultant EA profiles represent generic under 100 kW customers, segmented into eight different groups (Allera and Horsburgh, 1998):

- Domestic unrestricted customers (single-rate)
- Domestic economy 7 customers (two-rate), where the low rate period covers seven continuous hours
- Non-domestic unrestricted customers (single-rate/block tariff)
- Non-domestic non-maximum demand Economy 7 customers (two-rate), where the low rate period covers seven continuous hours
- The remaining four non-domestic maximum demand customers are subdivided by their load factor range: 20%, 20-30%, 30-40% and >40%

Figures 4.4 and 4.5 illustrate the nature of some of these profile classes. Figure 4.4 describes how the domestic profile can be scaled according to the number of occupants, both the overall consumption and peak consumptions are seen to increase with the number of occupants. Figure 4.5 depicts a number of industrial customers with different load factors. Industrial customers are classified by variations in load factor, which are largely dictated by the different industrial processes employed.

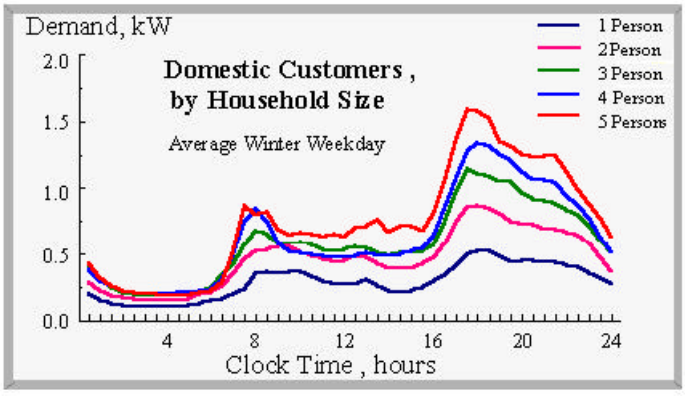

Figure 4.4: Domestic load profile shown as a function of household size (Allera and Horsburgh, 1998)

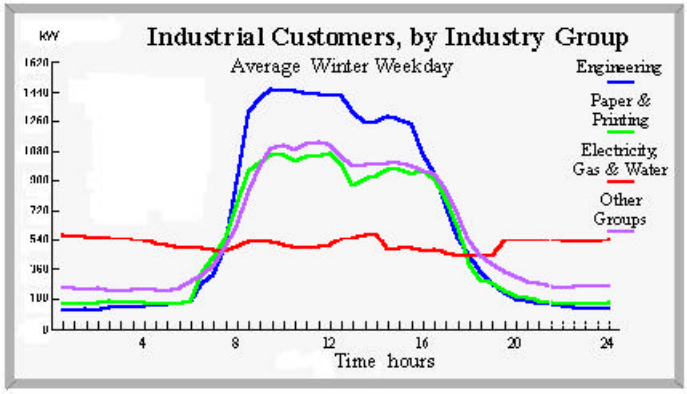

Figure 4.5: Load profiles of industrial customers with varying load factors (Allera and Horsburgh, 1998)

The requisites of the eight load classes were that firstly, they each represented a relatively homogenous group of customers and secondly, that each class was distinctly different from the others.

Single rate tariffs will not change with the time of day. Two-rate tariffs are applied to customers with a time switch, which controls part of the consumption, typically for water heating or storage space heating. Customers with a two-rate tariff will have switched loads controlled by the utilities depending on network system capacities. As

network capacity levels will fluctuate daily, the times at which switched loads are applied will vary. For this reason, two additional generic profiles are created for two-rate profile classes.

Distinctions are made between switched-loads and base-loads; to make allowances for the consumption of appliances such as refrigerators that are continuously in use and therefore alter the consumption of switched loads. To accommodate a variety of switching regimes, generic switched-load profiles are manipulated according to different time regimes and subsequently combined with the generic base-load profile to create a modified profile. For example, where the switching regime's duration exceeds the standard seven hours (00.30 - 07.30), the switched-load profile is simply 'stretched' to the required time-scale, while ensuring that the area under the curve remains constant, by reducing the peak values. Figure 4.6 describes the profile stretching technique, which essentially time-equalises a demand profile, the peak depicted for a seven hour regime is considerably greater than that of an eighteen hour regime and the area under both curves is the same. A similar approach is also used to reallocate a continuous seven hours period into separate sub-periods for split regime tariffs, where the low rate periods are for instance 02.30 - 07.30 hours and 14.00 - 16.00 hours.

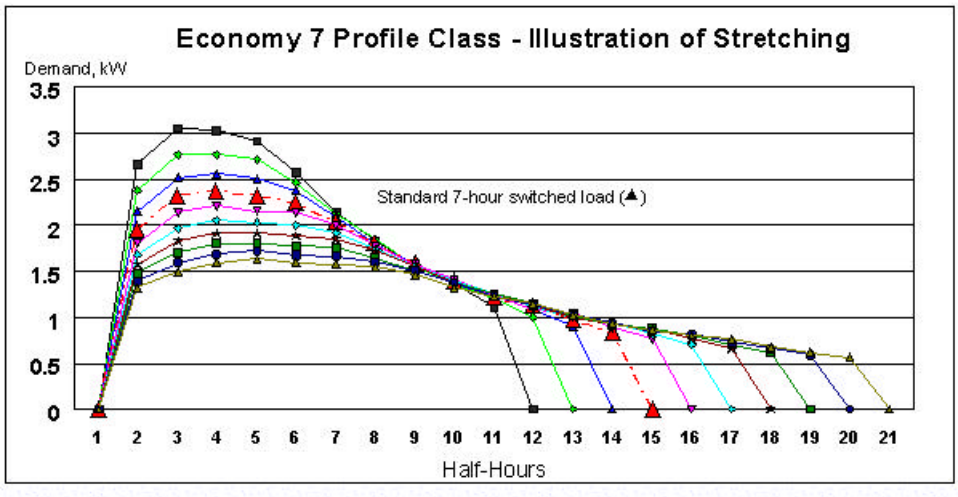

Figure 4.6: Profile Stretching (Allera and Horsburgh, 1998)

The Electricity Association's Load Research Group has built up a database of half-hourly customer demands for about 1200 domestic customers, which is updated annually. The load profile data is supplemented by details of customer appliance ownership and socio-economic characteristics. The data on customer characteristics enables analysis of load profiles with relation to household size, property type, lifestyle category, type of main heating and gas availability. (EA Load Research Group, 1998c). A project currently being undertaken by the Electricity Association (EA Load Research Group, 1998b), involves the collation of load data from 175 customers, for a variety of common household appliances. This project follows recently completed projects monitoring lighting load profiles. The first lighting project reported that lighting consumption is strongly associated with income and with the number of rooms and occupants in a dwelling (EA Load Research Group, 1998a). Other observations reported included seasonal variations in lighting loads and variations between weekday and weekend consumption patterns. A subsequent study (EA Load Research Group, 1999), reported the effect of introducing Low Energy (LE) lighting in the home and found an a 16% decrease in the average annual electricity consumption on lighting circuits due to the installation of LE light bulbs.

As load profile research data is collated, the various driving variables and their effects on load profiles will become increasingly defined. Load profiling research is advancing the understanding of different customer consumption patterns and will undoubtedly become more accurate as further information and experience, is accumulated. However, there are still a number of disadvantages in using load profiles as opposed to actual metered data. Trading on profiled (estimated) data introduces financial risks due to inaccuracies. A meter without communication, but with the ability to record half-hourly values and store them for a set period is now available. The deployment of such meters may minimise the risks associated with profiling (George and Prins, 1998a), allowing suppliers to trade on actual readings in the secondary reconciliation process, while simultaneously refining profiling methodologies and increasing their accuracy.

Load Profile data is usually available by typical seasonal days. By defining a number of seasonal profiles, for example spring, summer, autumn and winter days, the intermittent periods can be interpolated from the defined profiles to produce a complete annual demand profile.

4.4 Virtual Profiling: Building Simulation

An area where neither metering nor load profiling methods can be used to describe demand profiles is in the application to buildings in the design stage. Building simulation tools were developed to enable the analysis of building energy performance. This facilitated low energy building design and the subsequent analysis of energy efficient retrofits by quantifying energy savings. Building simulation can be a very accurate means of deriving load profiles. This method is not limited to the existing building stock and can therefore be used to predict load patterns of new developments. The currently available building simulation tools have the ability to model building processes to varying levels of detail and accuracy. The processes included in an integrated building model encompass; heat transfer, fluid flow, climatic effects, plant, control and electrical systems (Kelly, 1998).

The esp-r system (Clarke, 1985) describes a building in terms of 'control volume flux balances'. This technique involves the discretisation of a building into a number of small control volumes. A control volume is used to describe a region of space represented by a node, to which the principles of conservation of mass, energy and momentum are applied. Each of the finite volumes represents the various regions of the building (e.g. thermal zones, heating and air conditioning plant) within and between which energy can flow. The physical elements of a building are described using control volumes and created through the definition of boundaries around a region of space. The characteristics of each control volume can vary in size, shape and physical properties (e.g. from homogeneous to non-homogeneous, solid to fluid, etc.).

The fundamental physical processes (e.g. heat conduction, convection and storage, air and moisture flow, etc.) occurring within each control volume, are described using the laws that govern the conservation of mass, energy or momentum. The link between adjacent control volumes is represented by an energy or mass exchange. The transient energy and fluid flow processes occurring within a building can be quantified by the further definition of climate data, boundary conditions and control regimes. The quantification of time-series electrical loads can be used to define load profiles. This is of particular importance when applied to new buildings where consumption can not be measured or accurately described by existing load profile classes.

In addition to the esp-r system, a number of other building simulation tools exist which vary in their complexity but are similarly based on thermodynamic models of buildings, some of which were listed in chapter 2. The limitations of theoretical modelling programs are predominantly due to the difficulties incurred by users (Papamichael et al., 1997). The difficulties identified were, the time involved in preparing model inputs and the understanding of underlying modelling principles and implementation details. This was sited as being especially true in the case of sophisticated simulation tools, which rely on very detailed descriptions of the building and its context. Due to these inherent difficulties, simulation capability is still limited to a small number of specialised consultants. Thus, although the potential for obtaining a limitless number of demand profiles exists through simulation, the specialist knowledge requirement limits the generic use of this technique.

Alternative building demand prediction methods are based on empirical or regressive models, which require no knowledge of the physical processes that occur in buildings. However, these methods are based on historical data and can therefore not be used for new buildings. Two competitions known as ‘The Great Energy Predictor Shootouts’, were conducted to evaluate the most effective empirical or inverse regression models for modelling hourly whole building energy baselines (Harbel and Thamilseran, 1994),

(Harbel and Thamilseran, 1998). The competitions provided competitors with data sets and required different predictions based on the temporal data provided. Both competitions found that neural network techniques were the most accurate means for obtaining a model of a building's energy consumption. Neural networks are deployed in the absence of a working theoretical model and are based on mathematical data manipulation. These approaches employ regression techniques to find an approximate relationship between independent and dependent variables. When successful, these empirical models can be employed to predict the effects on dependent variables, of changing independent variables. A neural network is normally determined by nonlinearly mapping a number of input variables to the same number of output variables through a polynomial which passes through each of the data points (Feuston and Thurtell, 1994). This neural network is then 'trained', by replacing the original polynomial mapping function by one of any number of non-linear functions, which span the function space. The final function depends on the training algorithm used, of which there are many (Feuston and Thurtell, 1994).

4.5 Aggregated Profiling: The Database

The primary methods available for obtaining demand profiles have been reviewed. The individual merits of these different techniques are related to the characteristics of a site, for which a demand profile is required.

The availability of metered data, currently limited to larger electrical customers, provides the most accurate description of load behaviour and is preferable where the data is available.

Simulation techniques enable the effects of deploying individual technologies or a combination of complementary technologies, to be quantified. The barriers of simulation are dominantly related to specialist knowledge involved in both constructing building models that accurately reflect reality and in using simulation packages.

The quantification of load profiling observations could allow ‘rules’ to be applied to original metered profiles, to estimate modified profiles. For example, in considering the merits of advanced lighting technologies, a site’s metered profile could be fragmented into lighting and residual loads, with knowledge of typical lighting profiles and the site’s installed lighting capacity. The lighting profile could then be modified, by applying the rules of observation gained through load profiling. These rules may simply involve an increase in efficiency of a certain percentage, which could be applied linearly. Alternatively, in considering the effects of daylight control or occupancy sensors complex rules would need to be applied to the lighting profile, before recombining it with the residual profile. This combination of demand profiling techniques is what will now be termed aggregated profiling. Aggregated profiling enables demand profiles to be predicted, through the employment of any individual profiling technique or a combination of the techniques described.

The difficulty of accurately characterising temporal load behaviour through predefined load profiling classes is clearly illustrated in Figure 4.7. Depicted in Figure 4.7 is a comparison of normalised load profiles, of the domestic load profile from figure 4.3 and the two domestic profile classes (economy and unrestricted) designed by the Electricity Association's Load Research Group. It can be seen that neither of the profile classes accurately describes the load behaviour of the measured residential site. A number of fundamental differences between the profiles can be observed. Firstly, the base load for the measured profile is significantly lower, than in either of the predefined cases. Secondly, the morning peak in the measured data is more concentrated. Finally, the early evening peak described by the standard profiles occurs as afternoon electrical activity in the measured data. A peak occurring around ten o’clock, possibly associated with summer evening lighting is the only obviously shared characteristic. Because of the way load profiles are employed in settlement, the ability of standard profiles to describe individual sites is not considered of primary importance. However, the research being carried out by the Electricity Association's Load Research Group could

produce a number of invaluable rules, which could be applied to individual sites through engineering judgement. As data becomes available which describes consumption patterns associated with individual appliances as a function of some statistical relationships, these relationships and profile 'signatures' could be applied through rules to produce more accurate, site-specific demand profiles.

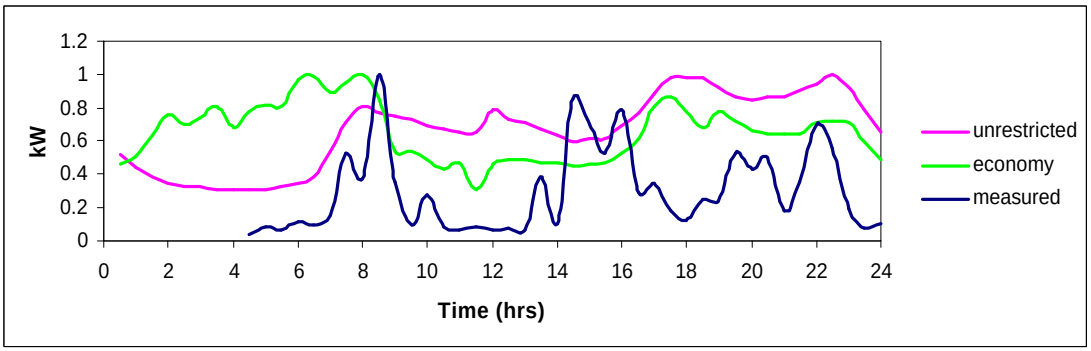

Figure 4.7: Comparison of actual domestic load profile with designed load profiles

Aggregated profiling is supported by the concepts of fragmentation and augmentation. Fragmentation refers to the process of fragmenting a sites demand profile into the individual profiles describing the consumption patterns of specific end use technologies. Fragmentation facilitates the process of defining more accurate site-specific profiles. In the example given above, it could be assumed that the lighting profile, of either of the standard domestic profiles, is a close approximation to that of the actual measured profile, the consumption of other loads, however, is poorly described. Profile fragmentation into a number of different sub-profiles, would allow modified sub-profiles to be recompiled to produce a more accurate load profile. The process of recompiling profiles is termed augmentation.

In a study carried out by the Florida Solar Energy Center (Parker et al., 1998), the energy use in ten conventional control houses built in 1993 was metered. Data was obtained at 15-minute intervals for a year on seven specific electrical end-uses. Weather and internal comfort conditions were also monitored, in conjunction with hot

water consumption and window ventilation status. Conclusions drawn from the field data obtained indicated that several very different energy usage patterns are prevalent in individual homes. Figure 4.8 illustrates the range of different consumption patterns observed in this study. The differences in energy use are clearly illustrated by the differences between the maximum and minimum demands shown. The variations in demands were primarily due to the different cooling strategies employed by occupants. Cooling energy in the houses varied by a ratio of approximately 5:1, with the interior thermostat settings found to account for 85% of the variation. Profiles such as the one depicted in Figure 4.8 were given for each of the electrical end uses studied, showing the range of maximum and minimum consumption patterns. As research continues in the field of demand characterisation, a database of various appliance profiles, together with rules or functions of primary influences such as, the number of occupants can be developed to support fragmentation.

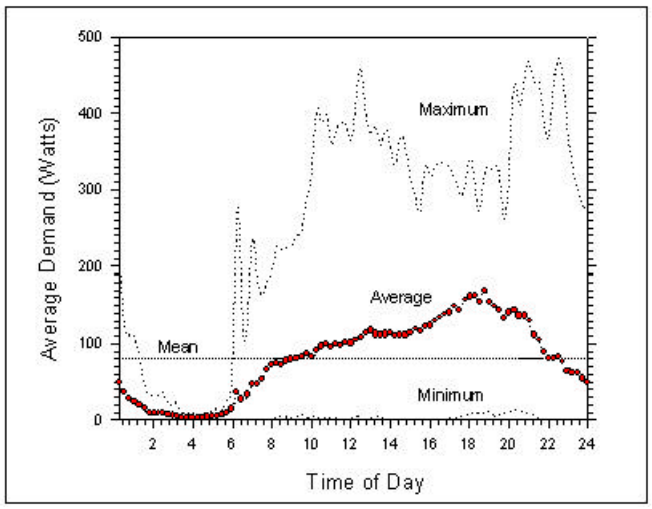

Figure 4.8: Daily Variations in Domestic Load Profiles form (Parker et al., 1998)

The Energy Information Administration (Energy Information Administration, 1993) presented 28 tables of data describing the consumption of energy used by households in the residential sector. The tables cover the following areas: major energy source; space

heating; air-conditioning; water-heating; refrigeration and appliances. Each of the tables presents non-linear regression estimates of annual energy consumption, which is therefore not profiled. However, it is divided into a number of categories, which illustrate some of the variables thought to influence energy consumption. The Table presented in Appendix A describes a variety of categories used to classify consumption. Profiled data could incorporate the regression coefficients related to particular end uses, to generate a number of household type profiles.

Fragmentation and augmentation can be applied independent of scale. Thus, if a profile for a particular grid supply point was known it could be fragmented into a number of customer profiles or vice-versa a number of customer profiles could be augmented to provide a grid supply point profile. Figure 4.9 illustrates an example of how individual profiles could be augmented to supply a community or grid supply point profile. The data shown describes the 1998 static load profiles, used by the Pacific Gas and Electric Company (Pacific Gas and Electricity, 1998).

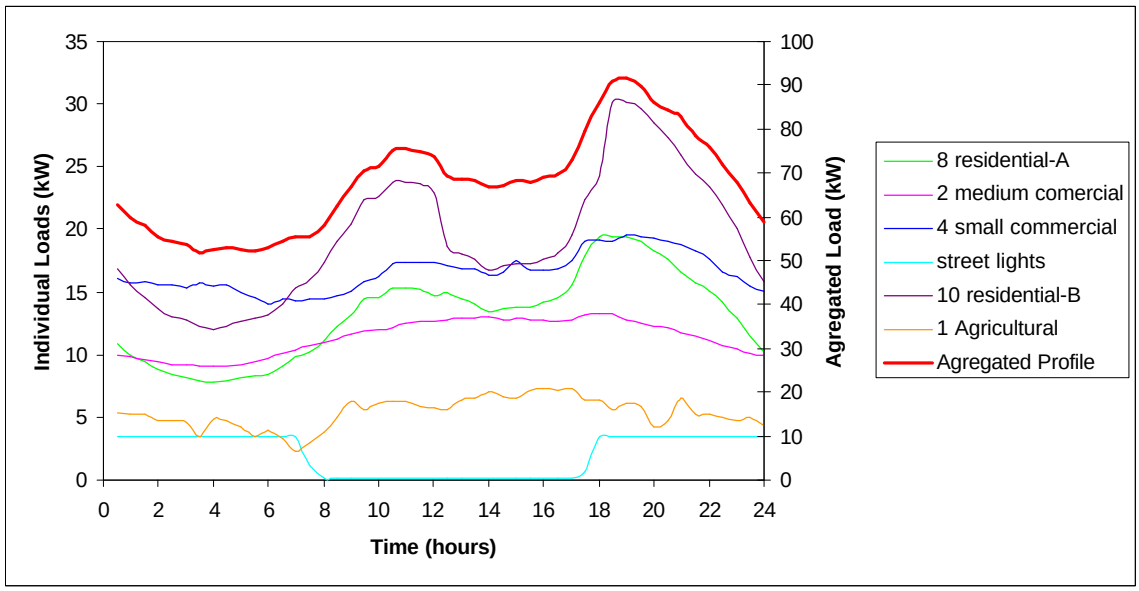

Figure 4.9: Augmentation applied to a number of individual customer type profiles

A Swedish study (Noren, 1999), analysed electrical loads in commercial buildings and developed typical non-dimensional load shapes for electricity consumption for six different categories of commercial buildings: schools, hotels, department stores, grocery stores and health buildings. The approach employed assumed that the building function determines the shape of the consumption pattern, which varies depending on the day type (i.e. weekday, weekend or holiday) and outdoor temperature. Annual electricity consumption figures are used to scale the profiles into actual load shapes. This approach results in the capacities of individual loads becoming less significant, than the way in which they are employed. Figure 4.10 describes some of these profiles for a typical weekday, given an outdoor temperature between 5 and 10°C. Regression analysis was carried out on the various profiles to identify the primary influences on demand. For example, it was identified that schools with kitchens had very different demand profiles to those without. A number of different relationships between buildings and demand patterns are being researched, consequently various different approaches to classifying profiles, e.g. by building function or by load factor, are being developed. These approaches can be used to complement each other, to provide a range of profiles for describing individual sites.

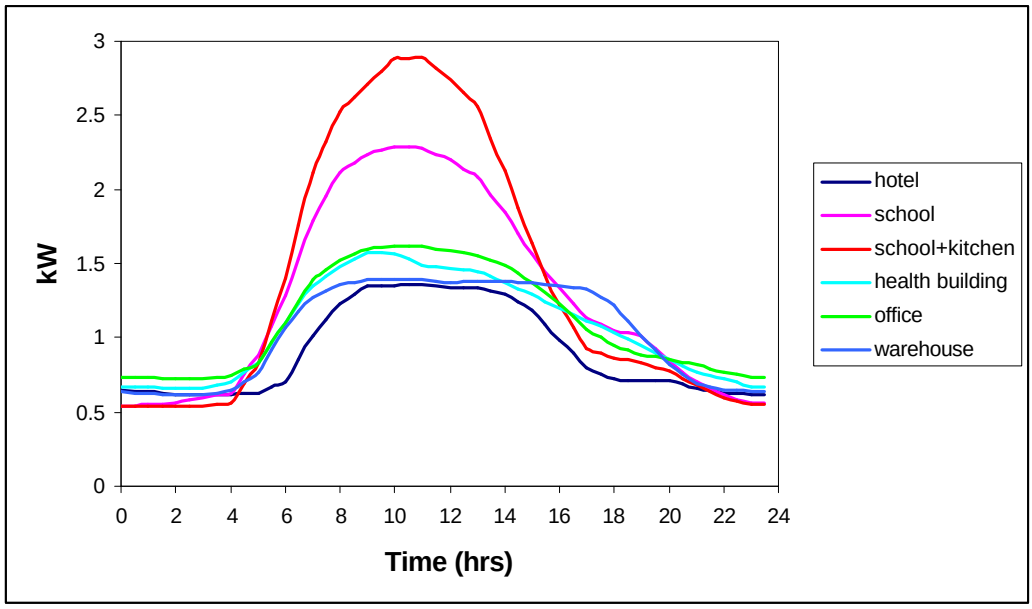

Figure 4.10: Weekday load profiles of various building functions for outdoor temperatures between 5-10 °C (Noren, 1999)

The Energy Efficiency Office in the Department of the Environment have produced a series of literatures entitled Energy Consumption Guides (Energy Efficiency Office) and Fuel Efficiency Booklets (Energy Efficiency Office) which quantify energy savings resulting from a variety of energy efficiency technologies. The Energy Consumption Guides have published savings by building function, e.g. offices, hotels, sports and recreation etc. and the Fuel Efficiency Booklets publish savings by different categories of technologies, such as boiler and refrigeration plant. The collation of these energy savings both by technology and by building function would make a powerful addition to the aggregated profiling environment. The savings resulting from certain energy efficiency measures together with rules which determine how the savings effect the shape of profiles could be used to manipulate reduced case profiles. Such a rule based strategy is ideally suited to aggregated profiling, as for example a sites profile could be fragmented, enabling technology specific savings to be applied to the relevant end use profile and subsequently the fragmented components could be augmented again to determine profile resulting from retrofits.

However, for a more accurate description of profiles resulting from retrofits, simulation could be deployed using a base case model together with models for a variety of retrofit options. Additionally, simulation could be employed to generate a number of end-use profiles, which are heavily dependent on building construction. These simulated profiles could be aggregated to predict the demand profiles for a variety of different constructions.

There is a variety of possible means for obtaining demand profiles; aggregated profiling is the framework in which each method can be deployed, depending on data availability. This enables community or grid supply point profiles to be produced, simply by selecting the particular amalgamation of profile types. Similarly, individual site profiles can be compiled from an aggregation of simulated profiles, standard profiles and actual measured profiles. This combination may describe seasonally consistent loads and loads which vary with temperatures or other known variables.

4.6 Summary

The various techniques used to obtain demand profiles have been reviewed. A framework has been presented in which every technique available can be used in parallel, to produce a rich data resource for describing load characteristics. This framework has been termed aggregated profiling and it is supported by the concepts of fragmentation and augmentation. Fragmentation allows profiles to be decomposed into sub-profiles which, describe some individual characteristic of a profile. Augmentation refers to the process by which these individual profiles can then be modified by some rule and consolidated. The collation of data that can describe the relationships between certain loads and their driving variables is beyond the scope of this work. However, this framework is used to derive profiles with data that is currently available to support the work that follows in the proceeding chapters of this thesis.

4.7 References

1. Allera S. V. and Horsburgh A. G., "Load Profiling for Energy Trading and Settlements in the UK Electricity Markets" , October 1998, London, URL:http://www.electricity.org.uk/services/lrg/dadsm2a2.html
2. Bailly Hagler Consulting, "Evaluation of NEES's Load Estimation, Settlement and Reconciliation System", Colorado, December 5, 1996
3. Braithwait Steven and Chung Sung. "Not Your Father' s TOU Rate: Price Response in the Presence of Interactive Communications Equipment," in Proceedings from the EPRI Conference on Pricing Energy in a Competitive Market, June 17–19, 1998.
4. Central Maine Power Company Chapter 321 Methodology Report #2, December 1, 1999, URL:http://www.cmpco.com/cep/profiles/methodology2.pdf
5. Clarke J.A., Energy Simulation in Building Design, Adam Hilger, Bristol, 1985.
6. CNN America, Inc., Iridium faces more woes, March 1, 1999 http://www.cnnfn.co.uk/digitaljam/9903/01/iridium/index.htm
7. Dick Alan, Electricity Association, UK, Competitive meter operation in the UK - four years on, Metering International 1, 1999
8. Electricity Association, An Analysis of Electricity Usage -The final report from the original (100 customer) lighting project, February 1998, URL:http://www.electricity.org.uk/services/lrg/light1.html
9. Electricity Association, Domestic End-Uses, End-use data relate almost wholly to the domestic sector, 2000, URL:http://www.electricity.org.uk/services/lrg/load_re3.html
10. Electricity Association, Domestic Sector, 2000, URL:http://www.electricity.org.uk/services/lrg/electr~1.html
11. Introducing Low Energy Lighting in the Home – an Impact Assessment, September 1999 URL:http://www.electricity.org.uk/services/lrg/light2.html

12. Energy Efficiency Office, Best Practice Programme, Energy Efficiency Office, Department of the Environment, Energy Consumption Guide, Energy Efficiency in Offices, Oct 1991
13. Energy Efficiency Office, Best Practice Programme, Energy Efficiency Office, Department of the Environment, Energy Consumption Guide 144, Energy Efficiency in Sports and Recreation Buildings: Technology Overview
14. Energy Efficiency Office, Best Practice Programme, Energy Efficiency Office, Department of the Environment, Energy Consumption Guide 18, Saving Energy in Schools
15. Energy Efficiency Office, Best Practice Programme, Energy Efficiency Office, Department of the Environment, Energy Consumption Guide 36, Energy Efficiency in Hotels
16. Energy Efficiency Office, Best Practice Programme, Energy Efficiency Office, Department of the Environment, Fuel Efficiency Booklet No 11, Economic Use of Refrigeration Plant
17. Energy Efficiency Office, Best Practice Programme, Energy Efficiency Office, Department of the Environment, Fuel Efficiency Booklet No 15, Economic Use of Gas Fired Boiler Plant
18. Energy Efficiency Office, Best Practice Programme, Energy Efficiency Office, Department of the Environment, Fuel Efficiency Booklet No 4, Compressed Air and Energy Use
19. Energy Efficiency Office, Best Practice Programme, Energy Efficiency Office, Department of the Environment, Fuel Efficiency Booklet No 8, Economic Thickness of Insulation on Hot-Pipes
20. Energy Information Administration, Household Energy Consumption and Expenditures 1993, URL:http://www.eia.doe.gov/emeu/recs/recs2c.html
21. Feuston B. P. and Thurtell J. H., Generalized Nonlinear Regression with the Ensemple of Neural Nets: The Great Energy Predictor Shootout, ASHRAE Transaction: Symposia or-94-17-3

22. George S. and Prins D, Final Report -Development of a Conceptual Metering and Settlement Design for Full Retail Competition in the National Electricity Market, Section 6 – Metering Technology Options, Benefits and Costs, 11 December 1998, URL:http://www.nemmco.com.au/future/retail/mt_sc838(d)v001.pdf
23. George S. and Prins D., Final Report -Development of a Conceptual Metering and Settlement Design for Full Retail Competition in the National Electricity Market, - Section 7 - Key issues in Metering, 11 December 1998, URL:http://www.nemmco.com.au/future/retail/mt_sc838(e)v001.pdf
24. George S. and Prins D., Final Report -Development of a Conceptual Metering and Settlement Design for Full Retail Competition in the National Electricity Market, Section 8 Other Issues, 11 December 1998, URL:http://www.nemmco.com.au/future/retail/mt_sc838(f)v001.pdf
25. Davis, What is TPC/IP?, URL: gopher://gopher-chem.ucdavis.edu/00/Index/Internet_aw/Intro_the_Internet/intro.to.ip/01_What_is_TCP_IP%09%09%2B,2000
26. Davis, TCP/IP Protocols, URL:gopher://gopher-chem.ucdavis.edu/00/Index/Internet_aw/Intro_the_Internet/intro.to.ip/02_TCP_IP_Protocols%09%09%2B, 2000
27. Harbel J and Thamilseran S., Predicting Hourly Building Energy Use – The Great Energy Predictor Shootout', ASHRAE Journal 1994
28. Harbel J. and Thamilseran S., The Great Energy Predictor Shootout II- Measuring Retrofit Savings, ASHRAE Journal, January, 1998
29. Kamat Vithal N, kVAh metering for environmentally conscious utilities, Metering International 1, 1999
30. Kelly N. J., Towards a Design Environment for Building Integrated Energy Systems: The Integration of Electrical Power Flow Modelling with Building Simulation, Phd. Thesis, Strathclyde University, October 1998.
31. McDiarmid M. D., Practical Considerations in Monitoring Building Energy Use, ASHRAE Transactions: Symposia, SA-96-8-3, 1996

32. Miller SH, Electronic meters allow innovative electricity tariffs, Metering International 4, 1998
33. Norén Corfitz , Load Shape Development for Swedish Commercial and Public Buildings –Methodologies and Results, Thesis for degree of Licentiate of Engineering, Lund Institute of Technology, Sweeden, 1999, URL: http://www.vok.lth.se/EEP/research/eeplm/forsk_uk.htm
34. Pacific Gas & Electric, 1998 Static Load Profiles, URL:http://www.pge.com/whats_new/issues/electric_restructuring/profiles/1998.html
35. Papamichael Konstantinos, La Porta John and Chauvet Hannah, Decision Making through Use of Interoperable Simulation Software, Proceedings of the Building Simulation ’97 Fifth International IBPSA Conference, Vol. II, September 8-10,1997, Prague, Czech Republic
36. Parker Danny S., Mazzara Maria D. and Sherwin John R., Monitored Energy Use Patterns in Low-Income Housing, Florida Solar Energy, URL: http://www.fsec.ucf.edu/~bdac/pubs.htm, 2000

Chapter 5: Supply Profiles

5.1 Introduction

Strategies for small-scale RE integration can be evaluated through the analysis of supply profiles from renewable technologies examined with respect to demand profiles. The opportunities for renewables to make significant contributions to the supply infrastructure are particularly evident where a supply profile can be employed to cancel the peaks in a demand profile. Various means for obtaining demand profiles were discussed in the previous chapter. The focus of this chapter is the acquisition of renewable supply profiles. As with demand profiles, the relevant information can be obtained through measurement. However, unlike demand profiles, which, with the exception of buildings in the design phase, are existential, supply profiles are largely virtual profiles, i.e. potential profiles that cannot be measured. Moreover, renewables are known to be extremely site specific as their output is dependent on climate and situation. Thus, a supply profile carefully monitored in one location will not correspond to the profile of the exact same technology in another location. For this reason, the emphasis of this chapter is on the prediction of profiles through mathematical models. The modelling approach avoids the significant costs associated with building test sites and the time required, to obtain supply profiles. Additionally, mathematical modelling can be applied to any location without loss in accuracy.

The prediction of temporal supply profiles from three renewable technologies: photovoltaic, wind and solar collector systems will be examined. These technologies have been selected, as they are currently considered to be the most viable of the renewable technologies. The modelling objectives were twofold: firstly, models were to be generic in nature to enable their use in the prediction of performance for varying designs of the same technology and secondly the models were to be based on input parameters which are readily available from manufacturers' specifications.

The derivations for each of the models are described in the following sections. The methodologies used could be applied to derive models for other technologies, enabling their performance prediction, and subsequent use in determining their effects on demand profiles. The models derived do not account for the limitations imposed by the building in which RE technologies are to be integrated. Building constraints such as the available integration surface area require prior evaluation through the examination of site plans and can subsequently be used to specify maximum RE capture areas.

5.2 Modelling Photovoltaic Generators

Intrinsic semi-conductor materials are characterised by covalent-bonding, which holds the crystal structure through the equally sharing of electrons. The electrical conduction properties of these materials can be manipulated through the deliberate addition of impurities, termed doping. Doping a semiconductor with atoms containing a surplus of electrons transforms the material into an n-type semiconductor in which electrons are comparatively mobile. Conversely, p-type semiconductors are doped with electron deficient atoms. The photovoltaic principal is based on a junction between p-type and n-type semiconductors, termed the p-n junction. In a state of thermal equilibrium, electrons are prevented from diffusing across the junction by the electro-static potential established between the opposing charges. The absorption of energy contained in photons of light causes the charges to move against the static electric field, where thermally excited electrons in the p-type material flow freely into the n-type material, which gives rise to the photon-induced current.

Many different PV modelling techniques are currently available which could be used to determine a specified PV systems supply profile. The very detailed level of simulation, suitable for cell design purposes, which can evaluate the current flows and voltage distributions throughout the cell (Maotro and Araujo, 1997), are not suitable for determining PV supply profiles for modules available on the market, as they require

detailed input parameters not available from manufacturers' specifications. On the other hand, over-simplified approaches, which determine annual energy outputs (Caamano and Lorenzo, 1996) as opposed to temporal profiles, are equally unsuitable. The electrical behaviour of a PV system is highly dependent on solar geometry and thermal performance, which cannot be neglected in the prediction of supply profiles. For this reason, circuit simulation software employed to model PV cells by equivalent electrical circuits (Katan et al., 1995), are not capable of examining variations to supply profiles resulting from changes in system configurations. Other models, which could be applied to produce supply profiles, require curve-fitting parameters (Russell, 1994), (Kelly 1998) determined through experimentation, and are therefore not generic in nature. Bryan Fry (Fry, 1998) reviewed three different mathematical techniques for predicting the performance of PV models. These models utilise a dimensionless diode curve fitting factor which neglect any imperfections in the cell, and assume the cell efficiency is independent of the intensity of incident radiation. These assumptions result in fairly accurate results at high levels of isolation, but become increasingly inaccurate at lower levels, particularly below 400W/m^2.

A generic model has been developed without the use of curve fitting factors which, either effect the accuracy of results or have to be determined through experimentation. This model can be applied to any PV configuration of silicon cells. The input parameters are manufacturers' data, situation and climatic parameters. The model encompasses solar geometry to calculate the angle of incidence of solar radiation on the PV surface. Reflection losses are subsequently evaluated depending on the solar angle of incidence. The portion of radiation incident on a panel's surface, which is not reflected is that which can result in a photon current. A thermal model, based on an energy balance is used to evaluate the panel temperature, which directly affects the power capacity of a cell. Finally, an electrical model is used to determine the supply profile. The physics of cell performance has been described extensively elsewhere (Kelly, 1998), (Fry, 1998), (Decher, 1997).

Duffie and Beckman (Duffie and Beckman, 1974) describe the various aspects of solar geometry, which have been summarised in Appendix B.1. Three components of incident radiation: direct, diffuse and reflected are calculated according to the methodology described in the Appendix B.1. These components are incident on an arbitrary surface at different angles. The losses incurred through reflection will depend on the angle of incidence of each of the components. By accounting for reflection losses, the actual radiation absorbed by the silicon, and therefore able to generate a photon current, can be obtained.

5.2.1 Losses by Reflection

Reflection losses is the term used to describe the portion of incident light which fails to be absorbed by the silicon layer, and includes both the light that is reflected and that which is absorbed. Reflectance losses are dependent on the angle of incidence of the incoming light, and on the material properties of a PV module. The angle of incidence for the direct component is obtained using Equation B.1.1., where the angle depends on the position of the sun relative to the panel surface. For the diffuse and reflected components, multiple angles of incidence exist. To simplify the process of determining the losses by reflection for these components, Brandemuehl and Beckman (Brandemuehl and Beckman, 1980) suggested the use of equivalent angles of incidences. These angles for both diffuse and ground reflected radiation are described in Equations 5.1 and 5.2, respectively, which assume the angles are dependent on the angle of tilt, τ, only.

$$\phi_{diff} = 59.7 - 0.1388 \cdot \tau + 0.001497 \cdot \tau^2 \qquad \text{Equation 5.1}$$

$$\phi_{r} = 90.0 - 0.5788 \cdot \tau + 0.002693 \cdot \tau^2 \qquad \text{Equation 5.2}$$

Where ϕ_{diff} = Effective angle of incidence for diffuse radiation

ϕ_{r} = Effective angle of incidence for reflected radiation

To estimate the reflectance losses, the relative portions of light, which are absorbed, reflected or transmitted require to be evaluated. Coefficients for absorption, reflection and transmission can be defined as functions of the wavelength and angle of incidence of incoming radiation. Experimentation has shown that the angular dependence on wavelength is relatively weak for a typical PV module encapsulation (Preu et al., 1995). By neglecting the dependence on wavelength, it is possible to estimate the fraction of solar radiation, which is successfully absorbed in the silicon layer of PV constructions. Employing three fundamental laws, which govern optical behaviour, together with the fact that for any transparent surface the sum of absorbtance, reflectance and transmittance must be unity (Duffie and Beckman, 1974), the portion of radiation absorbed by the silicon can be quantified. The optical laws used are described in Appendix B.2.

Figure 5.1 illustrates how these optical laws are used to evaluate the various components of reflected, absorbed and transmitted light from an incident beam, on an arbitrary interface between two mediums of refractive indices n1 and n2. The incident ray I, is shown incident at angle θ_1. The refracted angle, θ_2 is determined using Snells' law, and Fresnel's relationship is used to determine the reflected component. The incident light, which is not reflected, is transmitted into medium 2, and absorbed over its thickness t, according to Bougers' Law. A second beam is seen travelling from medium 2 back to medium 1. This beam represents an internally reflected beam R', incident at its refracted angle θ_3. This internally reflected component is reflected internally again R'', and the residual component is transmitted back to medium 1, τ'.

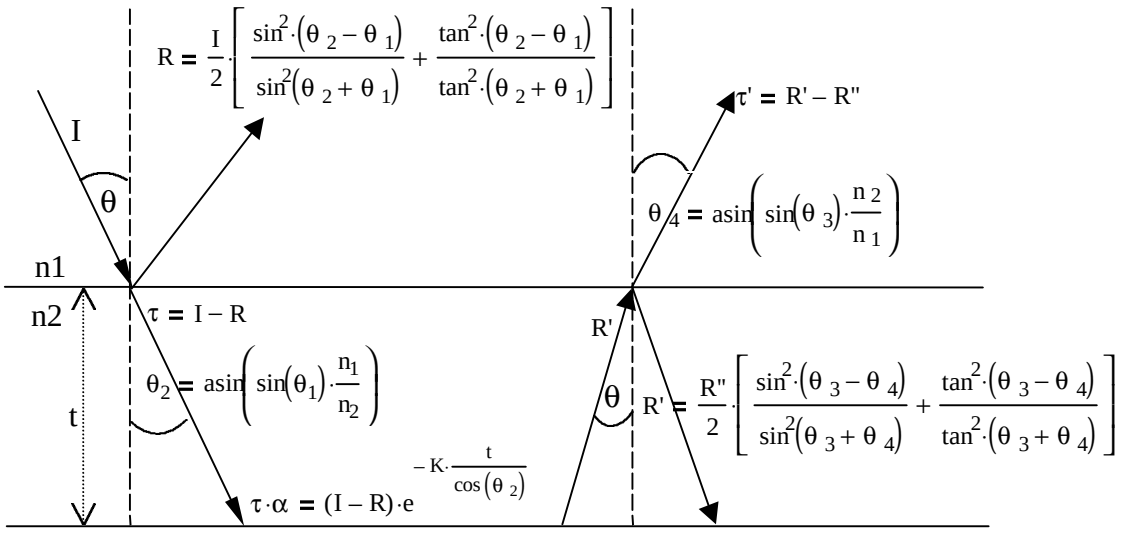

Figure 5.1: Optical characteristics for a single interface of two mediums with refractive indices n1 and n2

A typical PV construction will consist of multiple layers, and at each interface, the incident beam will be divided into a reflected and transmitted part, resulting in multiple reflections and interferences between the layers. Various approaches have been adopted in modelling the optical performance of PV modules. One approach used employs an empirical correlation for the reflectance of glass front PV modules as a function of incidence angle (Fry, 1998). The validity of such an empirical correlation will vary depending on the structural composition of the PV module. Other approaches employ ray tracing techniques (Lanzerstofer, 1995) (Preu et al., 1995), adopted for this work. Ray tracing 'follows' an incident beam through the various interfaces, the transmitted portion is subsequently traced to the next interface, whilst the reflected component is traced back to the previous interface. Rays are traced until the reflected component entering the silicon layer becomes negligible. Figure 5.2 illustrates the ray tracing methodology on the multiple layered structure defined in Table 5.1. The incident beam is reflected and transmitted at each layer. For clarity the multiple reflections, and subsequent transmissions are not shown.

Table 5.1: Material properties assumed for typical PV configuration (from Lanzerstofer, 1995)

Material	**Index**	**Thickness (mm)**	**Refractive Index**	**Coefficient of Extinction**
Air	0	-	1	-
Glass	1	2.0	1.52	0.05
EVA	2	0.5	1.48	-
Titandioxyd	3	0.000064	2.34	-
Silicon	4	0.5	3.6 ….. 6.9	-

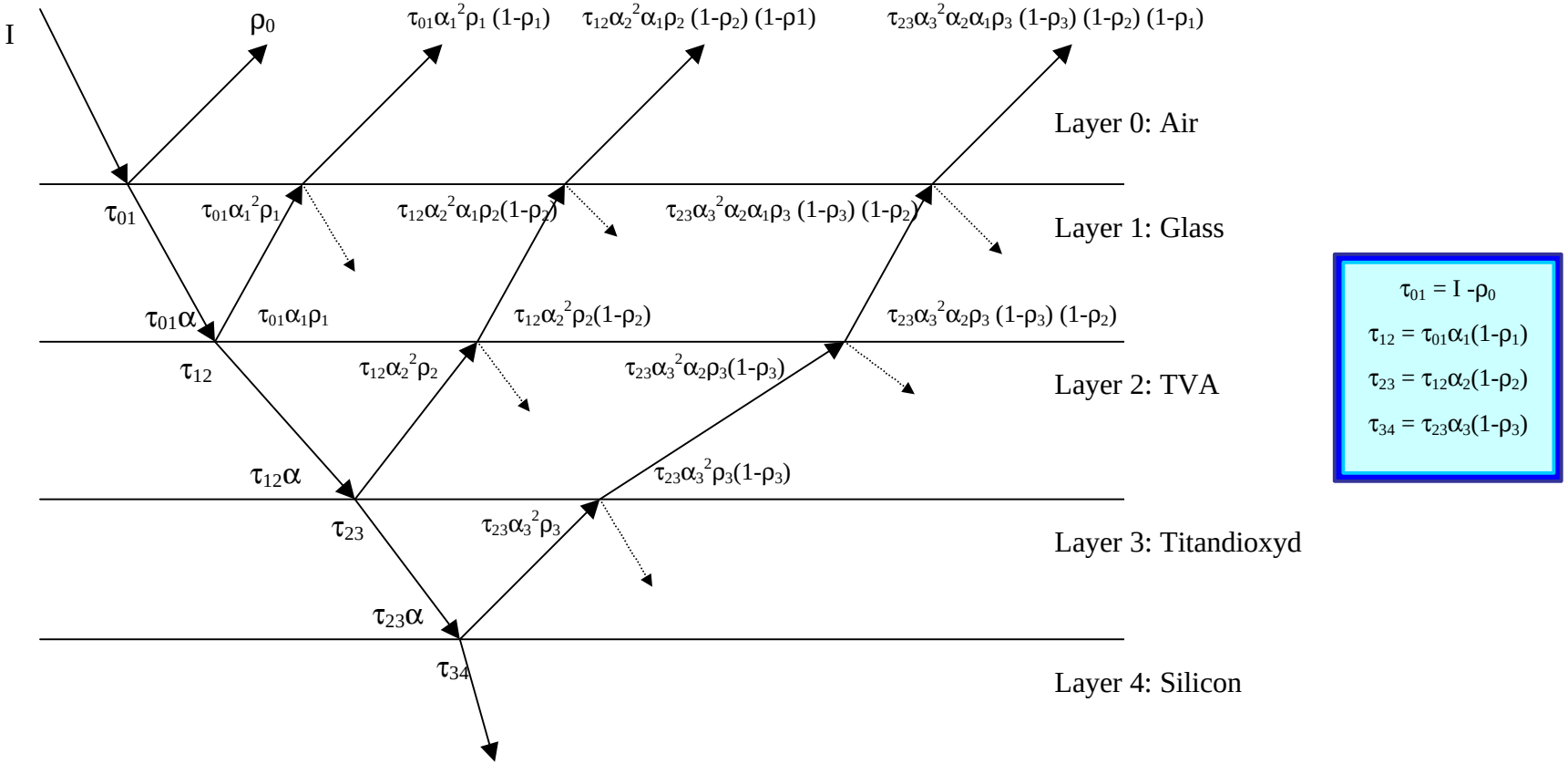

Figure 5.2: Ray tracing technique performed for a single

The optical characteristics in Table 5.1, are based on the construction of a typical silicon based module. The extinction coefficients, for all but the glass layer are neglected, as the other layers are so thin. This structure is assumed in calculations involving reflection losses. Figure 5.3 illustrates calculated reflection losses at a range of incident angles from 0 - 90 degrees. Two different structures are shown, the blue trace illustrates the radiation transmitted to the silicon layer for the four layered structure described, the second trace represents a three layered structure, identical to the four layered without the titandioxyd layer. A noticeable improvement in the radiation absorbed by the silicon layer can be seen, for the four layered structure. Both structures are very susceptible to oblique angles of incidence.

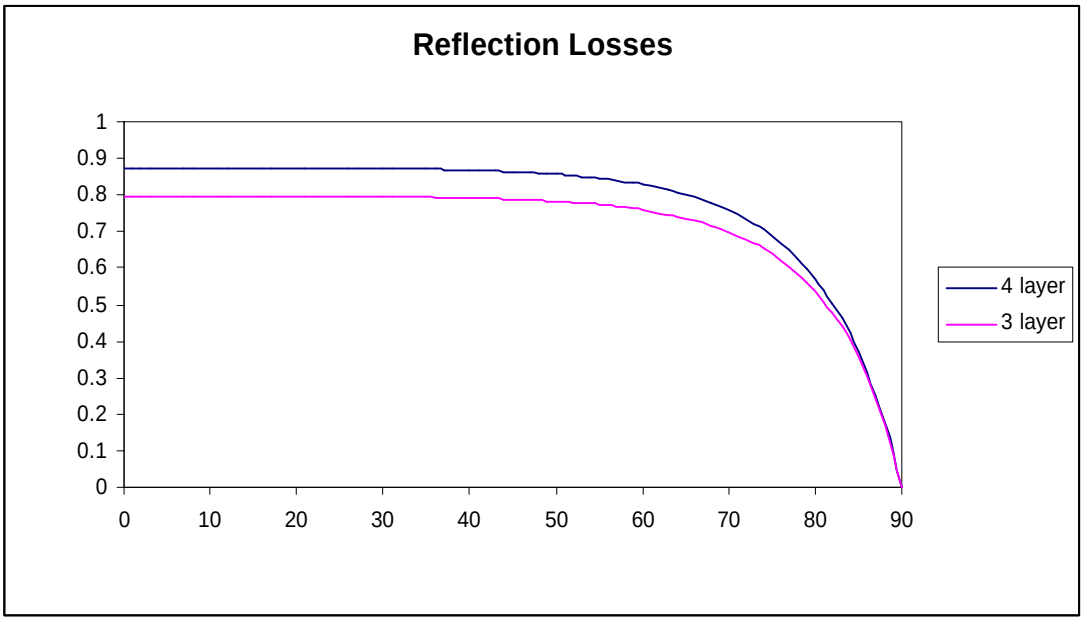

Figure 5.3: Net reflection losses for varying angles of incidence

5.2.2 Thermal Model

Temperature increases in PV cells result in reductions in open circuit voltage, which in turn reduce the power output. A temperature increase from 40 to 150°C can reduce the

power output by 60% (Decher, 1997). It is therefore vital to predict the panel temperature when modelling a PV system. PV-hybrid systems recover heat from the module, reducing the panel temperature and simultaneously producing a source of low-grade thermal energy. The heat available from a hybrid system is calculated to predict a thermal supply profile. Thermal demand and supply profiles can be examined in a similar fashion to electrical profiles to evaluate complimentary systems.

Figure 5.4 illustrates the various thermal exchanges modelled for a PV hybrid system. If a hybrid system is specified, the radiant exchange with the back wall, and convective heat losses from the panel to the air gap are considered. When modules are configured without heat recovery these terms drop out, leaving only the radiation exchanges with the sun and sky, convective heat losses due to wind conditions, and heat loss through power extraction, to be considered.

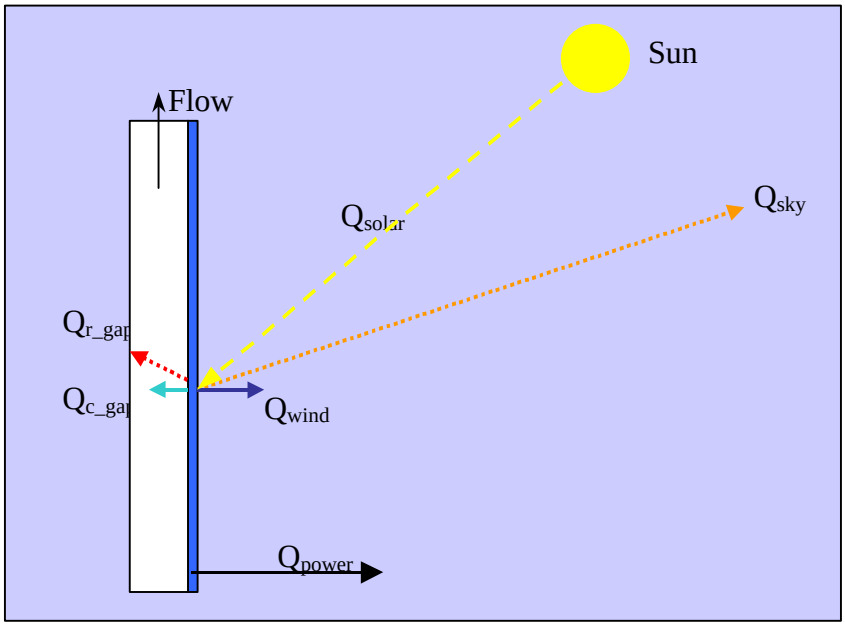

Figure 5.4: Thermal parameters considered in PV model

The derivation of solar radiation absorbed by the silicon Q_{solar}, was described in the previous section. Research activities in the field of solar collectors, has established the

relationships describing the thermal exchange between a surface and its environment. The equations employed to calculate the radiant exchange between the module and the sky, Q_{sky}, and the convective heat loss for an external PV surface exposed to wind, Q_{wind}, are given in Appendix B.3.

The radiant exchange between the back of a panel and wall in hybrid configurations is assumed to be that of two parallel grey surfaces, as described by Equation 5.3 (Rogers and Mayhew 1992).

$$Q_{r\_gap} = \frac{A \cdot \sigma \cdot \left(T^4 - T_{wall}^4\right)}{\frac{1}{\varepsilon} + \frac{1}{\varepsilon_{wall}} - 1} \qquad \text{Equation 5.3}$$

Where
- Q_{r_gap} = Radiant Exchange with wall
- ε = Emissivity of PV backing
- ε_{wall} = Emissivity of wall
- A = Surface Area of PV
- T_{wall} = Temperature of wall

The wall temperature is assumed to be at ambient temperature, provided the average ambient is above 10°C, otherwise the wall temperature is assumed to be 10°C, due to internal heating. This simplification is invoked as the detailed modelling of buildings is beyond the scope of this work. In sophisticated building simulation packages the wall temperature would be calculated, and the temperature gradients determined (Kelly, 1998).

Convection in the air gap will depend on whether the ventilation is forced or natural, on the air temperature and on the geometry of the air-gap. The approach adopted in predicting the convection heat transfer employs a number of empirical correlations with corresponding conditions for use, to calculate the Nusselt number. The Nusselt number

is defined as the dimentionless temperature gradient at a surface, and provides a measure of the convection heat transfer occuring at that surface (Incropera and DeWitt, 1996). The Nusselt number is used to calculated the convective heat transferr coefficient based on the previous air gap temperature calculated, whose calculation is described by Equation 5.4 (assuming constant atmospheric pressure).

$$T_{air} = \frac{Q_{c\_gap} + Q_{r\_gap}}{m \cdot c_p} + T_{prev} \qquad \text{Equation 5.4}$$

Where m = mass of air (m = volume×density)

c_p= specific molar heat capacity at constant pressure

T_{air} = Temperature of air at time, t

T_{prev} = Temperature of air at time, t-1

Q_{r_gap} = Radiative heat transfer in gap

Q_{c_gap} = Convective heat transfer in gap

The temperature of the air effects the various dimentionless parameters used to evaluate the Nusselt number, and the convective heat transferr coefficient. Air properties at different temperatures in the air-gap are determined from regression equations derived from tabulated values at 175-325 K (Rogers and Mayhew, 1992) for dry air at low pressure. The equations used are listed in Table B.1, in Appendix B.4, and all other dimensionless parameters used in calculating the convection heat transfer are given in Table B.2.

The subsequent correlations used to calculate the Nusselt number depend on whether a natural or forced ventiation system is used.

Where natural ventilation is specified, the driving forces are assumed to be buoyancy forces. More detailed fluid dynamic approaches have identified wind induced pressure differences between the top and bottom of the façade as another influential driving force

(Mattson et al., 1995), however such detailed analysis is beyond the scope of this work. Instead, empirical correlations for external free convection flows are employed (Incropera and DeWitt, 1996), which use the characteristic length L, defined by Equation 5.5, and assume a constant panel temperature to obtain the relevant dimentionless parameters.

$$L = \frac{A_s}{P} \qquad \text{Equation 5.5}$$

Where A_s = PV surface area

P = Perimeter length

Table B.3 summarises the various correlations, and the conditions for their use. Where panels are arranged vertically, one of two correlations is used. One of which applies to the entire range of Rayleighs numbers. The other can be applied where Rayleighs numbers are less than 10^9, and result in slightly better accuracy. For a vertical plate, the buoyancy force acts exclusively to induce fluid flow upwards, if the plate temperature is greater than the air temperature, or downwards when the plate is cooler. If the plate is inclined with respect to gravity, the buoyancy force has a component normal as well as parallel to the surface. A reduction in the parallel buoyancy force reduces the velocity along the plate. It is recommended that for inclinations, τ, between 0 and 60 degrees, g be replaced by $g \times \cos(\tau)$, when calculating the Grasshof number, after which the same correlations as for the vertical plate are used. For horizontal plates the buoyancy force is exclusively normal to the surface, and the flow patterns and heat transfer will depend strongly on weather the plate is hotter or colder than the air temperature.

Alternatively, forced convection may be specified in which case the driving force is due to mechanical ventilation, and a constant flow rate is assumed. In this case, the flow in the gap is treated as an internal flow in a circular tube. By employing an effective diameter as the characteristic length, the circular tube results can be applied to the non-

circular geometry found in PV-hybrid applications. The effective diameter used is the hydraulic diameter. The corresponding dimensionless parameters are shown in Table B.2 (Incropera and DeWitt, 1996).

$$D_h = \frac{4 \cdot A_c}{P} \qquad \text{Equation 5.6}$$

Where Ac = Flow cross sectional area

P = Wetted perimeter

Fully developed flow is assumed and the Reynolds number is calculated to determine whether the flow is laminar or turbulent. The correlations in Table B.4, are used for laminar flow (Reynolds numbers less than 2300) and where turbulent flow has been determined, a number of conditions are used to decide on the correlation used. These conditions are based on; the Reynolds number; the Prandtl number; the temperature difference between the PV surface and the air, and the geometry of the air gap. Both the conditions are corresponding correlations are given in Table B.6. The correlations for friction factors are given in Table B5. [All of the correlations used have all been obtained from Incropera and DeWitt, 1996]

The final heat loss is that which is removed through power production, Q_{pow}, the quantification of which is discussed in the proceeding section of this chapter. Once the various heat loss mechanisms and the solar radiation absorbed have been determined, an energy balance is used to establish the panel temperature. The Energy balance is described by Equation 5.7, which is solved for the panel temperature using the Newton-Raphson method.

$$m \cdot c \cdot \Delta T = Q_s - \frac{A \cdot \sigma \cdot \left(T^4 - T_{wall}{}^4\right)}{\frac{1}{\varepsilon} + \frac{1}{\varepsilon_{wall}} - 1} - \varepsilon \cdot A \cdot VF \cdot \sigma \cdot \left(T_{sky}{}^4 - T^4\right)$$

$$- A \cdot h_{wind} \cdot \left(T_a - T\right) - A \cdot h_g \cdot \left(T_a - T\right) - Q_{pow}$$

Equation 5.7

Where m = mass of silicon layer

c = specific heat of silicon

ΔT = change in panel temperature

The mass of the silicon layer is calculated using the panel dimensions and the typical silicon width of 0.5 mm. When a hybrid system has been specified the potential for heat recovery is evaluated by summating the energy loss through the radiant and convective components to the air gap. Figure 5.5 illustrates an example in the differences in a PV panel temperature obtained, for a system specified without heat recovery, with natural convection and with forced convection, at a flow rate of 2m/s.

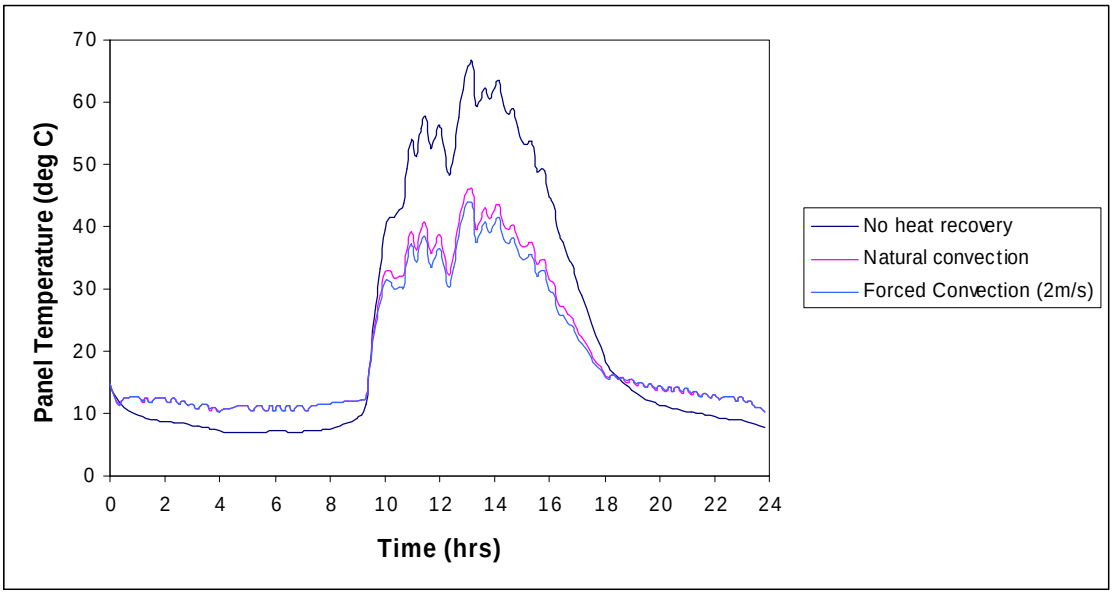

Figure 5.5: Panel temperatures resulting from different modes of heat recovery

5.2.3 Electrical Model

Figure 5.6 describes the equivalent electrical circuit used to model a PV cell. The p-n junction is represented by a current source, where the output I_S, is dependent on the photon flux. The current through the diode I_j, is used to represent recombining hole and electron pairs, which reduces the output from the cell. The cells internal resistance, R_i, is in series with the load resistance, R_L. The shunt in parallel with the p-n junction is the intrinsic self-shortening of the cell, which is usually small enough to be negligible in silicon cells. However, it has been shown that the inclusion of the shunt resistance enables the modelling of amorphous cells (Fry, 1998).

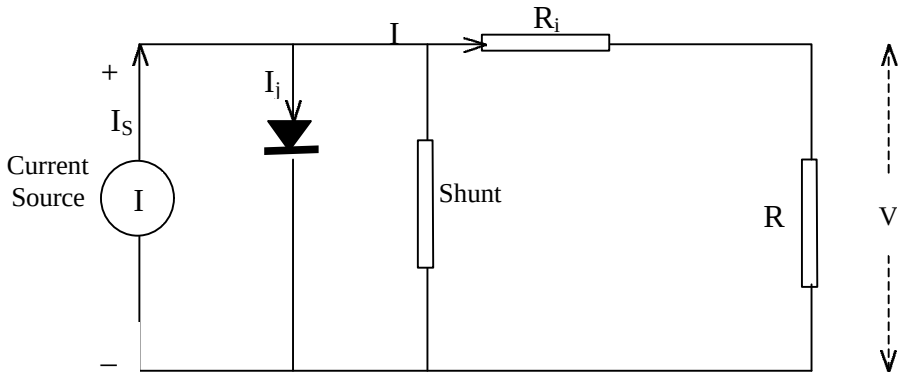

Figure 5.6: Equivalent circuit for a PV cell

This equivalent circuit is used to evaluate the dark and source currents, which enables the power output from a cell to be predicted using the methodology described below.

Dark current calculation

In the absence of a photon flux reaching the p-n junction, a static electric field is established as minority carriers diffuse into the majority carrier region. This diffusion establishes a current, known as the dark current, which is primarily dependent on cell

temperature, and on the diffusivity and lifetime of the minority carrier. The dark current, I_o, is defined (Decher, 1997) as:

$$I_o = 4 \cdot \left(\frac{2 \cdot \pi \cdot e \cdot m_e}{h^2} \right)^3 \cdot \left(\frac{\mu_h \cdot \mu_e}{L_h \cdot \sigma_e} \right) \cdot \left[\left(\frac{k \cdot T}{e} \right)^4 \cdot \exp\left(\frac{e \cdot V_g}{kT} \right) \right] \qquad \text{Equation 5.8}$$

Where e = Electron charge (1.602×10^{-19} Coulomb)

m_e = Electron mass (9.109×10^{-31} kg)

h = Planck's constant (6.626×10^{-34} kg)

μ_h = Hole diffusion velocity

μ_e = Electron diffusion velocity

σ_e = Electrical conductivity for electrons

v_g = Band gap (1.1 eV for silicon)

k = Boltzmann's constant (1.381×10^{-23} J/K)

T = Cell temperature (K)

Material property parameters such as the hole and electron diffusion velocities are typically not available from manufacturers' specifications. However, these parameters can be lumped together into a single material parameter, ξ, which enables Equation 5.8 to be reduced to 5.9.

$$I_o = \xi \left(\frac{k \cdot T}{e} \right)^4 \cdot \exp\left(\frac{e \cdot V_g}{kT} \right) \qquad \text{Equation 5.9}$$

Where

$$\xi = 4 \cdot \left(\frac{2 \cdot \pi \cdot e \cdot m_e}{h^2} \right)^3 \cdot \left(\frac{\mu_h \cdot \mu_e}{L_h \cdot \sigma_e} \right) \qquad \text{Equation 5.10}$$

The value of ξ can be obtained through the substitution of manufacturers performance data at standard test conditions (STC), as follows:

From the electrical equivalent circuit detailed in Figure 5.6, the diode current, I_j, is seen to be:

$$I_j = I_s - I \qquad \text{Equation 5.11}$$

Where I_S = Source current (A)

I = Output current (A)

The diode current is related to the dark current according to Equation 5.12. (Decher, 1997)

$$I_o = \frac{I_j}{\exp\left(\frac{e \cdot V}{k \cdot T} - 1\right)} \qquad \text{Equation 5.12}$$

Where, V is the voltage across an external load. Equating 5.9 and 5.12, rearranging the terms, and substituting in panel characteristics at STC, enables the material property term ξ to be evaluated, as described by Equation 5.13.

$$\xi = \frac{\frac{I_{s_{STC}} - I_{m_{STC}}}{\exp\left(\frac{e \cdot V_{m_{STC}}}{k \cdot T_{STC}} - 1\right)}}{\left[\left(\frac{k \cdot T_{STC}}{e}\right)^4 \cdot \exp\left(\frac{e \cdot V_g}{kT_{STC}}\right)\right]} \qquad \text{Equation 5.13}$$

Where I_S = short-circuit current at STC

I_m = maximum power point current at STC

V_m = maximum power point current at STC

T_{STC} = Reference temperature

Having obtained a value for ξ, dark current can be obtained using Equation 5.9.

Source current calculation

The source current, I_S, is linearly dependent on the solar radiation absorbed and on panel temperature.

This linear relationship can be evaluated by accounting for reflection losses. The reflection losses at STC and at the conditions under which performance is being predicted will usually be different and will in turn affect the quantity of solar radiation available at the p-n junction. It is therefore necessary to calculate the reflection losses in order to make use of the linear current-radiation relationship. The radiation used under standard test conditions is always directly normal to the panel surface and the consequential reflection losses can therefore be evaluated at an incidence of zero degrees.

The source current density, in the case of silicon cells, is known to increase with temperature at a rate of $10^{-4}Am^{-2}K^{-1}$ (Decher, 1997). This figure has been used to account for changes in current resulting from a deviation in the STC temperature.

Equation 5.14 describes the method used to predict the source current for silicon cells.

$$I_s = \frac{I_{STC} \cdot Q_{STC} \cdot r(0)}{Q \cdot r} + 10^{-4} \cdot I_{STC} \cdot (T - T_{STC}) \times A_p \qquad \text{Equation 5.14}$$

Where I_{STC} = Short circuit current at STC

Q_{STC} = STC Irradiance

$r(0)$ = Reflection losses at zero incidence

Q = Predicted solar radiation

r = Predicted reflection losses

T = Predicted panel temperature

T_{STC} = STC Temperature

A_p = Modules area

Voltage and Power Output

By combining Equations 5.11 and 5.12 (Decher, 1997), the load current I, of the equivalent electrical circuit can be calculated as follows:

$$I = I_s - I_j = I_s - I_0 \cdot \left[\exp\left(\frac{e \cdot V}{k \cdot T} \right) - 1 \right] \qquad \text{Equation 5.15}$$

For open circuit voltage ($R_L = \infty\ \Omega$), the load current I, is zero, resulting in the following relationship:

$$V_{oc} = \frac{k \cdot T}{e} \cdot \ln\left(1 + \frac{I_s}{I_o} \right) \qquad \text{Equation 5.16}$$

The temperature dependence of the open circuit voltage is clearly described by the above Equation, and its effect is illustrated in Figure 5.7.

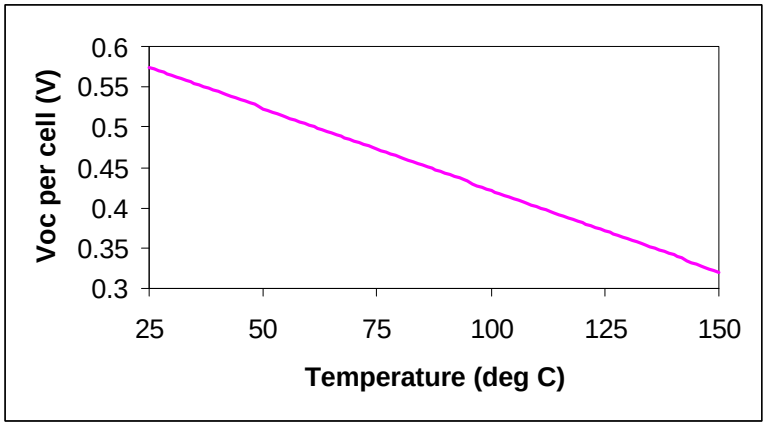

Figure 5.7: Effect of temperature on open-circuit voltage

The voltage across the external load can therefore be calculated by combining Equations 5.15 and 5.16 to give (Decher, 1997):

$$V = V_{oc} \cdot \frac{\ln\left[1 + \left(1 - \frac{I}{I_s}\right) \cdot \frac{I_s}{I_o}\right]}{\ln\left(1 + \frac{I_s}{I_o}\right)} \qquad \text{Equation 5.17}$$

The product of the open circuit voltage, $V_{oc,}$ and the source current $I_{S,}$ defines the power density of a cell. However, the actual power available from the cell is dependent on the load resistance. The ratio between the power obtainable and the power density is known as the fill factor, and is described by Equation 5.18 (Decher, 1997).

$$FF = \frac{I \cdot V}{I_s \cdot V_{oc}} = J \cdot \frac{\ln[\,1 + A \cdot (1 - J)\,]}{\ln(1 + A)} \qquad \text{Equation 5.18}$$

Where J, is the ratio of load current I and dark current I_o, and A is the ratio of supply current I_S, to the dark current.

The maximum operating condition, known as the maximum power point, is relatively close to the open circuit voltage and short circuit current condition. One approach used in predicting this optimum point has employed neural networks, trained on measured data (Hiyama and Kouzuma, 1993). The need for measured data has been avoided in this work, to preserve the generic nature of the model. Hence, the maximum power point is obtained by differentiating Equation 5.18 with respect to J, and setting the resulting expression to zero. Performing this operation yields the implicit expression for J, described below:

$$\ln[\,1 + A \cdot (1 - J)\,] = J \cdot \frac{A}{[\,1 + A \cdot (1 - J)\,]} \qquad \text{Equation 5.19}$$

A maximum power point tracker is a device, which will vary the load resistance for particular operating conditions, to optimise power output from the system. The power output is always calculated by assuming the PV system to be operating in conjunction

with such a device. This assumption is reasonable as building-integrated photovoltaic systems nearly all employ a maximum power point tracker (Fry, 1998). The above Equation is solved for J, using the Newton- Raphson technique, and provides a solution for the current flowing through a particular load resistance. The corresponding voltage can be calculated using Equation 5.18, enabling the power output from a single cell to be determined. The power output of a module is calculated by scaling the single cell output according to the module configuration and the number of modules contained within a system.

PV systems produce DC current, and where these systems are integrated into the electricity supply network, or used to supply AC loads, an inverter is required to convert DC to AC current. Inverters are power electronic converters, which convert DC at some voltage to AC at some voltage and frequency, transferring power with typically high efficiencies from DC to AC. The crudest inverter simply switches the DC input on and off at a specific frequency to produce the required AC output. Switching at a 50% duty cycle, where the on period equals the off period, gives a square wave with the mean output voltage half of the input voltage. More sophisticated inverters include complex topographies and control functions employed carry out switching at high speeds and produce a near perfect sinewave output, stepping up the voltage as necessary. In the UK, there are a number of regulations, which are influencing the design and use of inverters (Simmons, 2000). The first commercially available inverters were line commutated, followed by self-commutated and pulse width modulation inverters which include either line or high frequency transformers and often incorporate several stages of power conversion. More recently, designs include string-based units, transformer-less concepts, and multilevel converter technologies (Calais et al., 1999). All inverters consume some of the energy that they are converting and transferring from DC to AC. Generally, inverters operate at relatively low efficiencies below, and high efficiencies above, 25% of the inverter rated power (Simmons, 2000). The inverter efficiency η_{inv}, is included in the final power output P, of a PV system, and is described in the following relationship.

$$P = I \cdot V \cdot m \cdot n \cdot N \cdot \eta_{inv}$$ Equation 5.20

Where m = number of cells in series

n =number of cells in parallel

N = number of modules in specified system

A detailed electrical model of the inverter, which accounts for the switching losses and device impedance, requires information, which is not readily available from manufacturers specifications. Additionally, the rapid advances in inverter design further complicate the modelling process. Consequently, an approximation has been incorporated based on a typical inverter, characteristic performance curve. The approximation accounts for the losses in efficiency, at low percentage loading. The characteristic curve is described in Figure 5.8, and is obtained using Equation 5.21.

$$\eta_{inv} = e^{\frac{-(100-\eta_{max})}{pL}}$$ Equation 5.21

Where η_{max} = Maximum Efficiency at 100 percent load

pL = Percentage Loading

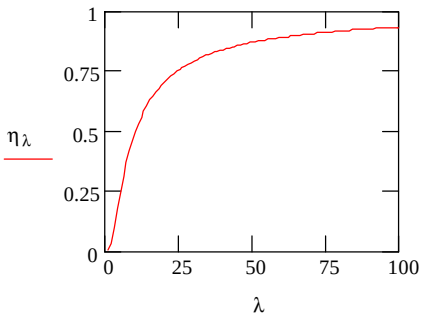

Figure 5.8: Characteristic Inverter Curve

5.3 Modelling Wind Energy Conversion Devices

The primary objectives in modelling wind systems were the same as for PV: that the model would be applicable to a variety of wind energy conversion systems, and that the inputs to the model could be obtained from manufacturers' specifications. A fundamental approach in determining performance requires the prediction of aerodynamic loads. The difficulties in predicting aerodynamic loads are driven by the combined influences of three-dimensionality, unsteadiness, and dynamic separation (Robinson et al., 1999). Three-dimensional cross flows as well as quasi-steady and unsteady separation events arise from both the stochastic nature of the inflow and a variety of turbine design parameters. Rapid changes in wind speed or direction dynamically alter the local angle of attack along the span. Additionally, the stall characteristics of the airfoils used over the tip region of the blades strongly affect the dynamics of the rotor. Low lift airfoils with gentle stall characteristics reduce blade dynamic excitations, whereas high-lift airfoils minimise blade solidity, enhance starting torque, and are more efficient in laminar flow conditions (higher lift-to-drag ratio) (Giguere and Selig, 1999). Because of these many influences, accurate and reliable prediction of wind turbine aerodynamics requires detailed data about wind flow and turbine design. Detailed models exist (Muljadi et al., 1998) which can predict high and low-speed shaft torques as a function of time. However, these models require detailed turbine data including blade geometry, rotor inertia, drive-train inertia, and stiffness and damping of the rotating shafts. The drive train stiffness of a particular turbine dictates whether drive train dynamics need to be included, and the pitch actuation system used will determine the actuator dynamics (Pierce and Fingersh, 1998)

The requirement to model performance based on manufacturers' data and climatic parameters constrained the approach to neglecting the fundamentals of detailed aerodynamic performance. Other models based on similar input requirements are either oversimplified or require comprehensive input data to predict performance. For example, a CAD tool for renewable energy systems (Enslin and Potgieter, 1996)

assumes rated power production for wind speeds with sufficient velocity, and neglects any power production in the run up to the devices rated power. Another example is that of the MORENA software package (Ramirez, 1998) which calculates power output from the standard equation;

$$P = \frac{1}{2} \cdot C_p \cdot \rho \cdot A \cdot V^3 \qquad \text{Equation 5.22}$$

Where C_p = Coefficient of performance

ρ = Air density (kg/m^3)

A = Swept area of blades (m^2)

V = Wind speed (m/s)

The power is calculated assuming a constant Coefficient of performance (Cp). However, Cp is a function of blade tip speed and pitch angle, as is illustrated in Figure 5.9. Blade tip speed varies with wind speed, and the blade pitch angle is variable for pitch regulated machines.

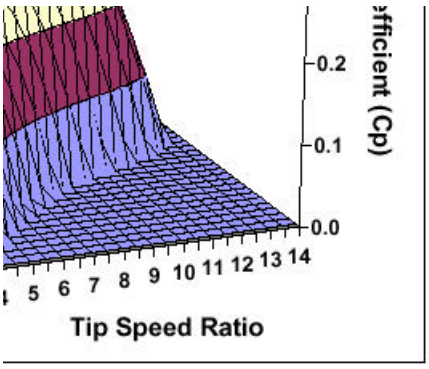

Figure 5.9: Power coefficient surface as a function of tip-speed ratio and blade-pitch angle. (All negative Cp values have been set to zero (Hand and Balas, 1999)

The approach taken by Loughborough University (Child et al., 1996) is to calculate power output using the empirical wind turbines power curve data as a look-up table. The approach adopted in this work is similar to that taken by Loughborough University but with an attempt to remove the extensive input data requirements. The method involves the mathematical characterisation of performance curves based on a limited number of points on the curve. Variations in accuracy between using a look-up table of performance curves and mathematically approximating performance curves are thought to be insignificant as climatic data will rarely capture actual wind dynamics.

Four wind turbine classes have been defined to account for marked differences in performance. The classification has been devised to account primarily for power regulation, which can be separated into unregulated, stall regulated and pitch regulated turbines. The final class of turbine is the ducted wind device (Webster, 1979) is

distinctly different from other turbines, as it exhibits sensitivity to wind direction (Pendas, 1999), due to its encapsulated design. Additionally, the ducted device is currently not being manufactured as it is in the early stages of development.

The turbine type classification dictates both the input data requirements and the mathematical procedures used in predicting power output. . The turbine-class-specific data requirements are outlined in Table 5.2. A number of other parameters, which are independent of the turbine class are required in the performance calculations including blade swept area, turbine (hub) height and the reference air density used by manufacturers to produce the empirical power curve. All parameters can be obtained from power curves, with the exception of the ducted wind turbine, for which no manufacturers' data exists. For the ducted wind turbine, the machine's orientation is the only turbine specific input parameter required.

Table 5.2: Turbine specific data requirements

Turbine Type	**Data Requirements**
Stall Regulated	Cut in wind speed and power Nominal power and associated wind speed Peak power and associated wind speed Cut out wind speed and power
Pitch Regulated	Cut in wind speed and power Nominal power and associated wind speed Cut out wind speed
Unregulated	Cut in wind speed and power Cut out wind speed and power
Ducted	Orientation

Temporal climate parameters are required to define the operating conditions, under which performance is to be predicted. Wind speed data is corrected for surrounding surface roughnesses and proposed turbine height. Subsequently these corrected wind speeds are used to estimate corresponding power outputs, which are then corrected to account for air density variations.

Wind speed corrections for surrounding surfaces and turbine height, are required as climate data is not necessarily obtained in the same conditions as those of turbine operation. The correction procedure and the basis for it are described in Appendix C. The power output at a corrected wind speed is calculated assuming a specified reference air density, and the calculated power output is subsequently corrected to account for variations in air density, as described by Equation 5.23 (Evans, 1996). This correction is based solely on temperature variations assuming constant atmospheric pressure. However, turbine altitude is typically much higher than the altitudes used to measure temperature, and no correction is included. Additionally, the reduction in atmospheric pressure at increased altitudes is neglected.

$$P = \frac{P_{ref}}{\rho_{ref}} \cdot \frac{R.A}{T_a} \qquad \text{Equation 5.23}$$

Where P = predicted power output

P_{ref} = uncorrected power output

ρ_{ref} = reference air density

R = ideal gas constant

A =atmospheric pressure

T_a = ambient temperature

5.3.1 Power Output Calculations

Once the wind speed has been corrected to account for the specified operational conditions, the corresponding power output is calculated according to the turbine class.

Unregulated Turbines

The relationship between wind speed and power output for an unregulated wind turbine is described in Figure 5.10. For wind speeds less than the cut in wind speed, or greater than the cut out wind speed, the power output is zero. Between these wind speeds, the power output follows a trend, which can be described mathematically by the statistical model a normal distribution curve. The normal distribution curve is given by Equation 5.24 (Scheaffer and McClave, 1982).

$$f(x) = \frac{1}{\sqrt{2\cdot\pi\cdot\sigma}}\cdot e^{\frac{-(x-\mu)^2}{2\cdot\sigma^2}} \qquad \text{Equation 5.24}$$

Where x = the value for which the distribution is determined

μ = the arithmetic mean of the distribution

σ = the standard deviation of the distribution

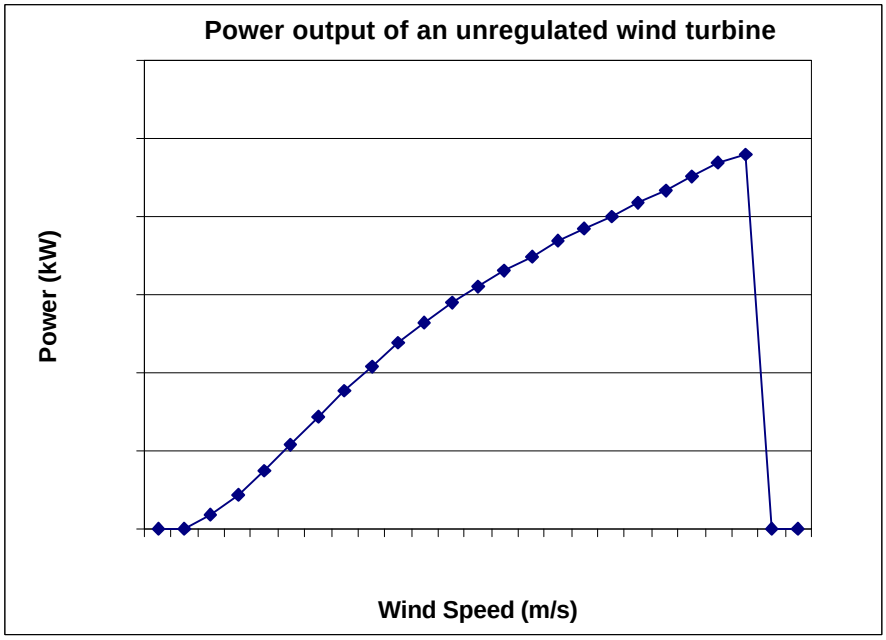

Figure 5.10: Power curve for an unregulated wind turbine

The normal distribution curve can be adapted to describe the performance of unregulated turbines by the substitution of manufacturers' performance characteristics. Equation 5.24 comprises a constant term, used as a scaling factor, which, for the purposes of this work is replaced by the maximum power output (achieved at cut out wind speed). The variable exponential term is used to predict the power output variations with wind speed, through the substitution of the arithmetic mean by the cut out wind speed. These modifications result in Equation 5.25

$$P = P_m \cdot e^{\frac{-(V-V_m)^2}{2\cdot\sigma^2}} \qquad \text{Equation 5.25}$$

Where P = Real power output (W)

P_m = Maximum power output (W)

V_m = Cut out wind speed (m/s)

V = Operating wind speed (m/s)

σ = Variable term dependent on wind speed

Calculating σ, for known power outputs at given wind speeds, enabled the use of regression analysis to determine the relationship between σ and wind speed. Figure 5.11 describes this relationship together with the resulting regressed equation (Equation 5.26) and the regression coefficient R^2. The regression coefficient indicates the accuracy of the equation, where a value of 1.0 is exact.

$$\sigma = -0.0507 \cdot V^2 + 1.0918 \cdot V + 5.1037 \qquad \text{Equation 5.26}$$

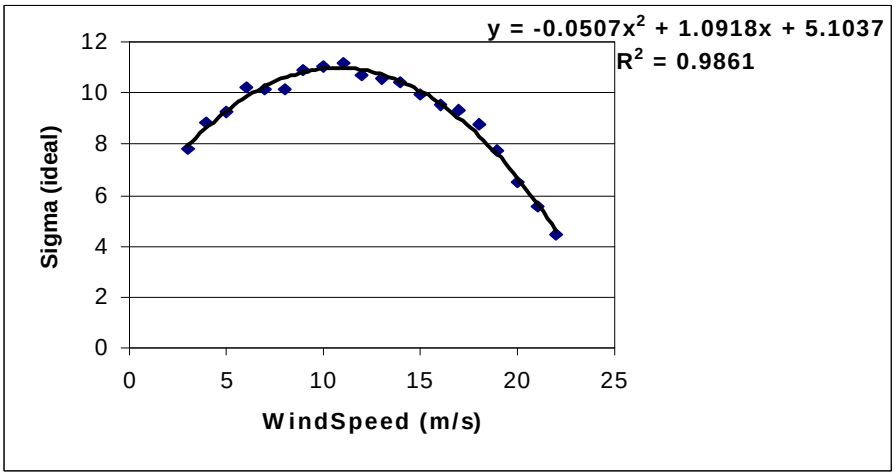

Figure 5.11: Result of analysis to determine the relationship between σ and wind speed for an unregulated wind turbine.

Thus the performance of an unregulated turbine is predicted by using the corrected wind speed to evaluate the σ term from Equation 5.26 which is used in Equation 5.25 to determine the power output.

Regulated Turbines

Larger wind turbines deploy power regulation systems to control the power output. Regulation is achieved through either active or passive control systems (Demontfort University, 2000). Active control includes varying the pitch of the whole blade or blade tips. This is achieved through negative feedback control to either reduce or increase the

winds' angle of attack, thereby altering the rotors aerodynamic characteristics. Passive control exploits the stall characteristics of the rotor blade, resulting in aerodynamic stall at high wind speeds without changing the blade pitch. These different regulation systems are used as further classification of regulated wind turbines into pitch or stall type turbines. Typical power curves for each type are illustrated in Figures 5.12 and 5.13

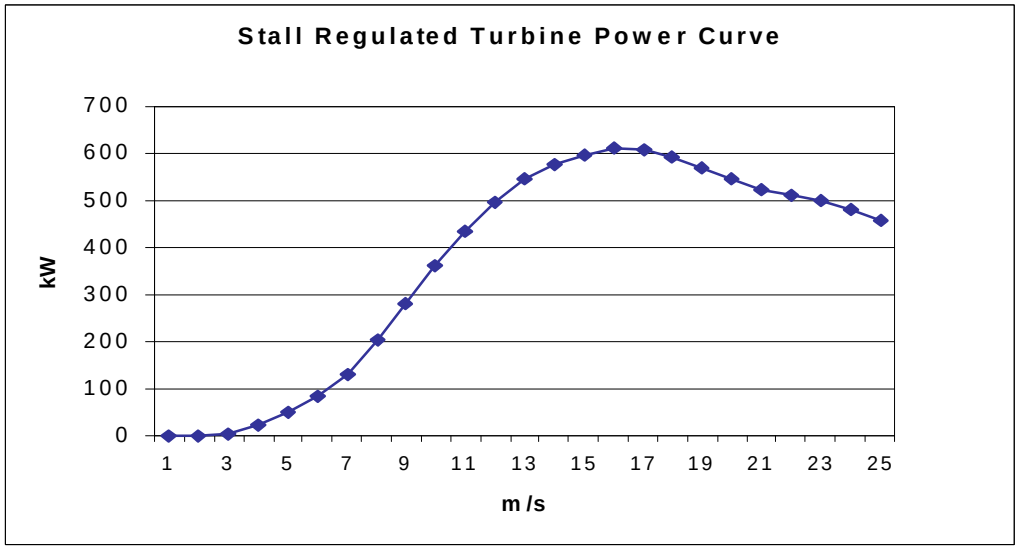

Figure 5.12: Typical power curve for a stall regulated wind turbine

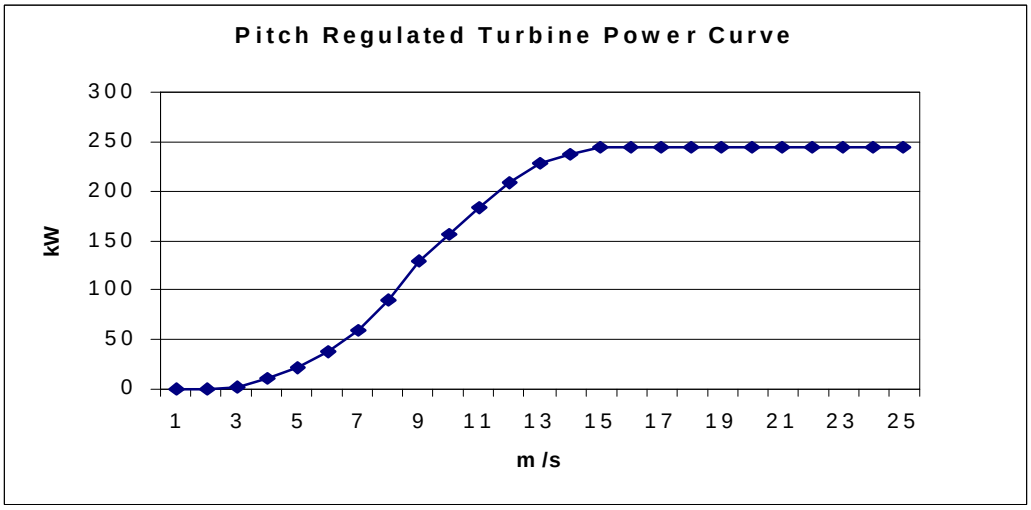

Figure 5.13: Typical power curve for a pitch regulated wind turbine

Three characteristic regions can be defined, which are approximated differently. Figure 5.14 illustrates the three stages to calculating the power output within each stage.

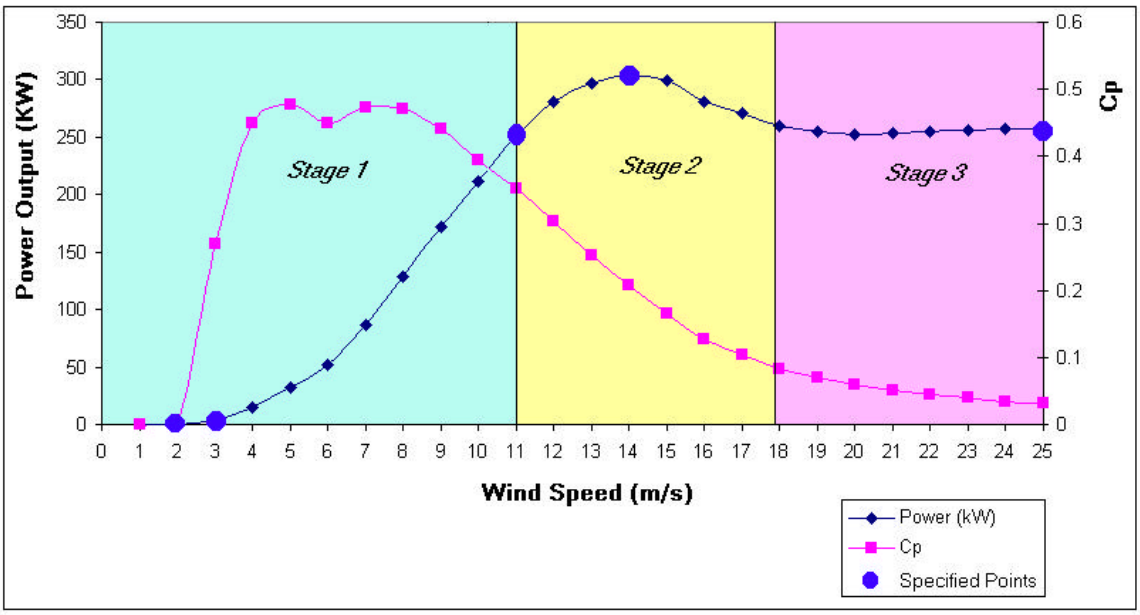

Figure 5.14: Three stages used to define regulated wind turbine performance

Both types of regulated wind turbines display similar performance characteristics up to the point where nominal output power is achieved. Following nominal output, the type of regulation systems dictates performance. Consequently, the region up to nominal output power can be described mathematically independent of the control mechanisms used in different turbine designs.

Stage 1: Start-up Region

The power output – wind speed curve in the start-up region does not follow the normal distribution trend used to describe unregulated turbines. The reason for this is thought to lie with the fact that larger turbines, which deploy regulation typically utilise two generators, a start-up generator for low wind speeds, and a larger one for wind speeds

approaching nominal. The dip seen in the Cp value during the start-up region in Figure 5.14 is thought to be due to generator change over.

The approach used in predicting power output in stage one, approximates the Cp value at a given wind speed, and subsequently uses Equation 5.22 to determine the corresponding power output. The method for calculating the Cp is based on a second-order polynomial curve fitting method, using specified point on the Cp – wind speed curve. Three points are required to define the Cp characteristic in the start up region, the cut-in, nominal and peak wind speeds, together with the corresponding power outputs. Additionally two more points are used which, both of zero Cp at wind speeds zero and cut-in minus one. These points are used to define four second-order polynomial equations. The polynomials used are based on Equation 5.27, which describes how Cp varies with wind speed, V. The coefficients a, b and c can be found using Equations 5.28, 5.29, and 5.30 respectively, where the various Cp and V values used are detailed in Table 5.3. Negative Cp values are not possible with this method as the portions of the polynomial curves used to characterise performance are always above the x-axis.

$$Cp = a \cdot V^2 + b \cdot V + c \qquad \text{Equation 5.27}$$

$$a = \frac{\frac{Cp_1 - Cp_2}{V_1 - V_2} - \frac{Cp_1 - Cp_3}{V_1 - V_3}}{\frac{V_1^2 - V_2^2}{V_1 - V_2} - \frac{V_1^2 - V_3^2}{V_1 - V_3}} \qquad \text{Equation 5.28}$$

$$c = Cp_2 - a \cdot V_2^2 - b \cdot V_2 \qquad \text{Equation 5.29}$$

$$b = \frac{Cp_1 - Cp_2}{V_1 - V_2} - a \cdot \left(\frac{V_1^2 - V_2^2}{V_1 - V_2} \right) \qquad \text{Equation 5.30}$$

Table 5.3: Parameters used in calculating polynomial coefficients.

	Polynomial 1	**Polynomial 2**	**Polynomial 3**
Cp_1	Cut-in Cp	0	0
V_1	Cut-in V	Cut-in V-1	0
Cp_2	Nominal Cp	Cut-in Cp	Cut-in Cp
V_2	Nominal V	Cut-in V	Cut-in V
Cp_3	Peak Power Cp	Nominal Cp	Nominal Cp
V_3	Peak Power V	Nominal V	Nominal V

For each of the Equations derived, the velocity at the maximum turning point is found by differentiating Equation 5.27, resulting in Equation 5.31. This velocity is substituted into Equation 5.27, to find the maximum Cp value resulting from each polynomial. These maximum values are subsequently used to define a descending order of sets of coefficients a, b, and c. From these ordered points two more polynomial equations are derived by taking the average of each of the coefficients, for coefficient sets 1 and 2, and 2 and 3.

$$V_T = \frac{b}{2 \cdot a} \qquad \text{Equation 5.31}$$

The top-four resultant polynomials are used to calculate the Cp value at wind speeds between cut-in and nominal. This range of wind speeds is divided into four, where each range is defined by the ordered polynomial equations.

The effect of this procedure is to trace the characteristic Cp curve as is illustrated in Figure 5.15 for a typical turbine. The actual Cp curve is shown together with points calculated using the ordered polynomials. The initial rise to a peak Cp value is rapid and is defined by the polynomial resulting in the highest Cp maximum value, and the subsequent Cp values are defined by the polynomial equations resulting in progressively lower Cp maximums.

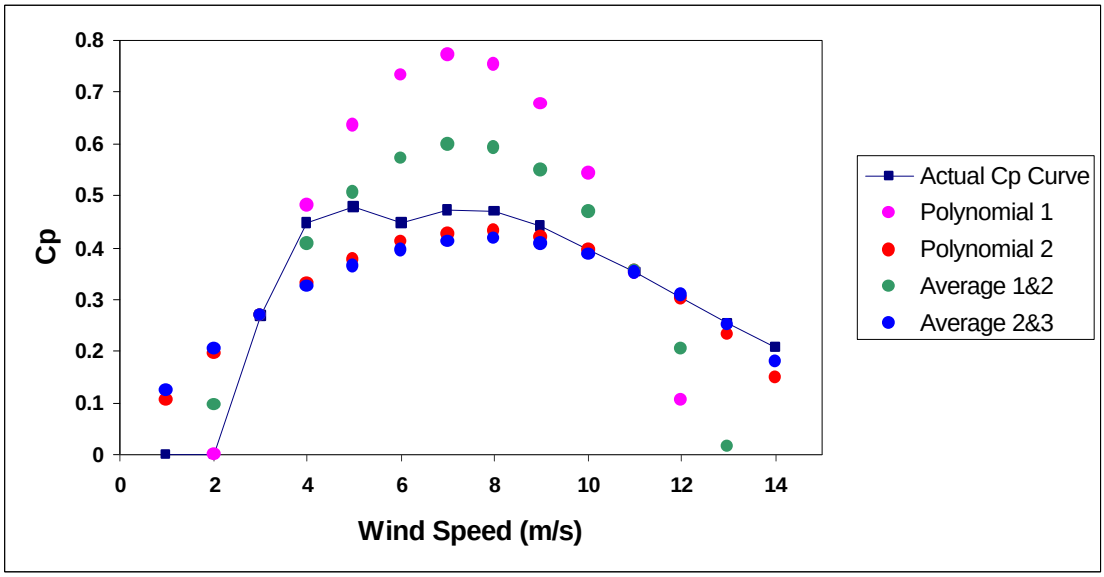

Figure 5.15: Polynomial Equations Used to Define Variations in Cp.

With Cp defined for a given wind speed, Equation 5.22 can be used to determine the corresponding power output.

Stages 2 & 3: Nominal to Cut-out Power Output Region

The Cp value after the nominal power output can be seen to fall off exponentially, as is clearly illustrated in Figure 5.14. However, at high wind speeds the use of Equation 5.22 to calculate power output using Cp values becomes very susceptible to large errors due to the V^3 term. For this reason the approach taken in estimating power output for

wind speeds grater than nominal, is based on approximating the power output curve directly. Pitch regulated turbines maintain nominal power output up until cut out wind speeds are achieved. Thus for pitch regulated turbines power output is predicted as the nominal power output for all wind speeds, between nominal and maximum wind speeds.

Stall regulated turbines display different characteristics in this region. Typically, power output is seen to increase from the nominal value to a peak value, followed by a reduction back to approximately the nominal value. Thereafter power performance curves can be seen to either continue decreasing or rise again just prior to cut out. The rise from nominal to peak power output is sinusoidal in nature and can be calculated using Equation 5.32.

$$P = P_n + \sin\left[\frac{\pi}{2}\cdot\frac{(V - V_n)}{(V_p - V_n)}\right]\cdot(P_p - P_n) \qquad \text{Equation 5.32}$$

Where P = Real Power output (W)

P_p = Peak Power output (W)

P_n = Nominal power output (W)

V_p = Wind Speed at Peak Power output (m/s)

V_n = Wind Speed at Nominal power output (m/s)

Once peak power is achieved, the typical performance curve can be seen to return to nominal power output, continuing with the sinusoidal characteristic. The rate of this decline is not typically symmetric to the rate of increase, taking on average an extra 2m/s before nominal power is re-achieved. This characteristic is therefore modelled using Equation 5.33.

$$P = P_n + \sin\left[\frac{\pi}{2}\cdot\frac{(V - V_n)}{(V_p - V_n + 2)}\right]\cdot(P_p - P_n) \qquad \text{Equation 5.33}$$

The final stage of the power curve for stall regulated turbines is predicted by assuming the power output from ($V_p - V_n + 2$) to the cut out wind speed to be linear. Thus, wind speeds within this range are used to determine corresponding power outputs through linear interpolation.

Ducted Wind Turbines

The ducted wind turbine presents a special case as it is currently in the early stages of development and hence manufacturers' data is not available. The algorithm developed for predicting the performance of this device was therefor derived from an analysis of field trial data, obtained for a prototype, tested at the National Wind Turbine Test Center (Grant et al., 1994). The data obtained was time-averaged over 10-minute periods for a total monitoring period of approximately 3 months, and shows the power output to be dependent on both wind speed and wind direction. A correction factor was evaluated to incorporate for the effects of wind angle of incidence on power output. Increases in angular incidence reduce power outputs, with angles greater than 75 degrees resulting in the cessation of power production. The magnitude of the reduction in power output is also proportional to the wind speed. The correction factor for misalignment was applied to the wind speed to obtain an expression for the power in the wind at the rotor. Clearly, the kinetic energy in the wind available at the rotor swept area is proportional to the angle of incidence, with obtuse angles reducing the wind power at the rotor. Regression analysis was used to evaluate the correction factor and was found to be related to the ratio of the angle of incidence to twice the maximum angle of incidence (75 degrees), as described by Equation 5.34. From Equation 5.34 it can be seen that for zero angles of incidence the wind speed at the rotor is the actual wind speed, and as the angle increases the effective wind speed is reduced.

$$V_c = V_w\left(1 - \frac{\theta}{2\theta_{max}}\right) \qquad \text{Equation 5.34}$$

Where V_c = Corrected wind speed of wind at the rotor

V_w = Wind speed

θ = Angle of misalignment

θ_{max} = Maximum angle of misalignment (75 degrees)

Having obtained an expression to correct the wind speed for the angle of incidence, the power of the wind at the rotor could be calculated as described by Equation 5.35.

$$P_w = \frac{1}{2}\rho \cdot A \cdot V_c^3 \qquad \text{Equation 5.35}$$

Where P_w = Power of the wind at the rotor (W)

ρ = density of air (kg/m^3)

A = rotor swept area (m2)

V_c = Corrected wind speed (m/s)

Regression analysis performed on the calculated power in the wind at the rotor and the power output from the turbine was used to ascertain the relationship between these two power characteristics, which essentially describes a function of the coefficient of performance Cp. The result of this analysis is shown in Figure 5.16.

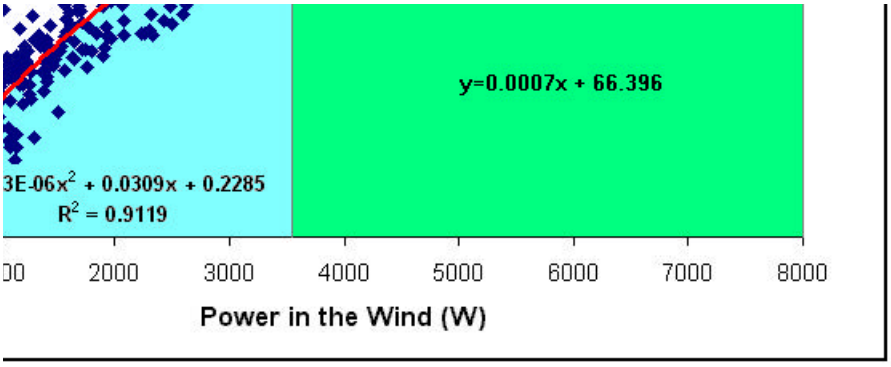

Figure 5.16:Result on regression performed on the ducted turbine power output and calculated power available at the rotor.

A regression coefficient (R^2) of 0.9119 was obtained, for the 2nd order polynomial described in Equation 5.36 which indicates that the equation is reasonably accurate in describing the relationship between the power in the wind and the turbine output for the data set provided. However, the inspection of Figure 5.16 shows that the polynomial is only valid for a portion of the test data, up to corrected wind speeds of approximately 22m/s. Corrected wind speeds greater than this appear to increase the power output from the turbine in a linear manner, as is illustrated in later portion of the graph shown in Figure 5.16. The linear equation pertaining to this section of the curve was calculated using two of the data points on it, and is described by Equation 5.37.

The analysis described gave rise to the following modelling technique used to predict the power output from a ducted wind turbine. Firstly, any wind incidence angles greater than 75 degrees result in zero power output. Provided the angle of incidence is within

this upper limit, the wind speed is corrected to account for misalignment and this effective wind speed is used to calculate the power in the wind at the rotor. For wind powers less than the limiting value of 3.5 kW, Equation 5.36 is used to predict the turbine power output, otherwise Equation 5.37 is used. The limiting value is thought to be a condition of significant turbulence, which inhibits the ability of the turbine to extract the power available.

$$P_t = -3 \cdot 10^{-6} \cdot P_w + 0.0309 \cdot P_w + 0.2285 \qquad \text{Equation 5.36}$$

$$P_t = 0.0007 \cdot P_w + 66.396 \qquad \text{Equation 5.37}$$

Where P_t = Power output of the turbine (W)

P_w = Power of the wind at the rotor (W)

The effects of microclimates on DWT performance can only be incorporated through site specific wind speed and direction measurements used as inputs to the model described.

5.4 Modelling Solar Water Heating

Solar water heaters utilise the suns' energy to provide a hot water supply. A mathematical model for such systems has been developed to generate simulated supply profiles for hot water. Typically, these systems comprise collectors and storage tanks, which can operate either actively, or passively. For active systems, an electric pump is employed to circulate fluid. Passive systems rely on natural convection. Three types of collectors are available: flat-plate; evacuated-tube; and concentrating. The most commonly utilised collectors in practice are the flat-plate, and the work to be presented focuses on the prediction of the hot water supply profiles from a flat-plate water heating systems. The output from a collector will depend on location, and positioning. Location sensitive technologies are significantly less intensive to investigate, through modelling than through monitoring.

The basic elements of a flat plate collector are detailed in Figure 5.17. With reference to this diagram, the collector can be observed to comprise a radiation-absorbing flat plate encapsulating a tube network, through which fluid circulates. An optional number of transparent covers, contained within a casing with back and edge insulation can also be employed. Solar radiation passes through the glazing material, if present and is absorbed by the plate. This thermal energy is subsequently transferred to the circulating fluid. To improve the efficiency of this process by reducing the heat losses from the system, insulation is typically included within the design. The overall energy absorbed by the plate, and the heat losses from the collector, will depend on the number of covers above the absorber plate. In this work the performance of three flat plate configurations; without and with single and duel cover systems are simulated using an appropriate mathematical model. The model to be described has been adapted from the work of Koo (Koo, 1998), which was initially developed to reproduce the performance data provided by manufacturers. However, manufacturers' performance data is only available for specified test conditions, and does not account for seasonal variations in climate or for the daily fluctuations in solar conditions.

The potential thermal gain from a flat plate collector is dependent on ambient temperature, solar condition, and also on the inlet temperature and flow rate of the circulating fluid. The inlet temperature is primarily determined by the characteristics of the storage tank through which the fluid flows. The flow rate will depend on whether fluid is forced through the system by a pump at a specific rate or if natural convection is used. A control algorithm based on the temperature difference between fluid inlet and outlet temperatures is used to determine whether fluid is circulating or not. Two separate techniques both based on an energy balance of the system are used to predict the performance of the system when fluid is circulating and when it is static.

Figure 5.17: Basic elements of a flat plate collector

5.4.1 Predicting Energy Flow in Collectors

Prior to describing the different energy balance methods employed to analyse circulating and stationary fluid conditions, an analysis of the energy flows for three collector configurations is described for a flat plate without glazing, and with single and dual cover systems. To evaluate the energy flows in a collector, all of the convection and radiation heat transfer mechanisms between the absorber plate, any parallel covers,

and the collectors' surroundings require to be considered. Clearly, the performance of a solar collector is dictated by the solar radiation incident on the collector surface. Appendix B.1 details the calculations required to evaluate the radiation incident on a surface. The method described in the previous section of this chapter describing the PV model (Section 5.2.1 Losses by Reflection) is subsequently used to determine the losses incurred by the incident radiation on penetrating transparent material.

Flat plates with No Covers

The heat transfer mechanisms, in a flat plate without glazing elements, are described in Figure 5.18. Collectors without covers enable the suns' radiation to be absorbed directly by the plate, and do not incur the losses associated with additional glazing. However, the absence of glazing increases the re-radiation of energy from the plate into the environment. Convective heat losses occur at the outer surface, and are predominantly influenced by the wind speed. The other heat loss mechanisms include the back and edge losses, and finally the energy transferred to the circulating fluid. The equations required to determine the various heat loss mechanisms illustrated have been taken from the work of Koo (Koo, 1999), and are described in Appendix D.1.

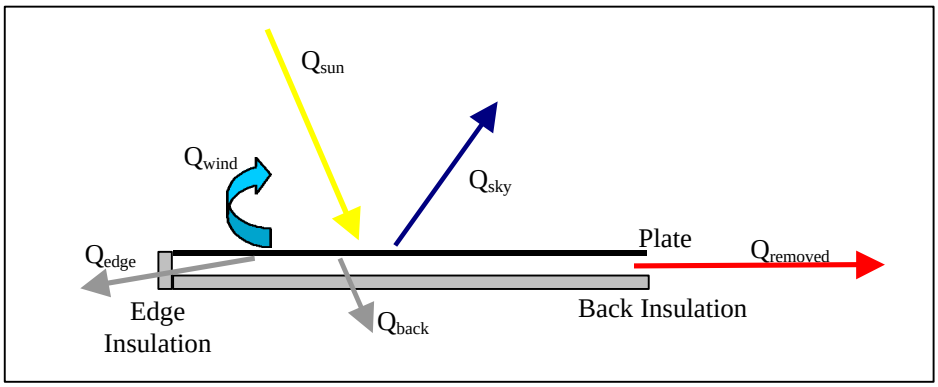

Figure 5.18: Energy flow in a flat plate collector without a cover system

Flat plates with One Cover

The heat transfer mechanisms for a flat plate with a single glazing system are shown in Figure 5.19. The additional glazing element introduces additional energy flows between the plate and the parallel cover. Energy is exchanged through convection in the air gap between plate and cover, and through radiation. The radiant energy exchange is shown diagrammatically as entering and leaving the covers' inner and outer surfaces, as the energy is transferred between the layers. The net radiation method (Siegel and Howell, 1992) is utilised to quantify these radiant energy terms together with the other heat loss mechanisms are described in Appendix D.1, and B.3.

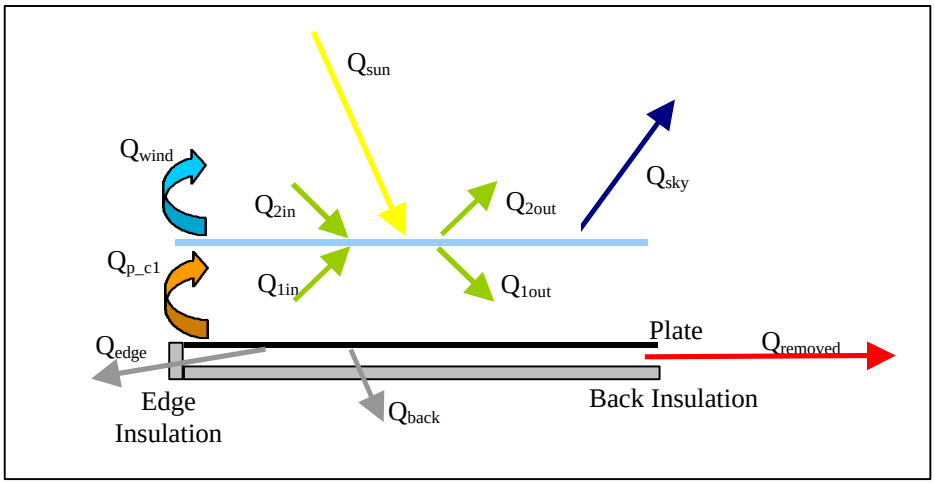

Figure 5.19: Energy flow in a flat-plate collector with a singe cover

Flat plates with Two Covers

A flat plate configured with two covers incurs yet more energy exchanges between the two covers, as shown in Figure 5.20. The mathematical description of this system is very similar to that for a single cover system. The net radiation method is again employed to quantify the radiant energy exchanges between plate and cover, and cover and cover.

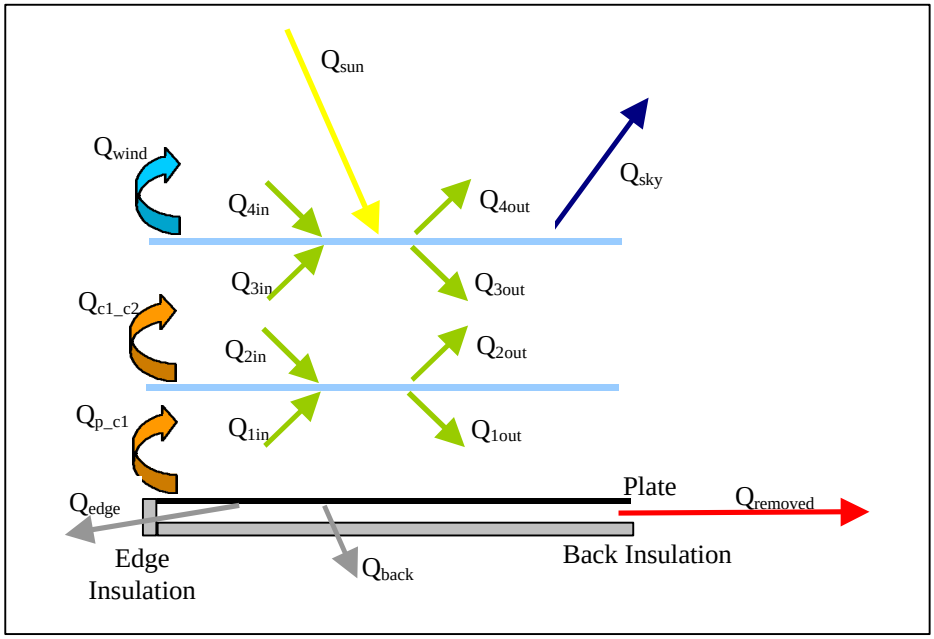

Figure 5.20: Energy Flow in a Flat Plate Collector with Two Covers

Flat plates Performance without Circulating Fluid

The above sections described the energy flows occurring in flat plates for the three different cover systems. When pumping is not included and fluid is stationary, it is still necessary to predict the temperature changes occurring in the system. The temperature of the plate and of the covers is determined by solving energy balance equations, using the Newton Raphson iterative technique. The energy balances used assume the heat removal term to be zero, as no fluid is circulating. A second assumption is that the mean fluid temperature is equal to the mean plate temperature, when fluid is not circulated. This assumption may be reasonable for a water system, but could not be implemented when air is used as the transfer medium.

The energy balance for the absorber plate of a flat plate collector without a cover system is described as:

$$m_p \cdot Cp_p \cdot \Delta T_p = Q_{rad} \cdot A_p - Q_{sky} - Q_{wind} - Q_{back} - Q_{edge} \qquad \text{Equation 5.38}$$

For a flat plate with glazing, it is necessary to predict both plate and cover temperatures as each parameter affects the energy flows throughout the system. The required energy balances for predicting these are:

$$m_p \cdot Cp_p \cdot \Delta T_p = Q_{rad_p} \cdot A_p - Q_{p\_c} - Q_{back} - Q_{edge} \qquad \text{Equation 5.39}$$

$$m_c \cdot Cp_c \cdot \Delta T_c = Q_{rad_c} \cdot A_p + Q_{p\_c} - Q_{sky} - Q_{wind} + Q_{RE} \qquad \text{Equation 5.40}$$

Where the net radiant exchange, Q_{RE} is the sum of the individual radiant components between plate and cover (Koo, 1999).

$$Q_{RE} = A_p \cdot (Q_{1in} - Q_{1out} + Q_{2in} - Q_{2out}) \qquad \text{Equation 5.41}$$

The incoming solar radiation (Q_{rad}) terms in Equations 5.39 and 5.40 are given different subscripts, as the radiation term used in the energy balance for the cover, is the radiation absorbed by the cover only, and that used in the plate energy balance incorporates the net reflection losses incurred.

A two-cover system requires the prediction of plate and cover temperatures and therefor three energy balances are used, as described below.

$$m_{c2} \cdot Cp_{c2} \cdot \Delta T_{c2} = Q_{rad_{c2}} \cdot A_p + Q_{c1\_c2} - Q_{sky} - Q_{wind} + Q_{RE2} \qquad \text{Equation 5.42}$$

$$m_{c1} \cdot Cp_{c1} \cdot \Delta T_{c1} = Q_{rad_{c1}} \cdot A_p + Q_{p\_c1} - Q_{c1\_c2} + Q_{RE1} \qquad \text{Equation 5.43}$$

$$m_p \cdot Cp_p \cdot \Delta T_p = Q_{rad_p} \cdot A_p - Q_{p\_c1} - Q_{back} - Q_{edge} \qquad \text{Equation 5.44}$$

Where

$$Q_{RE1} = A_p \cdot (Q_{1in} - Q_{1out} + Q_{2in} - Q_{2out})$$ Equation 5.45

$$Q_{RE2} = A_p \cdot (Q_{3in} - Q_{3out} + Q_{4in} - Q_{4out})$$ Equation 5.46

Flat plates Performance with Fluid Circulation

An iterative technique of balancing energy flows with circulating fluid developed by Duffie and Beckmann (by Duffie and Beckmann, 1974) is used to predict the performance of the collector under circulating conditions. This method evaluates the mean plate temperature, and simultaneously determines the useful gain from the collector. The methodology used is summarised below, a detailed description of the analysis and its derivation is presented elsewhere (by Duffie and Beckmann, 1974), and a summary of each of the calculations performed is given in Appendix D.2. Figure 5.21 describes the calculation procedure, assuming that the solar radiation absorbed has been determined. Firstly, an estimated mean plate temperature is used to calculate both the heat loss from the collector to the surroundings, and the heat transferred to the circulating fluid. These parameters are subsequently used to calculate the efficiency of the collector and the quantity of heat removed. This enables the useful gain from the collector to be quantified. The efficiency, heat removal and gain terms together with the fluid inlet temperature are used to ascertain the mean fluid and plate temperatures. This mean plate temperature is then used as the input to the described procedure and repeated until convergence occurs.

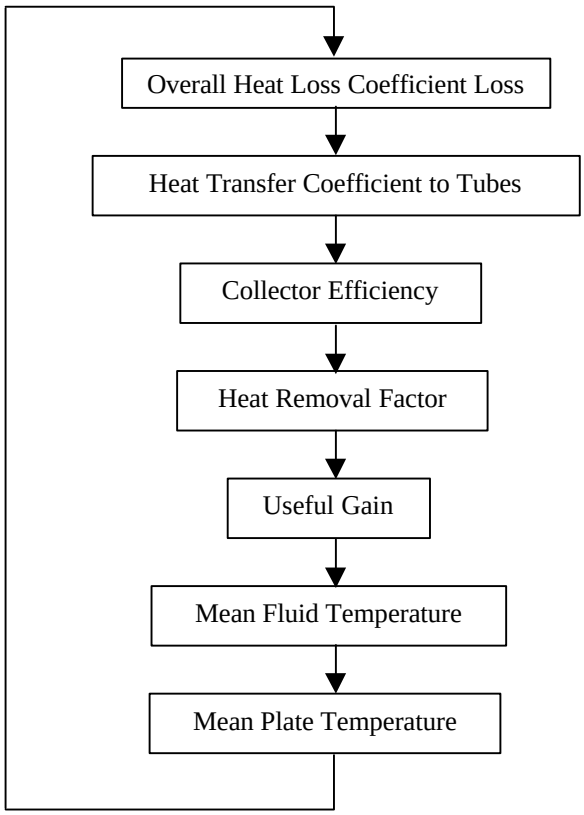

Figure 5.21: Iterative calculation process used to predict collector performance.

5.4.2 Predicting the Supply Profile from a Solar Collector System

The performance of the collector is largely determined by the inlet temperature and mass flow rate of the circulating fluid. Therefore, to accurately simulate a hot water supply profile the entire collector system requires to be analysed. The model developed applies to systems using water as the circulating fluid, however, collector performance utilising other liquids could be calculated similarly. The analysis of collectors using air as the circulating fluid, will require further refinement of the model presented. Examples of other fluid mediums used in collectors are anti-freeze solutions, which enable system operation through freezing conditions. Anti-freeze solutions are used together with heat exchangers, which transfer the solar gain to water in the storage tank.

Heat exchangers reduce the overall system efficiency, with mathematical models for various heat exchangers requiring to be incorporated to account for such losses.

The model developed enables the following hot water supply scenarios to be investigated:

1. A constant inlet temperature: this option enables supply profiles to be simulated and subsequently used to examine the effects of specific design characteristics of the collector itself. Additionally, this scenario aids the identification a bulk supply profile for large-scale studies, where the sizing of individual storage tanks may not be appropriate. However, it must be stressed here that although the resultant profile will produce an indication of performance, in reality the systems' inlet temperature will vary depending on the energy gained from the collector, and on the rate of heat removal through hot water demand.
2. A storage tank with no additional auxiliary heating system.
3. A storage tank with an inflow water heater, which supplies any additional heating requirements on demand.
4. A two-tank system, whereby a preheat tank is used, through which the circulating water flows, and an additional hot water storage tank which is kept at a minimum storage temperature by an auxiliary heating device.

The performance of each of these four systems will be influenced by the circulation control system defined. The circulation control system is used to specify the manner in which fluid is circulated through the tubes. In this model forced circulation is assumed with a specified flow rate. A controller acts to assume pumping only when a specified temperature difference between the fluid inlet and outlet temperatures is attained, therefore ensuring that pumping is justified. Additionally, the controller is used to discontinue operation during freezing conditions, if required. Natural convection has not been modelled as further work is required to estimate the flow rates resulting from changes in the temperature gradients, which produce the buoyancy forces.

Performance under constant inlet temperature conditions

Figure 5.22 illustrates the basic components incorporated in the hypothetical flat-plate collector system, assuming constant inlet temperatures conditions. Where forced circulation is being modelled, the controller acts to pump the fluid through the collector when the required temperature difference between the inlet, denoted the cold water temperature, T_{cw}, and the outlet or collector temperature, T_c, is reached. When this temperature difference is not attained, an energy balance is performed assuming no circulation. Additionally, if the controller is configured for freezing conditions, the average ambient temperature is evaluated and if below the freezing set point, the fluid is not circulated.

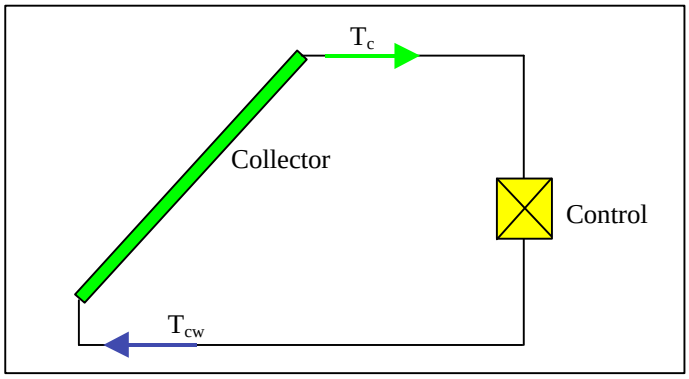

Figure 5.22: Hypothetical Collector Configuration Assuming Constant Inlet Temperature Conditions

Performance with Single Storage Tank and no Auxiliary Heating

A collector system configured with a storage tank, is illustrated in Figure 5.23. The fluid circulates through the collector and storage tank depending on the controller as discussed previously. The storage tank itself will incur heat loss to the environment, which is modelled according to Equation 5.47.

$$Q_{s\_loss} = \frac{k_s}{t_s} \cdot A_s \cdot (T_f - T_a) \qquad \text{Equation 5.47}$$

Where k_s = thermal conductivity of the storage tank insulation

T_s = thickness of storage tank insulation

A_s = surface area of storage tank

T_f = temperature of the fluid in the storage tank

The collector performance will be very influenced by the draw off from the tank. The tank draw off is given in the form of a hot water demand profile in kW. To obtain such a profile, the mass flow rate of hot water required over time, is multiplied by the specific heat capacity of water and the temperature difference obtained in heating cold water at 10°C to 65°C. Thus the mass flow rate associated with a hot water demand is calculated using Equation 4.48, and the heat lost from the tank, in meeting the demand is obtained from Equation 5.49.

$$m = \frac{Q_{demand}}{Cp \cdot 55} \qquad \text{Equation 5.48}$$

$$Q_{demand} = m \cdot Cp \cdot (T_f - T_{return}) \qquad \text{Equation 5.49}$$

The assumption that the supply temperature is 65°C, used in calculating the demand, is flawed with this configuration, as the assumed supply temperature may not be attained.

As the heat flows associated with the storage tank are all dependent on the temperature of the fluid in the tank, and energy balance is again used to determine the tank temperature and solved using the Newton Raphson method.

$$m \cdot Cp \cdot \Delta T = Q_{gain} - Q_{s\_loss} - Q_{demand}$$ Equation 5.50

Where Q_{gain} = Useful energy gained from the solar collector (i.e. Q_u)

From Figure 5.23, it can be seen that the calculated tank temperature is subsequently used as the collector inlet temperature.

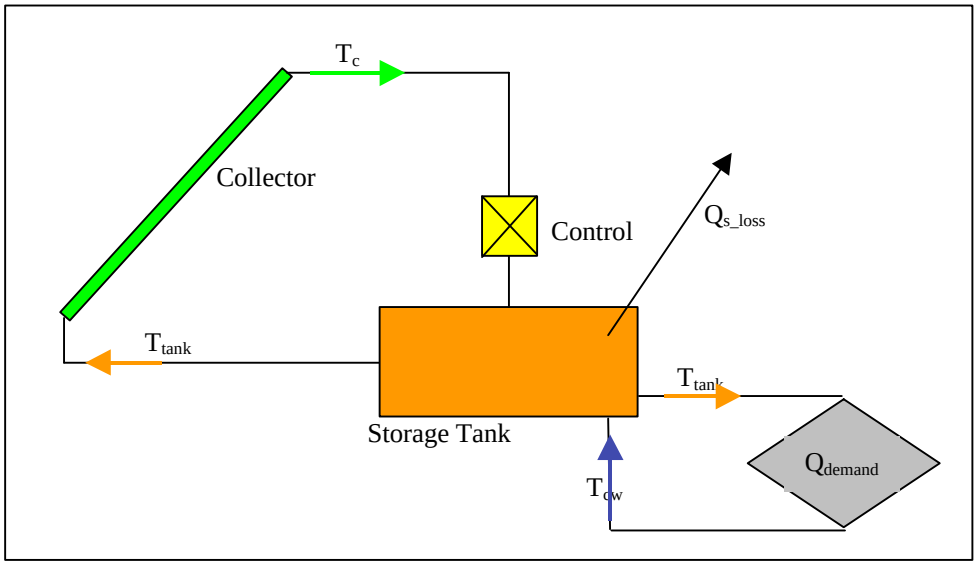

Figure 5.23: Collector system with storage tank supplying a hot water demand

Performance with Single Storage Tank and Flow-line Auxiliary Heating

Including an auxiliary flow line heater into the configuration just described enables the simulation of a more realistic hot water supply system, as some auxiliary heating system will typically be used in conjunction with the flat plate. Mathematically this configuration is treated just as it is without the flow-line heater. One additional equation is used to determine the power supplied by the auxiliary system, in providing the required supply temperature (assumed to be 65°C), Equation 5.51 describes this additional term.

$$Q_{heater} = m \cdot Cp \cdot (65 - T_f)$$ Equation 5.51

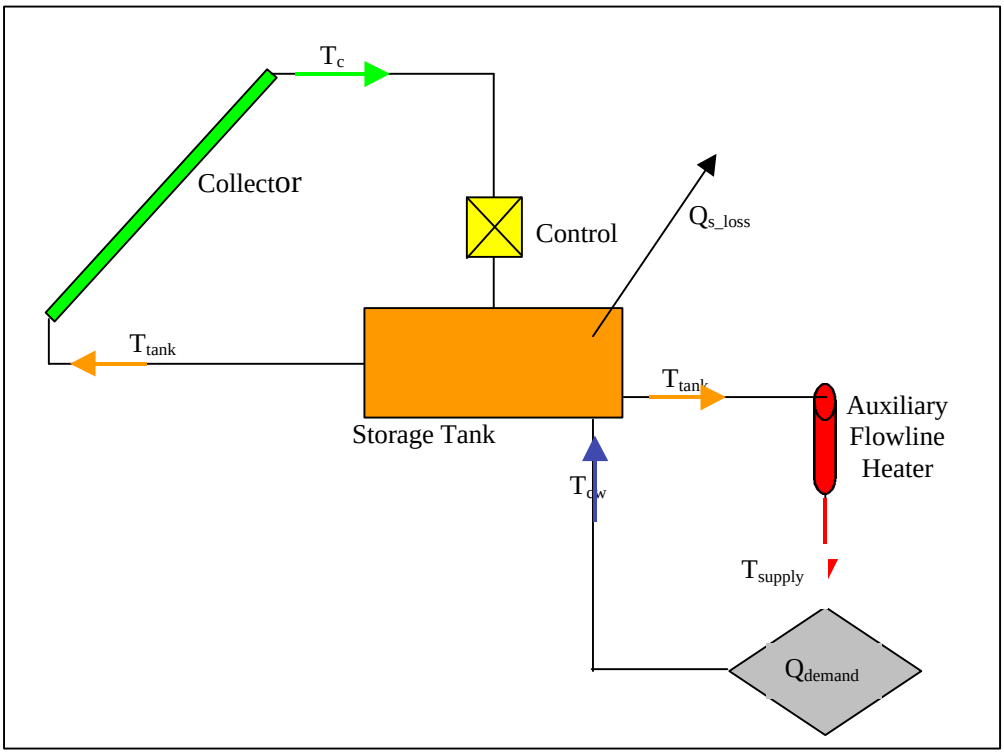

Figure 5.24: Collector system with storage tank supplying a hot water demand via a flow-line auxiliary heating system

Performance with Preheat and Constant Temperature Storage Tanks

Figure 5.25 describes a system configured with a preheat tank and a main storage tank. The main storage tank is kept at a set storage temperature, typically 65°C. A preheat tank is used to prevent such high temperatures being circulated through the collector, thereby diminishing the solar gain. Each of the tanks will incur heat losses to the environment, which are calculated using Equation 5.47 with respect to each of the tank fluid temperatures. The preheat tank will incur a heat loss to the main tank when hot water is drawn off. This heat loss equates to the heat gain in the main tank, and can be

obtained using Equation 5.52. The mass flow rate associated with the demand is that described by Equation 5.48.

$$Q_{tank1\_loss} = Q_{tank2\_gain} = m \cdot Cp \cdot (T_{f1} - T_{return}) \qquad \text{Equation 5.52}$$

Where T_{f1} is the temperature of the fluid in the preheat tank.

An energy balance equation for each of the tanks is required to evaluate the water storage temperatures. The preheat temperature is subsequently used as the collector inlet temperature, and the temperature of the main storage tank is used to find the additional heat supplied by an auxiliary heater to maintain the specified storage temperature.

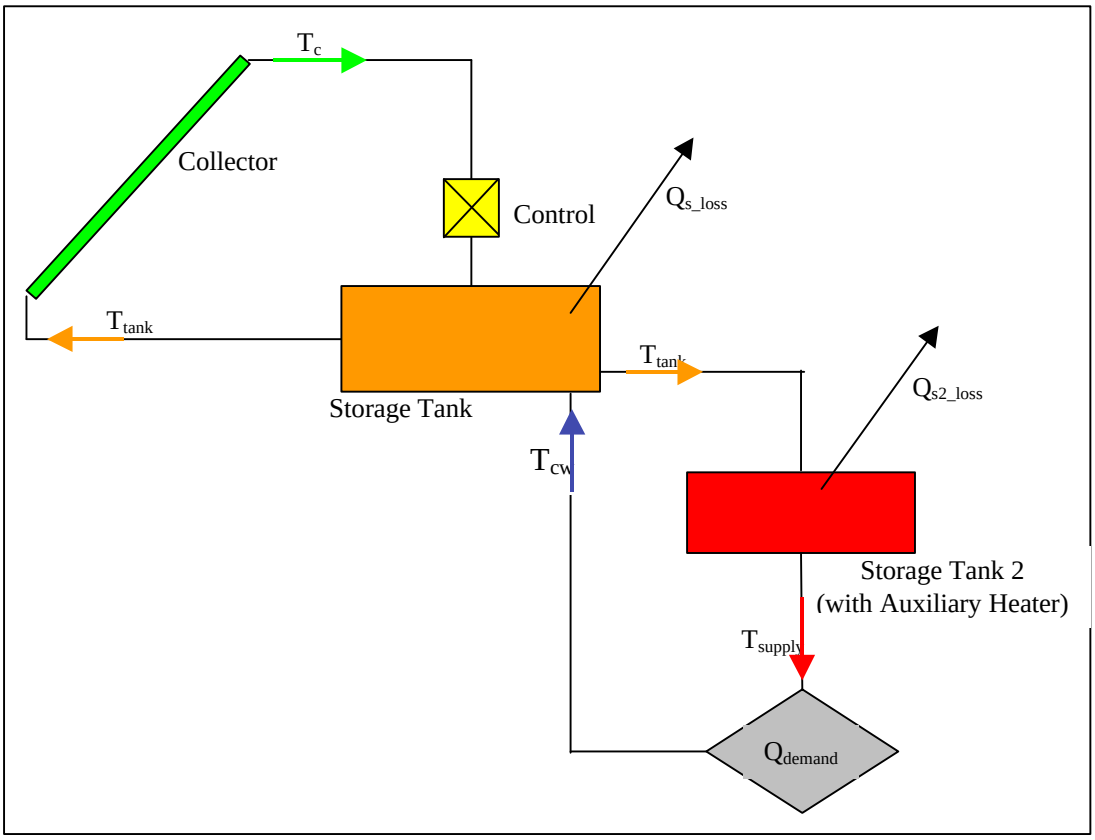

Figure 5.25: Collector system with preliminary and main storage tanks

$$(m \cdot Cp \cdot \Delta T)_{tank2} = Q_{tank1\_loss} - Q_{s2\_loss} - Q_{demand} \quad \text{Equation 5.53}$$

$$(m \cdot Cp \cdot \Delta T)_{tank1} = Q_{gain} - Q_{tank1\_loss} - Q_{s1\_loss} \quad \text{Equation 5.54}$$

The heat addition from the auxiliary system is therefor obtained as follows:

$$Q_{heater} = m \cdot Cp \cdot (65 - T_{f2}) \quad \text{Equation 5.55}$$

Summary of Calculation Methodology

The previous sections have described the calculations required to obtain supply profiles from a variety of solar collector systems. Four systems have been incorporated in the model; without storage, with storage (with and without an additional heating element), and finally with two storage tanks, a preheat tank and a main storage tank kept at a specified temperature by an auxiliary heating system. It is assumed that pumped circulation is employed, and a control system ensures the fluid is only circulated through the collector when a set temperature difference between collector inlet and outlet temperatures is attained. Separate energy balance techniques are employed to simulate the performance of a collector during fluid circulation, and to predict temperature changes within the system when the fluid is stationary. To obtain a hot water supply profile the collector is modelled temporally in conjunction with a hot water demand profile. The demand is required as an input parameter just as other driving variables e.g. climatic parameters, are required. The fluid, plate and cover temperatures within the system are calculated at each time step, and are used as the basis for subsequent calculations. Figure 5.26 describes a flow chart, which summarises the calculation process for each time interval.

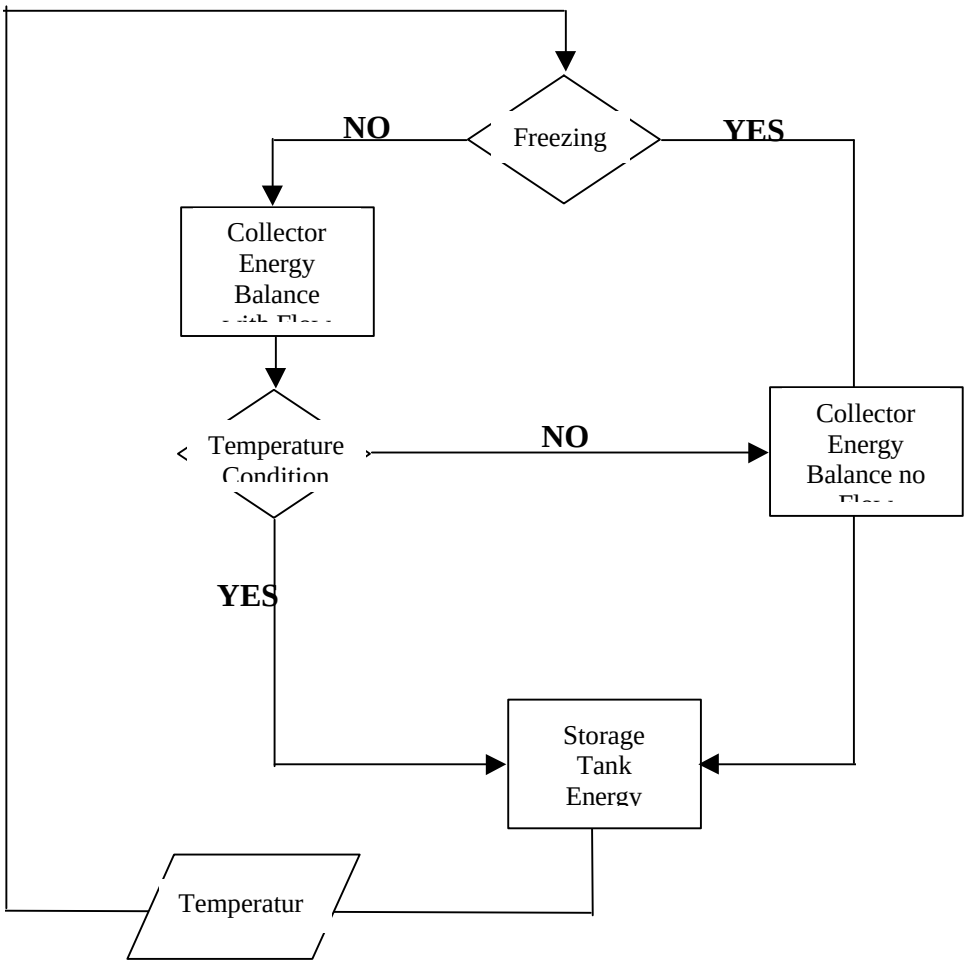

Figure 5.26: Flow chart summarising calculation process of flat-plate collector systems

5.5 Summary

Three modelling approaches have been described as a means for obtaining supply profiles from RE systems. Each method utilises temporal climatic data and manufacturers' data to predict the performance of characterised systems, accounting for the effects of location. The objectives in developing the models described were that the models be generic and thus applicable to a variety of systems independent of individual design attributes, and that model input parameters could readily obtainable from

manufacturers' data. The methods used to derive the models presented in this chapter could be applied to other renewable systems such as fuel cells, as manufacturers' data become available.

Each of the models presented account for effects of locality. The performance of RE systems is known to be very sensitive to the system surroundings. Accounting for locality enables location optimisation prior to instalment, where optimisation in the context of this work refers to the ability of a supply profile to meet that of a demand profile.

The PV model described is only generic for silicon cells. The characteristics of amorphous silicon differ significantly from mono and poly crystalline cells, and the mathematical description of this type of PV cell fell out with the bounds of this work. Additionally, no corrections have been included to account for the effects of shading of dust on the panel surface.

No corrections have been included for the non-availability of the wind turbine due to repair and maintenance. This factor could be incorporated by the reduction of power output by a user specified outage percentage, however in terms of correlating supply and demand profiles this approach would not result in a realistic indication of match. Other control systems present in wind turbine designs, such as load control, yaw control and aileron control, have not been encompassed. Analysis of the structural loading experienced by wind turbines is also not included.

The solar water-heating model was described for a number of different flat plate and storage tank configurations. The solar water heating system is unique to the other models because its performance is dependent on the demand for hot water. As with the PV model, the effects of shading and dust have been neglected.

5.6 References

1. Brandemuehl M. J. and Beckman W. A., “Transmission of Diffuse Radiation through CPC and Flat-Plate Collector Glazings,” Solar Energy, Vol. 24, pp. 511, 1980.
2. Caamano E. and Lorenzo E., Modelling and Financial Analysis Tools for PV Grid-connected Systems, Progress in Photovoltaics: Research and Applications, Vol. 4, 1996, pp295-305.
3. Calais M., Agelidis V.G. and Meinhardt M., Multilevel Converters for Single-Phase Grid Connected Photovoltaic Systems: An Overview, Solar Energy Vol. 66, No. 5, pp 325-335, 1999
4. Child D., Smith I. R., Infield D. G., Wind, Photovoltaic and Battery Electrical Power: Experience and Modelling of an Autonomous and Grid Connected System. International Journal of Ambient Energy, Volume 17, Number 3, July 1996.
5. Clarke J. A., Energy Simulation in Building Design, Hilger, Bristol 1985.
6. Decher Reiner, Direct Energy Conversion, Fundamentals of Electrical Power Production, Oxford University Press, 1997
7. Duffie, J.A. and Beckman W. A., Solar Energy Thermal Processes, John Wiley & Sons, New York, 1974
8. Enslin J.H.R. and Potgieter A. W., Computer Aided Design of Renewable energy systems. Elektron, Volume 8, issue 7.
9. Evans M. S., Plant Modelling and Simulation for Small Renewable Energy Systems. M.Sc. Thesis, University of Strathclyde, September 1994.
10. Fry Bryan, Simulation of Grid-Tied Building Integrated Photovoltaic Systems, Msc Thesis University of Wisconsin – Madison, 1998, URL:http://sel.me.wisc.edu/theses/fry98.zip
11. Giguère Philippe and Selig Michael S., Blade Design Trade-offs Using Low-lift Airfoils for Stall Regulated HAWTS, ASME/AAA Wind Energy Symposium, Reno, Nevada, January 11-14, 1999

12. Grant A.D., Nasr el-Din S.A., Kilpatric J., Development of a Ducted Wind Energy Converter. Wind Engineering Volume 18 , Number 6, p.297-303, 1994.
13. Hand M.M. and Balas M.J., Non-Linear and Linear Model Based Controller Design for Variable-Speed Wind Turbines, 3 rd ASME/JSME Joint Fluids Engineering Conference, San Francisco, California, July 18-23, 1999
14. Hiyama T. and Kouzuma S., Application of Neural //network To Prediction of Maximum Power From PV Modules, IEE 2nd International Conference in Power Control, Operation and Management, December 1993, Hong Kong. pp. 349-354.
15. Hollands, K. G. T., Unny, T. E., Raithby, G. D., and Lonicek, L, "Free Convection Heat Transfer Across Inclined Air Layers," Transactions of ASME Journal of Heat Transfer, Vol. 98, pp. 189, 1976.
16. Incropera, F. P. and DeWitt, D. P., Fundamentals of Heat and Mass Transfer, 4th Edition, John Wiley & Sons, New York, 1996.
17. Katan R. E., Agelidis V. G., Nayar C. V., PSPICE Modelling of Photovoltaic Arrays, 1995
18. Kelly Nicolas, Towards a Design Environment for Building-Integrated Energy Systems: The Integration of Electrical Power Flow Modelling with Building Simulation, PhD Thesis Strathclyde University, October 1998
19. Koo Jae-Mo,Development of a Flat-plate Solar Collector Design Program, MSc Thesis, University of Wisconsin-Madison, 1999.URL:http://sel.me.wisc.edu/theses/koo99.zip
20. Lanzerstofer S., Bauer G., Kepler Johanes, Losses by Reflection of Crystalline PV Modules, 13th European Photovoltaic Solar Energy Conference, 23-27th October 1995
21. Mattson M., Moshfegh B. Sandburgh M. and Stymnv H., Integration of PV elements in Building Components, KTH 1995
22. Markvart T. and Arnold R. J., Integration of Photo-Voltaic Convertors into the Public Electricity Supply Network, IEE, 1997
23. Maroto J.C. and Araujo G.L., Three-Dimentional Circuit Analysis applied to Solar Cell Modelling, 1997

24. Muljadi E., Pierce K and Migliore P., Control Strategy for Variable-Speed, Stall-Regulated Wind Turbines, American Controls Conference, June 24–26, 1998
25. Pendas I.A., Investigation of a Wind Energy Module. Final Year Project Thesis, University of Stathclyde, May 1999.
26. Petukhov, B. S., in T. F. Irvine and J. P. Hartnett eds., advances in Heat Transfer, Vol 6, Academic Press, New York 1970.
27. Pierce Kirk and Fingersh Lee Jay, Wind Turbine Control System Modelling Capabilities, American Controls Conference, Philadelphia, PA, June 24-26, 1998
28. Preu R., Kleiss G., Reiche K., Bucher K., PV-Module Reflection Losses: Measurement, Simulation and Influence on Energy Yield and Performance Ratio, 13th European Photovoltaic Solar Energy Conference, 23-27th October 1995
29. Ramirez M. A. S., Electrification of a Saline Based Dwelling by Means of a Stand-alone Rural Energy System. M.Sc. Thesis, University of Strathclyde, September 1998.
30. Robinson M.C., Hand M.M., D.A. Simms D. A., and Schreck S.J., Horizontal Axis Wind Turbine Aerodynamics: Three-Dimensional, Unsteady, and Separated Flow Influences, 3rd ASME/JSME Joint Fluids Energy Conference San Francisco, July 22, 1999
31. Rogers and Mayhew, Engineering Thermodynamics – Work and Heat Transfer 4th Edition, Longman Group Limited 1998,
32. Rogers G. and Mayhew Y., Thermodynamic and Transport Properties of Fluids –SI Units, Basil Blackwell Ltd, 1992.
33. Russell Miles C., Grid-tied PV System Modelling: How and Why, WCPEC; Dec 5-9, 1994; Hawaii
34. Simmons Anton, Building Integrated Photovoltaic Systems, Session 2: Technical Aspects of BIPV, The Electrical System and its Interaction with the Utility Grid, CREST, Loughborough University,URL:www.loughborough.ac.uk, 2000
35. Troen Ib, Lundtang Petersen: European Wind Atlas, Risoe National Laboratory, Risoe, Denmark, 1991, ISBN 87-550-1482-8, URL:http://www.risoe.dk/, 2000

36. Webster, G.W., Devices for Utilising the Power of the Wind, United States Patent 4152556, May 1979.
37. Yiqin, Y, Hollands, K. G. T., Brunger, A. P., “Measured Top Heat Loss Coefficients for Flat Plate Collectors with Inner Teflon Covers,” Proceedings of the Biennial Congress of the International Solar Energy Society, Denver, Colorado, USA, August 19-23, pp. 1200, 1991.
38. Wind Energy Reference Manual Part 1: Wind Energy Concepts URL:http://www.windpower.dk/tour/wres/calculat.html
39. De Montfort University, Wind Energy Training Course, Module 3 Technology, Section 2 Aerodynamics and Power Control. URL:http://www.iesd.dmu.ac.uk/~slb/m32potex.html
40. MacAdams, W. C., Heat Transmission, 3rd Edition, New York, McGraw Hill, 1954.
41. Siegel, R. and Howell, J. R., Thermal Radiation Heat Transfer, 3rd Edition, Taylor & Francis, New York, 1992.
42. Scheaffer Richard L. and McClave James T., Statistics for Engineers, PWS Publishers, 1982
43. Stanzel B., Chapter 6, External Longwave Radiation,
44. Gnielinski, V., Int. Chem. Eng., Vol. 16, pp. 357, 1976

Chapter 6: Matching Supply and Demand

The necessity for matching techniques pertaining to supply and demand profiles was discussed in Chapter 3. Chapters 4 and 5 described various techniques employed to obtain demand and supply profiles. This chapter examines methods, which enable sets of profiles to be analysed to quantify the match between supply and demand. The objective of matching is to ensure periods of generation coincide with periods of consumption. The accuracy of a particular match is dependent on the ability of the demand and supply profiles used in the analysis, to accurately portray reality. In the case of RE supply profiles, accuracy is a function of the climatic parameters used as inputs to the model. Data resolution will also affect the match statistics obtained. At very high frequency data in the order of seconds, a poor match may be obtained which if time averaged over half hourly intervals may result in a significantly improved scenario.

6.1 The Hierarchy of Profiles

Small-scale renewable systems at the building level do not financially benefit from grid export and in some circumstances grid export may not even be feasible due to limited system capacity. These systems should therefore be sized in such a way as to minimise grid export and ideally, to have the net effect of levelling demand profiles. In identifying supplies which level demands, the opportunities for renewable integration strategies become apparent, which have the additional benefits of improving the existing supply network and being relatively predictable in terms of demand forecasting. Demand side management activities are used in an attempt to smooth the system load curve by reducing or eliminating coincident peaks. A uniform load curve would enable generating plant to be run at optimum efficiencies, without the requirement for peaking plant. Additionally, without significant variability in demand, transmission and distribution systems could be sized according to base loads and the

tasks of tariff setting, energy trading settlement and demand forecasting would be facilitated. The ideal load curve could thus be described by a flat line. In terms of sustainability, this flat profile would additionally be of reduced energy consumption. By identifying coincident trends in supply and demand profiles, the opportunities for RE deployment in a DSM role become apparent. In order to quantify the effects of renewables it is suggested that demand profiles exist in a graded system or hierarchy. The ideal 'flat' profile will rarely occur in reality, but it can be seen as head of the profile hierarchy, where the degree of variability determines profile rank. Low ranking profiles may migrate up the hierarchy via different routes. The profile of an end-use appliance or process may be modified in two ways. Firstly, through an increase in efficiency that would reduce the energy content of the profile. Secondly, by some load management strategy aimed at reducing the magnitude or frequency of peaks in a profile. Increased efficiencies result from technological developments. Load management strategies encompass control methods and profile combinations. Cranfield University (Newborough and Augood, 1999) investigated various integrated control strategies for the management of a household's coincident peak power demands. The study illustrates the manner in which profiles of individual appliances can climb the hierarchy by control methods. Figures 6.1 and 6.2, taken from this study, illustrate the effects of improved control algorithms applied to an electric hob and a washing machine respectively. The reduction in 'peaky behaviour' resulting from improved control can be readily observed. Load management strategies can equally be applied to a set of appliance/process profiles that represent the profile of a particular site. By avoiding the coincident operation of appliances, the combined site-profile is levelled as the component profiles are distributed over time

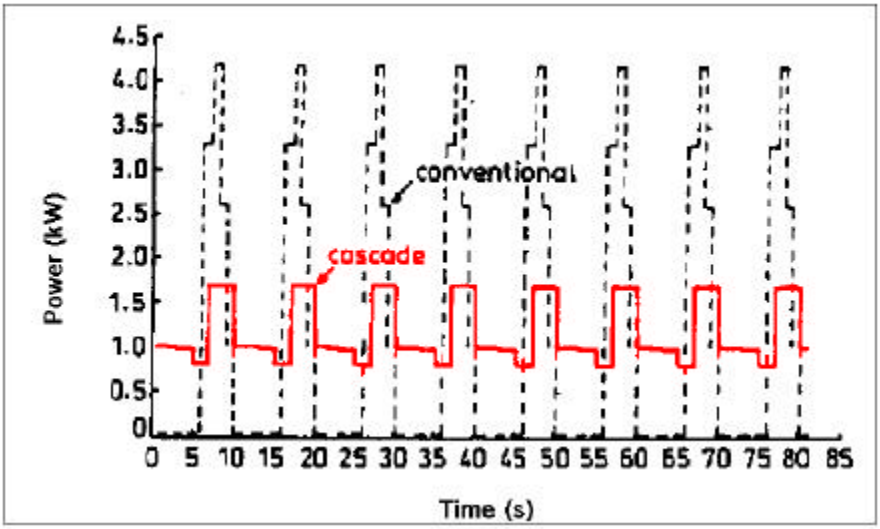

Figure 6.1: Comparison of the demand profiles associated with a conventional and load conscious control algorithms for an electric hob with four heaters (Newborough and Augood, 1999)

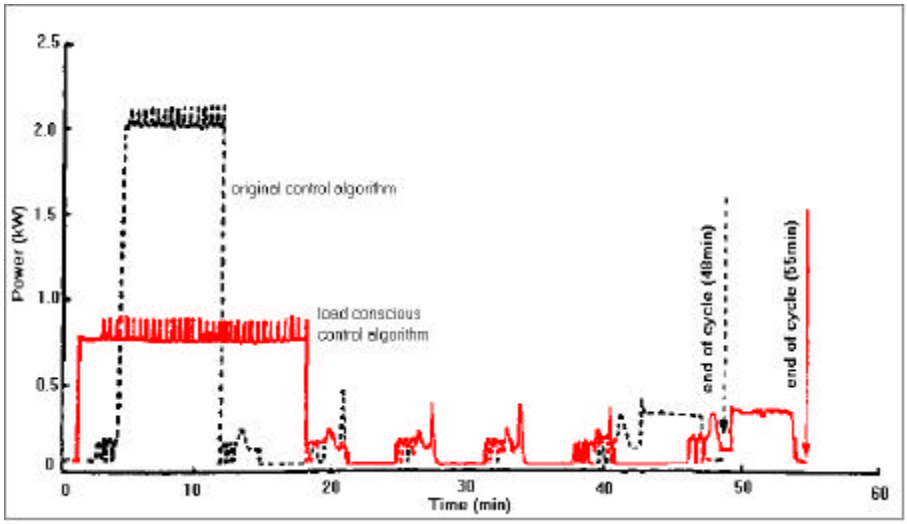

Figure 6.2: Comparison of the demand profiles associated with a conventional and load conscious control algorithms for a washing machine (Newborough and Augood, 1999)

Another strategy for increasing profile rank is through the combination of supply and demand profiles that mirror each others characteristic peaks. As the sign convention of supply and demand profiles is reversed, combining similar profiles of opposite sign leads to a cancelling out of peaks in a combination, resulting in an increase in the hierarchical status.

A profile's rank may be described mathematically simply by using the statistical parameters mean and variance. Mean describes the average energy content and variance the variability of a profile.

$$x_{mean} = \frac{1}{N} \cdot \sum_{n=1}^{N} x(n) \qquad \text{Equation 6.1}$$

$$\sigma = \frac{1}{N} \cdot \sum_{n=1}^{N} \left(x(n) - x_{mean}\right)^2 \qquad \text{Equation 6.2}$$

Where x_{mean} is the mean and σ the variance, N is the time period and x is the energy value at a given time n.

The ranking of demand profiles enables the benefits of deploying green technologies to be quantified. Both of mean and variance are inversely proportional to rank, with a decrease in either quantity resulting in an increase in rank. Rank is relative to a given period, which means a profile may score highly at certain times of the year and poorly at other times. Furthermore, rank is relative to the demand profile and although it enables different supply options to be compared in terms of their effect on a particular demand profile, it does not enable the comparison of different demands and supplies.

6.2 Match Assessment

Mathematical techniques are required to assess the temporal match between demand and supply profiles. A number of different statistical methods are available, which can be employed to define the match or goodness of fit between two profiles. These statistics will be examined using an example in matching renewable output with demand. There are two elements, which require to be considered in matching, magnitude and phase. Ensuring the magnitude of supply corresponds to that of the demand is the basis of energy matching and has been applied in other work (Ramakumar et al., 1992), (Iniyan et al., 2000). However, focusing on matching magnitudes alone could lead to the energy being supplied at times when demand for it is low. Thus, to ensure generation is not wasted, matching must encompass the relative phases of demand and supply.

The example used to demonstrate matching techniques considers a small commercial demand profile and the supply profiles from a 3 kW wind turbine system, and a 3 kW PV system, in a one-week period in June, with U.K. climate. Figures 6.3 and 6.4 illustrate the temporal match between the demand and the wind system and the demand and the PV system, respectively. Visual examination of these Figures demonstrates the difficulty in determining which, if any, of the RE systems is best matched to the demand. The wind system output is seen to increase throughout the week, with its most productive period occurring over the weekend where the demand is at its lowest. The PV system output is seen to exceed the demand over the midday hours on all but one day. Neither system meets the entire demand over the period shown and both sets of profiles contain periods when the supply exceeds the demand, which would either require to be grid exported or wasted.

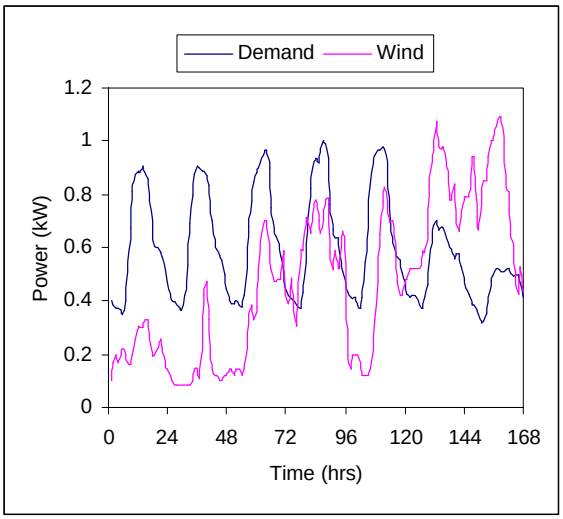

Figure 6.3: Matching with a wind system

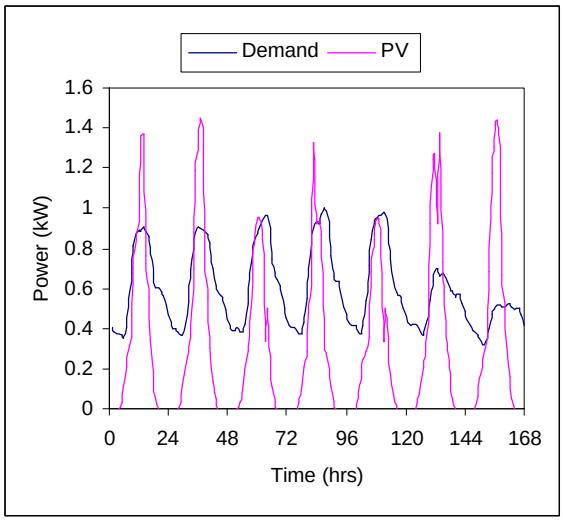

Figure 6.4: Matching with a PV system

Mathew et al (Mathew et al., 1999) defined an energy self-sustenance index for different energy measures based on temporal end use as described by Equation 6.3. A building's self-sustenance is therefore the ratio of the demand displaced by on-site generation, to the demand without generation. The optimal value for self-sustenance is taken to be unity, whereby all the sites demand could be displaced by on site generation. The difficulty with this index is that although it accounts for displaced energy, it neglects excess production.

$$ESS_x = \frac{\sum_{t=1}^{n} disp_{x,t}}{\sum_{t=1}^{n} dem_{x,t}} \qquad \text{Equation 6.3}$$

Where ESS_x = site energy self sustenance for energy type x

$disp_{x,t}$ = energy displacement by generation system, for energy type x, at time t

$dem_{x,t}$ = energy demand of a building without generation, for energy type x, at time t

n = total number of time steps

Similarly, match evaluation could be based on the area common to both profiles. The shared area, SA, is described by Equation 6.4 as the union, denoted by U, between the area under the demand and supply profiles. This value can be approximated by evaluating the area between the x-axis and the lowest value between supply and demand for every time step.

$$SA = \left(\int_0^n D(t)\,dt \right) U \left(\int_0^n S(t)\,dt \right) \qquad \text{Equation 6.4}$$

Where D(t) = demand profile

S(t) = supply profile

n = time period

When comparing scenarios where one of the profiles is common, i.e. a demand profile matched to a number of supplies or vice-versa, the shared area can be used to compare the individual matches. For the above example, the shared area in the wind scenario is 63.93 kWh, and in the case of PV is 44.84 kWh, indicating that the wind system is better matched to this demand. However, the shared area term becomes less meaningful when comparing matches between different demands and supplies. For example, if the demand were doubled and the number of panels in the PV system were doubled, the shared area term would double and so too would the residual. Thus, shared area needs to be expressed as a percentage of the demand area, as described in Equation 6.5, to be used as a valid means for comparing different sets of profiles.

$$\%SA = \frac{\left(\int_0^n D(t)\,dt\right) U \left(\int_0^n S(t)\,dt\right)}{\int_0^n D(t)\,dt} \qquad \text{Equation 6.5}$$

Although this term describes the portion of demand satisfied by the RE system, it gives no indication of excess supply. The excess supply, ES, can be obtained by subtracting the shared area from the supply area and expressing the result as a percentage of the supply as described in Equation 6.6. However, this now requires that both terms are included to make valid comparisons between different sets of profiles. Additionally, a question of priority is introduced, as to whether the importance is in meeting the demand or in using the supply. To achieve a perfect match both are equally important and in the case of a perfect match %SA would equal 100 and %ES zero. The addition of these terms yields an optimum value of 100, however non-perfect match values could range above and below this figure, making judicious comparisons difficult.

$$\%ES = \frac{\int_0^n S(t)\,dt - \left[\left(\int_0^n D(t)\,dt\right) U \left(\int_0^n S(t)\,dt\right)\right]}{\int_0^n S(t)\,dt} \,. \qquad \text{Equation 6.6}$$

The residual, r(t), of two profiles can be used to represent the combined profile and can be obtained by simply subtracting the supply at each time step from the demand, as described by Equation 6.7.. This is the profile the supply grid would ‘see’. There are two possible ‘net-profiles’, one where the excess supply is exported to the grid and one where it is dumped to some external load. The residual profiles from the above example are illustrated in Figures 6.5, where the excess is exported and in Figure 6.6, where the excess is dumped. It can be seen that the variability on the grid is increased in the case of exporting surplus energy production. However, dumping the surplus supply

will rarely promote the use of renewable technologies. The two ranking statistics: mean and variance, which represent the energy content and variability of a profile have been calculated for both export and non-export scenarios and are illustrated in Figure 6.7.

$$r(t) = D(t) - S(t) \qquad \text{Equation 6.7}$$

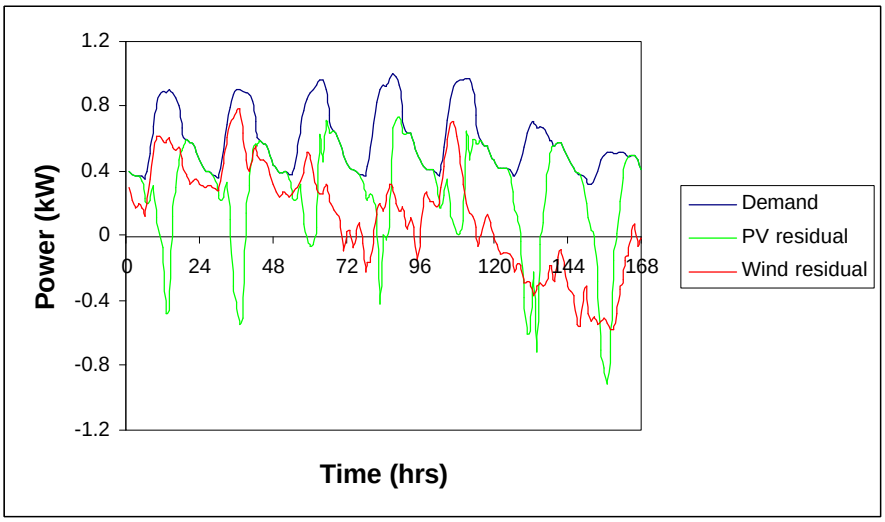

Figure 6.5: Comparison of original demand, residual profiles resulting from wind technology deployment and from PV deployment, with grid export.

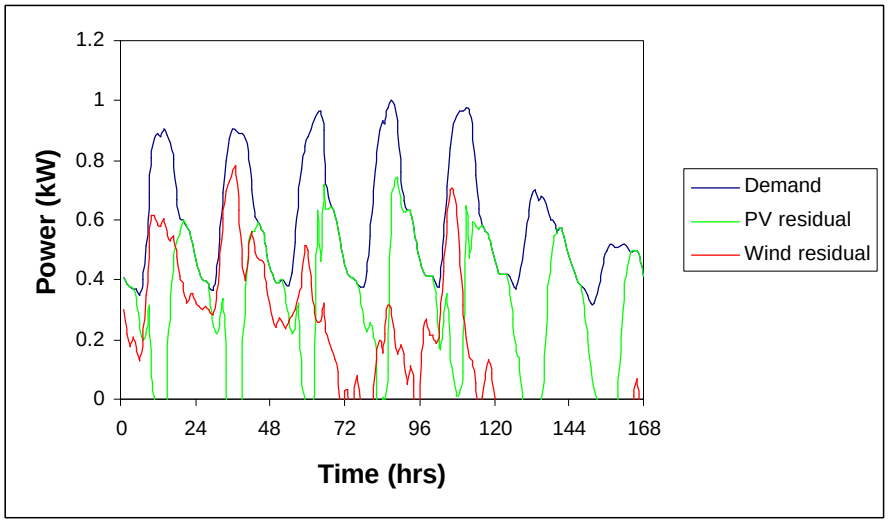

Figure 6.6: Comparison of original demand, residual profiles resulting from wind technology deployment and from PV deployment, without grid export.

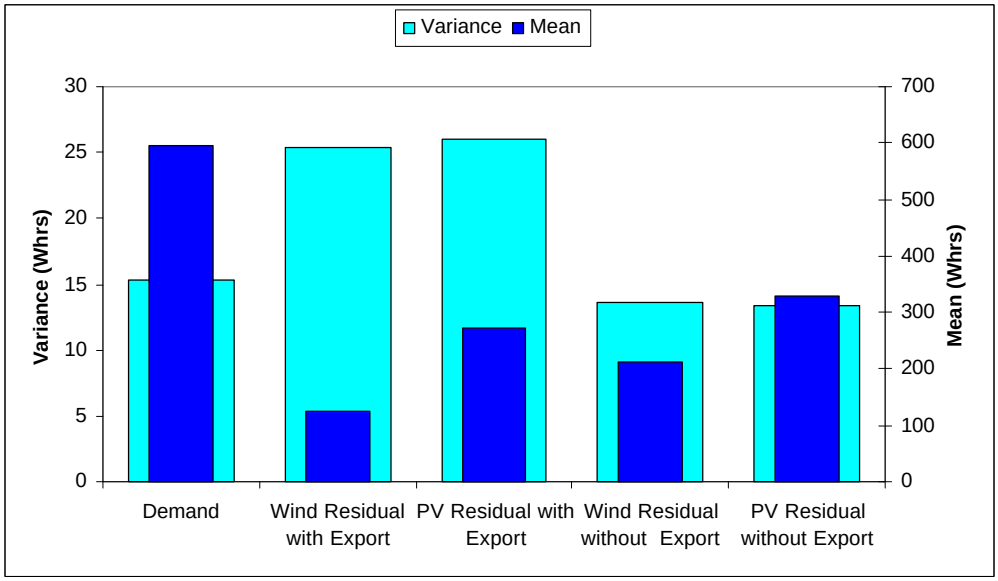

Figure 6.7: Comparison of statistics associated with the demand and different resultant demand profiles

Figure 6.7, illustrates the reduction in energy requirement due to RE deployment. In the cases associated with grid export this is particularly pronounced due to the negative values associated with exportation. The variability is increased significantly through grid export, which if this were to occur on a large-scale could result in grid instability. Without export, the variability is only reduced moderately and the unfavourable aspects of wasting RE are not accounted for. The rank of the demand profile can be seen to increase with RE integration without grid export, although with grid export improvements in rank become unclear. The match between demand and supply is not accurately described using this method.

A variety of statistical techniques can be applied to a profile pair to assess their match. The least-squares approach (Scheaffer and McClave, 1982) can be used to quantify the magnitude of deviation between two sets of data variables and has been used in quantifying differences in simulated time series (Dewson et al., 1993). This method can be applied to supply and demand profiles, where the least-squares value is obtained using Equation 6.8. This metric, will always yield a positive value, with a lower limit of zero indicating a perfect match and without an upper limit. The least-squares method can be used to compare different matches, with the lowest resulting value indicating the optimal match. In the current example, the least squares metric between the PV and demand profiles is 31.4557 and in the case of wind 20.924. It is clear that the match with the wind system is better than that of the PV. However, because of the lack of an upper limit, it is difficult to establish the difference in the quality of match. Where numerous profile pairs are to be compared, bands defining the quality of match are useful in processing various possibilities, although establishing such bands is extremely difficult where a worst case cannot be defined.

$$LS = \sum_{t=0}^{n} \left(D_t - S_t\right)^2 \qquad \text{Equation 6.8}$$

Spearman's Rank Correlation Coefficient (Scheaffer and McClave, 1982) describes the correlation between any pair of variables by calculating the degree to which the variables fall on the same least square line. Calculation of this coefficient will always result in a value between -1 and 1. A result of 1 indicates perfect positive correlation and –1 perfect negative correlation, i.e. as one variable tends to increase the other will decrease at the same rate. A value of zero denotes no correlation between the variables. The correlation coefficient, CC, between a demand and a supply profile, is calculated as described by Equation 6.9. For the previous example, the correlation between the PV profile and the demand is 0.115 and for wind 0.604. The figures again demonstrate the match with wind is superior. The coefficient is used to describe the trend between two data sets and does not consider the relative magnitudes of the individual variables. Thus, if the wind system were doubled in size the correlation coefficient would remain the same even though the excess supply would be far greater. Additionally, two profiles perfectly in phase with one another, but of very different magnitudes, would result in a perfect correlation, but not a perfect match. Nevertheless, it provides a measure of the potential match that could exist given changes to the relative capacities, i.e. through energy efficiency or altering the size of the RE system.

$$CC = \frac{\sum_{t=0}^{n} (D_t - d)\cdot(S_t - s)}{\sqrt{\sum_{t=0}^{n} (D_t - d)^2 \cdot \sum_{t=0}^{n} (S_t - s)^2}} \qquad \text{Equation 6.9}$$

Where D_t = demand at time t

S_t = supply at time t

d = mean demand over time period n

s = mean supply over time period n

Williamson (Williamson, 1994) describes an inequality coefficient used to validate prediction models used in thermal performance. The Inequality Coefficient, IC, describes the inequality in a time-series due to three sources: unequal tendency (mean), unequal variation (variance) and imperfect co-variation (co-variance) as described by Equation 6.10. The resultant coefficient can range in values between zero and one, with zero indicating a perfect match and one denoting no match. The inequalities in the above example are 0.375 and 0.299 for PV and wind, respectively. This metric is ideally suited to establishing bands of match, where matches resulting in inequalities between 0 and 0.1 could be termed good matches and bad matches are those resulting in values between 0.9 and 1.

$$IC = \frac{\sqrt{\frac{1}{n}\cdot\sum_{t=0}^{n}\left(D_t - S_t\right)^2}}{\sqrt{\frac{1}{n}\cdot\sum_{t=0}^{n}\left(D_t\right)^2} + \sqrt{\frac{1}{n}\cdot\sum_{t=0}^{n}\left(S_t\right)^2}}$$

Equation 6.10

6.3 Optimisation

The future success of renewable technologies relies on revealing the roles where their use is both beneficial and notable. The possible supply and demand combinations are limitless, however in many cases the combination will not promote the use of renewable technologies. Large industrial loads would dwarf the output from a $20m^2$ PV façade, implying that the technology is futile; whereas, the same façade combined with a domestic load, which consisted of low daytime base loads such as refrigerators due to the occupants being at work, would require grid export and would render the project with an unfavourable payback period. Thus, for the promotion of renewables, it is vital that the supply and demand combinations are well matched. The classic example is that of PV rooftop projects being used to offset air-conditioning demands (Byrne et al.,

1996). However, even this comparatively narrow focus, combinations of air-conditioning and PV systems, could be optimised to reveal specifics regarding the operating patterns of air-conditioning and the configuration details of a PV system which best promote their combination.

Optimisation is the process of finding the conditions that give maximum or minimum values of a function (Stoeker, 1989). In the context of evaluating supply and demand combinations, which promote the use of renewables, the search condition involves the maximum match. The variables, which need to be considered, include the demand patterns which follow those of the renewable source, but also location parameters such as the angle of tilt of a PV system, or the hub height of a wind turbine. The abundant possible combinations require a search procedure to evaluate the optimum. Stoecker (Stoeker, 1989) reviews a number of different search procedures used in optimisation. A precise optimum can never be known (Stoeker, 1989) particularly when dealing with the highly variable and irregular nature of demand and renewable supply profiles. Instead, an interval of uncertainty can be defined by optimising the match between profiles. This interval of uncertainty represents characteristic demands which can be 'taken out' by specific RE supply configurations. The combination may represent that of an appliance demand, a site's demand or the demand associated with a number of different demand profiles, combined with either a single RE supply configuration or an aggregation of supplies.

Profile ranking parameters such as the mean and variance enable high priority demand profiles to be identified and changes resulting from RE Integration to be quantified. A profile whose variance is high represents a peaky profile, which incurs additional supply infrastructure costs. Such profiles are high priorities as any levelling technology has advantages, which surpass the savings in energy costs. High variance is indicative of requiring either or both forms of green technologies: energy efficiency and renewable energy. Two search methods will be presented which can identify optimal solutions to low ranking profiles, both of which are based on exhaustive searching. Exhaustive

searches are the most widely used type of search (Stoeker, 1989) as they evaluate every possible solution. The first search procedure described identifies the optimal match, using statistical evaluation. The second utilises the Fast Fourier Transform technique (Cooley and Tukey, 1996) to focus the search by identifying similarities in the frequency domain. Both search methods indicate promising matches between types of profiles over a defined time frame, thus what may produce an optimum result in the summer, could equally result in a poor match in the winter. Optimisation requires a number of iterative searches to evaluate the specifics of the supply and demand profiles.

6.4 Search Orders

Three exhaustive search methods can be applied in the optimisation of supply and demand matching. The methods can be differentiated by their search order, which directs the result. Firstly, a best overall search includes every possible combination of supply and demand profiles and results in an optimal result, which could include both multiple supplies and demands. Secondly, a demand led search finds the optimal supply profile combination for each demand scenario. The inverse of this, i.e. a supply led search, is the third search method.

6.4.1 Best Overall Search

The best match overall involves obtaining the match statistics for all the possible supply and demand combinations. Single demand profiles are matched with single supplies according to Equation 6.11. The summation sign used in this equation is employed to represent the combinatorial order as opposed to a literal summation, thus Equation 6.11 infers that every individual supply profile is combined with every individual demand profile.

$$M_{1D} = \sum_{i=1}^{s} \left(S_i + \sum_{j=1}^{d} D_j \right) \qquad \text{Equation 6.11}$$

Where M_{1D} = match order for single demands

s = number of supply profiles

S_i = supply profile i

d = number of demand profiles

D_j = demand profile j

Following the single demand profiles, coupled demand profiles are matched with single supplies as described by Equation 6.12. Again, the summation sign represents the combinatorial order and the equation states that every individual supply profile is combined with every possible set of two demand profiles.

$$M_{2D} = \sum_{i=1}^{s} \left[S_i + \sum_{j=1}^{d} \left(D_j + \sum_{k=j+1}^{d} D_k \right) \right] \qquad \text{Equation 6.12}$$

The match order for three demands, M_{3D} and that for four, M_{4D}, are described by Equations 6.13 and 6.14. This pattern of matching is continued until the number of demands in combination, matched to the individual supplies, is equal to the total number of demands. For example, with eight demand profiles, each individual supply profile would eventually be matched with all eight demands.

$$M_{3D} = \sum_{i=1}^{s} \left[S_i + \sum_{j=1}^{d} \left[D_j + \sum_{k=j+1}^{d} \left(D_k + \sum_{l=k+1}^{d} D_l \right) \right] \right] \qquad \text{Equation 6.13}$$

$$M_{4D} = \sum_{i=1}^{s} \left[S_i + \sum_{j=1}^{d} \left[D_j + \sum_{k=j+1}^{d} \left[D_k + \sum_{l=k+1}^{d} \left(D_l + \sum_{m=l+1}^{d} D_m \right) \right] \right] \right] \qquad \text{Equation 6.14}$$

Once single supplies and multiple demands are matched, the procedure is reversed and multiple supplies are combined with individual demands, with the match statistics noted after every combination. Thereafter, multiple supply and multiple demand profiles are combined. Equation 6.15 describes how two supplies are matched with two demands, this equation is expanded until all demands are combined with all supplies and every possible match statistic is obtained. A limit incorporated into this search procedure is that multiples of the same profile are never used, otherwise the search would be infinite.

$$M_{2D+2S} = \sum_{i=1}^{d} \left[D_i + \sum_{j=i+1}^{d} \left[D_j + \sum_{k=1}^{s} \left(S_k + \sum_{l=k+1}^{s} S_l \right) \right] \right] \qquad \text{Equation 6.15}$$

6.4.2 Led Search Methods

Led searches are modified versions of the best overall search, which only include single profiles of the search type, i.e. a demand led search will only evaluate a single demand profile in combination with every possible amalgamation of supply profiles. A led search will find a solution for each priority ‘A’ profile made up of a single or set of priority ‘B’ profiles, where priority ‘A’ profiles lead the search. This reduces the number of possible combinations and increases the results set, enabling the identification of a field of focus for profile types. A demand led search identifies the

types of supply best matched to each demand, from which more detailed studies for each demand scenario can be initiated. A supply led search classifies the best types of demand profiles, to couple with the different supply technologies.

6.5 Statistical Search Method

Statistical searches calculate one or more of the statistics described in the previous section to filter the various combinations in search of the optimal condition or conditions. The search proceeds through one of the combinatorial orders described, evaluating the statistics associated with each match. These statistics are subsequently compared with one another to find the optimal solution. Where the maximum match condition is defined by a single variable, i.e. the inequality metric, the match(s) resulting in the minimum of this value produce the optimal solution.

Where multiple condition variables are used, for example, the correlation coefficient, the shared area and the inequality coefficient, a filtering procedure is required to evaluate the profile combination which best meets each of the criteria. The filtering process involves an array of results describing each of the combination possibilities, for each condition variable specified. The process is initiated by finding the optimal combination of profiles to meet each of the condition variables in turn. The combinations are subsequently compared and the filtering process is terminated if a profile combination satisfies each condition variable. Where this is does not occur, the defined optimal condition for each condition variable is expanded to enable a larger number of combinations to meet the required conditions. For example, the optimal inequality index would be defined as any inequality less than 0.2, as opposed to the true optimum value of zero. The profile combinations are subsequently filtered for each of the condition variables to find those that succeed in satisfying the newly defined interval of uncertainty. The results for each condition are again compared to find the combination(s) that satisfies all the conditions. Where no profile combination is found,

the intervals of uncertainty are expanded once more, and filtering is resumed until a profile combination is found to satisfy each condition.

6.5.1 Example of Best Overall Search with Statistics

Consider the example shown in Figure 6.8, illustrated are a mixed set of supply and demand profiles. The demand profiles range in weekly consumption from 100 kWh for a residential profile, up to 700 kWh for an industrial profile. The supply profiles include a number of different PV configurations and wind turbines ranging in size up to a 10 kW. This example clearly demonstrates the difficulty of supply and demand matching, as the optimum combination could consist of a mix of demand and supply profiles. Following the best overall search procedure for these 14 profiles generates 16,129 possible combinations. With this scale of data processing, computer technology is essential.

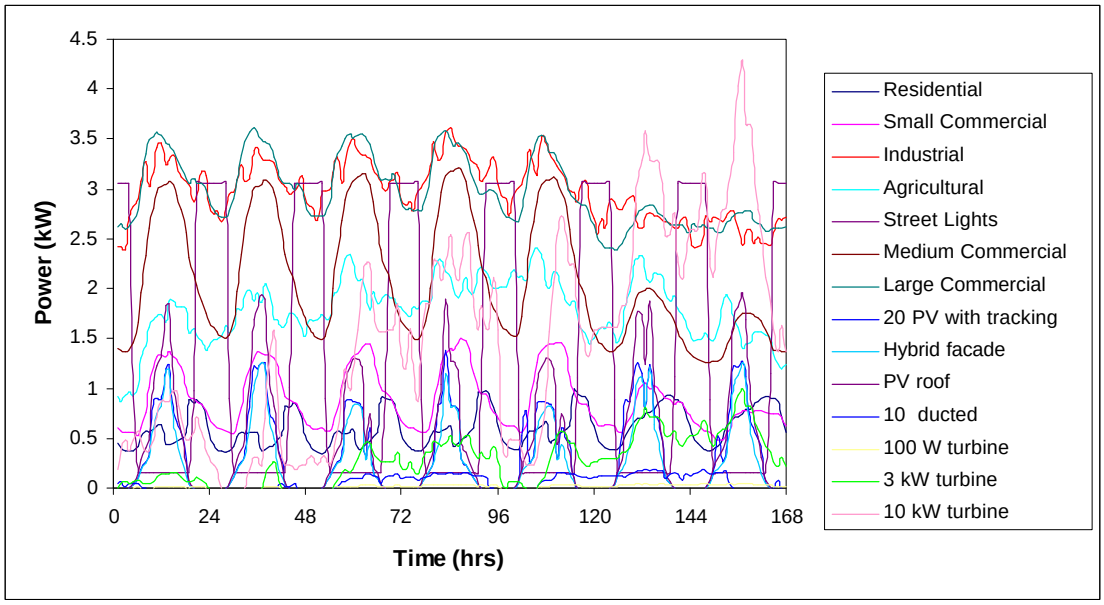

Figure 6.8: Example of matching numerous profiles.

These combinations were filtered to find the best match using a single variable search, based on the inequality metric to define the quality of match between profiles, the result

is illustrated in Figure 6.9. The inequality metric for this combination is 0.27 and the correlation 0.42. The combined supplies incorporate 20 mono-crystalline PV panels with solar tracking devices, a PV-hybrid façade consisting of 30 vertical south-facing mono-crystalline panels, 10 ducted wind turbines facing southwest, a 100 W and a 10 kW wind turbine. These supplies are matched to the combined profiles of a small commercial and an agricultural demand. From this Figure, it can be seen that the PV systems meet the mid-day peaks and the wind systems help to meet some of the demands base load.

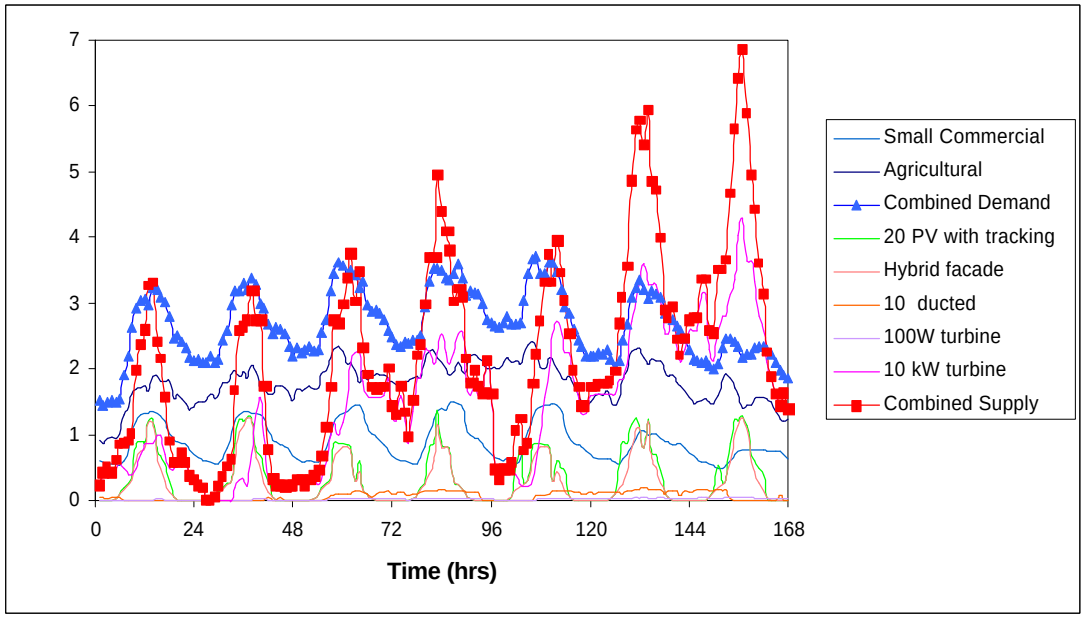

Figure 6.9: Best supply and demand match based on the inequality metric

A different result is obtained if the correlation coefficient is used as the filtering variable, as is illustrated in Figure 6.10, where the correlation is 0.62 and the inequality 0.43. The best correlation is achieved with a small commercial demand profile, combined with a PV hybrid façade and 10 ducted wind turbines, all of which were encompassed in the best match scenario. These results enable the scope of the search to be refined, eventually leading to system sizing. The optimisation process is only valid

over the period for which it is performed and should therefore be performed on a range of periods encompassing typical annual seasons over a full year.

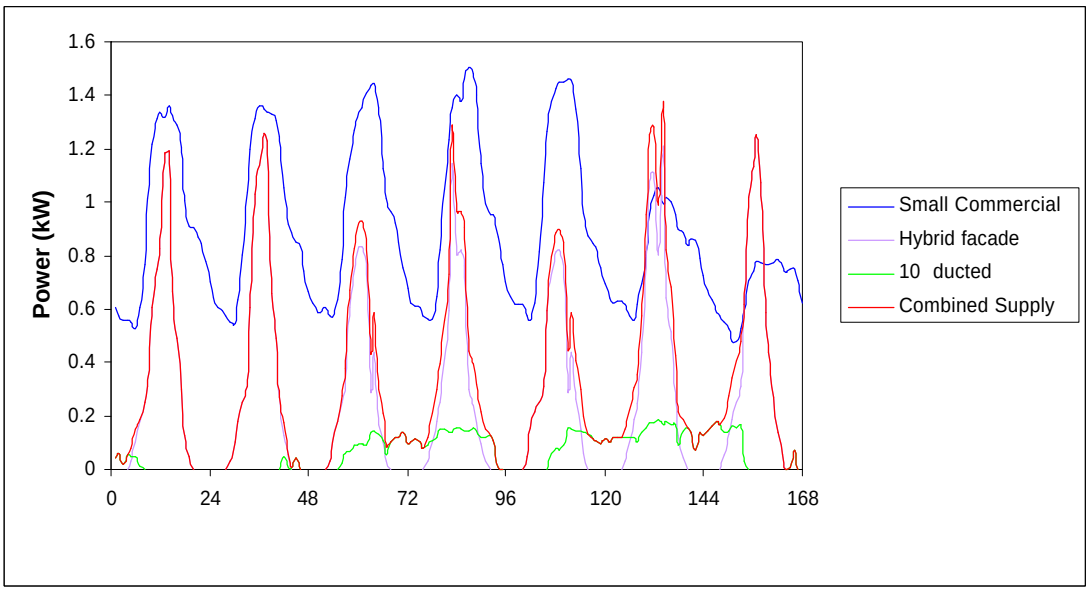

Figure 6.10: Best supply and demand match based on correlation.

6.5.2 Example of Lead Search with Statistics

Carrying out a demand led search on the profiles used in the previous example, requires the evaluation of 127 possible combinations for every demand profile, giving 889 in total. This reduces the data processing required for the best overall search by 95%. The results obtained from a demand led search for this example are detailed in Table 6.1 and the profile combinations are shown in Figure 6.11. It can be seen that, the small commercial profile is best matched with a combination of 20 PV panels with tracking, 10 ducted turbines, a 100 W and a 3 kW turbine. Examining area's of deficit supply, enables certain observations to be made which could increase the match. For example in the match illustrated for the small commercial demand and an afternoon deficit is observed which could possibly be met by a west facing PV system. However, the

addition of such a system will also contribute to the supply peaks seen around noon, thereby increasing energy wastage or export.

Table 6.1: Statistics from best per demand led search

Demand	Supply	Inequality	Correlation	Shared Area	RE	Export	Import
Residential	10 ducted, 100 W turbine, 3 kW turbine	0.35	0.29	53.49	60.9	7.27	46.36
Small Commercial	20 PV with tracking, 10 ducted, 100 W turbine, 3 kW turbine	0.29	0.48	96.61	118.93	22.18	53.24
Industrial	20 PV with tracking, PV roof, 10 ducted, 100 W turbine, 10 kW turbine	0.31	0.02	322.54	395.43	72.08	176.65
Agricultural	Hybrid Façade, 10 kW turbine	0.29	0.26	219.55	293.34	73.08	79.74
Street Lights	10 ducted, 10 kW turbine	0.53	-0.22	91.39	257.09	164.9	107.81
Medium Commercial	PV roof, 10 kW turbine	0.3	0.2	244.96	323.11	77.38	104.27
Large Commercial	20 PV with tracking, PV roof, 10 ducted, 100 W turbine, 10 kW turbine	0.3	0.15	325.23	395.43	69.39	173.96

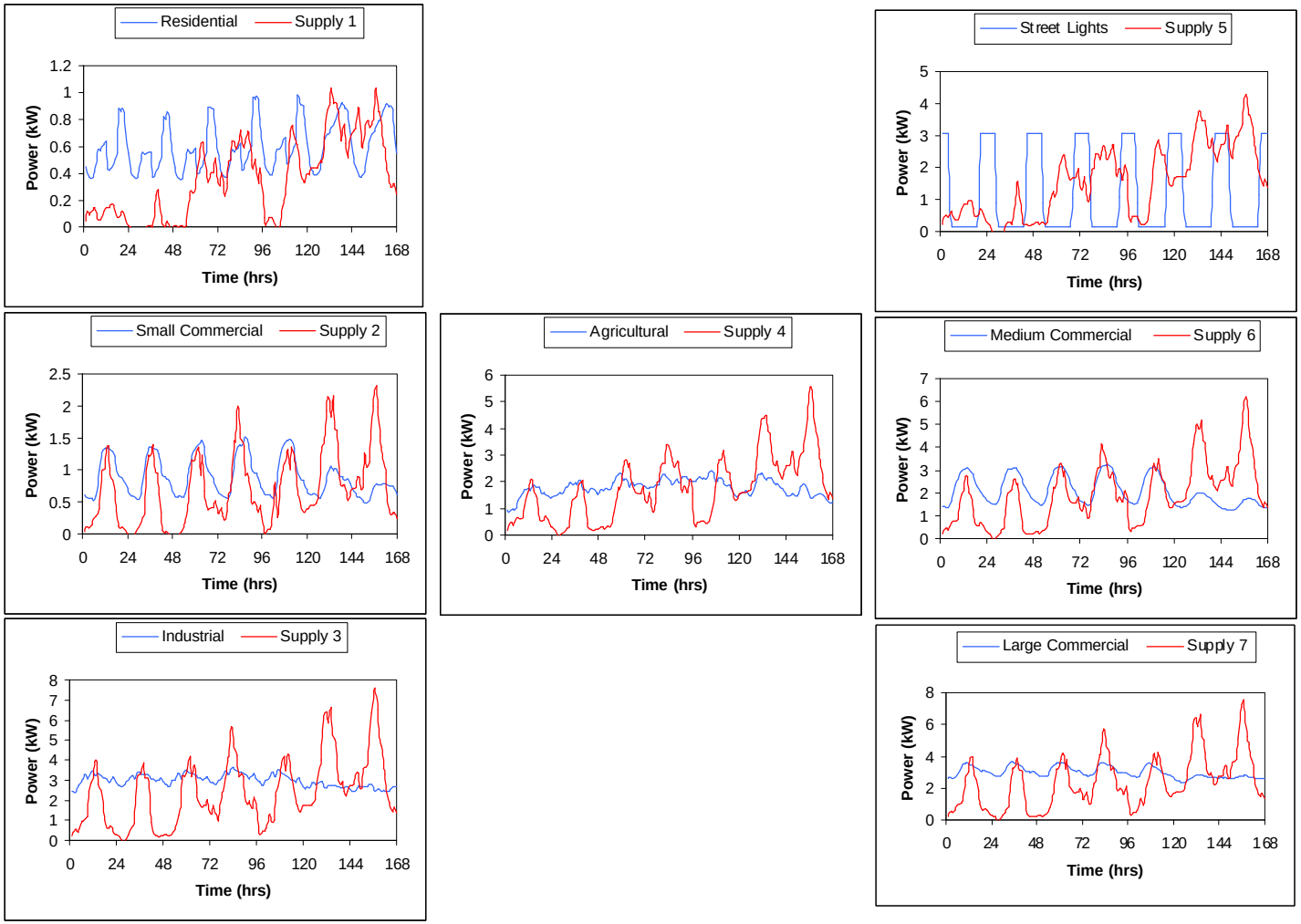

Figure 6.11. Results for best per demand search

6.6 Fast Fourier Transform Search Method

The alternative to a statistical search is to transform the time series to the frequency domain, and search for similarities in the occurrence of peaks. Figure 6.12 illustrates a time series profile, and Figure 6.13 shows the profile after it has been transformed to the frequency domain.

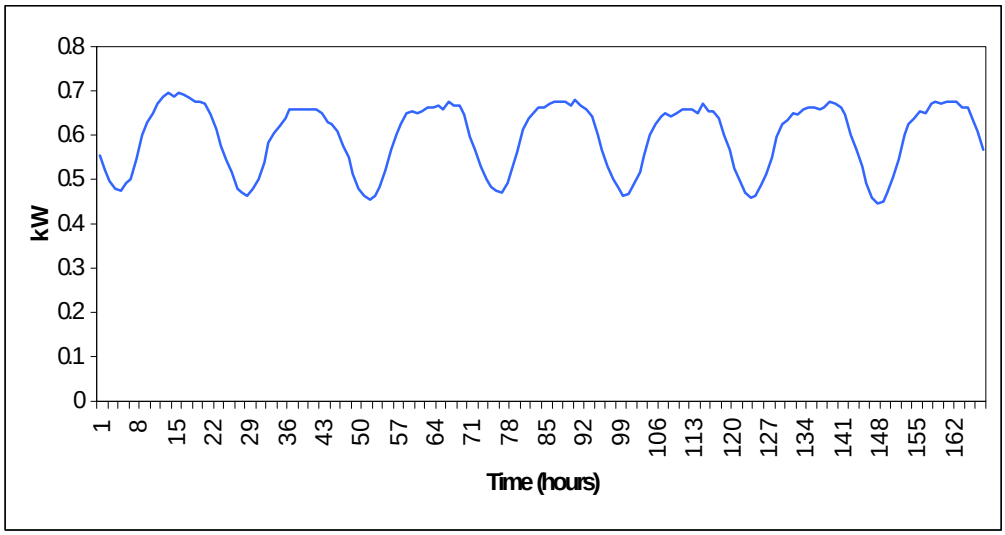

Figure 6.12: A weekly profile shown in the time domain

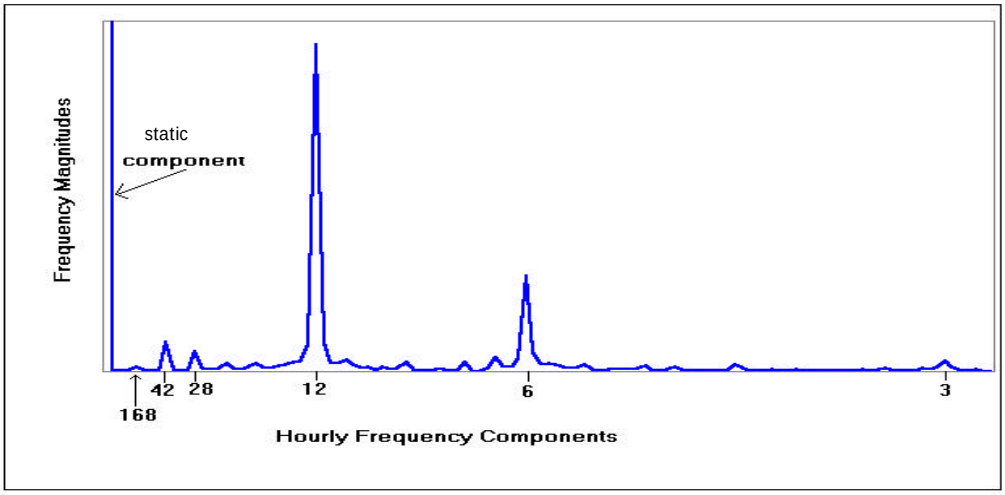

Figure 6.13: The weekly demand profile illustrated in Figure 3.7 in the frequency domain

Transforming to the frequency domain requires decomposing the time variant profile into simpler component waveforms. The first frequency transformation technique in wide use was the Fourier transform (Goodyear, 1971), the Fourier series expansion decomposes a waveform (profile) into sinusoidal components. The amplitudes and phases of these individual sinusoids can be plotted along a frequency axis to provide the spectrum of a signal and give a complete description of a periodic function. However, a profile is represented by a discrete time sequence, as opposed to a continuous waveform. Each value represents an independent time variable whose value is only known at discrete instants in time. The discrete Fourier transform (DFT) is a mathematical procedure used to determine the harmonic or frequency content of a discrete signal sequence (Lyons, 1996) and is described by the following Equation:

$$X(m) = \sum_{n=0}^{N-1} x(n) \cdot e^{\frac{-j \cdot 2 \cdot \pi \cdot n \cdot m}{N}} \qquad \text{Equation 6.16}$$

Where X(m) = the discrete frequency domain sequence

X(n) = the discrete time domain sequence

n = the time domain index of the input samples

m = the index of the DFT output in the frequency domain

N = the total number of input samples

Equation 6.16 can be expanded using Euler's relationship, described by Equation 6.17, to Equation 6.18.

$$e^{-j \cdot \phi} = \cos(\phi) - j \cdot \sin(\phi) \qquad \text{Equation 6.17}$$

$$X(m) = \sum_{n=0}^{N-1} x(n) \cdot \left(\cos\left(\frac{2 \cdot \pi \cdot n \cdot m}{N} \right) - j \cdot \sin\left(\frac{2 \cdot \pi \cdot n \cdot m}{N} \right) \right) \qquad \text{Equation 6.18}$$

Equation 6.18 describes each X(m) DFT output term as the sum of the point for point product between an input sequence of signal values and a complex sinusoid. The exact frequencies of the different sinusoids depend on both the sampling rate at which the original signal was sampled and the number of samples. The magnitude and phase of each of the frequency components are defined by Equation 6.19 and 6.20, respectively.

$$X_{mag}(m) = |X(m)| = \sqrt{X_{real}(m)^2 + X_{imag}(m)^2} \qquad \text{Equation 6.19}$$

$$X_{\phi}(m) = \tan^{-1}\left(\frac{X_{imag}(m)}{X_{real}(m)}\right) \qquad \text{Equation 6.20}$$

The most efficient means of calculating the discrete Fourier transform by employing an algorithm described by Coley and Tukey known as the Fast Fourier Transform (FFT) (Coley and Tukey, 1996). This algorithm requires the DFT input data size to be 2^k, where k is a positive integer of 2 (i.e. 2^6, 2^8, 2^{10} etc). The profiles used to define demand and supply over specific periods (i.e. a day, week, month or year) rarely contain the required 2^k number of data points. It is frequently suggested to augment the data with zero values, however: Bach and Meigen (Bach and Meigen, 2000), suggest that this technique, known as zero padding, leads to spurious results, which can be overcome by re-sampling the data. The procedure used in this work to transform any time series profile into a representative profile containing the required number of input values involves the evaluation of the even positive integer, k, the interpolation rate, ir, and the sampling rate, sr, relative to the number of time steps, N. The value of k is defined as the next highest even positive integer obtained from the division of ln(N)/ln(2). The profile is re-samples four times, to ensure the frequency component related to the period over which the profile is defined, is identified. Thus, the number of FFT input values, m, used is 2^{k+2}. The sample rate, sr, and interpolation rate, ir, are related to m and N as $N \times ir/sr = m/4 = 2^k$. The sample rate is determined by repeatedly dividing the number of time steps, N, by two for as long as the result is an integer and sr is the number of divisions possible and the interpolation rate is $2^k \times sr/N$. Table 6.2 illustrates some examples.

Table 6.2: Examples of FFT parameters evaluated for different numbers of time steps

Time steps, N	**k**	**FFT input values, m**	**Sample rate, sr**	**Interpolation rate, ir**
24	6	256	3	8
48	6	256	3	4
96	8	1024	3	8
168	8	1024	21	32

The resulting spectral analysis enables the identification of the base frequency component which, is related to the profile period and the dominant frequency components within the profile, i.e. those frequencies with the greatest magnitudes. Employing this method to determine the phase of the dominant cyclic components, defined by the relative magnitudes of the frequency bins, enables profiles to be defined by five variables. These five variables, representing the five most dominant cycles within the profile, can be compared to find profiles with similar dominant cycles. Any of the three search procedures described above can be used to systematically compare the phases and magnitudes of the dominant cycles contained within the profiles. The comparison of these cycles is done by allocating scores for cycles with similar phase and magnitude components. First, each of the five dominant cycles for every profile is identified and defined by an identification value, where the most dominant is zero, and the fifth most dominant is four. To obtain a FFT score, a supply and demand combination must have at least one phase difference within a specified tolerance, of the five dominant cycles. within each profile for a demand and supply combination, the scoring procedure is initiated with the zero component of the demand profile(i.e. the most dominant cycle) whose phase is compared to the zero component of the supply profile. Where the phase difference between the two components is within the set tolerance a partial score of (5-0)x(5-0) is given, the magnitudes are subsequently compared for cycles within the phase tolerance, and where these are within the tolerance and additional score based on the identification number is given (again (5-

0)x(5-0)). Thus profiles whose dominant cycles contain phase and magnitude overlap defined by a tolerance, are assigned a temporary sore of 50, where only the phases are within the tolerance a score of 25 is given. The scoring continues by comparing the zero demand component with the one supply component. The scoring system is the same, thus where phases overlap between these cycles, a score of 20 can be obtained ((5-0)x(5-1)), which is doubled if the magnitudes are also within the tolerance. This temporary scoring continues until the four demand component is scored against the four supply component, which can achieve a maximum score of 2 ((5-4)x(5-4) for phase + (5-4)x(5-4) for magnitude). Initially the tolerance is set to zero, therefor only those cycles exactly in phase with one another can generate a score. Should no combination of profiles have any exact phase overlap, the tolerance is iteratively increased until at least one set of profiles is contains a set of dominant profiles whose phase differences are within the defined tolerance.

$$\chi = \left[\sum_{S_{ph}=0}^{5} (5 - S_{ph}) \cdot \sum_{D_{ph}=0}^{5} (5 - D_{ph}) \right] + \left[\sum_{S_m=0}^{5} (5 - S_m) \cdot \sum_{D_m=0}^{5} (5 - D_m) \right]$$

Equation 6.21

Where χ = score

S_{ph} = Phase of dominant cycle within supply profile

S_m = Magnitude of dominant cycle within supply profile

D_{ph} = Phase of dominant cycle within demand profile

D_m = Magnitude of dominant cycle within demand profile

With multiple profiles in combination every demand involved is systematically paired with every supply and given a FFT score as described above, the individual scores are summated and the summation divided by the number of profiles given in the combination. This division ensures that good frequency matches are not shrouded by

the inclusion of unnecessary combinations. This method is applied to reduce the data processing requirements associated with the calculation of FFT results for combined profiles.

Applying a best-overall FFT search to the example given in Figure 6.3 results in the best match illustrated in Figure 6.14. Visual examination of Figure 6.14 demonstrates quite clearly that there are shared frequency cycles between supply and demand. The correlation coefficient for this result is 0.45 and the inequality metric 0.44. The FFT search is useful in the optimisation of types of technology suited to particular demand characteristics. However, the approach neglects magnitude matching and may not be sensitive to subtle variations in supply technologies e.g. PV tilt angles.

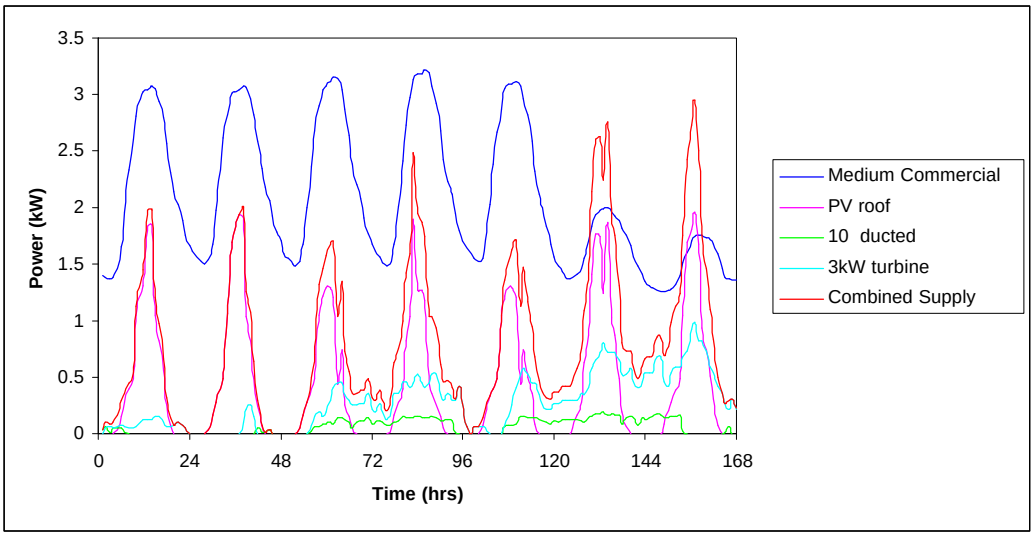

Figure 6.14: FFT Result

6.7 Summary

A variety of search and match evaluation techniques have been described, to optimise the RE options for given demand scenarios. It has been shown that the optimal condition is very sensitive to the filtering variable used to find that condition. The deployment of the Fast Fourier Transform technique to compare frequency cycles in a profile yields optimised results, which do not necessarily yield statistically favourable results. A perfect match is easily assessed, however rating a match in degrees of 'goodness' becomes less clear. Storage, which has not yet been considered can have a significant effect on matching and needs to be considered prior to establishing the best metric to use in filtering search results. This is the focus of the subsequent chapter.

6.8 References

1. Bach Michael and Meigen Thomas, Do's and don'ts in Fourier analysis of steady-state potentials, URL:http://www.augenklinik.uni-wuerzburg.de/projects/meigen2.htm, 2000

2. Byrne J., Letendre S., Govindarajalu C., Wang Y., Evaluating the economics of Photovoltaics in a Demand-Side Management Role, Energy Policy, Vol. 24, No. 2, pp. 177-185, 1996.

3. Cooley JW, Tukey J, An algorithm for the machine calculation of complex fourier series. Math Comput, Vol 19, No. 90, April 1996 pp.297-301

4. Dewson T., Day B., Irving A. D., Least Squares Parameter Estimation of a Reduced Order Thermal Model of an Experimental Building , Building and Environment 1993

5. Goodyear C. C., Signals and Information, Butterworth & Co. (Publishers) Ltd., London 1971

6. Iniyan S., Sumathy K., Suganthi L., Samuel A. A., Sensitivity Analysis of Optimal Renewable Energy Mathematical Model on Demand Variations, Energy Conservation & Management, 41, pp.199-211, 2000

7. Lyons Richard G., Understanding Digital Signal Processing, Addison-Wesley Publishing Company 1996

8. Mathew Paul, Hartkopf Volker, Mahdavi Ardeshir, Towards the Building as a Power Plant: Computational Analysis of Building Energy Self-Sustenance, 1999

9. Newborough M. and Augood P, Demand-side Management Opportunities for the UK Domestic Sector, IEE Proceedings of Generation, Transmission and Distribution, Vol 146. No 3, May 1999

10. Ramakumar R., Abouzahr I., Ashenayi K., A Knowledge-Based Approach to the Design of Integrated Renewable Energy Systems, IEE Transactions on Energy Conversion, Vol. 7, No. 4, December, 1992

11. Scheaffer Richard L. and McClave James T., Statistics for Engineers, PWS Publishers, 1982

12. Sears F. W., Zemansky M. W., Young H. D., University Physics (fifth edition), Addison-wesley Publishing Company, 1978

13. Stoeker W. F., Design of Thermal Systems, 3rd Edition, McGraw-Hill International Editions, Engineering Series, 1989

14. Williamson T. J., A Confirmation Technique for Thermal Performance Simulation Models, University of Adelaide, Austrailia, 1994

Chapter 7: Improving the Match

Incorporating auxiliary systems can have a profound effect on the ability of a renewable system to match a given demand profile. The classic example can be described by a PV system whose output peaks during the middle of the day, exceeding the corresponding demand and is zero during the night. Storage in this instance could change a poor match to a good match by storing the excess generation until times when generation is low. Back up systems can be used together with a RE technology to meet consistent deficiencies producing a theoretically perfect match. There are, however, economic considerations that have to be examined to ensure any deployment of auxiliary systems is beneficial. Additionally many tariff structures available today are not based on a single price per kWh, but vary according to system loads, thus RE production at certain times of the day may be more beneficial than at others. The best metric for describing match is the inequality metric introduced in the previous chapter, but a holistic approach is required if auxiliary systems are to be incorporated, which can evaluate the benefits of their incorporation. Additionally another metric needs to be defined which can be used to describe a 'potential match', based on the inclusion of some form of storage and/or backup system. To support this work, mathematical models will be described for a battery and for a back up generator. Secondly, a method for analysing the effects of tariff selection is described and finally a potential match metric is defined. An illustrative example will be used to show the effects of some of the different auxiliary choices available when RE deployment is being considered.

7.1 Battery Storage

In order to predict the effects of energy storage on the ability of a renewable energy system to meet a demand, it is necessary to model rechargeable battery performance. Rechargeable batteries are able to accept, store and release electrical energy. The most common, well-developed and successful battery is the lead acid cell (Decher, 1997). It

is used in many applications ranging from starting automotive vehicles to industrial and leisure applications. Industrial batteries are also known as deep-discharge or deep-cycle batteries because they can be discharged to 80% of their rated capacity. Generally, all rechargeable batteries used with renewable energy systems of the are Lead-Acid type, with typical efficiencies of 85-95%. There are some Nickel-Cadmium batteries in use, but for most purposes they are too expensive and have low efficiencies (typically around 65%). Nickel-Iron batteries are also available, again these have poor efficiencies (60-70%) with voltage variations that make them more difficult to match up with standard 12v/24/48v systems and inverters (Northern Arizona Wind & Sun, 1999). Furthermore, battery memory problems arise in batteries employing nickel chemistry. These batteries have a naturally uneven electrode material, which will show a preference for activity in some patches and become relatively inactive in others, when the batteries are repeatedly put through shallow charge/discharge cycles or as a result of recharging partly depleted cells or prolonged overcharging. The consequential phase changes result in a loss in capacity as the cell's characteristic voltage is reduced (Accu Oerlikon Ltd, 2000).

It is not the purpose of this work to examine the various electro-chemical and physical processes that occur within the battery. Detailed models of this nature can be found elsewhere (Hiram and Nguyen, 1987), (Newman and Tiedemann, 1997),(Notten et al., 1998). The purpose of this work is to identify mathematical techniques that accurately define the generic performance of deep-discharge lead acid batteries. Goldstein and Case (Goldstein and Case, 1978) model battery performance by employing typical charge and discharge curves and assume sets of linear relationships between terminal voltage and state of charge. Child *et al*. (Child et al., 1996) use one of two battery models. The first relies on a user-specified constant discharge efficiency, also used by Evans (Evans, 1994), while the second is based on the Shepherd model. Shepherd (Shepherd 1965) describes a numerical method for fitting a battery discharge equation to a particular set of discharge curves. The method involves the determination of six empirical values, using eight data points on two separate discharge curves. Manwell

and McGowan (Manwell and McGowan, 1993) introduced a new model based on chemical kinetics. The model utilises battery discharge data to define the width of and the conductance between two tanks, one which holds the available charge and another that holds the chemically bound charge. Voltage is modelled as a linear function of state of charge. Protogeropoulos *et al* (Protogeropoulos et al., 1994) developed a model to predict battery voltage both under static and dynamic battery charging and discharging. The model was further developed to include effects of temperature of discharge and charge (Morgan *et al*., 1997). The model is dependent on two sets of five empirical values, one set for charge and the other for discharge characteristics. The empirical values need to be obtained through laboratory testing for any battery under investigation.

The battery model developed in this work is generic to any lead-acid battery and by avoiding the use of empirical values does not require battery testing to enable performance prediction. The mathematical description of a battery is based on manufacturers' data and does not describe electro-chemical reactions.

7.1.1 Battery Performance

In this work the purpose of predicting battery performance is to predict the power flows associated with charging and discharging modes of operation. The modelling objective was therefore to predict the power which can be obtained from a battery when a supply fails to meet a demand and that which can be absorbed by the battery when the power generated by a supply technology exceeds that required by a demand. The model described assumes the battery system to be operating in conjunction with a charge regulator, whose function is to regulate both the charging voltage and current to prevent battery damage from overcharging. The circuits depicted in Figure 7.1 are taken from a standard electrical circuit text (Davis, 1992) and describe battery charging and discharging. During discharge the battery, represented by a voltage source, E, and an internal resistance, r, discharges a current, I, to an external load resistance. During

charging a charger represented by a constant voltage source, V, and an internal resistance, $r_{charger}$, supplies a charging current to the battery.

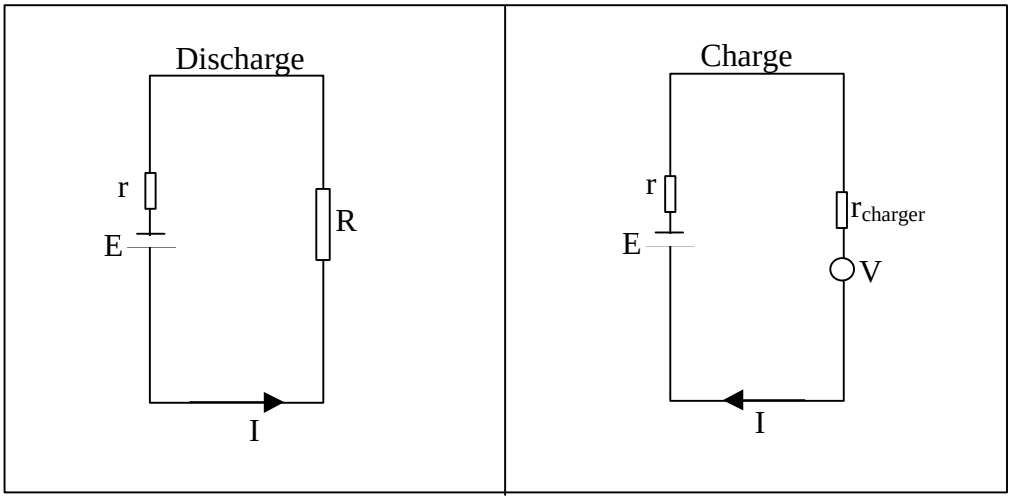

Figure 7.1: Circuits describing battery discharging and charging

The changes in the battery's open circuit voltage during charge and discharge can be described by Equation 7.1, where the sign convention for a discharge current is positive and a charging current is negative.

$$V_{oc_t} = V_{oc_{t-1}} - I \cdot r \qquad \text{Equation 7.1}$$

As in this work the objective is to predict battery power flows Equation 7.1 had to be used to describe the power delivered by or to the battery during discharge or charging. This was done by multiplying every term in Equation 7.1 by the charging or discharging current, resulting in Equation 7.2 (as $P = I \times V$).

$$P = I \cdot V - I^2 \cdot r \qquad \text{Equation 7.2}$$

From Equation 7.2, it can be seen that the power delivered or absorbed by the battery is dependent on its open circuit voltage, the discharge/charge current and on the battery's internal resistance. In order for the work to proceed the following assumptions are made:

- The battery's internal resistance is assumed to be constant
- The charging current is a function of both the power available and the battery's state of charge
- The discharge current is a function of both the power required and the battery's capacity
- The open circuit voltage of the battery is a function of its state of charge

A battery's state of charge describes the charge (in coulombs) stored, and the current describes the rate at which this charge is dissipated or accumulated. The fundamental prerequisite of this work was to establish the relationship between open circuit voltage and state of charge.

Open-circuit Voltage and State of Charge

Various electro-chemical and physical processes occur within a battery, which result in overpotential and ohmic losses, which alter a battery's open circuit voltage. These phenomena can not be modelled without modelling the electro-chemical processes, which in turn require modelling input parameters that are typically not available from manufacturers' specifications. Typical open-circuit voltage and state of charge data for lead acid cells can be found in various publications (Northern Arizona Wind & Sun, 2000), (Excide, 2000/2001). The data presented is generic for all lead-acid cells, except the gel-cell type for which 0.2V must be subtracted. Typically, discharged cells are characterised by a voltage of 1.75V and fully charged cells by 2.12V. This open circuit voltage – state of charge data was used to obtain a mapping function between the two parameters. Employing regression analysis on the published data led to the derivation of a 6th order polynomial mapping function. It is stressed here that this 6^{th} order polynomial is purely a mapping function without theoretical basis. Its use is contained

within the limits of 0-100% battery charge and within these limits is 99% accurate. The data and the result of the regression analysis are illustrated in Figure 7.2.

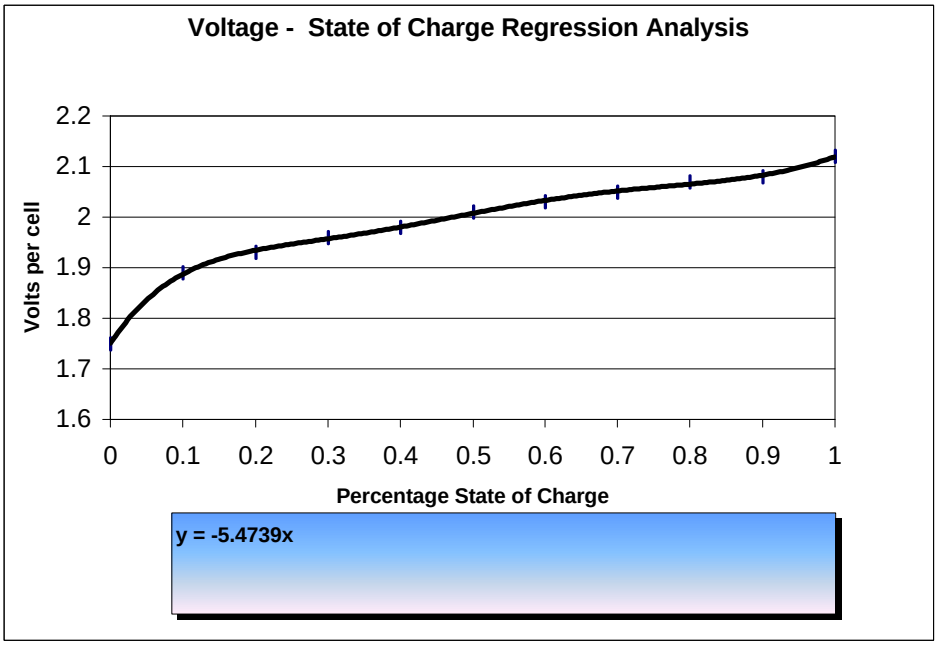

Figure 7.2: Regression analysis performed on cell voltages and state of charge.

As batteries consist of a number of series connected cells, the cell voltage may be scaled to represent any battery as described by Equation 7.3.

$$V = N \cdot \left(-5.474 \cdot SOC^6 + 22.67 \cdot SOC^5 - 35.57 \cdot SOC^4 + 26.97 \cdot SOC^3 - 10.4 \cdot SOC^2 + 2.171 \cdot SOC + 1.75\right)$$

Equation 7.3

Where V is the open circuit voltage of a battery (V), N is the number of series connected cells in the battery and SOC is the battery's percentage state-of-charge (%/100). The number of cells in a battery can be calculated by assuming the nominal voltage of a cell is 2V and therefore dividing the batteries nominal voltage by two.

7.1.2 Modes of Battery Operation

Battery Discharge

The first parameter required to predict battery discharge performance, is the discharge current required to meet the deficit power between supply and demand. Thevinin's theorem (Davis, 1992) was employed to derive an equation, which would convert the power requirement into a current requirement. With reference to Figure 7.1, Thevinin's theorem describes the current in the circuit as:

$$I = \frac{V}{R + r} \qquad \text{Equation 7.4}$$

Since

$$P = I^2 \cdot R \qquad \text{Equation 7.5}$$

$$P = \left(\frac{V}{R + r}\right)^2 \cdot R \qquad \text{Equation 7.6}$$

Equation 7.6 can be solved for R, to give

$$R = \begin{bmatrix} \frac{1}{(2 \cdot P)} \cdot \left[-2 \cdot P \cdot r + V^2 + \left(-4 \cdot P \cdot r \cdot V^2 + V^4\right)^{\left(\frac{1}{2}\right)} \right] \\ \frac{1}{(2 \cdot P)} \cdot \left[-2 \cdot P \cdot r + V^2 - \left(-4 \cdot P \cdot r \cdot V^2 + V^4\right)^{\left(\frac{1}{2}\right)} \right] \end{bmatrix} \qquad \text{Equation 7.7}$$

Both solutions were substituted into Equation 7.4, as described by Equation 7.8 and a method of back-substitution demonstrated that Equation 7.9.a was derived from the real root and 7.9.b the imaginary. Thus, the kW demand is transformed to a discharge current requirement using Equation 7.8.a.

$$I = 2 \cdot V \cdot \frac{P}{\left[V^2 + \left[-V^2 \cdot \left(-V^2 + 4 \cdot P \cdot r \right) \right]^{\left(\frac{1}{2} \right)} \right]}$$

Equation 7.8.a

$$I = 2 \cdot V \cdot \frac{P}{\left[V^2 - \left[-V^2 \cdot \left(-V^2 + 4 \cdot P \cdot r \right) \right]^{\left(\frac{1}{2} \right)} \right]}$$

Equation 7.8.b

Having established the current required of the battery, the next stage in modelling discharge is to evaluate to what degree this current requirement may be met, which will depend on the charge stored within the battery. The charge stored in a fully charged battery is described by its capacity, which is a function of the discharge current. A battery will deliver less energy the quicker it is discharged. In liquid lead-acid cells, the effect is so pronounced that a deep cycle battery, capable of delivering 100 amp-hours over a 20-hour period, might delivery only 45 amp-hours in one hour.

This phenomena is due to Peukert's Effect, first noted by Schroder (1894) and most clearly defined by Peukert (1897), who described declining capacity at increasing rates of discharge as a logarithmic curve (Ure, 1998). Batteries can be described by their Peukert exponent values, which are directly related to the internal resistance of the battery. The higher the internal resistance, the higher the losses while charging and discharging, especially at higher currents. However, typical manufacturers' data typically do not include the Peukert value and give the internal resistance as a constant. To determine the relationship between capacity and discharge current, regression analysis was performed on capacity and discharge time data for a number of lead acid batteries. Figure 7.3 illustrates an example of the results obtained from this analysis for three different 12-Volt deep cycle batteries (manufactured by the U.S. Battery Manufacturing Company).

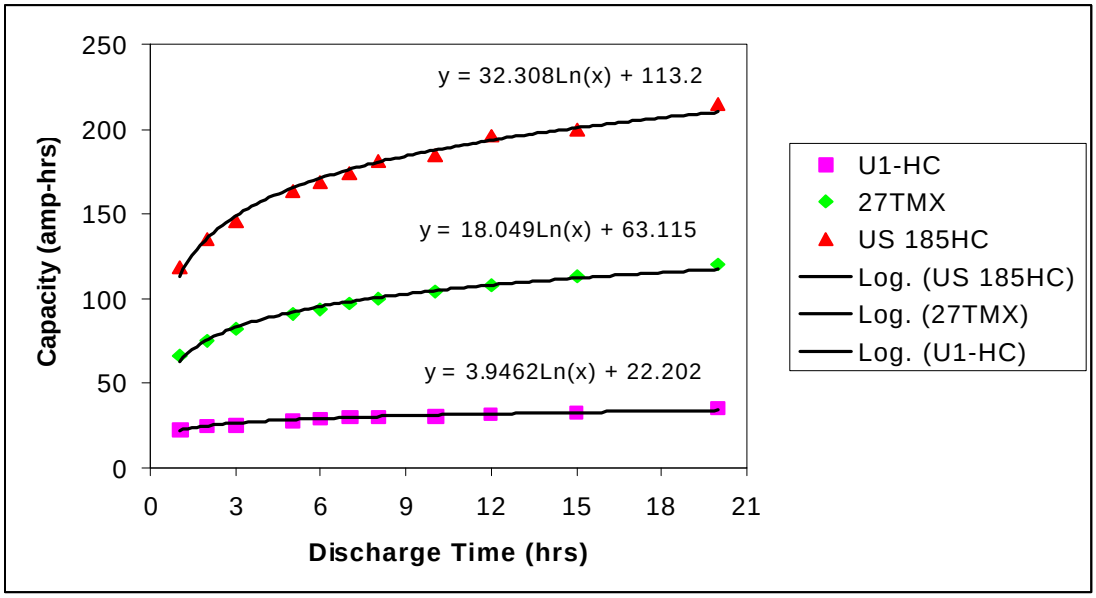

Figure 7.3: Capacity-time to discharge relationship of typical deep-discharge batteries (U.S. Battery Manufacturing Company, 2000)

With reference to this figure it may be observed that the relationship between battery capacity and rate of discharge can be described mathematically as:

$$C = A \cdot \ln(t) + B \qquad \text{Equation 7.9}$$

Where C is the battery capacity (Ahrs) and t is the time to full discharge (hours). The discharge current can be obtained by dividing the capacity by the time to full discharge (in hours). The constants A and B will vary with different battery configurations and internal resistances. These constants can however be derived for any battery by specifying two capacity values (C_1 and C_2) specified for different discharge rates (t_1 and t_2), as described below.

$$A = \frac{C_1 - C_2}{\ln(t_1) - \ln(t_2)} \qquad \text{Equation 7.10}$$

$$B = C_1 - A \cdot \ln(t_1) \qquad \text{Equation 7.11}$$

The charge stored in the battery is calculated by first assuming the battery is fully charged and its capacity at the required discharge current is determined. This capacity is subsequently multiplied by the percentage state of charge to determine the actual charge stored relative to the discharge current.

The time taken to fully discharge a fully charged battery, t_d, can be calculated by rearranging Equation 7.9, and substituting for the capacity ($C = I \times t$) to give:

$$t_d = \exp\left[\frac{-\left(B - I_r \cdot t_d\right)}{A}\right] \qquad \text{Equation 7.12}$$

Where I_r is the discharge current required. Equation 7.12 is solved iteratively for the discharge time, t_d, and subsequently used to calculate the capacity of the battery for the required discharge current. The capacity calculated represents the charge required to be stored in the battery in order for it to supply the required discharge current.

$$Q_r = I_r \cdot t_d \qquad \text{Equation 7.13}$$

The charge available, Q_a, in the battery is calculated from the state of charge:

$$Q_a = SOC_{t-1} \cdot Q_r \qquad \text{Equation 7.14}$$

The charge supplied, Q_s, by the battery over a time period, t , at the discharge current required is:

$$Q_s = I_r \cdot t \qquad \text{Equation 7.15}$$

Knowing the charge to be supplied and charge stored in the battery enables the resultant charge Q, to be calculated.

$$Q = Q_a - Q_s \qquad \text{Equation 7.16}$$

To determine whether the battery charge control system will allow this discharge current the resultant charge is compared to the charge at a specified deep discharge level, given by Equation 7.17.

$$Q_{dd} = SOC_{dd} \cdot Q_a \qquad \text{Equation 7.17}$$

Where the resultant charge is less than the deep-discharge charge, an itterative process is initiated which gradually decreases the current requirement until the battery is capable of supplying the current, without discharging below the deep discharge level.

The power dissipated to the load, P, is calculated using Equation 7.2 and the resulting state of charge is mapped to the corresponding open-circuit voltage (Equation 7.3).

Battery Charge

Battery charging takes place in 3 basic stages: bulk, absorption and float.
Bulk Charge : Current is transmitted at the maximum safe rate until the open-circuit voltage rises to near full charge voltage (80-90%).
Absorption Charge: The voltage remains constant and current gradually tapers off as the internal resistance increases during charging.
Float Charge: After the battery reaches full charge, the charging voltage is reduced to a lower level to reduce gassing and prolong battery life.

Figure 7.4 shows typical charging characteristics of a battery (Accu Oerlikon Ltd, 2000). As the terminal voltage of the discharged battery rises, its current acceptance decreases. Bulk charging is illustrated over the initial period, where the charging current is limited to the maximum safe rate to avoid cable overheating, typically this is the battery capacity at the 20-hour rate divided by 4. During the bulk charging phase the charge can be seen to increase linearly. Absorption charging is illustrated by the exponential decay in the current, due to increased internal resistance. During this

charging phase, the voltage remains constant. Peukerts effect on battery charging is illustrated in the logarithmic trend in the charging curve. The battery is fully charged once the current stabilises at a low level for a few hours. This final stage is the float charge.

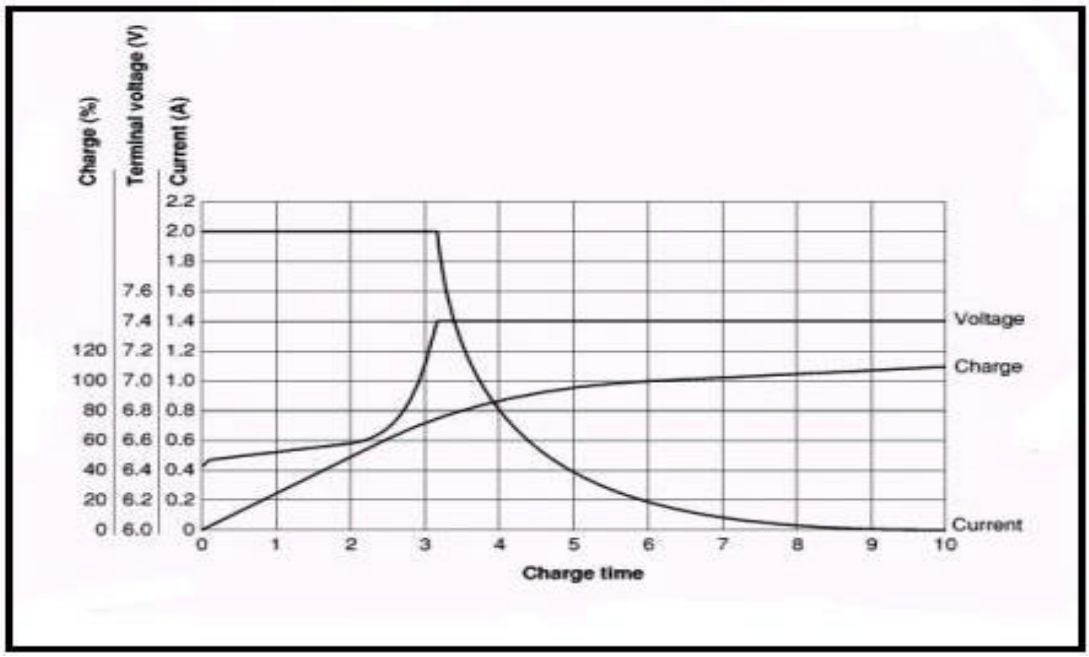

Figure 7.4: Battery charging characteristics (Accu Oerlikon Ltd, 2000)

Battery charge is modelled assuming the use of a charge-regulator designed to prevent overcharging. Without charge-regulation, the battery would quickly be damaged from overcharging. Just as battery discharge is dependent on the state of charge of the battery, so is battery charging. The state of charge dictates the rate a battery will accept charge, if at all. Assuming for the moment that the excess supply generated is sufficient to meet the charging current requirements, battery charging is modelled according to its state of charge. The bulk charging phase is modelled by assuming the maximum charging current is supplied to a battery when its state of charge is below 75%. No distinction is made between absorption and float charging, and this phase has been modelled as follows:

Referring to Figure 7.4, it can be observed that the charging current decreases exponentially as the batteries ability to accept charge is reduced. Furthermore, the charge accepted is equal to the integral under the current – charge time curve. As no other data relating to battery charging characteristics was found, the data presented in Figure 7.4 was assumed to be typical of all lead acid batteries. The data was scaled to represent a single cell, and regression analysis was employed to describe the exponential current decay.

$$I_c = I_{max} \cdot e^{-t} \qquad \text{Equation 7.18}$$

Where I_c = charging current required at time t(A)

I_{max} = maximum charging current (A)

t = time for current to decay from I_{max} to I_c (hrs)

In order to predict the charge accepted by a battery, the current at the beginning and end of a charging interval, require to be evaluated. To do this a number of assumptions were made. The charge stored in a fully charged battery Q_f, is assumed to be the charge of the battery's capacity rated at 20 hours.

$$Q_f = 72000 \cdot C_{20hs} \qquad \text{Equation 7.19}$$

The charge required at the beginning of the charging interval is assumed to be an ideal charging current I_{c_ideal}, defined as that which would be required to recharge the battery fully in the given charge interval, t.

$$I_{c\_ideal} = \frac{\left(100 - SOC_{t-1}\right) \cdot Q_f}{t} \qquad \text{Equation 7.20}$$

Substituting this ideal charging current into Equation 7.18, enables the corresponding charge time to be determined. The charge time at the end of the simulated charging interval, t2, is the sum of the initial charge time, t1, and the charge interval, which enables the charging current at the end of the charging interval to be obtained using Equation 7.1.8. Thus, the change in charge, ΔQ, accumulated in the battery can be described by Equations 7.23 and 7.24.

$$\Delta Q = \int_{t}^{t+1} I\,dt \qquad \text{Equation 7.23}$$

$$\Delta Q = \left[-I_{max} \cdot \exp(-t2) + I_{max} \cdot \exp(-t1)\right] \times \Delta t \qquad \text{Equation 7.24}$$

The current available for charging the battery can be found by solving Equation 7.2 for I, resulting in one of the following, real and imaginary solutions.

$$I = \begin{bmatrix} \frac{1}{(2 \cdot r)} \cdot \left[-V + \left(V^2 + 4 \cdot P \cdot r\right)^{\left(\frac{1}{2}\right)} \right] \\ \frac{1}{(2 \cdot r)} \cdot \left[-V - \left(V^2 + 4 \cdot P \cdot r\right)^{\left(\frac{1}{2}\right)} \right] \end{bmatrix} \qquad \text{Equation 7.25}$$

Using the real solution, enables the charging current available $I_{A,}$ to be determined from the open circuit voltage at the previous time step $V_{t-1,}$ the internal resistance, r and the excess power P.

$$I_A = \frac{1}{(2 \cdot r)} \cdot \left[-V_{t-1} + \left[\left(V_{t-1}\right)^2 + 4 \cdot r \cdot P \right]^{\left(\frac{1}{2}\right)} \right] \qquad \text{Equation 7.26}$$

Where the current available is less than that required, it is assumed that all the charge delivered by the available current can be accepted. Where the current is greater than

that required, only that which is required is used, thereby assuming a charge controller is being used.

The state of charge after charging is calculated as a percentage of the fully charged condition, as described by Equation 7.27 and used to evaluate the open-circuit voltage with Equation 7.3.

The power used, in charging the battery is calculated according to equation 7.2, where P is the power used in battery charging, I the average charging current, V the nominal battery voltage and r the internal resistance (Ω).

$$SOC_t = \frac{(100 - SOC_{t-1}) \cdot Q_f + \Delta Q}{Q_f} \qquad \text{Equation 7.27}$$

Self-Discharge

Batteries that are stored for long periods will eventually lose all their charge. This "leakage" or self- discharge varies considerably with battery type, age and temperature. It can range from about 1% to 15% per month. The rate of self-discharge is typically specified as a percentage loss in capacity over a storage period, typically in the order of months. By assuming the rate of self discharge specified by manufacturers to be linear, self discharge can be incorporated as described by Equation 7.28 (assuming a month has 30 days). Self-discharge is incorporated when the battery is neither charging nor discharging.

$$\delta_{SOC} = \frac{\%\delta \cdot C}{\delta t \cdot 30 \cdot 24 \cdot \Delta T \cdot C_{TC}} \qquad \text{Equation 7.28}$$

Where δ_{SOC} = state of charge reduction due to self-discharge

$\%\delta$ = specified percentage reduction in capacity over discharge period (% / months)

δt = specified discharge period (months)

C = rated capacity (Ahrs)

C_{TC} = Temperature compensated capacity (Ahrs)

ΔT = time period of discharge (hrs)

7.1.3 Other Factors Affecting Performance

Battery Ageing and Life-span

The depth of discharge (DOD) plays an important role in battery life-span. A battery "cycle" is one complete discharge and recharge cycle. It is usually considered to be discharging from 100% to 20% and then back to 100%. However, there are often ratings for other depth of discharge cycles, the most common ones are 10%, 20% and 50%. Battery life is directly related to how deep the battery is cycled each time. If a battery is discharged to 50% every day, it will last about twice as long as if it is cycled to 80% DOD. If it is cycled to only 10% DOD, it will last about 5 times as long as one cycled to 50%. Obviously, there are some practical limitations on this. Manufacturers' specifications will indicate the number of life cycles at a specified deep-discharge level. Battery life is simply estimated by counting the number of cycles as they are simulated and comparing them to the number specified by the manufacturer.

As batteries age their capacities are decreased and they require increased charging times and/or have a higher amperage at the end of the charge. The life-span of a battery will vary considerably with how it is used, how it is maintained and charged, temperature and other factors. Life-span can be seriously reduced at higher temperatures - most manufacturers state this as a 50% loss in life for every 8°C over a 25°C cell temperature. Life-span is increased at the same rate if below 25°C, but capacity is reduced. This tends to even out in most systems - they will spend part of their life at higher temperatures and part at lower. Battery life expectancy due to factors other than

the number of cycles is not accounted for due to the high variability involved. For the same reason battery ageing effects are neglected.

Temperature Effects on Battery Performance

Operating temperatures will affect a battery's performance in a number of ways.

- Self-discharge rates increase with increased temperatures
- Battery capacity is directly proportional to temperature.
- Battery life is inversely proportional to temperature.
- Battery charging voltage changes with temperature. It will vary from about 2.74 volts per cell at - 40°C to 2.3 volts per cell at 50°C.

Accounting for temperature effects is complicated by the size of a battery bank (i.e. its thermal mass) and any insulation used to protect a battery from temperature fluctuations.

The effects of temperature on battery life are neglected as the effects of time spent at higher temperatures is assumed to be cancelled out by time spent at lower temperatures.

The effect of temperature on battery capacity is illustrated in Figure 7.5. The effect is assumed to be linear between temperatures of -20°C and 20°C and also between 20°C and 60°C, but at a different rate. The linear temperature effects are applied to the two rated capacities used to define a battery, at the beginning of every time-step calculation. As these capacities are subsequently used in modelling all modes of battery operation, temperature effects are accounted for. Battery discharge rates are evaluated utilising the rated capacities. Battery state of charge is modelled as a percentage of the fully charged capacity, rated at the 20-hr rate, to which temperature effects are applied. State-of-charge is mapped to the battery voltage, which ensures temperature effects on voltage are incorporated. Battery charging currents are assumed un-effected by temperature as temperature compensation is included in the majority of battery charge control systems. However the effect of applying a certain charging current over a period of time will

vary depending on temperature, as the amount of charge stored by the battery will vary with temperature. Finally, self-discharge is modelled as a percentage reduction in capacity, therefore a percentage change in a temperature effected capacity, will account for the effects in self discharge.

Equation 7.29 and 7.30 are used to establish temperature effects of temperatures below and above 20°C respectively.

$$C = C_{ref} \cdot \frac{0.875 \cdot (T + 20) + 65}{100} \qquad \text{Equation 7.29}$$

$$C = C_{ref} \cdot \frac{0.25 \cdot (T - 20) + 100}{100} \qquad \text{Equation 7.30}$$

Where C = capacity with temperature compensation

C_{ref} = capacity prior to temperature compensation

T = operating temperature (assumed to be ambient temperature)

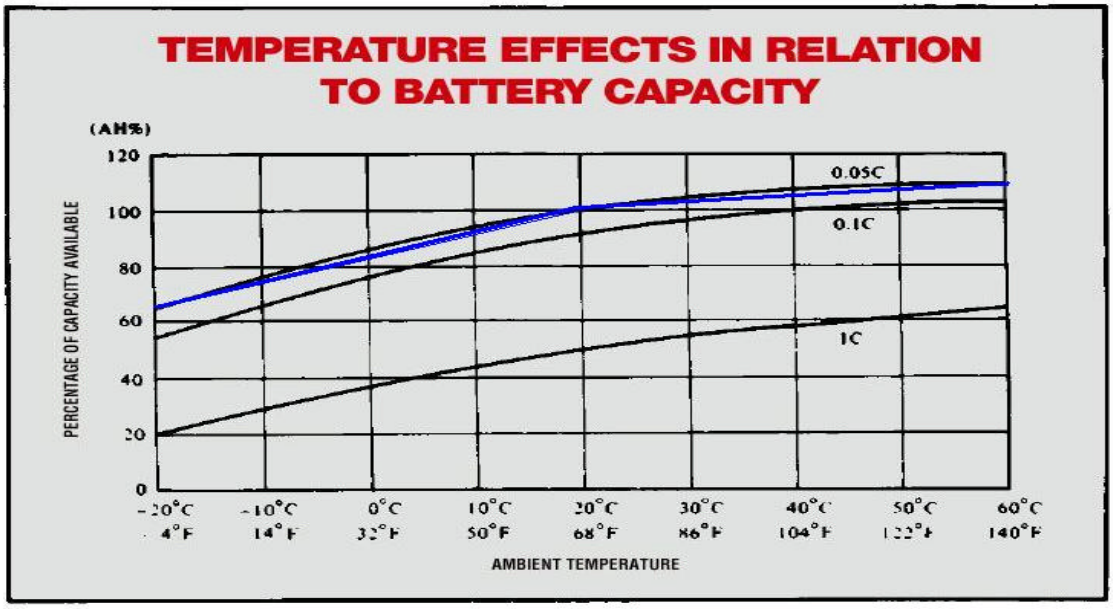

Figure 7.5 Temperature effects on battery capacity (Yaussa Batteries, 2000)

Battery Configurations

The discussion so far has related to a single battery. For battery banks including multiple batteries connected in series or parallel, standard electrical circuit theory is employed to model the effects of configurations.

Identical batteries connected in series maintain the same capacity as a single battery. The total internal resistance is the sum of the internal resistances of the batteries and the total open-circuit-voltage is the sum of the open-circuit voltages.

Connecting secondary cells in parallel in theory leads to greater current capacity. In practice, however, poor current sharing during both charging and discharging will cause serious cell imbalance and early failure. The effects of this phenomenon are not accounted for and parallel batteries are modelled theoretically. Theoretical treatment of parallel-connected batteries results in the same open-circuit voltages as a single battery, a total capacity that is the sum of the capacities and a reduced internal resistance.

7.1.4 Sample Results

Referring back to the example profiles used in the previous chapter, the small commercial demand profile has been combined with a mixture of supplies consisting of 20 PV panels with tracking, a PV hybrid Façade, 10 ducted wind turbines and a 100 W wind turbine. To demonstrate battery modelling four series connected batteries rated at 215 Ah (at 20 hours) have been modelled, with the deep-discharge level set at 30%. Figure 7.6 shows the demand and supply profiles and that of the supply with battery storage and Figure 7.7 describes the state of charge of the battery bank over this one-week period. During the initial 12-hour period the demand exceeds the supply, but is met by the battery, which initially is fully charged. The midday supply then exceeds the demand and is used to re-charge the battery. The initial recharging can be seen to occur faster than when the battery system approaches its fully charged condition. The charging process successfully absorbs all of the excess supply and during this time

supply and demand are perfectly matched. However the evening demand is greater than in the morning and the battery fails to meet the entire load, discharging rapidly to its deep-discharge level. At this point no power is supplied from either the primary supply or the battery, in order to meet the demand power has to be imported from the grid, or it will not be met. Recharging occurs around noon on every subsequent day. The next four days however, produce insufficient excess supply to bring the battery back up to full charge. Over the weekend the demand is significantly reduced and this coincides with a particularly productive period for the combined RE system and the supply exceeds the battery's ability to absorb it, leaving an excess which is either wasted or exported to the grid.

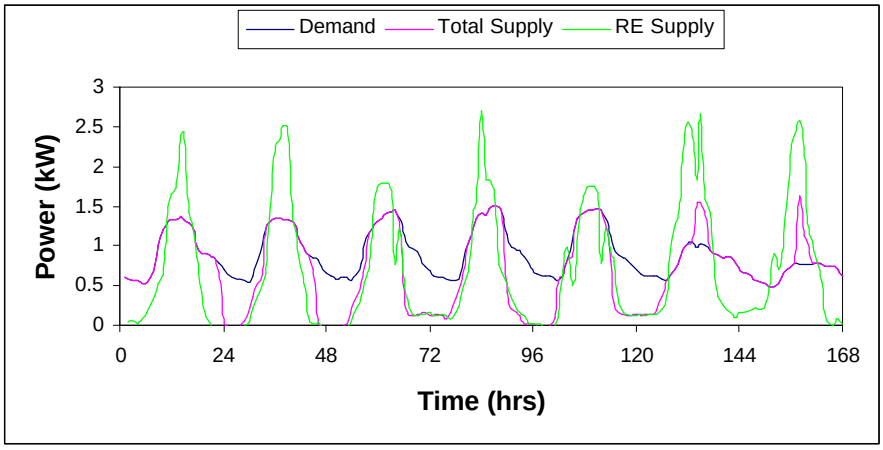

Figure 7.6: Comparison of demand, supply and supply with battery storage profiles

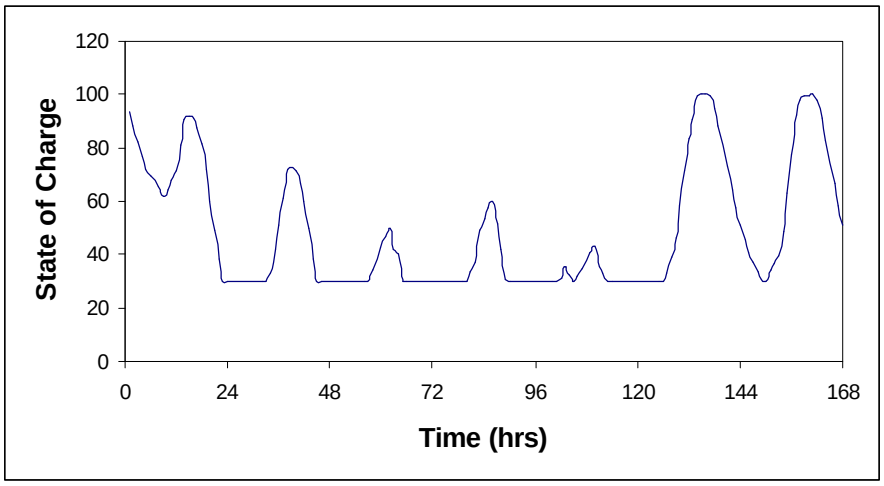

Figure 7.7: Changes in battery state of charge

This example was modelled again using 8 batteries in series to illustrate the effects of increasing the overall capacity and using 4 batteries in parallel to examine the theoretical differences in battery configuration, whilst neglecting the adverse effects of current sharing in the parallel arrangement. Figure 7.8 illustrates the differences in residual power resulting from the three different battery configurations. Figure 7.9 shows the corresponding differences in states of charge. It can be seen that by doubling the capacity the length of time a fully charged system can supply a load is increased significantly and its capacity for absorbing excess supply is also increased, however the charge and discharge rates are reduced. Parallel configurations compared with batteries in series charge less rapidly but discharge at approximately the same rate, which demonstrates that series configurations are superior, even when the effects of current sharing are neglected. Table 7.1 illustrates the differences in match statistics resulting from the use of the different battery systems. The results show that by incorporating storage the match is improved and that the improvement is related to the storage capacity. The results also illustrate that series configurations are superior to parallel.

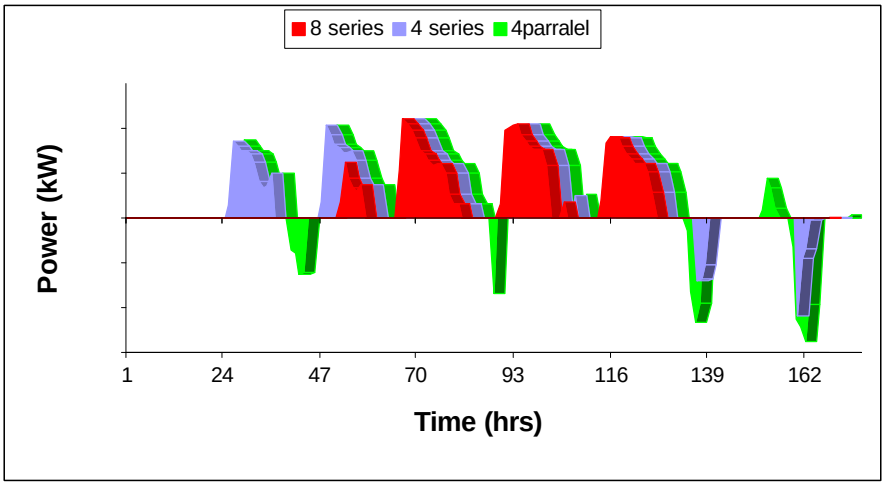

Figure 7.8: Comparison of the effects of different battery configurations on residual power

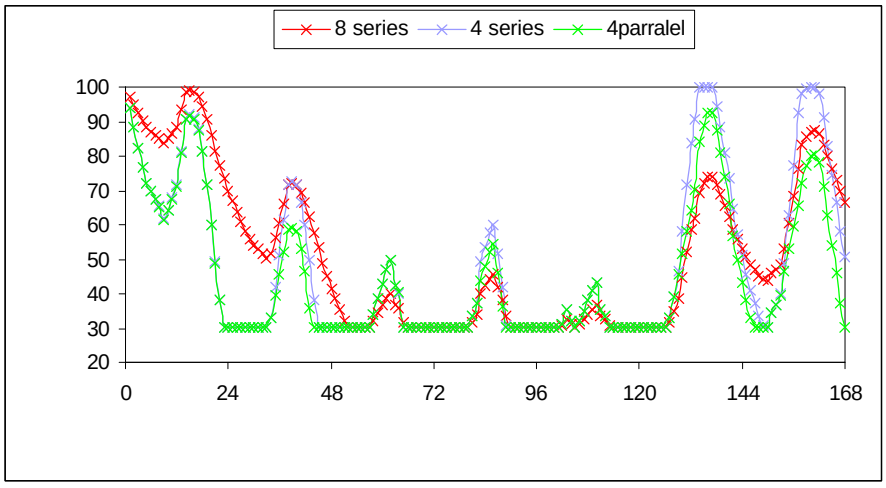

Figure 7.9: Comparison of the states of charge of different battery configurations

Table 7.1: Comparison of match statistics of different battery configurations

Storage	Correlation	Inequality	Excess (kWh)	Deficit (kWh)	Battery discharge (Ahrs)	Battery charge (Ahrs)
None	0.6	0.33	33.78	64.09	-	-
4 Series	0.78	0.20	3.03	35.01	638.96 @ 48V	584.24 @ 48V
8 Series	0.81	0.16	0.00	24.10	423.76 @ 96V	332.98 @ 96V
4 Parallel	0.74	0.22	8.75	37.26	2367.26 @ 12V	1958.61 @ 12V

7.2 Back-up Generation

Diesel generator sets are frequently used as stand-by power units. Engine performance can be modelled in different levels of precision. Liu and Karim (Liu and G. Karim, 1996) describe a highly detailed model used in simulating the combustion processes. Such an approach was considered unsuitable due to the requirements of engine geometry and operational parameters, which are not available from manufacturers' standard specifications. Kelly (Kelly, 1998) describes another approach used in the simulation of CHP systems, where by performing a one-dimensional energy balance for the cycle-averaged combustion process, the mechanical work output can be calculated. This approach again requires the specification of a number of parameters unavailable from specifications and utilises empirical values best obtained from test data. As the objective of this work is to gain an understanding of performance prior to installation and based solely on manufacturers' data, methods employing empirical data are unsuitable. Evans (Evans, 1994) suggested the use of engine performance charts to find the most efficient point of engine operation and model performance based on a generator running at this point. However, it is not always possible to couple an engine's most efficient point of operation with a generator, as generators are designed to operate at a fixed rotational speed. The approach adopted here utilises performance charts to obtain data related to fixed speed operation. The speed is ascertained through Equation 7.31 and is based on the number of generator pole pairs and the supply frequency.

$$S = F \cdot \frac{60}{n}$$ Equation 7.31

Where S = engine speed (rpm)
F = supply frequency (Hz)
n = number of generator pole pairs

An example of an engine performance chart is given in Figure 7.10, where the method used in determining operating characteristics for the maximum power output condition at a specified speed is illustrated. In this example the operating speed specified is 1500 rpm which could correspond to the engine being coupled with a generator incorporating 2 pole-pairs supplying power at a frequency of 50 Hz. From the operating speed, the specific fuel consumption at that speed and the engine torque and power output at this torque, can be obtained. This information is sufficient for obtaining a first approximation of the generator-set performance.

The total power required of the generator, P_g, can be obtained by calculating the magnitude of the real, P_r, and reactive, Q, components of the power deficit.

$$P_g = \sqrt{P_r^2 + Q^2}$$ Equation 7.32

The power required from the generator can be translated into that required by the engine P_e, by accounting for the efficiency of the generator, η, and its power factor, θ, as described by Equation 7.33

$$P_e = \frac{P_g}{\eta \cdot \theta}$$ Equation 7.33

If the power required is greater than that which can be supplied by the generator-set, then the output is simply set at the maximum generation conditions. Where there is no deficit the generator is not required and the output is set to zero. Where some intermediate power requires to be satisfied, the engine torque is reduced to reduce the power output whist maintaining the generator speed. Since power is equal to the product of torque and angular velocity (Hannah and Hiller, 1994) and the velocity remains constant, the operating torque T, can be calculated from Equation 7.34.

$$T = \frac{P_e}{P_m} \cdot T_m \qquad \text{Equation 7.34}$$

Where Pm = power output at maximum torque for operating engine speed
Tm = maximum torque at operating engine speed

Specific fuel consumption, SFC, is given in the units g/kWh, thus by calculating the power output from the engine, P_e and assuming this remains constant over a specified time interval, t, the actual fuel consumption, FC, in grams, can be calculated as follows:

$$FC = P_e \frac{SFC}{t} \qquad \text{Equation 7.35}$$

By outputting the percentage of engine loading and the fuel consumption an indication of both engine performance and fuel requirements is obtained.

Diesel engines can vary considerably in size and can be large enough to provide an entire community with its power requirements. A community scenario, made up load profiles for 2 agricultural loads, a school, 4 shops, 30 standard and 5 large residential premises, street lighting and traffic control, has been used to illustrate the results obtained by modelling diesel generators. Figure 7.11 shows the demand profile met exactly by the generator and the percentage of engine loading required to meet the demand. Figure 7.12 illustrates the demand profile and the profile from a 300 kW wind turbine. Figure 7.13 shows the wind turbine combined with the diesel generator used to meet the demand and the generator loading.

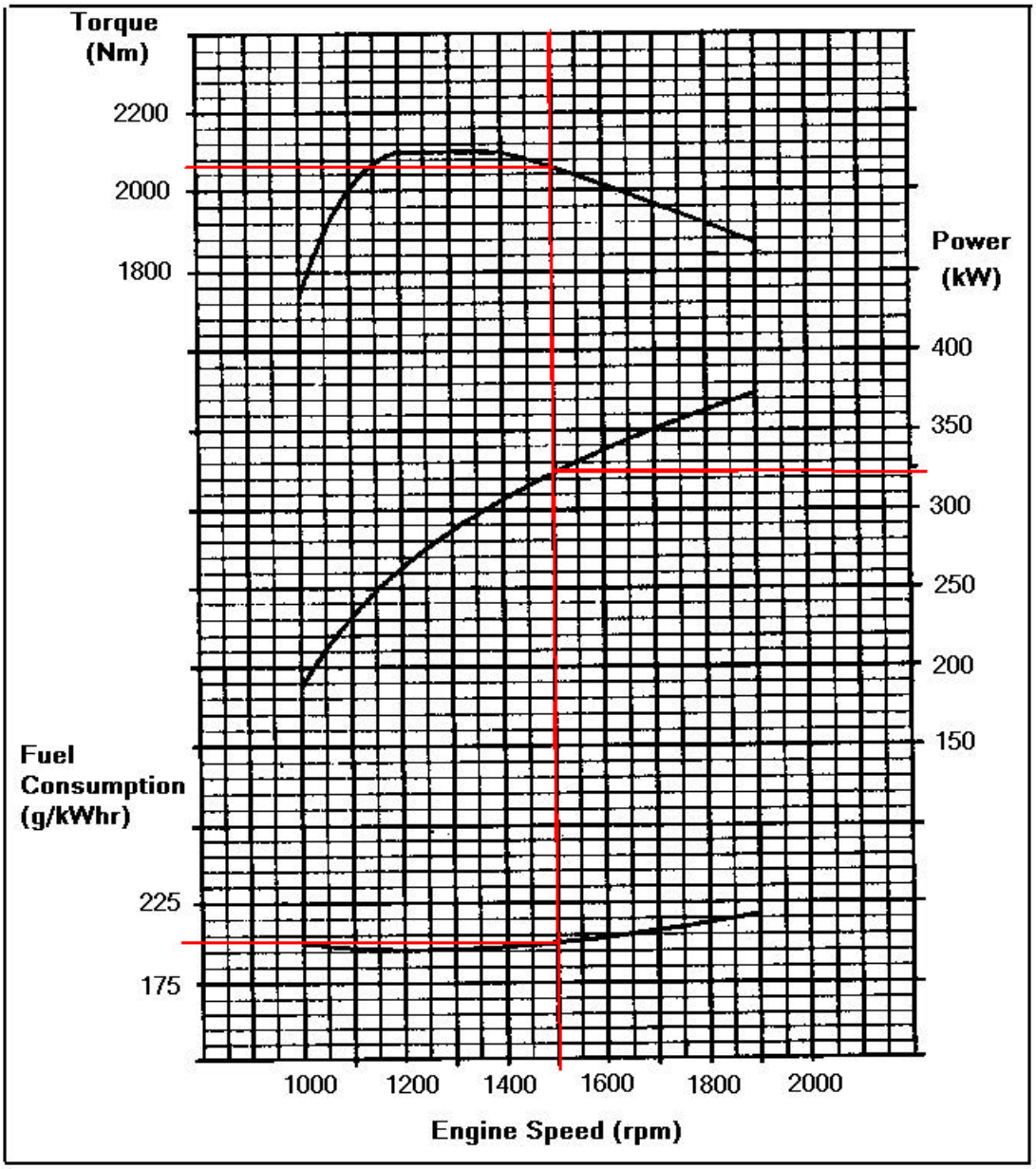

Figure 7.10: Typical Engine Performance Curve (Cummins Engine Company Ltd, 1994)

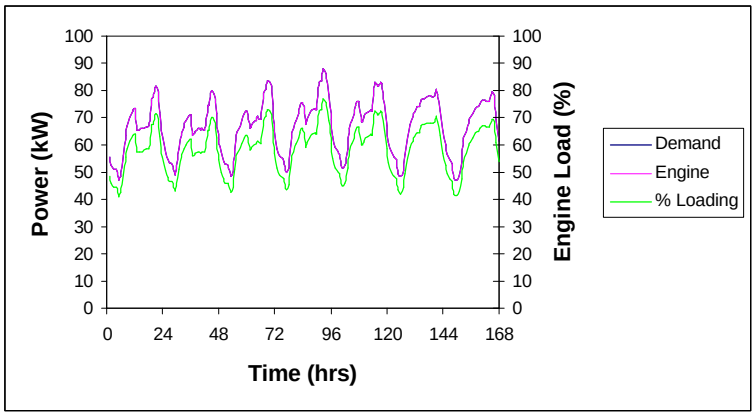

Figure 7.11: Community demand and generator supply

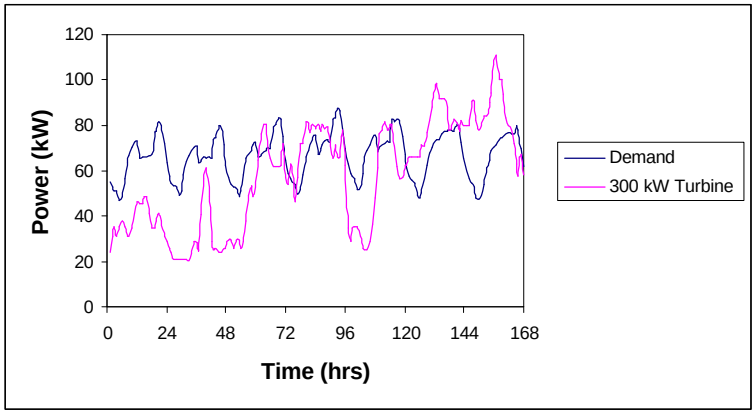

Figure 7.12: Community demands and wind turbine supply

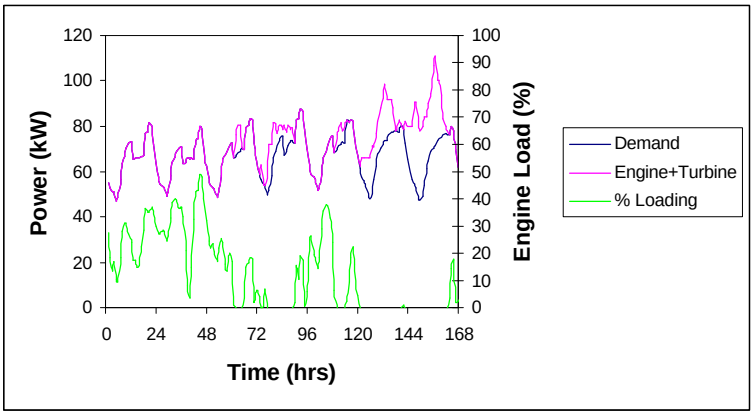

Figure 7.13: Community demand and combined wind turbine and generator supply

These figures illustrate that generators are ideally suited to making up deficit supply, but cannot store any excess, therefore if diesel generators are to be incorporated into a hybrid supply system the renewable energy systems should ideally be slightly undersized to prevent wastage. Secondly, to prevent excess generator cycling, the role of the renewable is to eliminate peak demands thereby enabling more continuous engine operation. Although running at full load will result in engine wear, running at very low loads is an inefficient use of the generator. Table 7.2 illustrates the match statistics for the three examples given above and the fuel consumption for the generator cases. From this table it can be seen that although the generator used autonomously results in a perfect match, there is a fuel penalty associated with it. The wind turbine on its own results in a considerable deficit, which is easily supplied by the generator with a 78% reduction is fuel consumption. However, where the diesel and wind system are used together the engine is loaded at 20% of full load for much of its operation, this indicates that a smaller generator may be more appropriate in such a scenario.

Table 7.2: Comparison of supply systems with and without generator

Supply	Correlation	Inequality	Excess (kWh)	Deficit (kWh)	Fuel Consumption (kg)
Generator	1	0	0.00	0.00	3211.77
Wind Turbine	0.30	0.18	956.39	2499.99	-
Wind Turbine & Generator	0.65	0.07	956.39	0.00	716.91

7.3 Tariff Structures

A variety of tariff structures exist, designed to meet different electricity consumption patterns. Typically tariffs can encompass either a single kWh price, night and day time prices, evening and weekend reduced rates or rates which charge a certain premium for an agreed number of initial units and another for any units consumed above this limit (Scottish Power, 1999). Additional service charges are also applied either daily or monthly. Calculating the cost of electricity consumption, with respect to different tariff options, enables tariff optimisation and an economic evaluation of saving resulting from RE generation. Tariff accounting simply involves summating the kWh required by the grid and applying cost functions which will depend on the tariff and either the day type, time of day, running kWh total or a combination of these. For example, Tariff A utilises a one-price structure of x pence/kWh and a standard charge of y pence/day, the total cost of an electricity consumption, c, over a period, p, will therefore equal $x \times c + y \times p$. Tariff B, on the other hand is divided into a day and night rate, where day-time and night-time units are priced at x and y pence/kWh and a standing charge of z pence/day is applied. In this case the consumption during defined day hours is kept separate from the night-time consumption to calculate the total electricity cost.

Incorporating tariff analysis in matching exercises enables an economic analysis of savings made through the deployment of RE systems. To demonstrate the effect of different tariffs a demand profile has been met entirely by the grid and priced using two different tariffs. Tariff 1 is a business tariff with a reduced weekend and evening rate and tariff 2 uses a fixed price per kWh, independent of time of use. The demand is subsequently combined first with a PV façade and then with a 10 kW wind system and the tariffs are applied to the deficit portion met by the grid. The profiles from the PV and wind systems relative to the demand are shown in Figures 7.14 and 7.15, respectively. The PV system never exceeds the demand whereas the wind system does towards the end of the week. The price for grid exported power changes every half-hour depending on the lowest bid from large-scale generators. To include a realistic

approximation for a tariff structure for exported power a detailed analysis of price trends would be required, which was out with the scope of this work, thus, excess production is treated as wasted electricity.

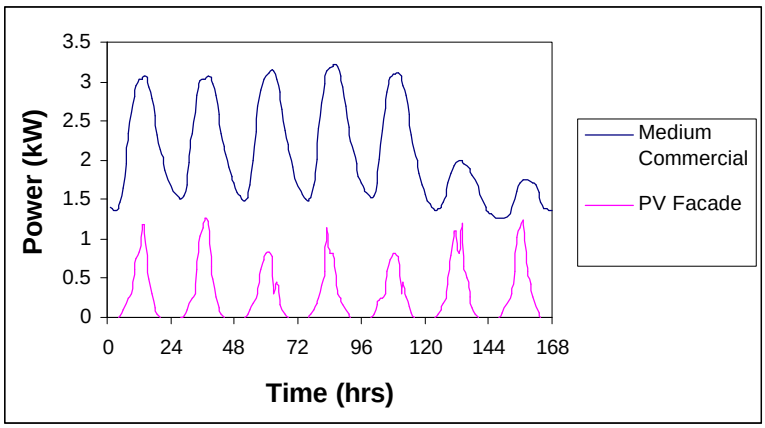

Figure 7.14: Demand and PV profiles

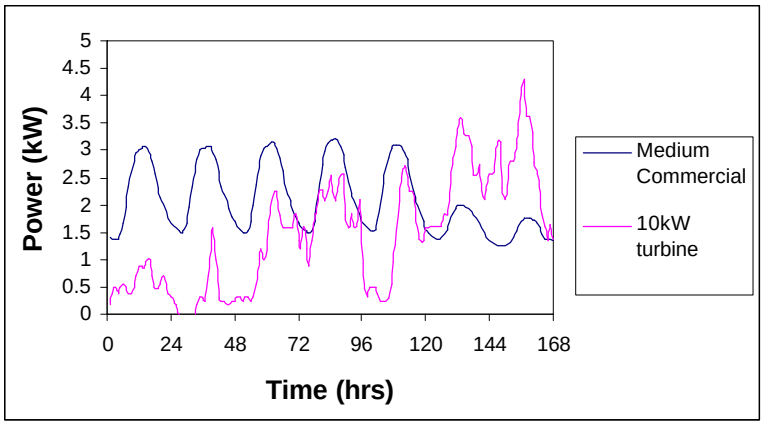

Figure 7.15: Demand and wind turbine profiles

Figure 7.16 compares the difference in electricity costs and total cost, which includes standing charges. Although the standing charge for tariff 2 is less than for tariff 1, the total cost for tariff 2 is still greater in each of the cases presented. Figure 7.16 quantifies the savings made by deploying the different RE systems over this one-week

period. To obtain an estimated pay-back, tariff analysis needs to be carried out on an annual basis. However, what is clearly demonstrated is that pay-back periods are relative to tariff prices and tariff analysis is beneficial in negotiating favourable arrangements.

Ideally RE system costs should be incorporated in any economic analysis relating to RE deployment. However, generic capital cost functions are difficult to establish as costs vary with a number of factors such as whether export facilities are required, proximity to grid connection, installation and commissioning costs, and project scale. As RE system costs are both site-specific and likely to change significantly in the future, their inclusion was considered beyond the scope of this work.

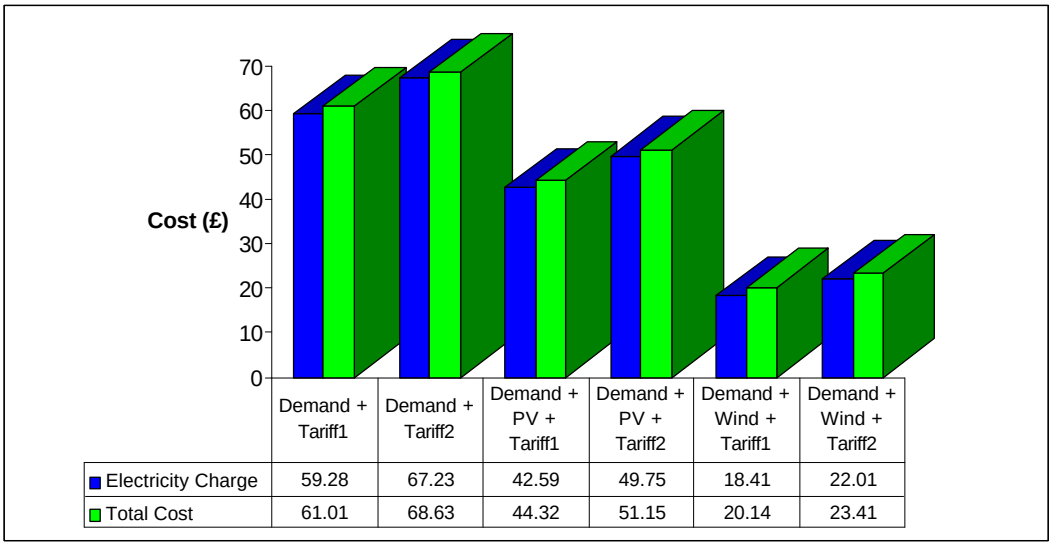

	Demand + Tariff1	Demand + Tariff2	Demand + PV + Tariff1	Demand + PV + Tariff2	Demand + Wind + Tariff1	Demand + Wind + Tariff2
Electricity Charge	59.28	67.23	42.59	49.75	18.41	22.01
Total Cost	61.01	68.63	44.32	51.15	20.14	23.41

Figure 7.16: Tariff price analysis.

7.4 Potential Match Assessment

The inequality metric described in the previous chapter was shown to be the best indicator of 'goodness of fit'. Another useful indicator is that of a potential match. Since matching has been shown to be an iterative process in optimisation, a potential match index could be used to evaluate supply and demand combinations, which could potentially achieve near excellent matches, using some form of auxiliary system. It is clear however that a very bad match, where the supply is considerably less than the demand, could be transformed to a perfect match with an adequately sized generator, possibly to the detrimental operation of that generator. Thus the conditions for a potential match must consider this, as well as the fact that continuous under supply from an RE system cannot be combined with battery storage as these conditions will never allow the battery to recharge. Correlation and FFT parameters are useful in picking out similarities in the trends of the profiles, but neither accounts for relative magnitudes involved.

The net residual area relative to the shared area quantifies the impact of the supply on demand without providing any indication of whether the profiles are in phase with one another. Two separate potential match indices are required to define the potential match that could be obtained through improved storage and through the inclusion of some back-up supply system. The potential match with storage can be quantified by combining the correlation coefficient and the residual area relative to the shared area. Equation 7.36 describes the parameters used to derive this metric and Equation 7.37 shows how it is calculated.

$$PMS = \frac{A_r}{A_s} + CC \qquad \text{Equation 7.36}$$

Where PMS = potential match with storage

A_r = residual area

A_s = shared area

CC = correlation coefficient

$$PMS = \frac{\left(\int_0^n D(t)\,dt\right) - \left(\int_0^n S(t)\,dt\right)}{\left(\int_0^n D(t)\,dt\right) \cup \left(\int_0^n S(t)\,dt\right)} + \frac{\sum_{t=0}^{n} (D_t - d)\cdot(S_t - s)}{\sqrt{\sum_{t=0}^{n} (D_t - d)^2 \cdot \sum_{t=0}^{n} (S_t - s)^2}} \qquad \text{Equation 7.37}$$

The potential match with back-up supply also requires the use of the correlation coefficient to pick out trend similarities, however where back-up systems are used it is preferable that the primary supply does not exceed demand as this represents periods of energy wastage. Thus the potential match with back-up supply can be defined by Equation 7.38.

$$PMBS = CC\,2 \quad \frac{1}{N} \cdot \sum_{n=1}^{N} D(t) - S(t) \qquad \text{Equation 7.38}$$

Where PMBS = potential match with back-up supply

D(t) = Demand at time t

S(t) = Supply at time t

N = number of time steps

Potential match metrics can be used as a filtering variable in the search procedures described in the previous chapter. Employing the storage potential match metric on the profiles used in the previous chapter, shown in Figure 6.8, the best potential match is that of a small commercial demand combined with 20 PV panels with tracking, a PV roof and 10 ducted wind turbines. The two profiles are shown in Figure 7.17, it is clear because of the excess supply, a storage facility is required to improve the match. Figure

7.18 illustrates the effect of incorporating ten 215 Ahr batteries in series to provide this storage, starting with a fully charged battery bank and setting the deep-discharge level to 30%. Because the battery is fully charged to begin with it is unable to accept some of the excess supply initially, also evident from Figure 7.18 is that the deep-discharge level prevents the battery supplying the demand during days 4 and 5. However if the battery is initially at 85% of the fully charged condition and is permitted to discharge to 10%, then the entire load can be satisfied, as is shown in Figure 7.19. This example illustrates how a potential match assessment can be useful in cases where auxiliary systems are to be incorporated.

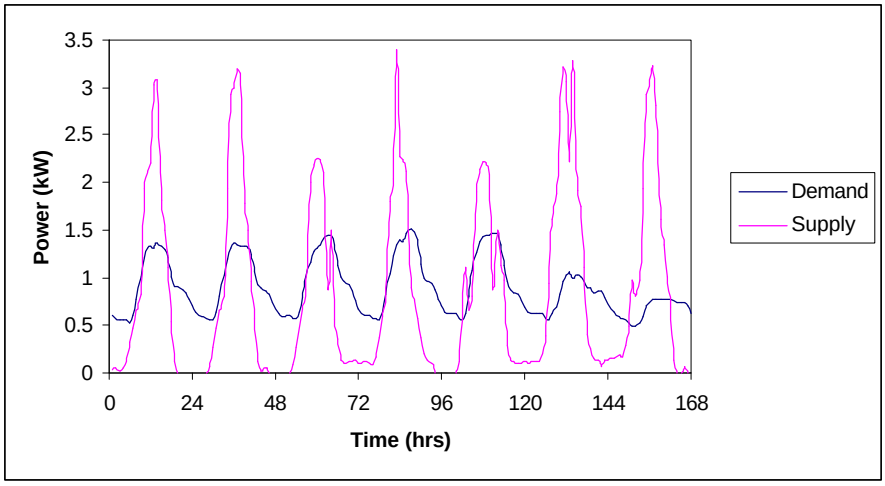

Figure 7.17 Best potential match with storage from example given in Figure 6.8

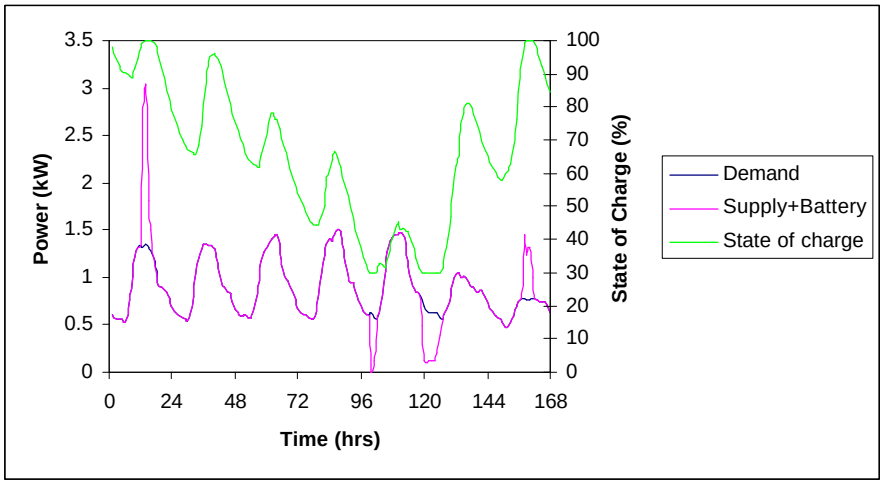

Figure 7.18: Effect of combining battery bank with 30% deep-discharge level

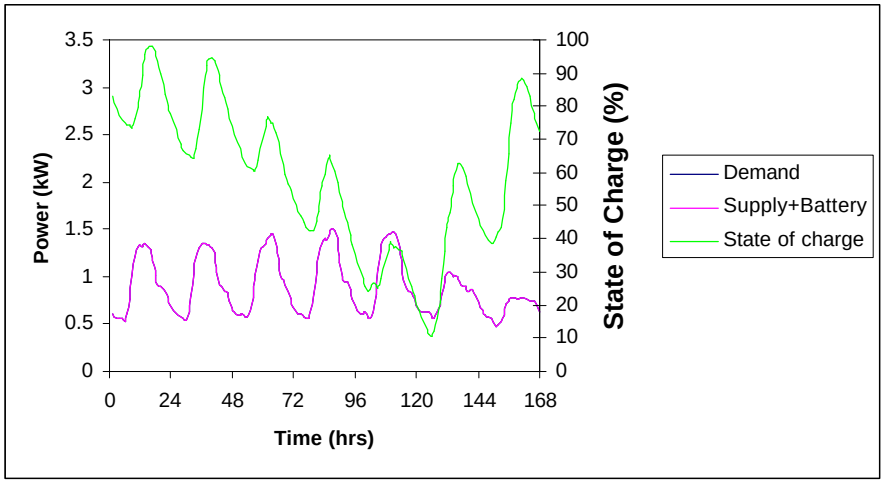

Figure 7.19: Effect of combining battery bank with 10% deep-discharge level

7.5 Summary

Mathematical models have been developed for both battery systems and back-up generators. These auxiliary systems can often be used to enhance a match between a renewable energy supply and a demand. Mathematical modelling of these systems is the most efficient means of evaluating their performance under different conditions. Furthermore it is the most economic means of ensuring auxiliary systems are sized optimally. A procedure for tariff analysis has been demonstrated which is useful both in quantifying the savings resulting from RE deployment and for any tariff negotiation. Two mathematical definitions for metrics of potential match with storage and with back-up supply have been described and shown to be useful in evaluating matches which best benefit from auxiliary system incorporation.

7.6 References

1. Accu Oerlikon Ltd Copyright (c) 1996, 1997, 1998, 1999, 2000. accu-info@accuoerlikon.com
2. Child D., Smith I.R. and Infield D.G., Wind, Photovoltaic and Battery Electrical Power: Expeience and Modelling of an Autonomous and Grid Connected System, International Journal of Ambient Energy, Vol 17, No3, July 1996.
3. Cummins Engine Company Ltd., N500E Truck Engine Technical Data Sheet, April 1993
4. Davis T. J., Circuit Calculations, Butterworth-Heinemann Ltd., 1992
5. Decher Reiner, Direct Energy Conversion, Oxford University Press 1997
6. Evans Mark S., Plant Modelling and Simulation for Small Renewable Energy Systems, Msc Thesis, University of Strathclyde, Spetember 1994.
7. Excide Recommended Fitments Catalogue, 2000/20001
8. Goldstein Lawrence H. and Case Glenn R., PVSS – A Photovoltaic System Simulation Program, Solar Energy, Vol 21, pp 37-43, 1978.
9. Hannah J. and Hiller M., Mechanical Engineering Science, 2nd Edition, Longman Scientific & Technical, 1994
10. Hiram Gu and Nguyen T.V., A Mathematical Model of a lead Acid Cell, Journal of Electrochemical Society, December 1987, pp. 2953-2960
11. Kelly Nicolas, Towards a Design Environment for Building-Integrated Energy Systems: The Integration of Electrical Power Flow Modelling with Building Simulation, PhD Thesis Strathclyde University, October 1998
12. Liu Z. and Karim G., Simulation of Combustion Processes in gas-fuelled diesel engines, Proceedings of the Institution of Mechanical Engineers, Vol. 221, Part A, pp. 159-169., 1996
13. Manwell James F. and McGowan Jon G., Lead Acid Battery storage Model for Hybrid Energy Systems, Solar Energy, Vol. 50, No. 5, pp.399-405, 1993

14. Morgan T. R., Marshall R. H., Brinkworth B. J., ‘Ares’ – A refined Simulation Program for the Sizing and Optimisation of Autonomous Hybrid Energy Systems, Solar Energy, Vol 59, No 4-6, pp 205-215, 1997.
15. Newman John and Tiedemann William, Simulation of Recombinant Lead-Acid Batteries, Journal of Electrochemical Society, Vol 144, No 9, September 1997, pp. 3081-3090.
16. Northern Arizona Wind & Sun, All about Deep Cycle Batteries, URL: http://www.windsun.com/Batteries/Deep_Cycle.htm, 1999
17. Notten P.H.L., Kruijt W.S. and Bergveld H.J., Electronic Network Modelling of Rechargeable Batteries, Journal of Electrochemical Society, Vol 145, No 11, November 1998, pp. 3774-3782.
18. Oerlikon, URL: http://www.accuoerlikon.com/html/accuframe6.htm
19. Protogeropoulos C., Marshall R. H., Brinkworth B. J., Battery State of Voltage Modelling and an Algorithm Describing Dynamic Conditions for Long-Term Storage Simulation in a Renewable System., Solar Energy, Vol 53, No 6, pp 517-527, 1994.
20. Scottish Power, Domestic Pricing Information, Gas & Electricity in your Area, April 1999
21. Scottish Power, Electricity Prices for Buisness Customers (Designated Sites), April 1999
22. Shepherd C.M., Design of Primary and Secondary Cells, Journal of Electrochemical Society, July1965, pp. 658-664.
23. U.S. Battery Manufacturing Company, URL: http://www.usbattery.com/specs1.htm, 2000
24. Ure George, Application Note: Why Batteries Shrink, 12/01/98 URL:http://www.cruisingequip.com/ftp/Battery%20Shrink.pdf
25. Yuassa Batteries, URL: http://www.yuasa-exide.com/pdfs/NP1.2-6.pdf, 2000

Chapter 8: MERIT – Towards a Software Solution

The methodologies and mathematical models presented in the previous chapters have been used to create, through the use of rapid prototyping, a software program to provide a structured methodology for performing matching exercises. This chapter describes the program both from the user perspective and from a software engineering viewpoint. The program is entitled MERIT and has been developed to investigate supply and demand matching. The implementation platform is Visual C++. In chapter 4, it was pointed out that theoretical modelling programs were limited to a small number of specialised consultants, because of the difficulties incurred by users. The principal pitfalls identified were time requirements in data input and due to a lack of understanding of the underlying modelling principles, difficulties in accurately specifying the modelled scenario. The fundamental aim in the creation of MERIT was to ensure its use was not limited to specialist knowledge and could be used by computer literate individuals to investigate various supply and demand strategies, without the need for prior knowledge of different technologies.

Figure 8.1 illustrates the elements comprising MERIT; the principal components are:

- Central program manager: This component allows accesses the other components, directing the user through a project specification in an intuitive way. The program manager allows current projects to be saved and opens previous projects.
- Boundary Condition Specifier: Enables the selection of climate files and periods of investigation.
- Demand Specifier: Enables profile selection from a profile database and/or profile importation from an external source. Additionally, this component provides the route to the profile designer from which profiles can be created.
- Supply Specifier: Enables the specification of renewable supply technology parameters (based on manufacturers' data) from which system performance is

simulated. These specifications can be loaded from and saved to relevant databases. Alternatively, profiles can be imported from external sources. Supply simulation is done within this component.

- Auxiliary System Specifier: Enables the specification of auxiliary system parameters and contains the same functionality as the supply system specifier with the exceptions that auxiliary system performance simulation is not carried out as this stage and auxiliary profiles cannot be imported. Auxiliary systems are classed as such because their performance is dependent on the supply/demand systems they are combined with, and can therefore not be simulated until the supply and demand combination is known.
- Matcher: Reports match statistics between selected supplies and demands and simulates the performance of auxiliary systems. This component contains a matching search engine to find optimum combinations in terms of selected criteria. (All profiled data can be exported from the matcher.)
- Reporter: Reports details of selected profiles and results from search procedures.

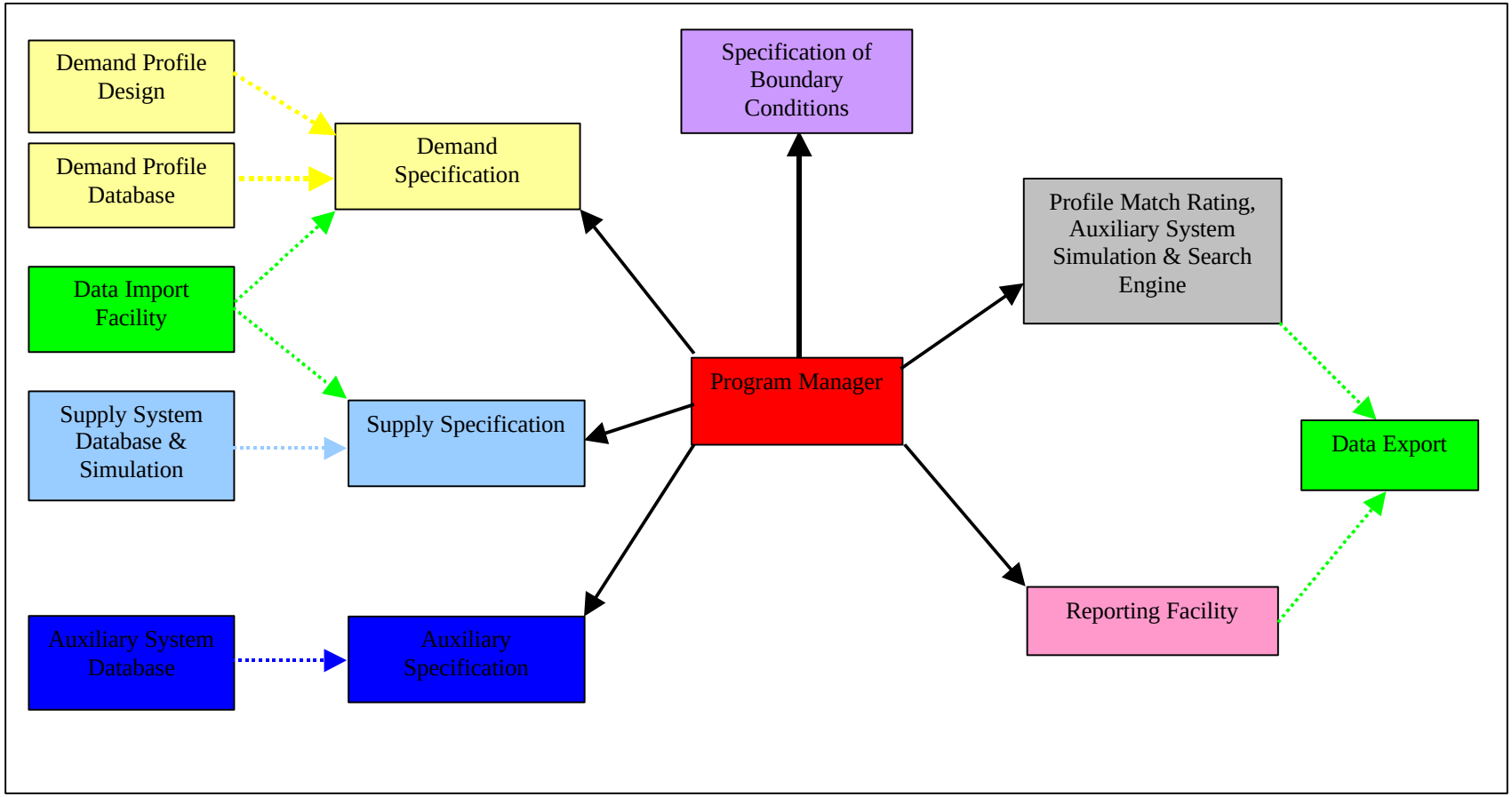

Figure 8.1: Principal components of MERIT

8.1 Software Architecture

The principal software objective was to provide a structure that could be evolved on a task-sharing basis in future, whereby new or modified models could be efficiently incorporated and maintained. These objectives resulted in the development of MERIT using Object-Oriented Programming (OOP). OOP is defined (Grady, 1991) as: *a method of implementation in which programs are organised as co-operative collections of objects, each of which represents an instance of some class and whose classes are all members of a hierarchy of classes united via inheritance relationships*. The essence of the OO paradigm is that a program can be composed of independent objects, communicating via messages (Clarke et al., 1992). The modular approach facilitates the addition of new models through the incorporation of new classes, which can be derived from a common base class containing any common functionality and thus re-using existing code. Reusing developed classes enables faster development with improved reliability and design consistency (Electric Library's Free Encyclopaedia). The programming language selected for the implementation was C++ (Stroustrup, 1999). The principal reasons for its selection were as follows:

1. Modules created are isolated from changes made in other modules, thus changes in one module will not ripple to other modules. Once created, modules are reusable in that the high level modules do not depend upon the low level details and so can be reused in a different detailed context.
2. Run Time Efficiency. C++ is a statically typed language, which performs run time binding by indexing a table of pointers. Dynamically typed languages perform run time binding via looked up tables, with a loop and a token matching algorithm. With this procedure it is impossible to precisely describe the time required for such an operation and is generally of the order of dozens, or even hundreds of microseconds. Indexing a table of pointers always requires exactly the same amount of time and for each implementation is of the order of one or two microseconds. This makes C++ an excellent choice for applications that have intense real time requirements. It also

makes C++ a good choice for component libraries that ‘might’ be used in intense real time applications (Martin,1995).

3. Memory management: C++ is possibly the best language to provide control over how memory is managed (Martin,1995). The disadvantage with this is that dynamically allocated memory, which is not ‘freed’ can lead to memory leaks. Because of this, a developing environment had to be selected capable of tracking heap problems.

The development environment selected was the Microsoft Visual Studio, which as well as providing heap tracking, encompasses the Microsoft Foundation Class Library (MFC), which is an "application framework" for programming in Microsoft Windows. This framework ensures developed programs are compatible with any Microsoft Windows operating system. Statistics have shown that of all the operating systems in use over the past year, Windows NT holds the majority at 60.51% (OS Statistics, 1999). Thus building a Windows application clearly widens the scope for potential users. MFC provides much of the code necessary for managing windows, leaving only the addition of application specific code to create a working tool, which clearly reduces the development time.

8.2 MERIT from a Users Perspective

A new user could carry out an initial investigation into RE deployment within 30 minutes following the subsequent procedure. First a climate file together with the dates of interest would be selected. Secondly, standard demand profiles would be selected from the database of demand profiles to best replicate the demand(s) of interest. Having thus defined the demand, a variety of RE supply technologies could be selected from the various databases and if desired a rage of auxiliary technologies. Thereafter the match facility would be used to investigate the various combinations, this process may be manual or may involve the auto-search mechanism which enables the best supply and demand combinations to be evaluated automatically by MERIT. A

comprehensive study would require further investigation through a process of refining demand profiles and configuring supply technology choices, however within a very short time frame the reasonable options would become apparent.

Figure 8.2 illustrates the central project manager; the dialog contains buttons to provide access to the other components. The four project progress reporting views detail the boundary conditions and the demand, supply and auxiliary systems selected. To initiate a new project, the first task is to specify the analysis conditions, as the dates selected direct the program to select the relevant portions of demand profiles and the climate conditions to use in the simulation of RE systems. The user is prevented from any other action (other than exiting) by the disablement of other buttons. Once these conditions have been specified the user is free to define profiles, where every profile selected appears in the relevant reporting view. The natural order of progression follows the top-to-bottom, left-to-right order of the buttons on the dialog, i.e. specify analysis conditions, specify demand, specify supply and auxiliary supply, carry out matching, generate a report, save the project and finally exit the program. This order is flexible, provided the analysis conditions have been specified, enabling selected profiles to be augmented, removed or replaced. After exiting any of the other main dialogs, e.g. demand/supply specification, the program returns to the manager with updated reporting views, to summarise the user's progress. At any point a project can be saved for completion, alteration, re-investigation or reference at a later stage.

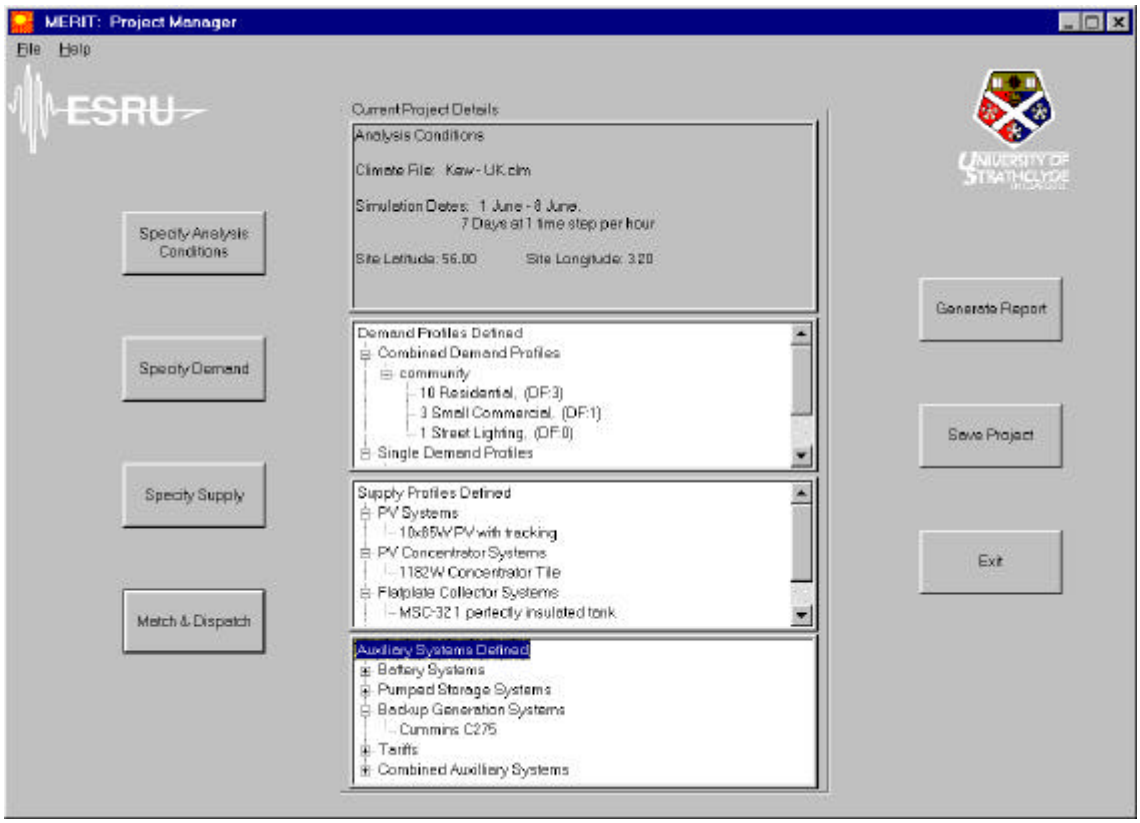

Figure 8.2: MERIT's project manager

The analysis conditions, specified at project initiation can be altered during a project, enabling different 'design weeks' to be analysed and/or different climates. When this is done all the simulated profiles are re-simulated for the new conditions and the relevant portions of the demand profiles selected are extracted from the annual demand profiles to reflect the new period. Analysis conditions are specified via the dialog shown in Figure 8.3, after the selection of the desired climate file. The details of the climate file are stated in a summary box, which informs the user of the dates available for selection and the longitude and latitude of the site. Any dates within the time-scale available may be used as the basis of an investigation with the frequency of calculation defined by the time-steps per hour. Climate data is interpolated if the resolution selected is greater than that contained within the file. The longitude and latitude may be edited for hypothetical studies.

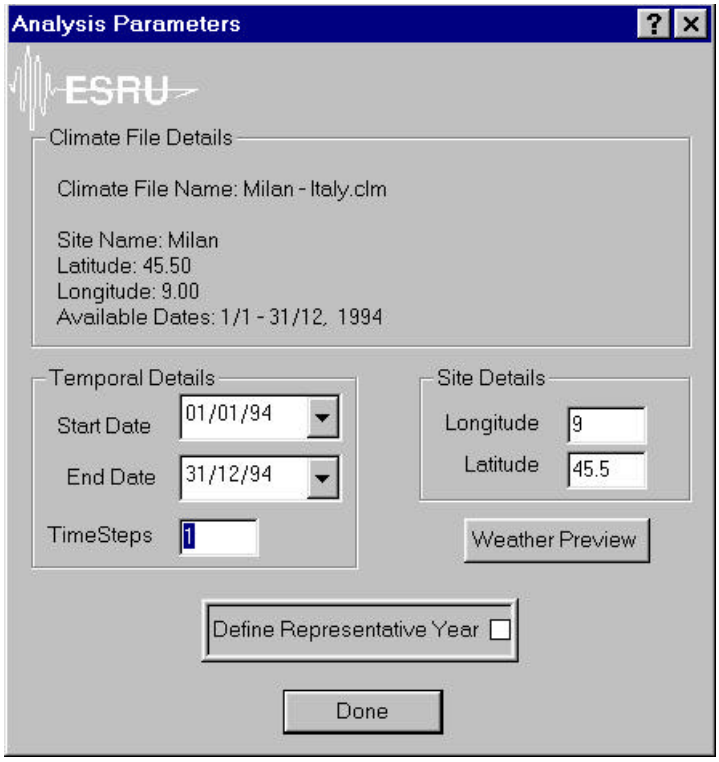

Figure 8.3: Boundary condition specification dialog

The weather preview button is provided for users wishing to investigate particular climatic effects on RE performance, for example, if a period of high solar insolation was of interest, a weather preview of the summer months would reveal the periods containing the appropriate solar radiation. The weather preview is shown in Figure 8.4. This dialog contains a graph to display the climatic parameters selected via check boxes, which allow the user to switch certain climate variables on or off, to clarify the data of interest.

An additional feature enables the user to define a representative year comprising seasonal days, weeks or months for either three or four seasons. The dialog for specifying the representative year is shown in Figure 8.5.

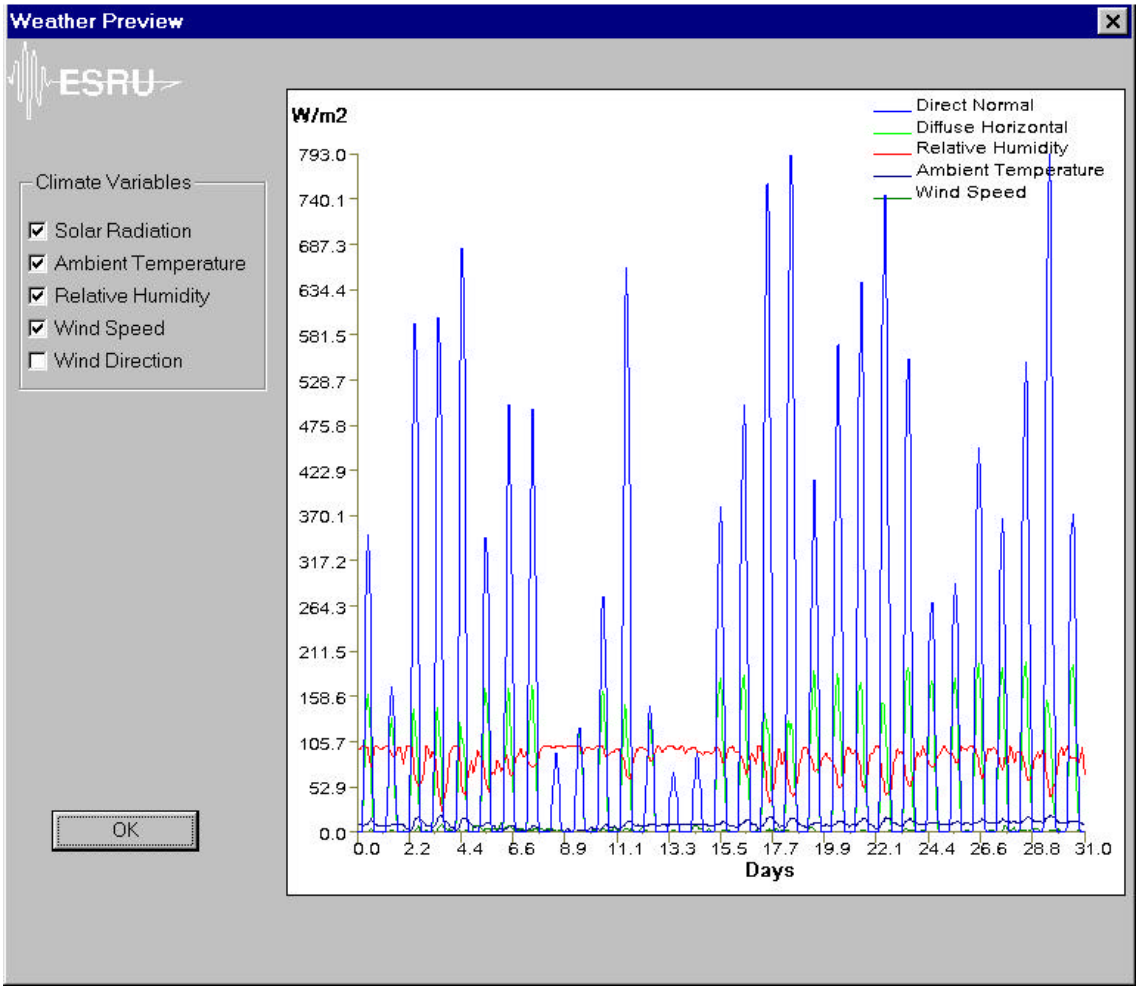

Figure 8.4: Whether preview dialog

By specifying a representative year the user is able to analyse supply and demand matches, which include seasonal changes in profile characteristics, without having to wait for the data processing times associated annual profiles.

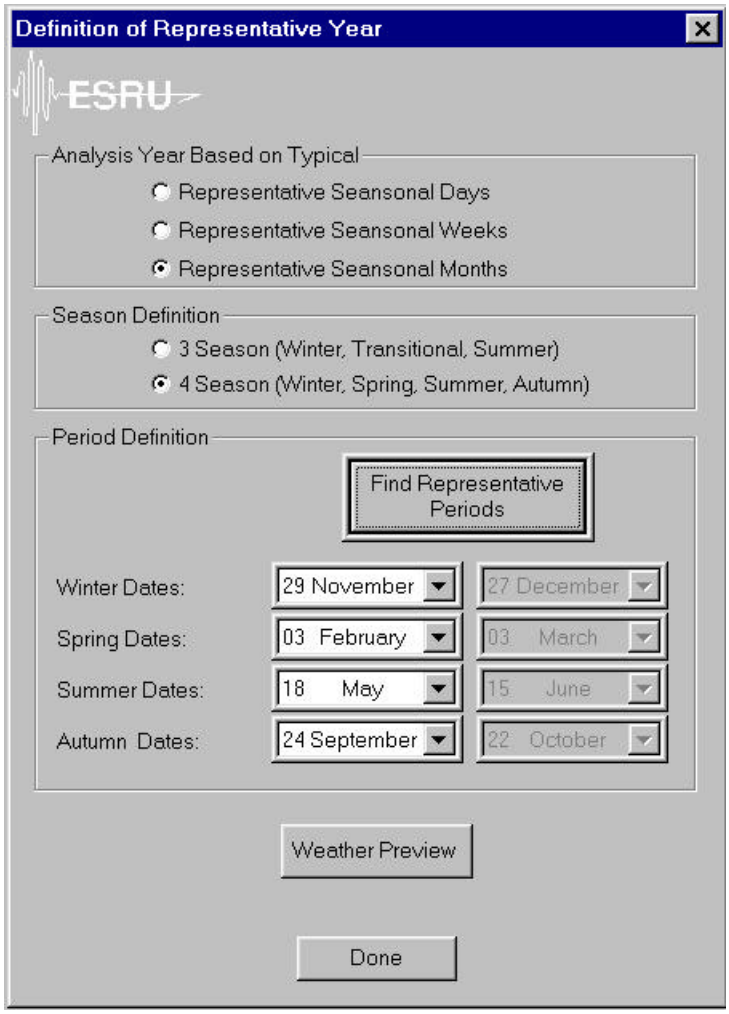

Figure 8.5: Representative year definition dialog

Having selected the appropriate climate conditions demand and supply profiles may be specified. The demand, supply and auxiliary specification dialogs are of the same format as shown in Figure 8.6 for demand and 8.11 for supply. The common features include:

- The ability to select a profile individually or to combine it with that of another profile prior to selecting the composite profile.
- A graph showing the profile for browsing purposes.
- The ability to delete a profile selected.

- The ability to edit a composite profile either by deleting one or more of the sub-profiles or by augmenting another profile.
- The ability to save profiles, which are not held in a database, i.e. imported profiles or combined profiles for analysis in different project.
- The ability to import data from an external source (not included in auxiliary specification).

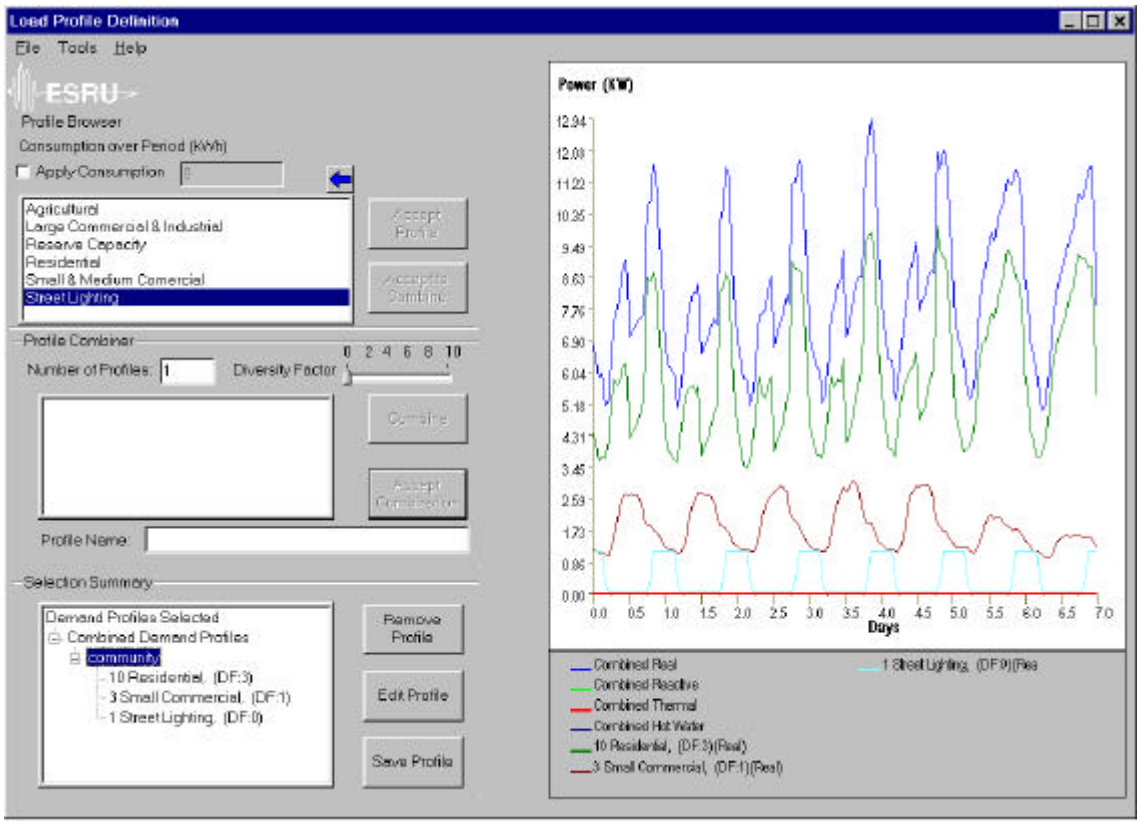

Figure 8.6: Demand specification dialog

The demand specific feature is a database of profiles sub-divided by demand-type, which can be browsed, scaled to a specified consumption over the given period, and selected. Profiles from the database can be selected in multiples e.g. 10 residential profiles. In selecting multiples, the user can specify a diversity factor, which introduces a degree of variability between profiles. The database can be augmented by selecting to

add a ‘designed profile’ to the database. ‘Designed profiles’ are user defined profiles created via the ‘profile designer’. The profile designer is shown in Figure 8.7. This feature allows the user to create annual demand profiles from a number of daily profiles. In the U.K. the demand profiling information is available in ‘typical day’ format, which will include differences in day type e.g. weekend/weekday and seasons. These typical days can be used to interpolate the demands occurring throughout the year. The specification of ‘Profile Effects’ (Figure 8.8) provide the means to turn limited demand data into annual profiles. Specification of a degree of variability introduces random fluctuations in the profile, representing random elements of consumption. This variability can be applied throughout the profile or just to data above the base load. The effects of temperature can be included by specifying a reference temperature and a power deviation from this temperature expressed in W/°C. The temperature deviation can be limited to specified times, i.e. heating times or applied to the entire day.

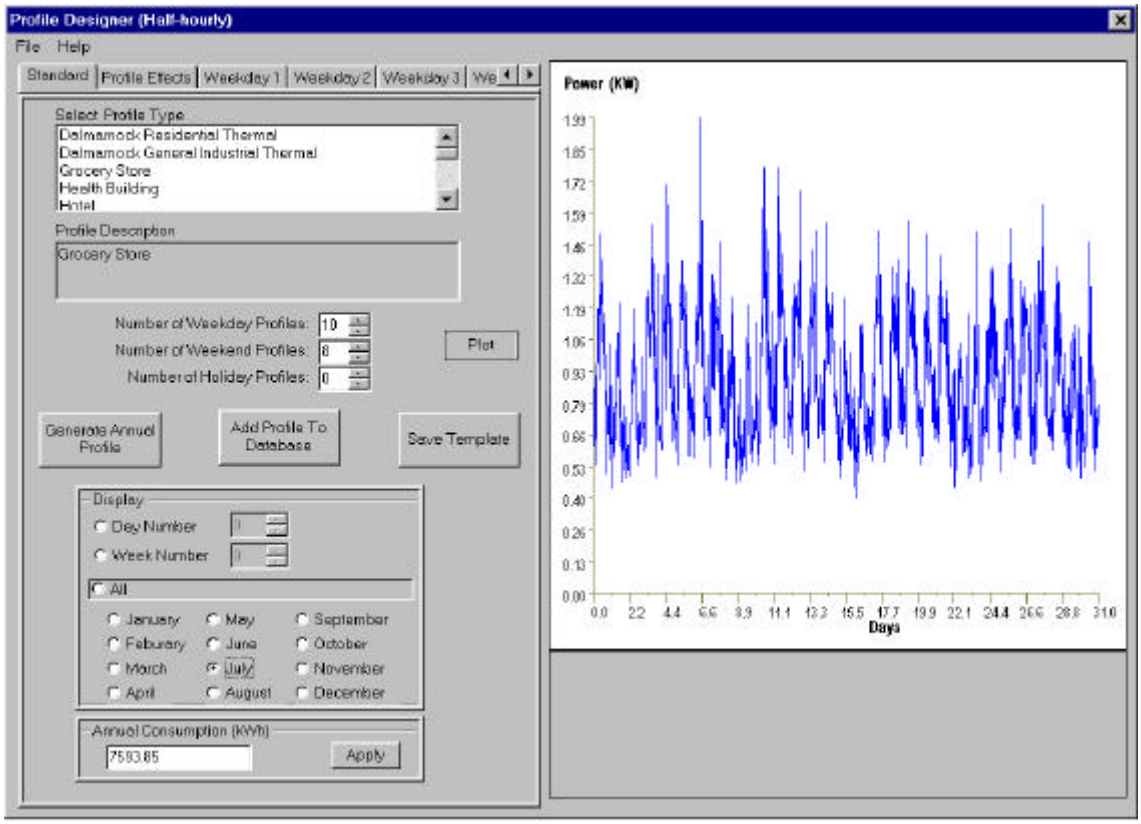
Profile Designer (Half-hourly)
File
Help
Standard
Profile Effects
Weekday 1
Weekday 2
Weekday 3
Select Profile Type
Dalmamock Residential Thermal
Dalmamock General Industrial Thermal
Grocery Store
Health Building
Hotel
Profile Description
Grocery Store
Number of Weekday Profiles:
10
Number of Weekend Profiles:
8
Number of Holiday Profiles:
0
Plot
Generate Annual Profile
Add Profile To Database
Save Template
Display
Day Number
Week Number
All
January
February
March
April
May
June
July
August
September
October
November
December
Annual Consumption (kWh)
7593.85
Apply
Power (KW)
1.99
1.85
1.72
1.59
1.45
1.32
1.19
1.06
0.93
0.79
0.66
0.53
0.40
0.26
0.13
0.00
0.0
2.2
4.4
6.6
8.9
11.1
13.3
15.5
17.7
19.9
22.1
24.4
26.6
28.8
31.0
Days

Once a satisfactory profile has been created it can be added to the demand database of profiles for selection.

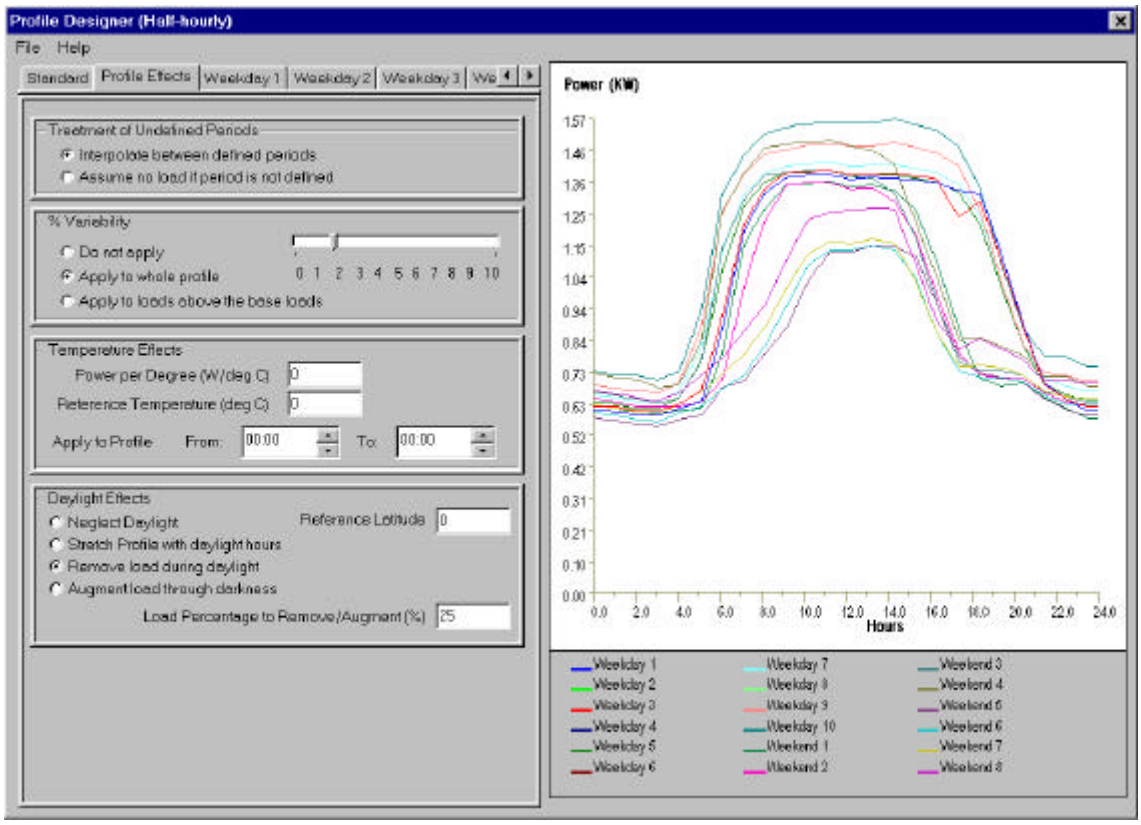

Figure 8.8: Profile designer effects specification

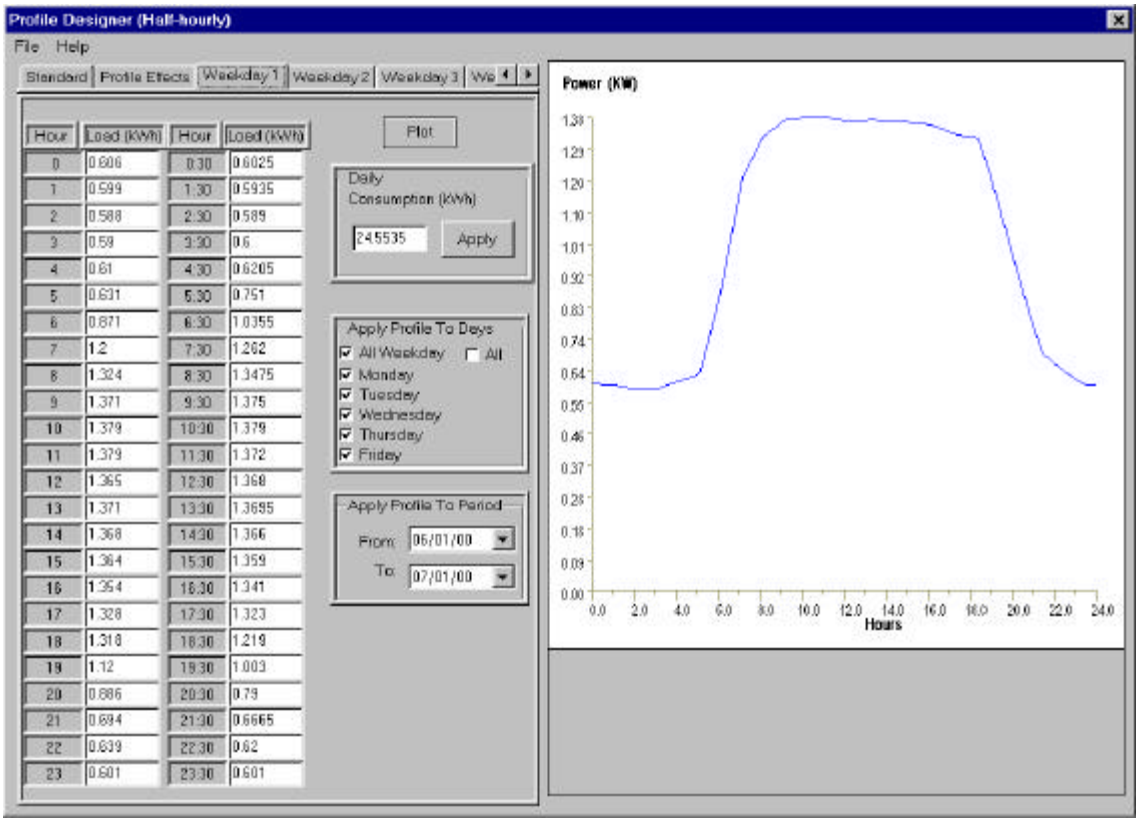

Figure 8.9: Profile designer day type specification.

The alternative to selecting a profile from the database, in the case of demand specification, or to simulating a supply profile, is to import the data from an external source, such as another simulation package or from measured data. External data from a text file can be imported via the import dialog shown in figure 8.10. The format of the original text file is flexible, as data can be imported either column or row wise and the separators can be comas, spaces, tabs, semicolons or some other defined character. The one condition for import is that the resultant number of data points is equal to the total number of time steps specified by the analysis conditions. If this condition is not met, the dialog will not exit, but instead state the condition to allow the user to change the starting and/or finishing rows/columns to ensure compatibility. The user can select whether the profile relates to real or reactive power or to a thermal or hot water profile.

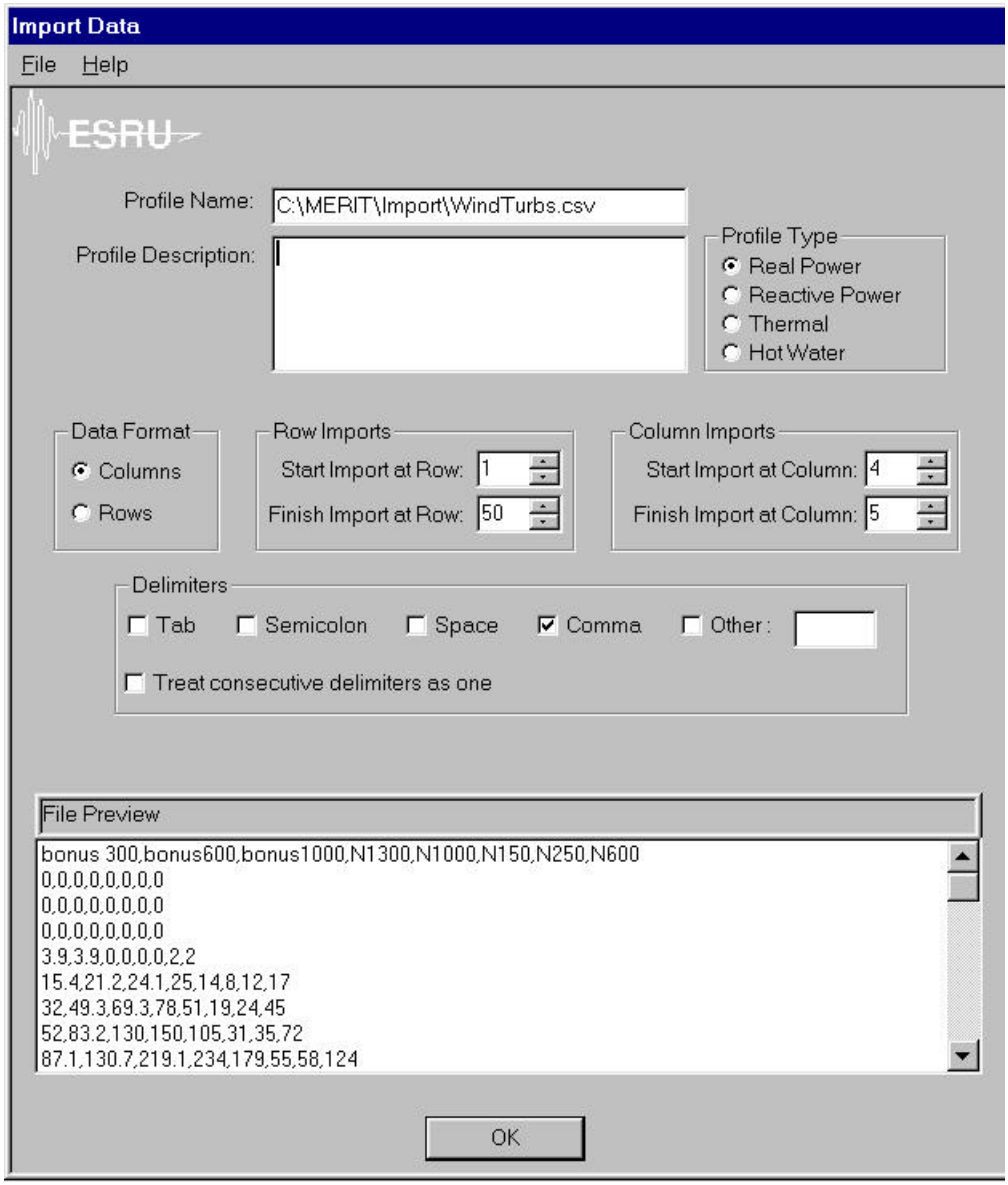

Figure 8.10: Import data dialog

On exiting the import dialog, the profile is presented on the graph and is subsequently available for selection, either individually or in combination with other profiles, as a demand or as a supply profile.

Figure 8.11 illustrates the supply selection dialog whose interface is very similar in format to that of the demand selection dialog. Supply profiles, which are not imported, are simulated using the climatic conditions and manufacturers specifications. An example input sheet is given in Figure 8.12 for PV systems.

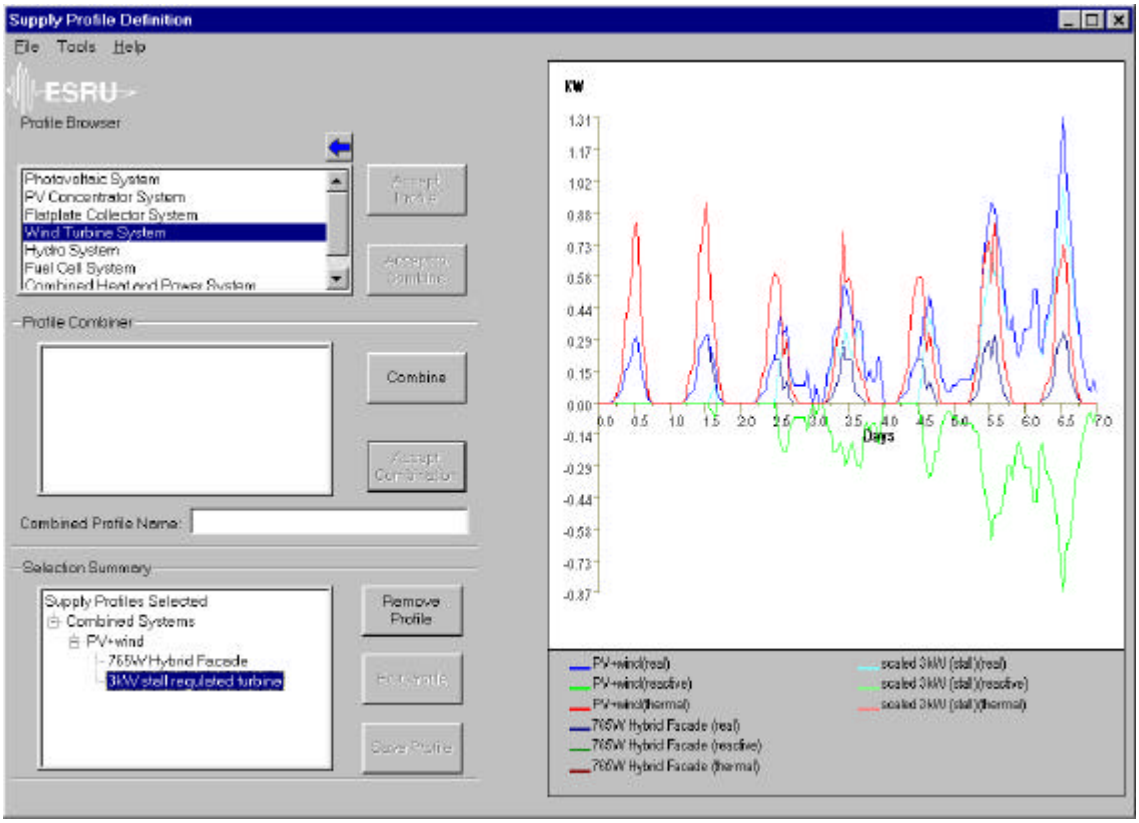

Figure 8.11: Supply Specification Dialog

Every profile is given a name for identification purposes and calculations are based on the input parameters. Databases of various supply and auxiliary systems are provided.

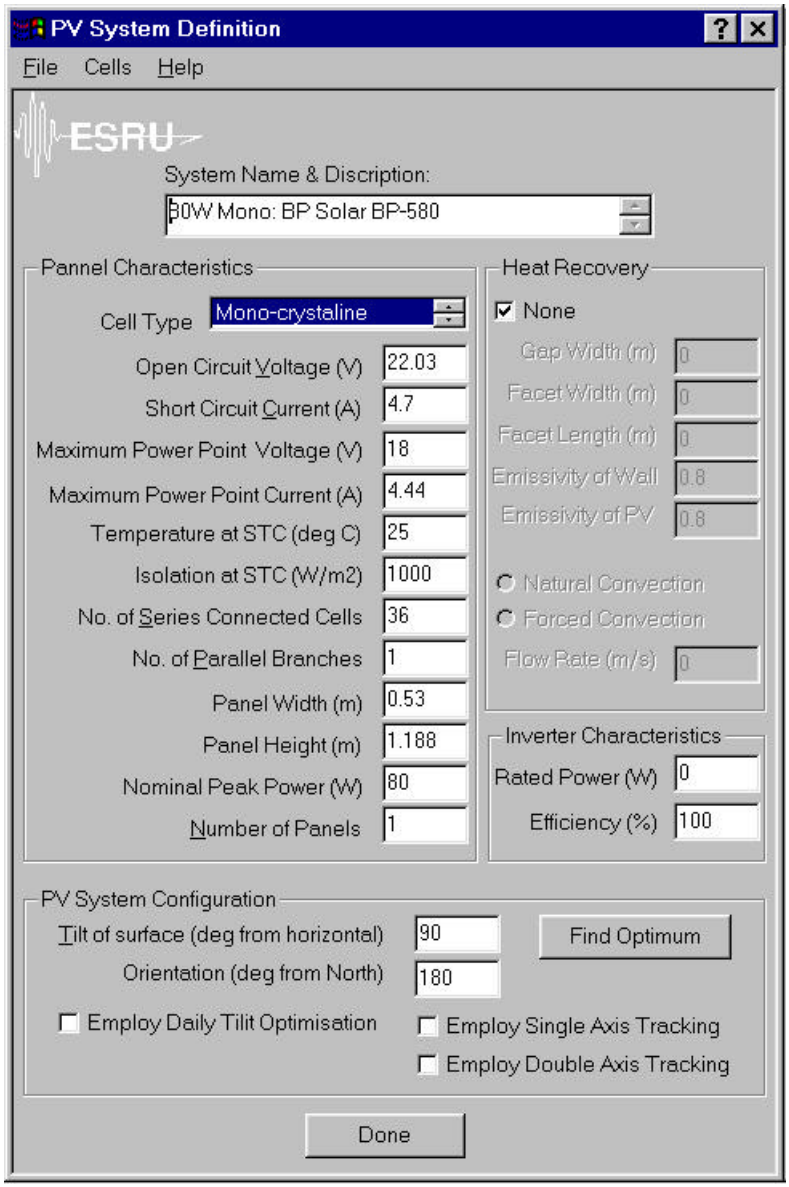

Figure 8.12: Supply System Specification (PV)

Where a specific system is to be simulated the user will be required to refer to the data-sheets provided for the technology and input the data fields manually. New data may be added to the database for future use simply by saving the configuration. Once the performance has been simulated, the resultant profile is plotted on the graph and becomes available for selection. Auxiliary systems can not be simulated at this point as

their performance is dependent on how they are combined with a demand and supply profile. Their simulation occurs during the matching phase of a project.

On entering the matching dialog the selected demands, supplies and auxiliaries appear as rows of buttons, which can be identified by ‘hovering’ over a button to produce its identification, as shown in Figure 8.13. Profile combinations can be investigated manually by simply selecting different profiles. Three graphs and a set of match statistics detail selected combinations. The first graph illustrates the demand profile with the supply superimposed. The second shows the residual components, with portions above the x-axis representing the deficit and portions below the excess. The third graph is only active when an auxiliary system is selected and details its performance, in the case of a battery system state of charge is plotted, in the case of a generator percentage loading and in the case of a tariff price fluctuations.

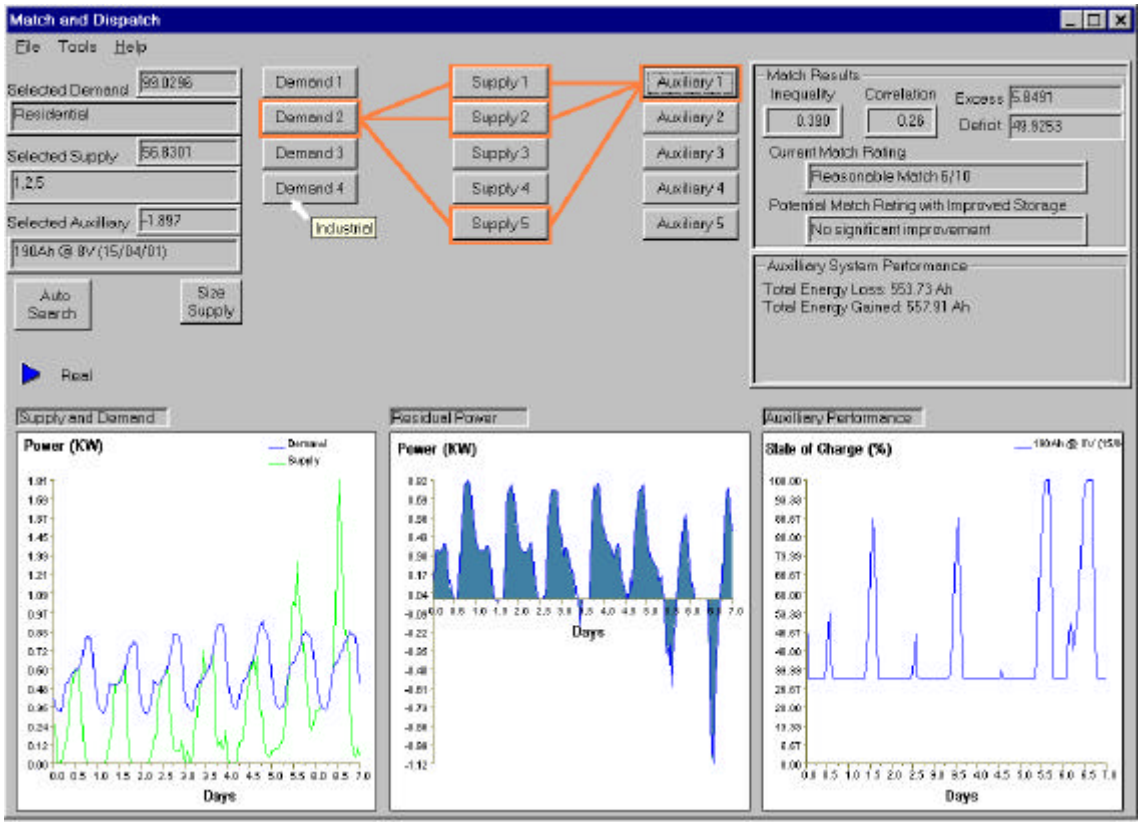

Figure 8.13: Matching Facility

The match statistics presented include the inequality metric, the correlation coefficient, the net excess and net deficit, together with a verbal rating and score-out-of-ten for the match and the potential match, given better auxiliary facilities. An auxiliary performance box details certain aspects of system performance: in the case of batteries, the charge gained and lost; in the case of back-up generators, the fuel total consumption and in the case of tariffs the electricity price and standing charge over the period and the total grid supply cost. The size supply button will inform the user of the multiples of a selected supply profile required both to meet the peak in the demand profile and to ensure the demand is not exceeded at any point.

The search procedure can be initiated by the auto-search button which allows the user to select the criteria for the search, as shown in Figure 8.14.

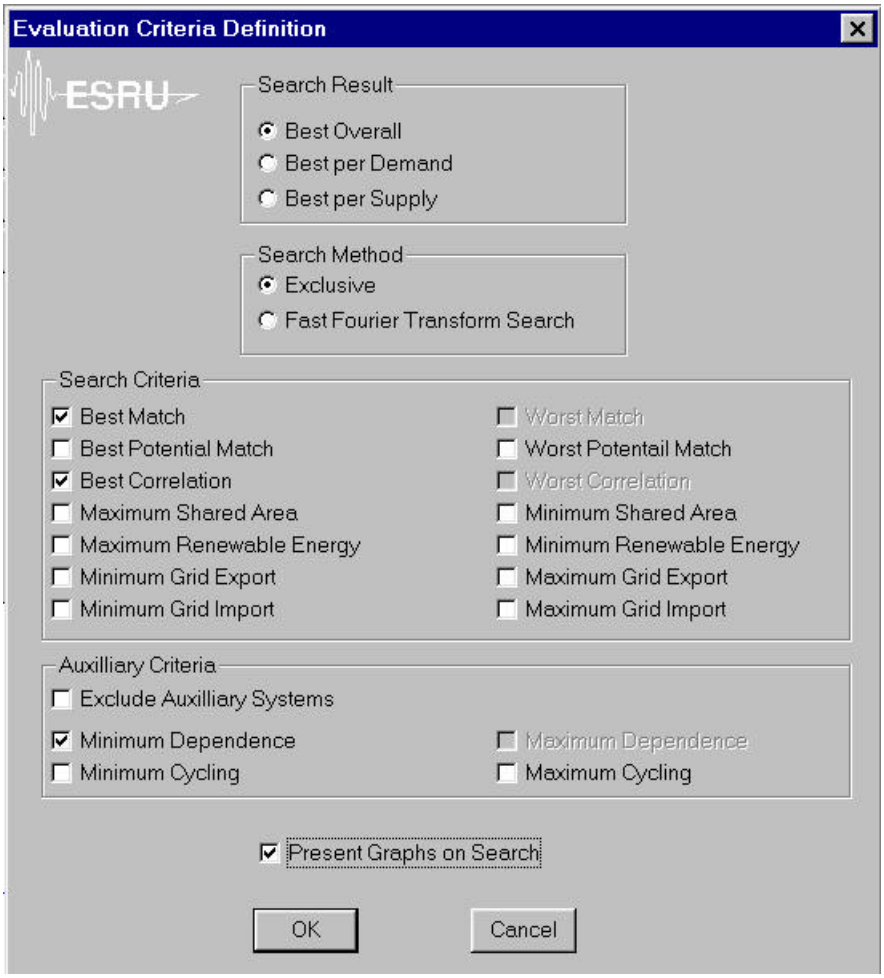

Figure 8.14: Search criteria selection

The criteria selected can either refect the best combinations to meet certain condtions, or, alternatively, the worst, so they may be eliminated from further investigation. All match results are presented via a scroll button in case of multiple combinations. These results, together with the selected criteria are stored in a match results file which can be viewed in the reporting dialog. The reporting dialog also states the defined input variables for each profile as shown in Figure 8.15.

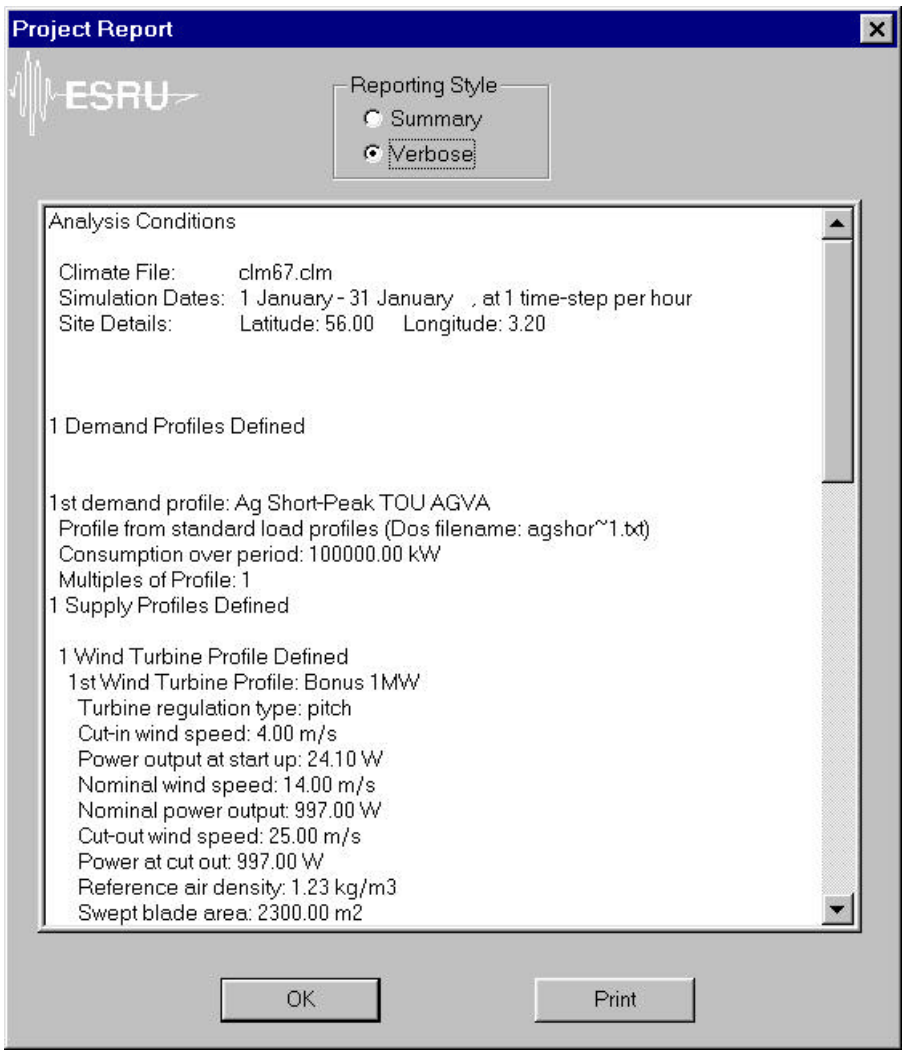

Figure 8.15: Reporting dialog

8.3 Applicability

MERIT can be used for a range of applications and by a range of users. The potential users include engineers, utilities, private power developers, renewable technology product suppliers, energy consultants, energy managers, architects, researchers and community planners. Merit has been distributed amongst a range of users for testing and the feedback received on the user interface and functionality has been incorporated. The current deployment sites include Highland Regional Council (energy managers), Scottish Power and it subsidiary Manweb (electricity supply), Buro Happold (building services engineers) and Strathclyde University (researchers). MERIT has been designed to assist the optimisation process of developing renewable energy integration strategies, however, the following functions could also be satisfied by the program's capabilities:

- renewable system sizing
- auxiliary system sizing
- pre-installation, renewable systems positioning studies
- identification of potential renewable technology markets
- load management investigations
- tariff negotiation

Two case studies are presented in the subsequent chapter to demonstrate the application of MERIT.

8.4 Software Design

8.4.1 Classes

Merit has been designed using the 'Object Oriented' approach (Grady, 1991). Probably the most powerful aspect of using the OO approach lies in the ability to define

inheritance relationships, whereby new objects are derived from base classes, which contain common functionality and thus re-uses existing code. Reusing developed classes enables faster development with improved reliability and design consistency.

Demand, supply and auxiliary profiles are all derived from a base profile data class, the class hierarchy is described in Figure 8.16. The data class is responsible for the storage and access of time series data irrespective of their nature. Derived from this class are the demand, supply and auxiliary container classes, which hold the functions common to the nature of the profile. These profile types are distinctly different from each other and require different parameters and access functions, which ensure a profile is derived and manipulated according to its nature. For example a demand profile will require the filename for its annual profile and its net consumption over the defined period, to scale the profile. Supply and auxiliary profiles on the other hand will require the parameters needed in simulating their performance. An auxiliary profile will depend on its interaction with selected supply and demand objects, whereas a supply profile can exist in its own right. Derived from each of these classes are definition classes to account for differences in parameters and calculations relevant to each class. Thus a PV profile will require certain cell parameters and functions to predict its performance, which are distinctly different from a wind devices parameters and functions. However both can be manipulated as supply profiles which contain time-series data, just as a demand profile. Composite or hybrid profiles are containers for a number of like-natured profiles, enabling the definition of for example a community demand profile or a renewable hybrid system.

8.4.2 Memory

Memory management in MERIT is of primary importance, because memory requirements are proportional to both the number of profiles selected and the temporal definitions of those profiles. Thus in the analysis of annual performance at 1 hour intervals, every profile will result in a minimum of 8760 data points, which if real,

reactive and thermal profiles coexist in a profiles definition is trebled. The ‘stack frame’ is an area of memory that temporarily holds the arguments to the function as well as any variables that are defined local to the function and is set up whenever a function is called. When an object is defined as a frame variable, its constructor is automatically invoked at the point where the definition is encountered, to allocate the memory for an object of a given class type. When the object goes out of scope, its destructor is automatically invoked to deallocate this memory when objects are destroyed. The key advantage of allocating objects on the frame is that they are automatically deleted. A disadvantage of frame allocation is that frame variables cannot be used outside their scope. Additionally, for large objects, it is often better to use the heap instead of the stack for storage since stack space is often limited. Objects allocated on the heap are not destroyed when the scope in which they are defined is exited. Global objects are in scope for the duration of the program. MERIT employs two global objects and a number global pointers to objects. All profiles are defined as global pointers, whose memory is allocated as and when required. The global objects used are the climate-object, which contains pointers to climate data and functions for accessing that data and the simulation-period-object, which defines the time scales involved in a project.

Memory is managed in merit through the use of the stack, the heap and binary file storage. The profiled data class is defined as a pointer to the heap whose memory is allocated only when it is required. This pointer becomes nested in that all the permanent definition classes exist as global pointers for which their memory is allocated when they are in use and deallocated with the data stored in binary files when not. Thus all profile classes occupy the heap when they are in use and all interface classes utilise the stack. When an interface is exited, it is destroyed and its memory usage released, just as other classes used in the creation of merit only exist whilst they are in scope. This design has ensured that the memory usage at any time is the program is kept to a minimum.

8.4.3 Analysis Conditions

When the analysis conditions are defined, the climate and simulation period objects are initialised and the memory required to hold the climatic parameters is allocated. These two objects can be considered as permanent throughout the duration of the program and their functions and data are accessed throughout, in defining demands, simulating supply and auxiliary systems.

8.4.4 Profile Selection

The process of creating and utilising profiled classes is described in Figure 8.17. Whilst profiles are being 'browsed' they are held in temporary definition classes, which are created through the definition interface. The interface has access to the various databases containing the necessary information to create different profile types. Alternatively, the user may define new systems, with the option of storing them in the relevant database.

Once a profile is defined, a temporary definition class is created and if it is selected it is copied into a permanent definition class and the temporary object deleted. When a permanent profile class is not in use either for performing calculations or for viewing, its data is stored in a binary file, thereby minimising its size.

8.4.5 Search Procedure

During the searching procedure the definition classes involved in a given combination are activated for the duration required to obtain the search results and then deactivated, i.e. put into storage. Minimising memory requirements promotes fast calculations and helps to ensure the program can run on machines with limited memory resources. Each of the search results (correlation coefficient, shared area, inequality metric, net excess etc.) is stored in an indexed array. This indexed array is then passed into an array

sorting class, which filters the array for the condition variable. If the ideal condition is not met by any of the possible combinations of profiles the accepted interval range is extended iterativly, until a combination or a set of combinations satisfy the condition. Where multiple variables are used, the same iterative procedure is employed for each variable and the index(es) of the combinations are compared until at least one combination can satisfy each variable condition.

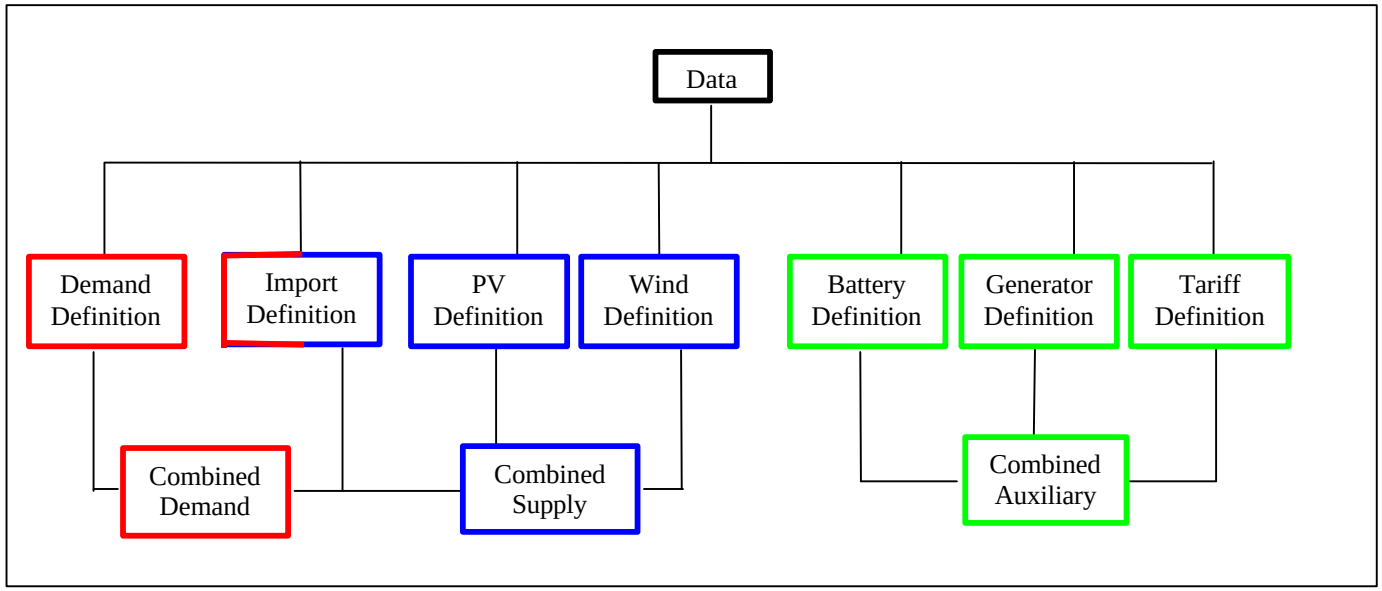

Figure 8.16: Profile class hierarchy

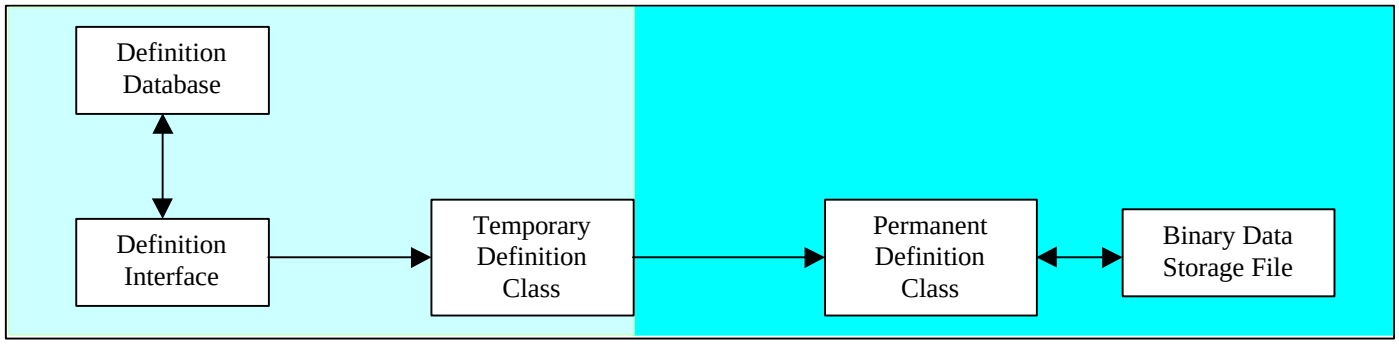

Figure 8.17: Profile creation process

8.5 Validation

8.5.1 PV Model

To validate the PV model described in Chapter 5, test data obtained from BRE was compared with predicted results. The data obtained was measured at 10-minute intervals, over a 24-hour period, on the 18th September 1995, at the BRE ScotLab test site. The PV system parameters used to define the mathematical model are listed in Table 8.1. The Inverter size and efficiency and emissivity of the back wall were estimated, as this data was not available. The radiation data was measured directly at the front of the cells; consequentially the individual components of direct, diffuse and reflected radiation could not be separated. The angle of incidence of radiation was assumed to be that of the direct radiation component, as it would be the dominant component for the majority of the day. To compensate for the errors in predicting the reflection losses, the inverter efficiency was over-estimated.

Table 8.1: Input parameters for PV validation exercise.

PV Properties	
Number of modules on façade	4 in parallel
Number of cells per module	150 in series
Open circuit voltage	91.8 V
Short circuit current	20 A
Maximum Power	1416 W
Voltage @ maximum power point	75 V
Current @ maximum power point	18.88 A

Inverter Size	1500 W *
Inverter Efficiency	98%*
Hybrid Construction	
Facet length	5.95 m
Facet Width	3.2 m
Air gap	0.74 m
Emissivity of back wall	0.7*
Climatic Parameters	
Latitude	55deg
Orientation	Due south
Global Vertical Solar	M
Wind Direction	M
Wind Speed	M
Ambient Air Temperature	M

[* - Estimated values for unknown parameters]

[M – measured at 10 minute intervals]

A measure of the accuracy of the thermal model is demonstrated in Figures 8.18 and 8.19. Figure 8.18 illustrates the predicted panel temperature against the average panel temperature measured. Deviations in temperature during periods of no solar radiation are predominantly due to the simulation period. The air gap was not vented at the time of experimentation, which resulted in some storage of heat gained during proceeding period. The air gap temperature was initialised to be that of the ambient air temperature, which was lower than that measured, resulting in greater heat losses and hence lower panel temperatures. To compensate for this the thermal inertia of the panel was increased by increasing the silicon width from 0.5 mm to 0.9 mm. Other deviations in the predicted and measured case are within ± 5%, as is illustrated in Figure 8.19, where 5% error bars are shown on the measured values. The differences can be

attributed primarily to errors in the prediction of reflection losses, as these have a direct effect on the radiation absorbed.

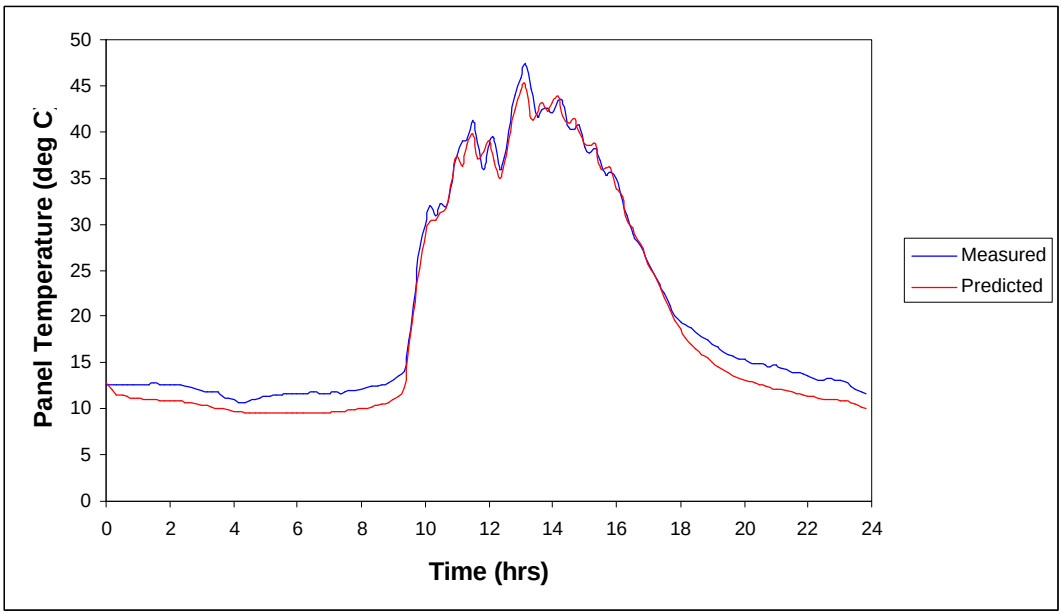

Figure 8.18: Modelled and Measured Panel Temperatures.

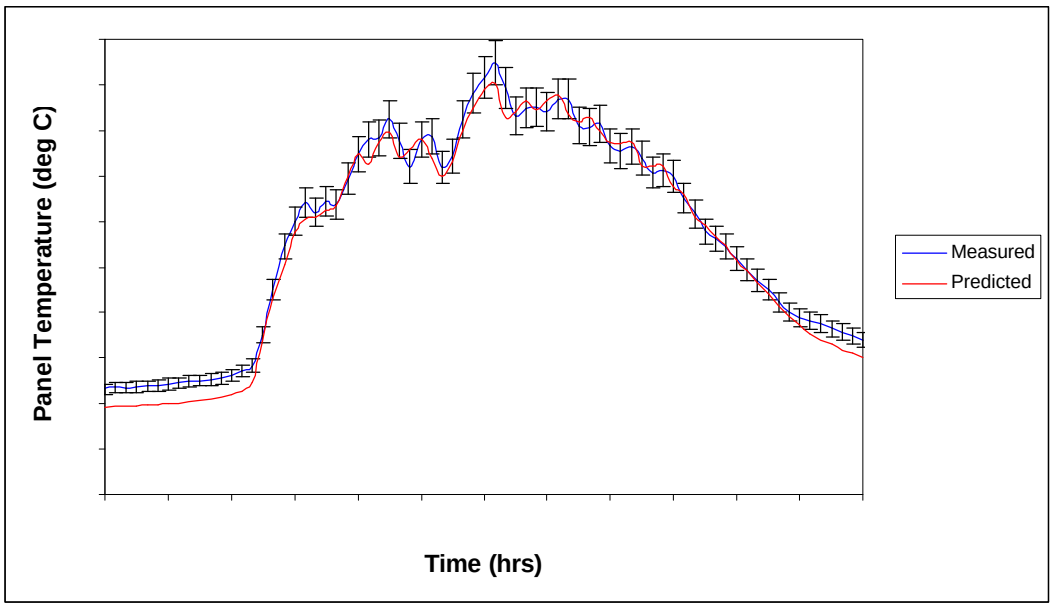

Figure 8.19: Errors in Predicted Panel Temperatures

Figure 8.20 illustrates the differences in predicted power output and actual measured output. Errors in temperature prediction clearly lead to errors in PV output. Additional errors will be incurred through the inability of separating the different radiations, resulting from errors in predicting reflection losses and consequently in the prediction of absorbed solar radiation.

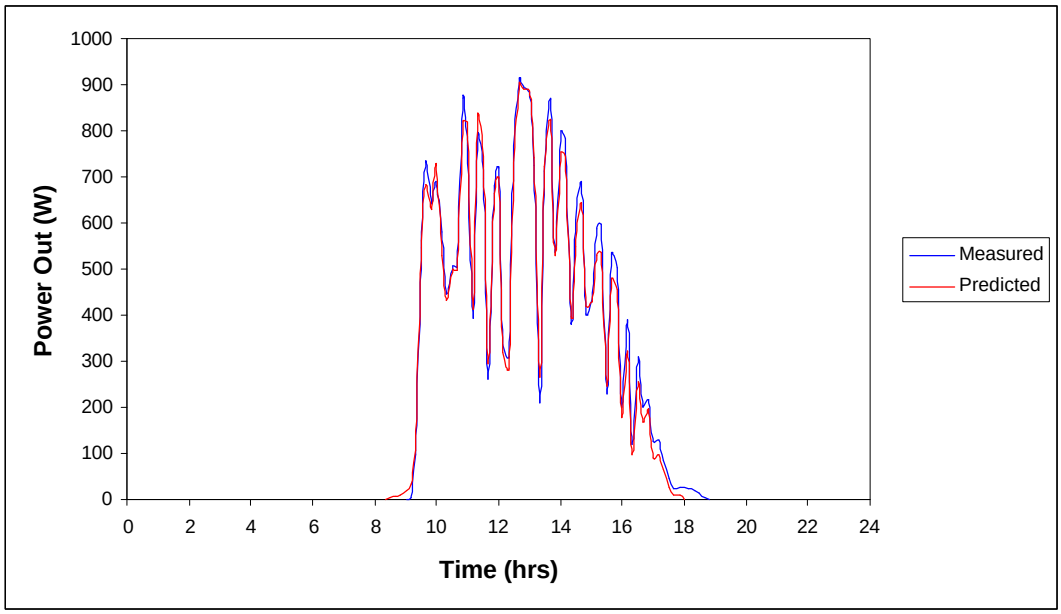

Figure 8.20: Modelled and Measured PV Power Output.

Figure 8.21 illustrates the sensitivity of the calculation to reflection losses. To demonstrate the effects of reflection losses, the power output was calculated for panel orientations of 160° and 200°. For the southeasterly facing surface (160°) the reflection losses become significant towards sunset hours. This is reversed for a southwesterly surface (200°) where losses are seen during sunrise hours. During sunrise and sunset hours, the portions of diffuse and reflected radiation components are more significant, which explains some of the deviations seen during those times.

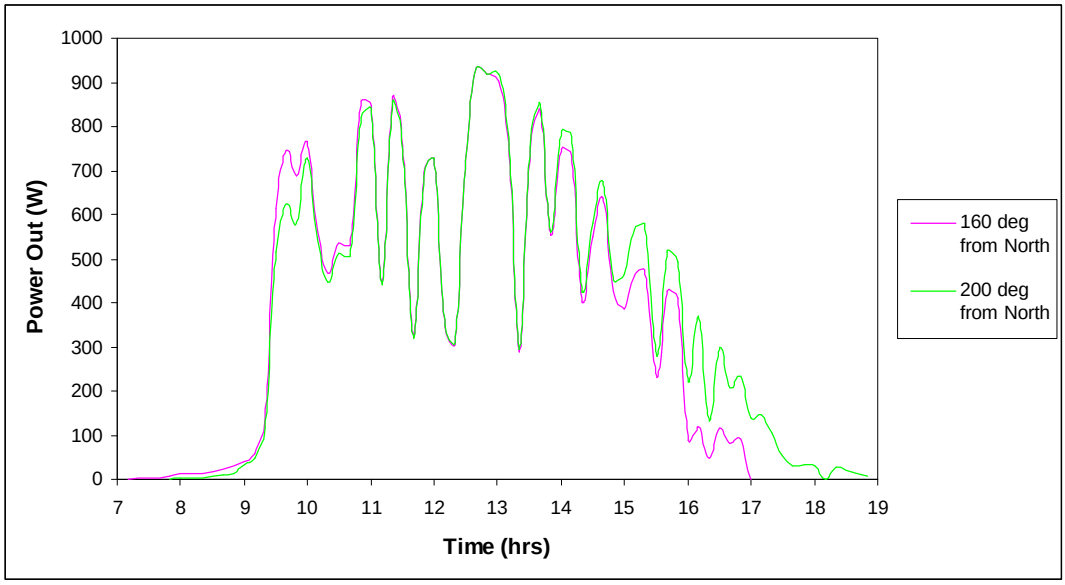

Figure 8.21: Sensitivity to orientation

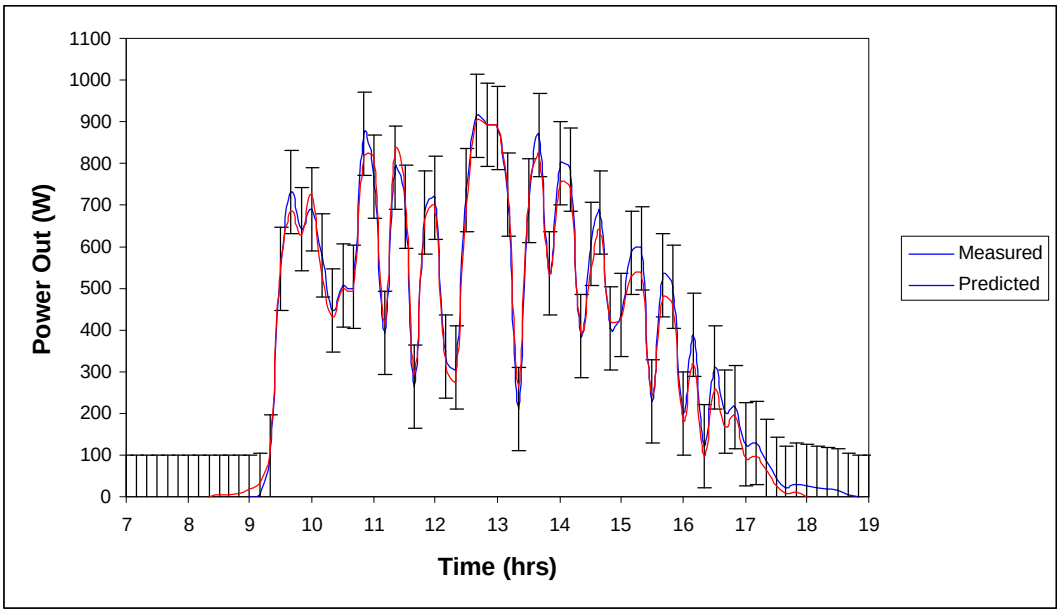

Figure 8.22: Percentage errors of predicted power output against measured power

8.5.2 Unregulated Wind Turbine Model

Wind turbine performance data under realistic operating conditions was not available, and the model was validated by its ability to represent performance curves obtained from a turbine manufacturer. The results obtained from predicting power for wind speeds between the cut-in and cutout points, compared with a manufacturer's power curve are illustrated in Figure 8.23. The agreement between predicted and actual results indicates the suitability of using the normal distribution curve to describe performance.

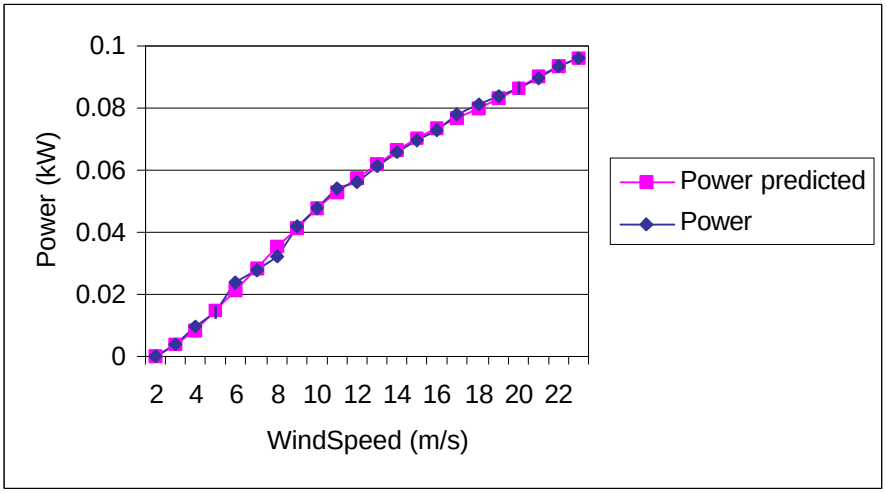

Figure 8.23: Predicted power output against actual power output

8.5.3 Regulated Wind Turbine Model

Again measured performance data was not available and the regulated wind turbine models were validated by their ability to reproduce the power curves supplied by manufacturers. A cross-section of turbines varying in size from 150 kW to 1.0 MW rated power output were employed in the validation. The results illustrated in Figure 8.24 indicate that good correlation between predicted and actual power output is achieved. Figure 8.25 describes the errors obtained using the modelling technique described. The errors are greatest during stage one calculations, which rely on the prediction of Cp values. As a first approximation of performance characteristics, the predictions are reasonably accurate with errors in the range of ± 15%. Given realistic fluctuations in wind speed, true performance becomes extremely difficult to predict and the methodology presented is thought to be an efficient means to obtaining wind turbine supply profiles, independent of size or particular design characteristics.

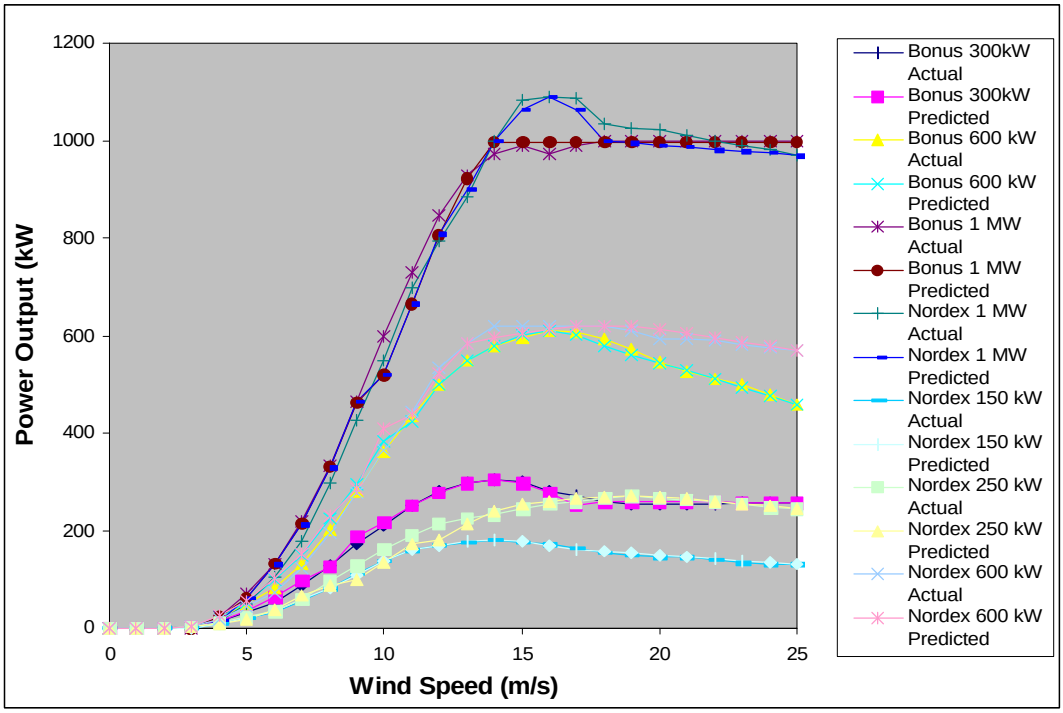

Figure 8.24: Predicted and actual power curves for a variety of wind turbines

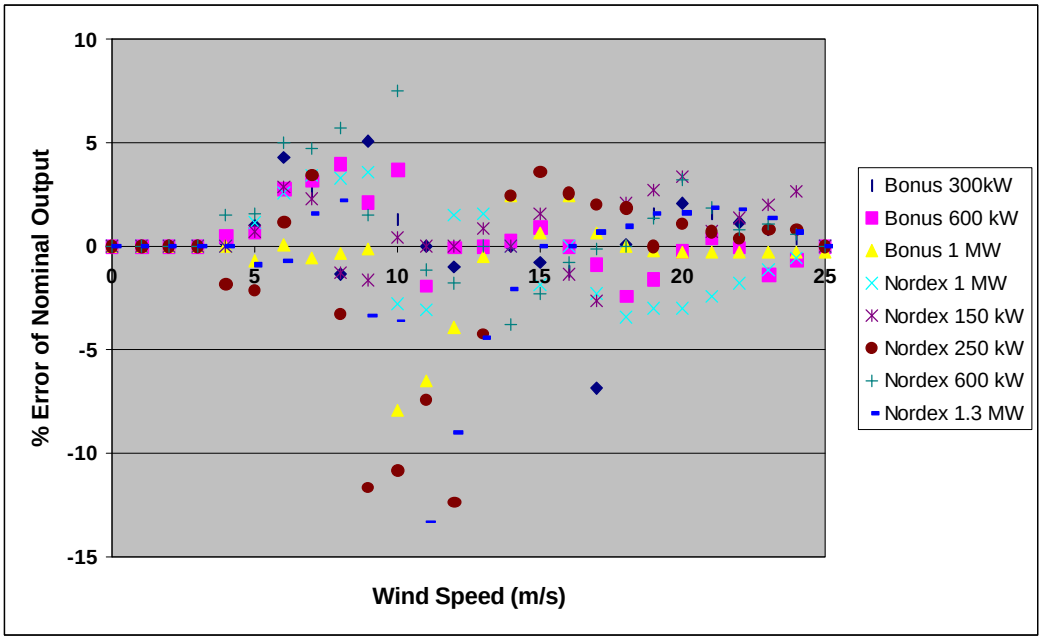

Figure 8.25: Prediction errors for a variety of wind turbines

8.5.4 Ducted Wind Turbine Model

To validate the ducted wind turbine prediction methodology, 39 days of the field test data was extracted and used as the input data for the derived model and to compare predicted results with power outputs measured. The result is illustrated in Figure 8.26, where good agreement between predicted and measured power outputs can be seen. The correlation coefficient over the data set was calculated as 0.92. However, the predicted results tend to be slightly lower in magnitude than those measured, in certain places. Some errors may be as a result of experimental errors largely as a consequence of time-averaged wind and turbine performance data, although the majority are likely to be as a result of inaccuracies in the predictive equations used. The data set used to establish the influencing relationships between power output and wind characteristics was relatively limited and the analysis of more extensive data is recommended. Nevertheless, the greatest errors in predicting the performance of any wind energy

conversion device is likely to be in the wind data itself, which is difficult to measure accurately. Thus, the results were considered to be satisfactory. It is stressed that although good agreement has been achieved between predicted and actual performance, this model can not claim to be generic and can be applied only to the device constructed for the previously mentioned field trials.

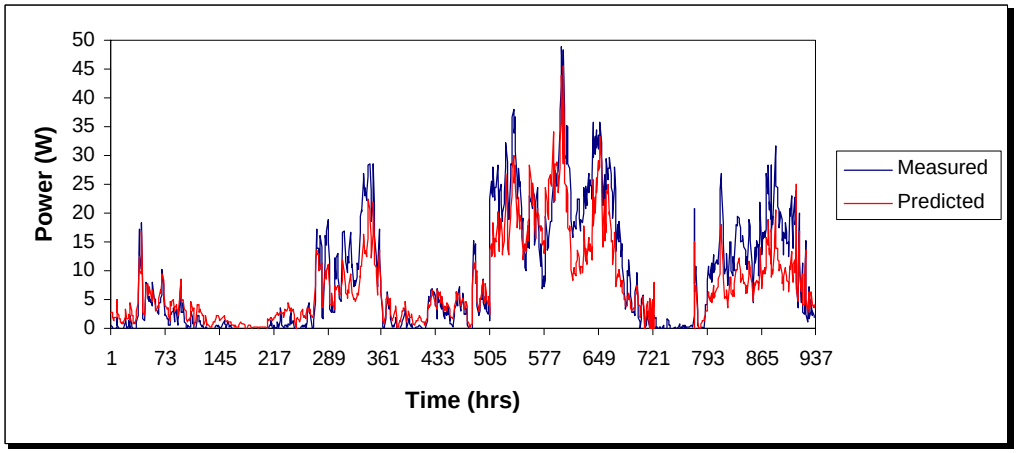

Figure 8.26: Comparison of measured and predicted power outputs of a ducted wind turbine

8.5.5 Flat-plate collector model

The lack of comparative data meant the flat plate model could not validated as the other models were. Test simulations were performed to ensure the results were conceivable. Figure 8.27 illustrates the results obtained for simulations performed under ideal collector operation (i.e. with a constant inlet temperature) with different cover systems. Where no cover has been specified the peaks in power output under high solar isolation conditions can be seen to be slightly higher than for the collectors with covers. The same trend can be seen when an additional second cover is added to a single cover configuration. However, these peaks are not maintained for long without a cover system, as the solar radiation absorbed is not stored within the cover. The effect of a

cover system can therefor be seen to increase the length of time over which thermal gains can be accumulated.

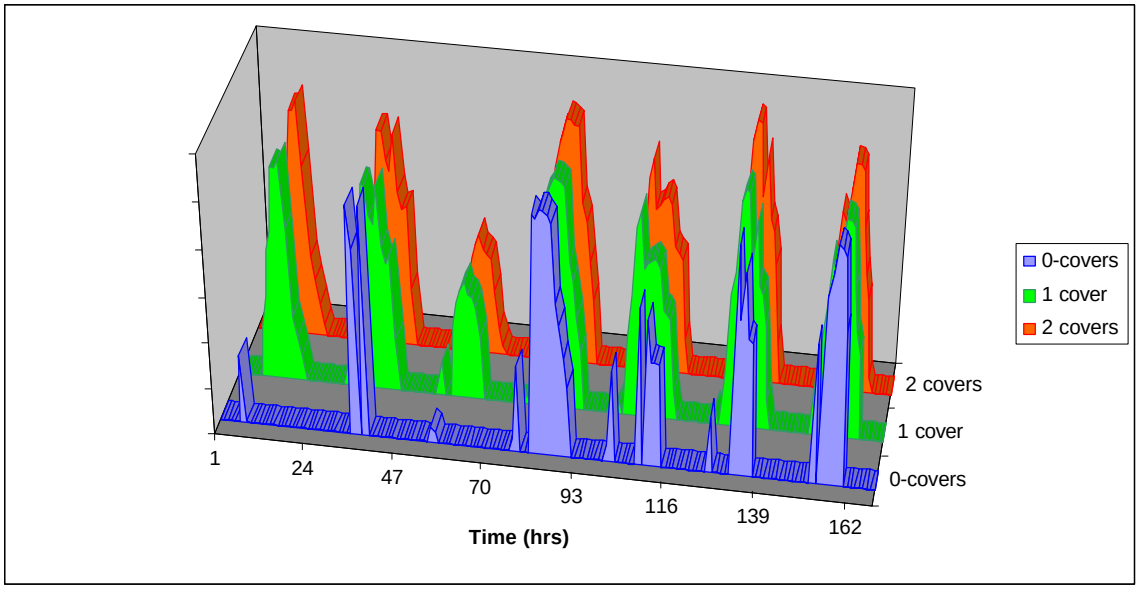

Figure 8.27: Comparison of performance of three different cover systems.

The performance of a single tank with auxiliary heating will be more efficient than a two-tank system, where one tank is kept at 65°C, as heat losses to the environment are increased in the latter. A simple test performed on the validity of the model demonstrated this to be true. Additionally if both systems were configured with perfect insulation, their performance was seen to be the same, as would be expected.

Figure 8.28 illustrates the results obtained for a four-day period of a collector system with a perfectly insulated storage under three different loading scenarios. The loads used were modelled as continuous hot water requirements, of increasing magnitudes. All other parameters, including the initial conditions within the tank were set to be the same for each system. At the start of the simulation the performance of each system can be seen to be the same, with the rate of solar gain collection increasing with solar irradiance. However, with the lowest demand case the heat removal from the tank is

slow and the resultant collector inlet temperatures begin to limit the solar gains. The pump control was specified not to circulate water unless the outlet temperature was a minimum of 1°C higher than the inlet. When the fluid is not being circulated, none of the solar energy transferred to the collector is removed, resulting in periods of no gain. On day one, a temporal shift in operation cycles is evident, as the highest demand case is able to remove heat from the tank more rapidly; it is able to resume operation more quickly than the other systems. By the second day, the lowest demand case can not attain the required 1°C temperature difference until late in the day, as the tank temperatures are too high.

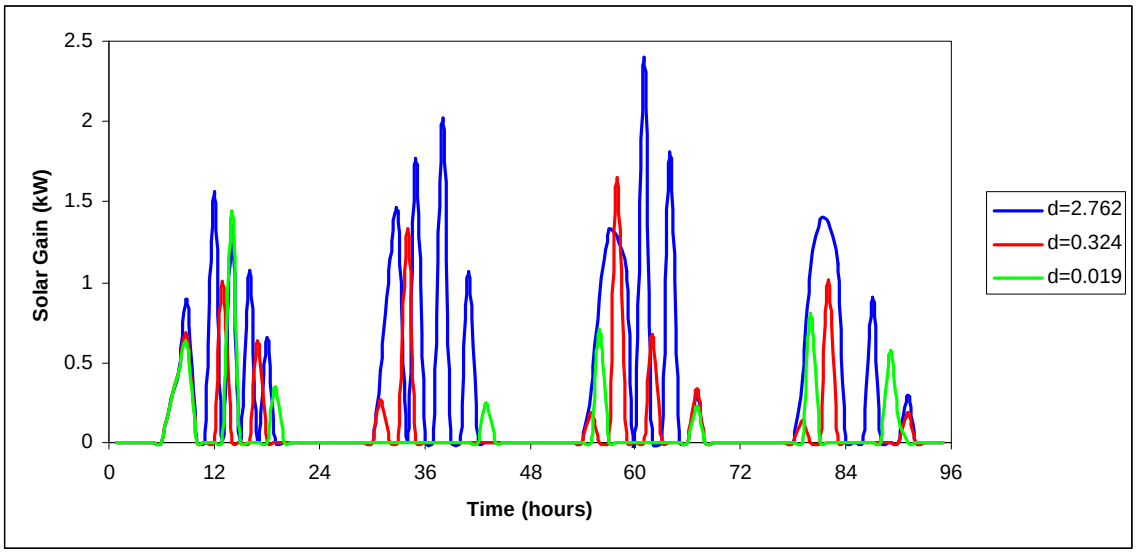

Figure 8.28: Performance of a perfectly insulated storage tank under varied load

8.5.6 Other Models

The battery and generator models described were validated through a series of manual calculations to verify performance under constant demand conditions and in the case of the battery constant supply.
The simulated and calculated results were the same indicating that the implementation of the model is correct. However, results require to be compared with measured data to validate the modelling philosophy adopted.

The application of tariffs was validated by applying a known tariff to a residential profile of known consumption (from billing information) and comparing the total cost with that of the electricity bill.

8.5.7 Search Engine

The search engine was validated by importing a fictitious profile both as a demand and as a supply together with a number of other profiles and the best match was found to be that of the two identical profiles.

8.6 Summary

The hypotheses presented throughout this work have been used as the basis of a software package designed to evaluate the degree of match between supply and demand profiles. The package has been described from the users' perspective where the primary objective was ease of use and from the software perspective where the goal was to minimise memory requirements, promote the speed of calculations and enable future development on a task sharing basis. Various aspects of the software implementation have been validated and some of its current and potential applications discussed.

8.7 References

1. Booch Grady, Object Oriented Design with Applications, The Benjamin/Cummings Publishing Company, Inc., California 1991.

2. Clarke J., Tang D., James K. and MacRandal D., The Energy Kernel System – Final Report for Grant GR/F/07880, November 1992.

3. Electric Library's Free Encyclopedia, URL: http://www.encyclopedia.com/

4. Martin Robert C., Why C++, Object Mentor Associates, 4 Apr 1995, URL: http://www.progsoc.uts.edu.au/~geldridg/cpp/rmwhycpp.htm

5. OS Statistics: August 1999 to present, URL:http://www.attrition.org/mirror/attrition/os.html, 5th August 2000

6. Stroustrup Bjarne, An Overview of the C++ Programming Language, The Handbook of Object Technology (Editor: Saba Zamir), CRC Press LLC, Boca Raton, 1999

Chapter 9: The Application of MERIT

The final focus of this work was to test the robustness and applicability of MERIT. Two case studies are presented which use the tool to perform supply and demand match analyses. The first case illustrates a detailed investigation of a single building. The second employs MERIT in the analysis of a community-scale project. These case studies have been selected to illustrate MERIT's wide ranging applicability: the tool can provide decision support irrespective of the scale and the level of uncertainty involved in a project. It can be applied both where supply strategies are technically constrained, and where high levels of uncertainty apply.

9.1 The Lighthouse Building

The Lighthouse building in Glasgow, designed by Charles Rennie Mackintosh, was refurbished to celebrate Glasgow's selection as UK City of Architecture and Design 1999. The refurbishment presented a unique opportunity to demonstrate the urban deployment of small-scale renewable energy systems. A portion of the building, the viewing gallery, was the focus of a simulation exercise to identify those passive and active technologies that could be usefully deployed. A description of the design methodology, utilising the MERIT system is presented.

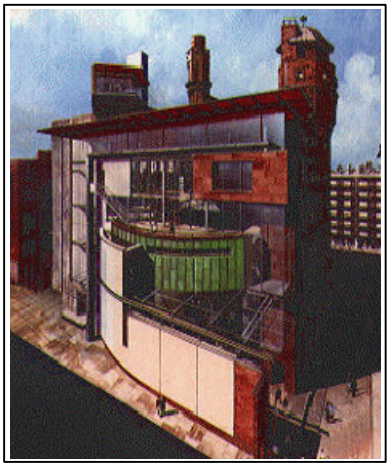

Figure 9.1: The lighthouse building in Glasgow.

9.1.1 Demand scenarios

Three demand scenarios, relating to the building's lighting, small power and space/water heating systems, were considered: a base case corresponding to typical installed capacities; a reduced case corresponding to good practice energy efficiency; and an aggressive case which corresponds to an intense energy reduction strategy.

Lighting

The lighting capacity for the viewing gallery was 25 W/m^2, with an area of 34 m^2. As a result, the base case lighting demand was considered to be 850W, between the hours of 8am and 9pm, irrespective of season or day type. The profile generator module of MERIT was subsequently employed to generate the reduced case, assuming daylight control is applied to 75% of the lighting capacity. The annual consumption of the reduced profile was halved to represent the aggressive lighting reduction case, and is synonymous with the use of energy efficient luminaires.

Small Power

The small power demands for the portion of the building were considered to include the limited use of electrical appliances. For example, vacuum cleaning, the use of projection equipment, refreshment machines, refrigeration and security lighting. A single small power profile was generated by using a variable profile above a base load and used to represent continuous loads such as refrigeration and security lighting. The annual consumption was considered to be 930kWh, with a peak demand of 300W.

Space Heating

The maximum capacity of the space heating system was 5kW. This maximum was applied during the winter period between 8am and 2pm, with a considerably reduced top-up heating period employed until closing time. Additionally, the top-up space heating was assumed to increase towards the later part of the evening. The transitional base case profile was considered to contain a maximum heating load in the morning for two hours. The summer period was defined without the use of heating plant. These three profiles, used to represent days within the various seasons, were subsequently employed to interpolate intermittent periods, resulting in an annual consumption of 3950kWh. A 20% reduction was applied to the base case annual consumption to generate a reduced case scenario, and a 50% reduction was applied to give the aggressively reduced heating profile.

Water Heating

The hot water demand profile was generated for two types of sanitary fittings, firstly the standard tap and secondly the spray-tap. Spray tap sanitary fittings reduce the flow rate of standard tap fittings and therefore the daily demand, by one third (C.I.B.S. Guide, Section B5), (BS CP 310). With a recommended hot water end use temperature of 45°C (McLaughlin, 1981) together with a hot water supply temperature of 65°C and a cold water supply temperature 10°C, the hot water demand was determined by using two thirds of an estimated maximum daily hot water demand per person. The maximum daily demand per person for an office type building is likely to be 15 litres

(C.I.B.S. Guide, Section B5), but as this figure is based on a typical eight hour working day, it was used to evaluate a person-hour equivalent. Assuming the viewing gallery to have around 30 visitors in a typical day, each with a stay of 30 minutes, gives approximately 2 office person hours. Based on the tap flow rate fitting, the daily hot water demand was estimated to be around 13860 kJ ($mC_p\Delta T$), and this was used in the base case scenario. The reduced consumption figure (4620 kJ) was applied to both the reduced and aggressively reduced demand scenarios. The consumption figures were used in the profile generator of MERIT, together with a variable profile representing hot water requirements, between the hours of 7.00am for cleaning purposes, and 9.00pm at closing. The annual profiles were provided a high variability factor, as the hot water demand of the site was likely to be irregular.

9.1.2 Supply Options

The lighthouse building is category A listed and situated in the city centre, which introduces a number of planning restrictions limiting the possibilities for deploying RE technologies. The roof area and south facing façade were identified as potential deployment areas, with a further restriction that only the south and west facing exposures of the roof area could incorporate visual alterations. Further planning restrictions required that the rotors of any wind turbines deployed needed to be concealed from public view. Consequently eliminating the use of conventional wind turbines. A number of supply technologies were investigated using a series of matching analyses as described in the proceeding sections.

Matching Strategy

The matching strategy was undertaken in three phases. The first involved an elimination procedure to enable the more focused second phase of the study. The second phase was concerned with optimising the supply options. The final phase required a detailed analysis of the performance of favoured supply technologies in conjunction with energy

storage. Each phase is described to illustrate the levels of decision support provided by the tool.

Phase 1: Considering the Options

The initial demand supply matching approach involved specifying a number of technically feasible supply technologies and utilising the search engine of MERIT to find the best matches for each of the three demand scenarios. The supply technologies chosen were physically constrained to the available deployment areas at the site. The following technologies were considered:

a) A vertical photovoltaic component comprising nine 85W monocrystalline panels operating in hybrid mode to provide both an electrical and thermal output. In this mode of operation the electrical performance of the PV is improved.
b) A second hybrid façade, the same as (a) but comprising 18×85 W monocrystalline panels (utilising the entire available south facing wall area).
c) Four 85 W monocrystalline panels operating in conjunction with double-axis solar tracking devices to maximise their output. The number of PV trackers employed were constrained to enable PV rotation, without creating shading for neighbouring panels.
d) A PV concentrator tile system horizontally mounted on the roof with a peak capacity of 1182W.
e) A hybrid system consisting of four west facing ducted wind turbines, with a PV panel incorporated into the aerofoil section of each wind generator. A system such as this has two advantages over deploying one or the other technology. Firstly, the device's power density is increased, and secondly the turbulent air leaving the turbine cools the panels, enabling them to operate at higher efficiencies. The PV components were specified at tilt angles of 40° τo the horizontal to maximise solar capture in the transitional and summer seasons.
f) As (e) but south facing. The south facing roof edge is shorter than the west an only enabled 3 wind-PV hybrid component to be specified.

g) Four west facing ducted wind turbines (no PV component).
h) Three south facing ducted wind turbines (no PV component).
i) Two flat plate collectors roof mounted at 40 degrees.

Thermal and Electrical Analysis

The best match search option was used in conjunction with the best result per demand, with the search carried out for four seasonal typical week periods. The results indicated that in the base case demand the best electrical match was achieved utilising supply options (b) through (h) giving an inequality index of 0.33. The supply technologies suggested for the reduced scenario were options (c), (e) and (f), with inequality indexes of 0.39. The aggressively reduced demand was best matched to the supply options (a), (f) and (g), with inequality indexes of 0.35. Examination of the above results indicates that the best match index was obtained for the base case demand. However, each of the individual supply technologies were sized according to maximum deployment areas, and although the façade could be used in conjunction with some of the technologies envisaged for the roof space, it is technically impossible to deploy them all. Assuming there were no sizing limitations, the economics of this supply and demand match would still be comparatively unfavourable. The supply options for the reduced demand were economically more favourable, but again there is competition for roof space and the selected technologies are all purely electrical components, with none capable of offsetting the thermal demand. In the case of aggressive demand reduction the inequality index is only marginally larger than that for the base case but with the selected technologies capable of being deployed together. Additionally, the façade component will generate warm air, which can be used to off set the thermal demand.

Hot Water Analysis

The solar water heating system was configured with 2 collectors, a 30ltr hot water tank, and an auxiliary flow line heater. A two-tank system would not be required due to the low flow rates associated with this type of site. Preliminary simulation for both tap and spray tap scenarios are considered for four typical seasonal weeks, and described in Figures 9.2, and 9.3, respectively. Both demand scenarios are observed as relatively uniform, and the supply profile exhibits seasonal variation as expected. The heat recovered from the system can be seen to be greater with the larger draw off (i.e. tap installation).

A comparison between Figures 9.2 and 9.3 illustrates that by increasing the hot water draw off from the collector tank, the supply potential, over the four seasonal weeks, is increased by 50% due to the resultant decrease in collector inlet temperature. The auxiliary heater is required to provide 56% of the overall demand, with the solar collector providing the residual, 44%. 4.8kWh of the supply gained over the four-week period being lost to the environment. In the case of a spray tap installation, the reduced supply potential is able to meet 71% of the demand, with the residual 29% being met by the auxiliary heater. Increased losses to the environment of 8.4kWh are as a result of increased storage temperatures. Although considerable portions of the hot water demand could be realised through the deployment of a solar water heating system, the nature of the site rendered this option unfavourable. The study focuses on part of the building only, although the hot water supply network has been designed for the entire building. The retrofit required was not deemed an economic option, given that the demand predicted could be highly variable, with long periods of no draw off possible, adversely affecting system performance.

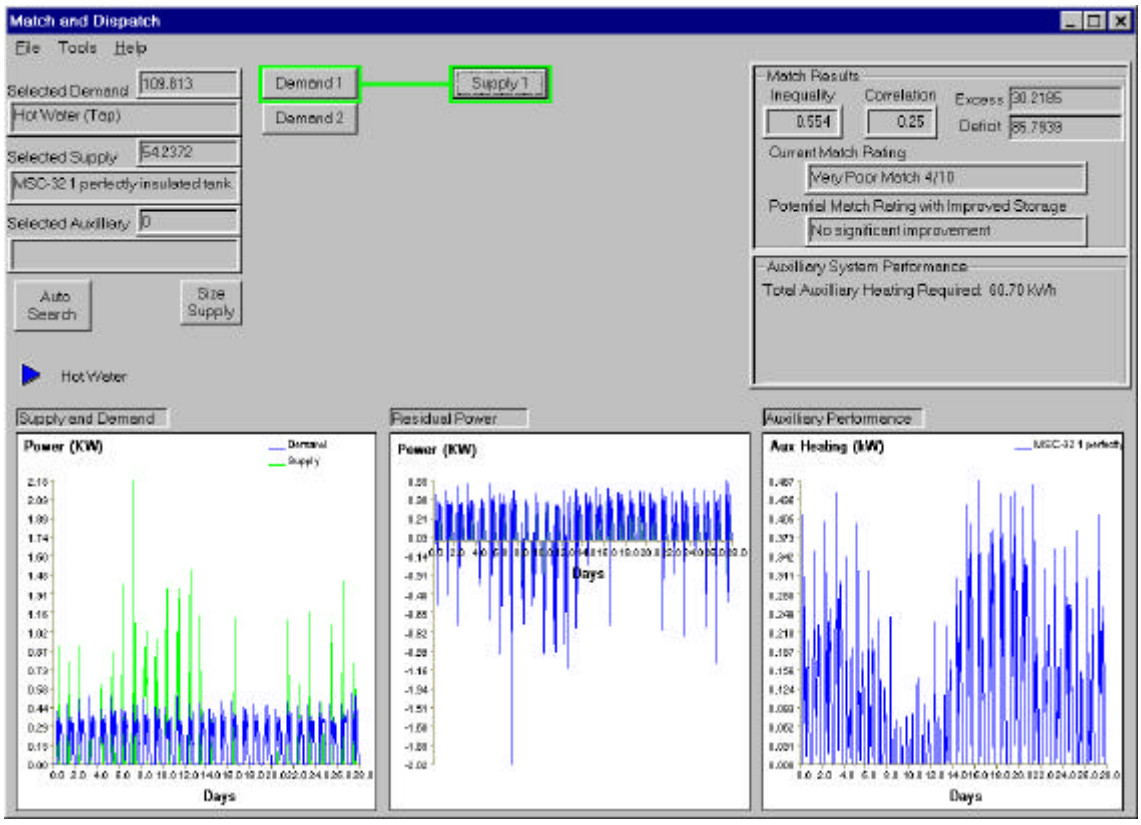

Figure 9.2: Hot water demand with standard tap fittings and flat plate collector supply

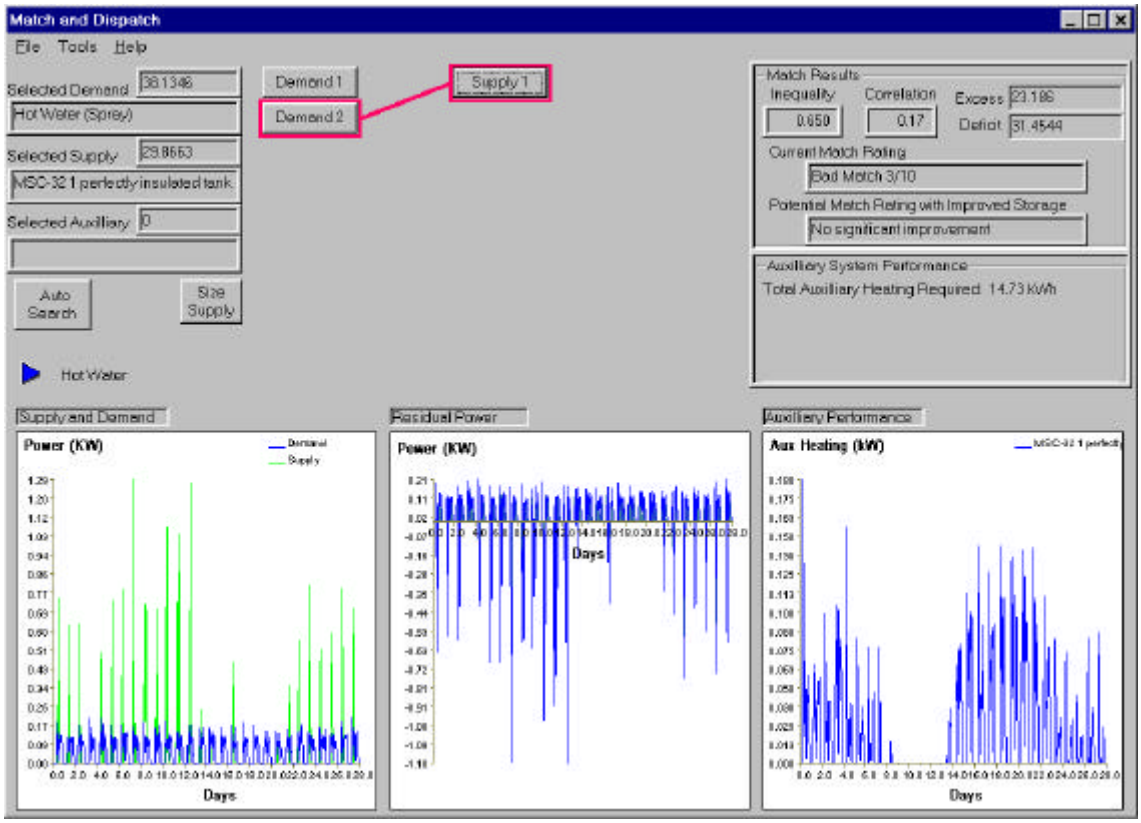

Figure 9.3: Hot water demand with standard tap fittings and flat plate collector supply

Phase 2: Renewable Energy Optimisation

Phase 1 of the lighthouse study demonstrated that high power demands were not conducive to renewable deployment constrained by energy capture areas. It was therefore concluded that demand required to be minimised prior to evaluating optimal supply technologies. Phase 2 of the study was consequently focused on the aggressively reduced demand scenario. To avoid problems of competing deployment areas, a second search was performed, by coupling possible technologies together. The two façade areas were selected in combination with the solar tracking PVs, the concentrator tiles, and the ducted wind turbine and PV spoiler systems. The inequality indexes for each technology sets, over a complete year, are provided in Figure 9.4.

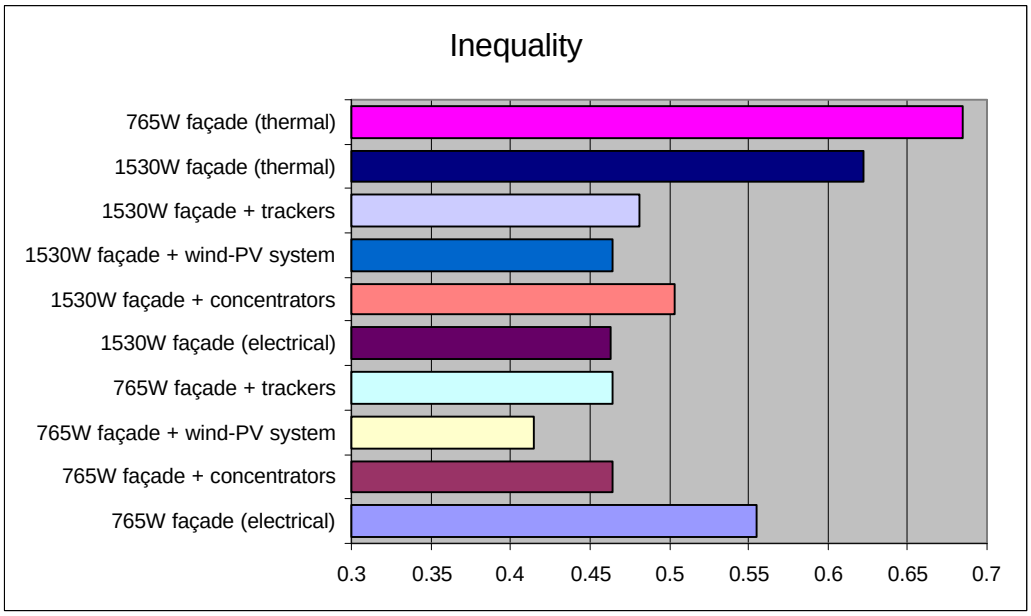

Figure 9.4: Inequality metrics obtained for a variety of RE combinations deployed with the aggressively reduced demand scenario

From Figure 9.4 it may be observed that the thermal matches in both façade sizes are poor. This is to be expected as the summer thermal demand is zero, and corresponds to the maximum supply period. The larger façade area gives a marginally better result, due to its increased capability in meeting winter demands. The match results are shown in Figures 9.5 and 9.6 for the 1530W and 765W facades, respectively. The unused energy in the summer is significantly more in the larger façade, whereas the difference in winter deficit is small, also more energy is lost during transitional periods. Figure 9.4 shows that on the electrical side the best match of the specified technologies is achieved using the smaller façade together with the full set of ducted wind turbines. A further annual search was conducted to examine the results obtained for the smaller PV façade, together with the PV-ducted technologies, and with the ducted wind turbines without the additional PV components, as these were proposed in the initial investigative search.

The results from this second search indicated that the west facing turbines should be employed without PV and the south-facing turbine with PV. This combination of technologies resulted in an inequality of 0.41, compared with the previous inequality of 0.42 for a full configuration of wind-PV systems. The difference between the two results can be observed to be small, and consequentially neither of the configurations are discounted at this stage.

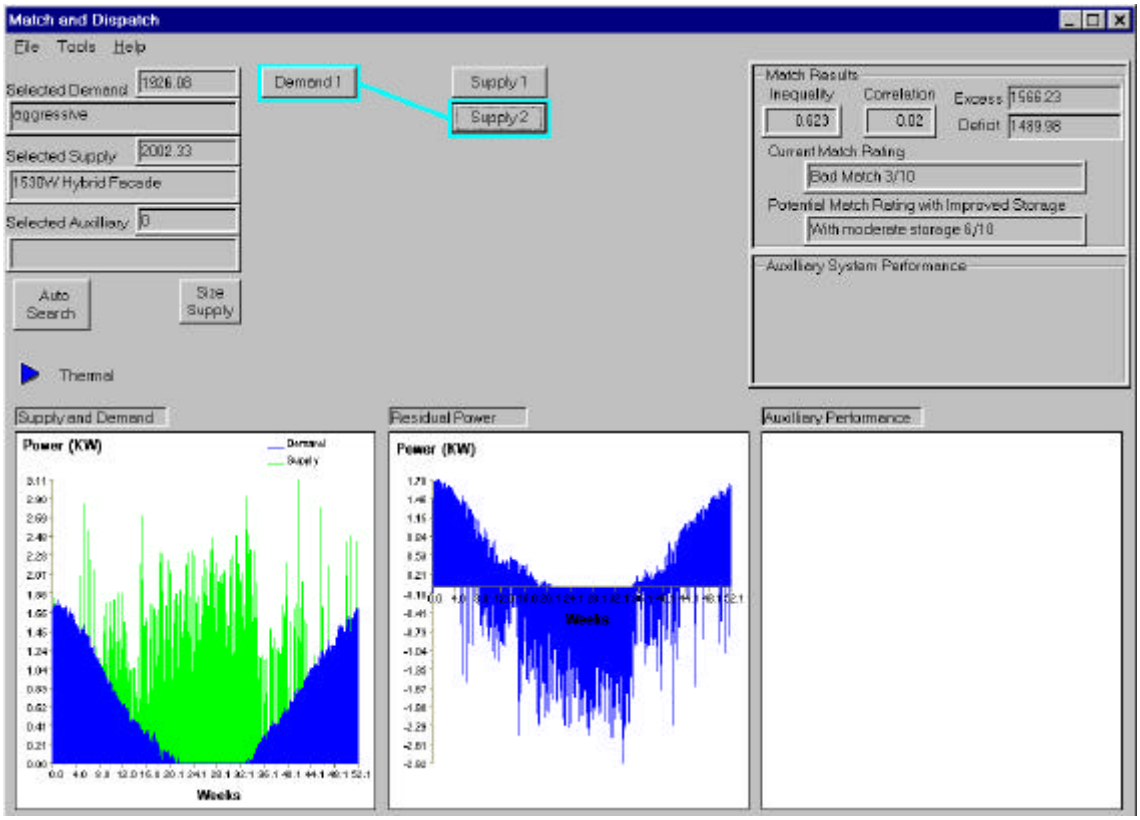

Figure 9.5: Thermal performance of a 1530W PV-hybrid component with Lighthouse thermal demands

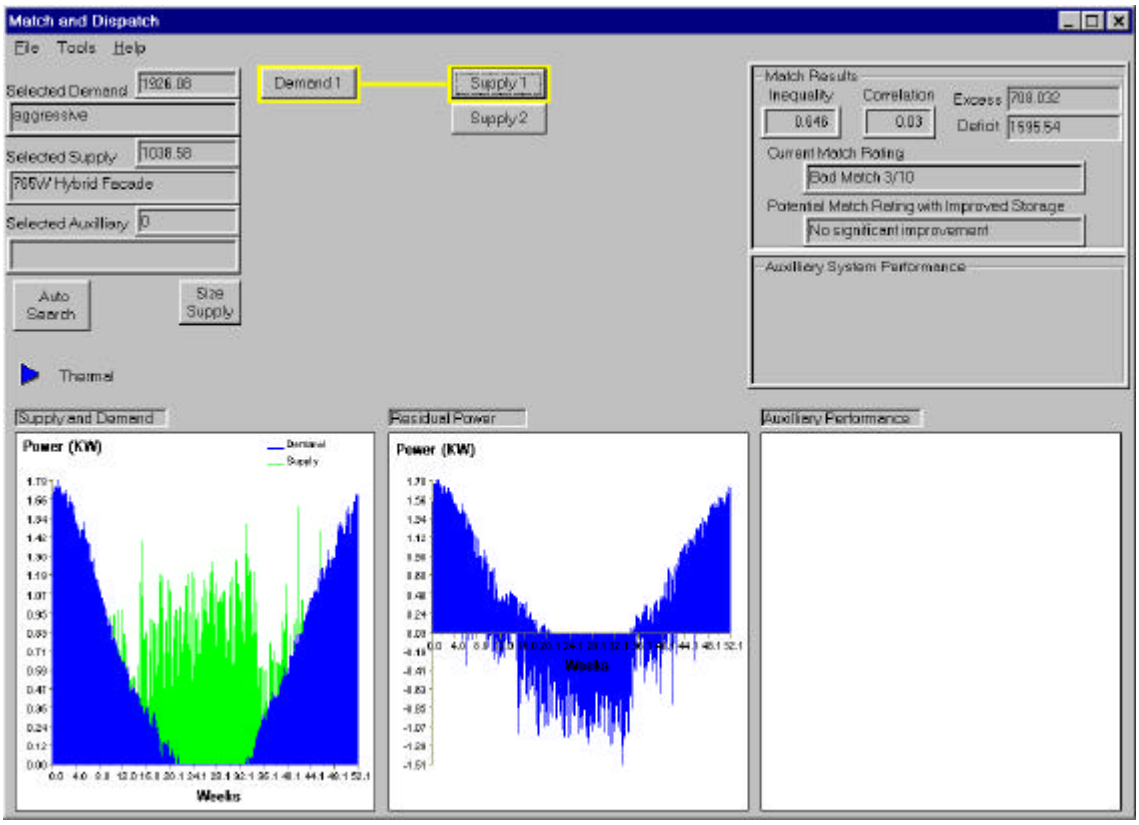

Figure 9.6: Thermal performance of a 765W PV-hybrid component with Lighthouse thermal demands

Phase 3: Auxiliary System Selection

The supply potential of the renewable systems investigated was not sufficient to consider grid-export via a parallel connection to the public electricity supply network. This option has the potential of selling excess production through the pool, at pool prices, i.e. in competition with large-scale conventional generating plant. Additionally, grid export requires compliance with numerous regulations (Engineering Recommendations G59/1, 1990), (Engineering Recommendations G5/3, 1976) and the

use of expensive power conditioning and inverter systems, to ensure the power quality of the electricity supply network is not adversely affected. Two other options were possible: either install a dedicated low voltage DC supply, or alternatively use an AC supply, powered from a battery storage system via an appropriate power converter. Losses associated with power conversion are avoided with the dedicated DC supply, although a DC supply has the disadvantage of requiring specialised electrical appliances. Employing a battery storage system together with an AC supply was the favoured choice, as the storage system provided a means of regulating demand and supply mismatch.

The final stage of this study therefore focused on sizing a battery storage system to further improve match statistics and hence evaluate which of the two supply strategies was optimal. Three sizes of battery bank were specified, with a charge control system that would draw electricity from the grid in the event of reaching a discharged state of 80%. The battery banks considered were four series connected 12V batteries of 60Ah, 80Ah and 215Ah capacities. Given that the most likely time for battery recharging would be the evening, the tariff selected provided a discounted rate for evenings and weekends. This final analysis involved the comparison between four possible renewable energy options, together with the three sizes of battery bank. The four renewable technology possibilities all included the 765W PV hybrid component on the south façade, together with the following roof space configurations:

- 4 west facing ducted wind turbines and 3 south facing ducted wind turbines
- 4 west facing ducted wind turbines and 3 south facing ducted wind turbines with PV aerofoils
- 4 west facing ducted wind turbines with PV aerofoils and 3 south facing ducted wind turbines 4 west facing ducted wind turbines with PV aerofoils and 3 south facing ducted wind turbines with PV aerofoils

The results from an annual simulation, illustrating the inequality metric, excess generation (not absorbed by the battery bank), and electricity cost, are presented in

Figure 9.7. The figure shows that by reducing installed capacity both the frequency, and magnitude of excess generation are reduced, and the inequality metric is improved. However, the converse is that lower excess inevitably correlates to lower net generation, and therefore increased deficit. This trend is further observed by the electricity cost increase with a reduction in installed capacity. The costs illustrated are electricity costs only, neglecting the standing charge, and compare with an electricity cost of £123.81 for the site without renewable deployment. As would be expected the figure illustrates that the greater the installed capacity, the greater the generation and the lower the electricity cost associated with grid export. Additionally, it may be noted that increasing the battery bank capacity, improves the inequality metric, and reduces the excess wasted energy, without increasing the electricity cost to recharge the battery.

Figures 9.8 through 9.10 depict the performance of the highest deployment of RE, i.e. a hybrid façade with ducted wind turbines and integral PV aerofoils, over 4 seasonal days with two different battery storage capacities. Figures 9.11 through 9.13 illustrate the performance of the minimum RE case, i.e. a hybrid façade with ducted wind turbines. Inspection of the figures indicates that the higher installed RE capacity system depends less on the grid to recharge the battery than the lower RE case. Additionally, it may be observed that although the cost of recharging a larger battery bank is higher than for a reduced capacity battery, the frequency of recharging is less.

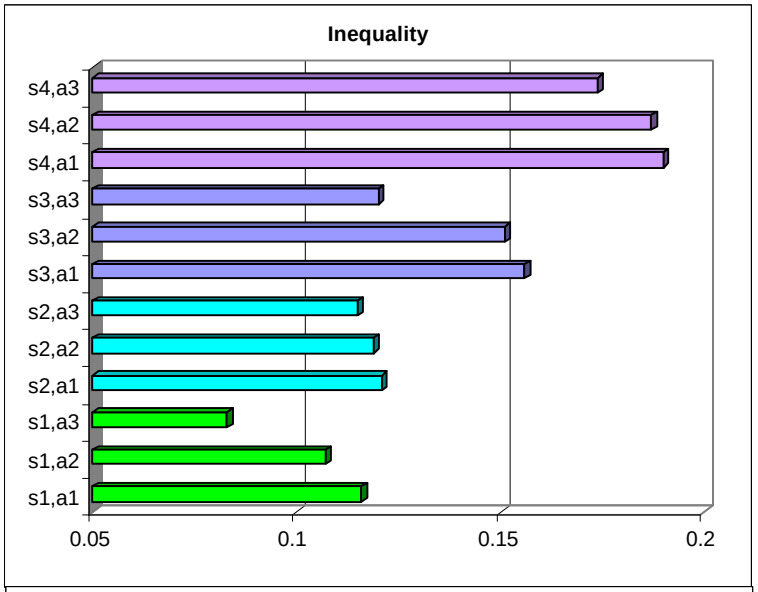

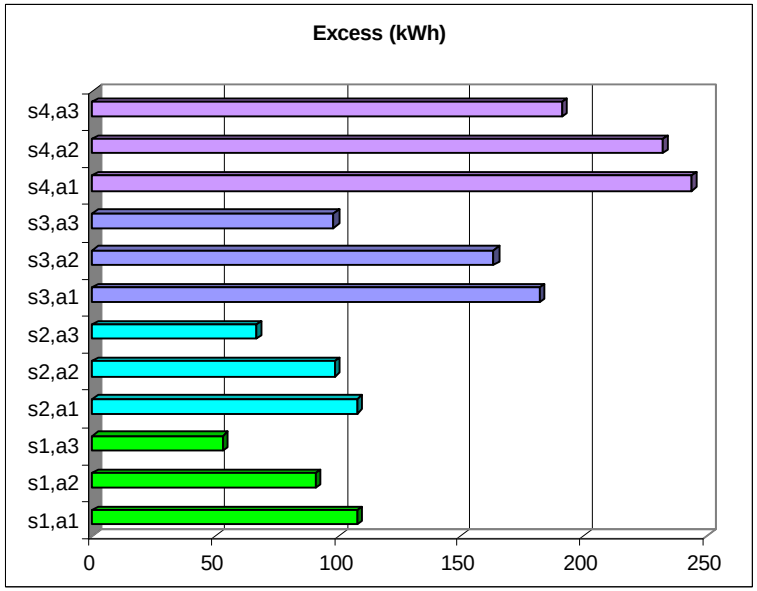

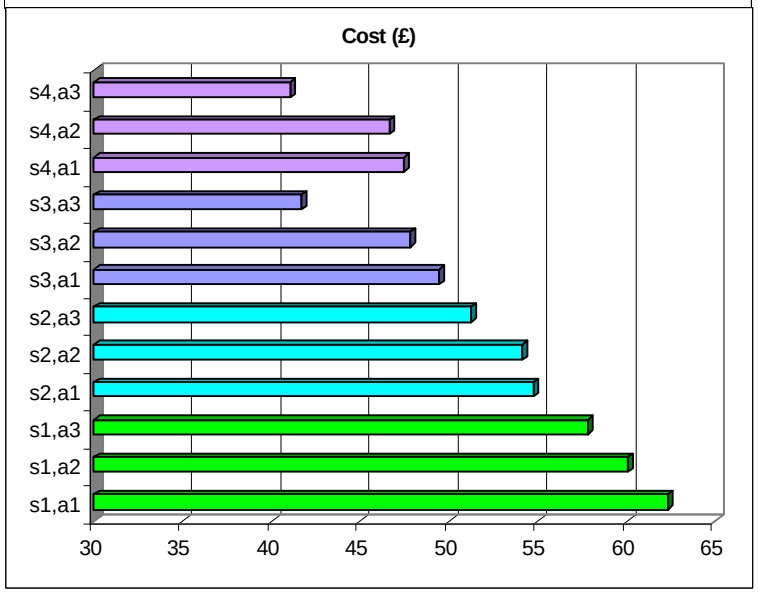

Supply Code	Technology
s1	PV façade + DWT west +DWT south PV façade + DWT west +PV-DWT south PV façade + DWT south + PV-DWT west PV façade + PV-DWT south + PV-DWT west
a3	4x215Ah @12V

Figure 9.7: Supply option comparisons

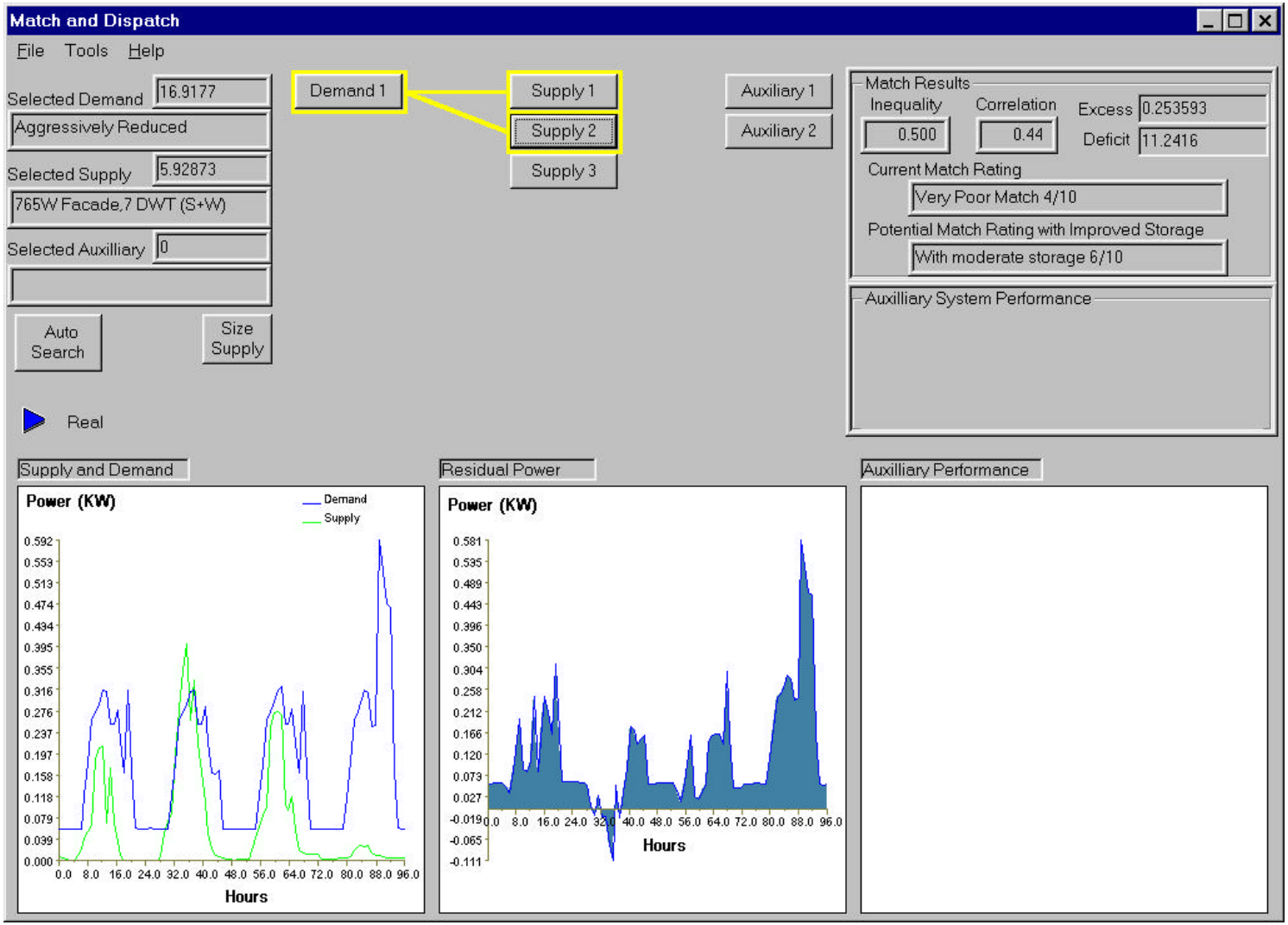

Figure 9.8: Seasonal performance of lower capacity RE supply option

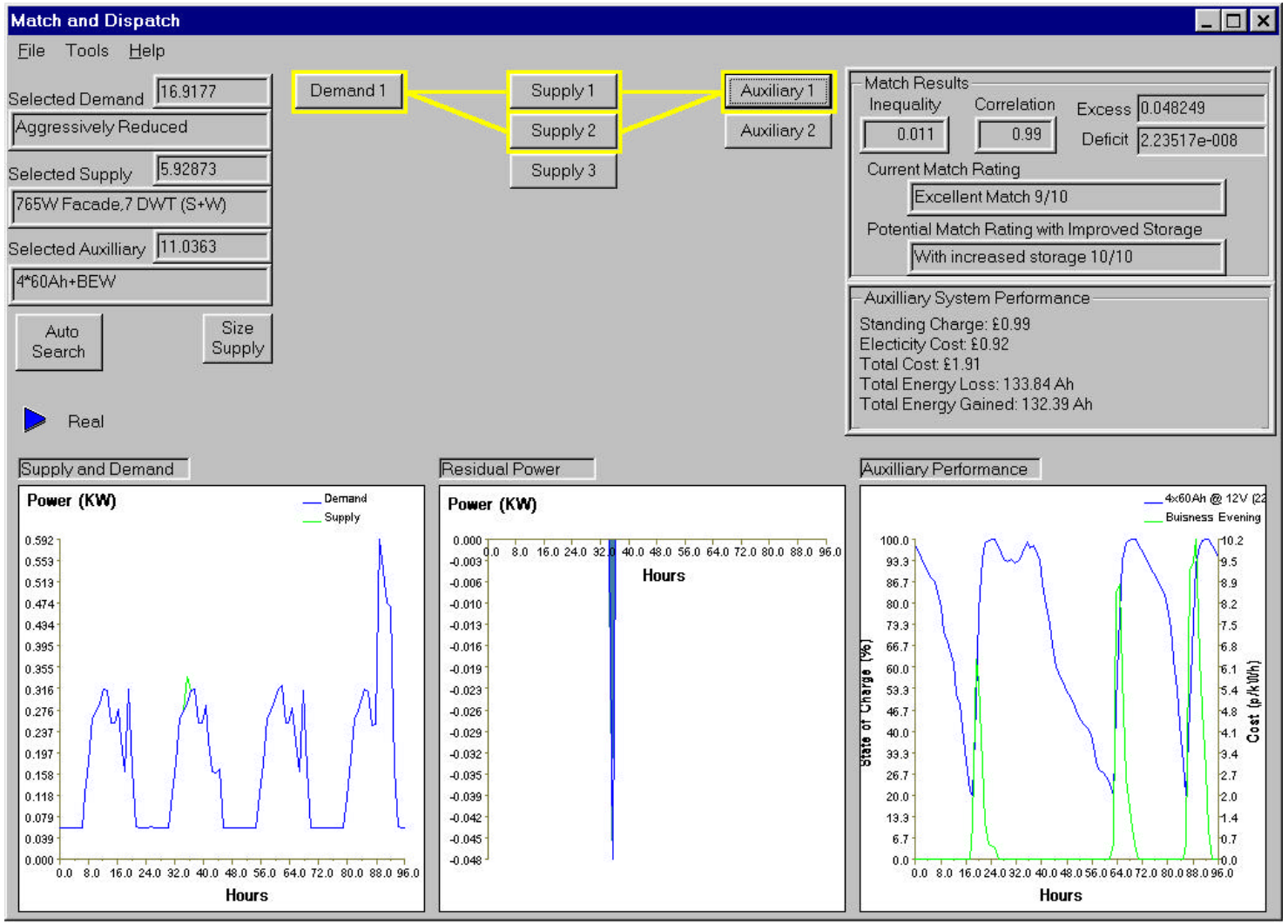

Figure 9.9: Seasonal performance of lower capacity RE supply option with lower battery storage capacity

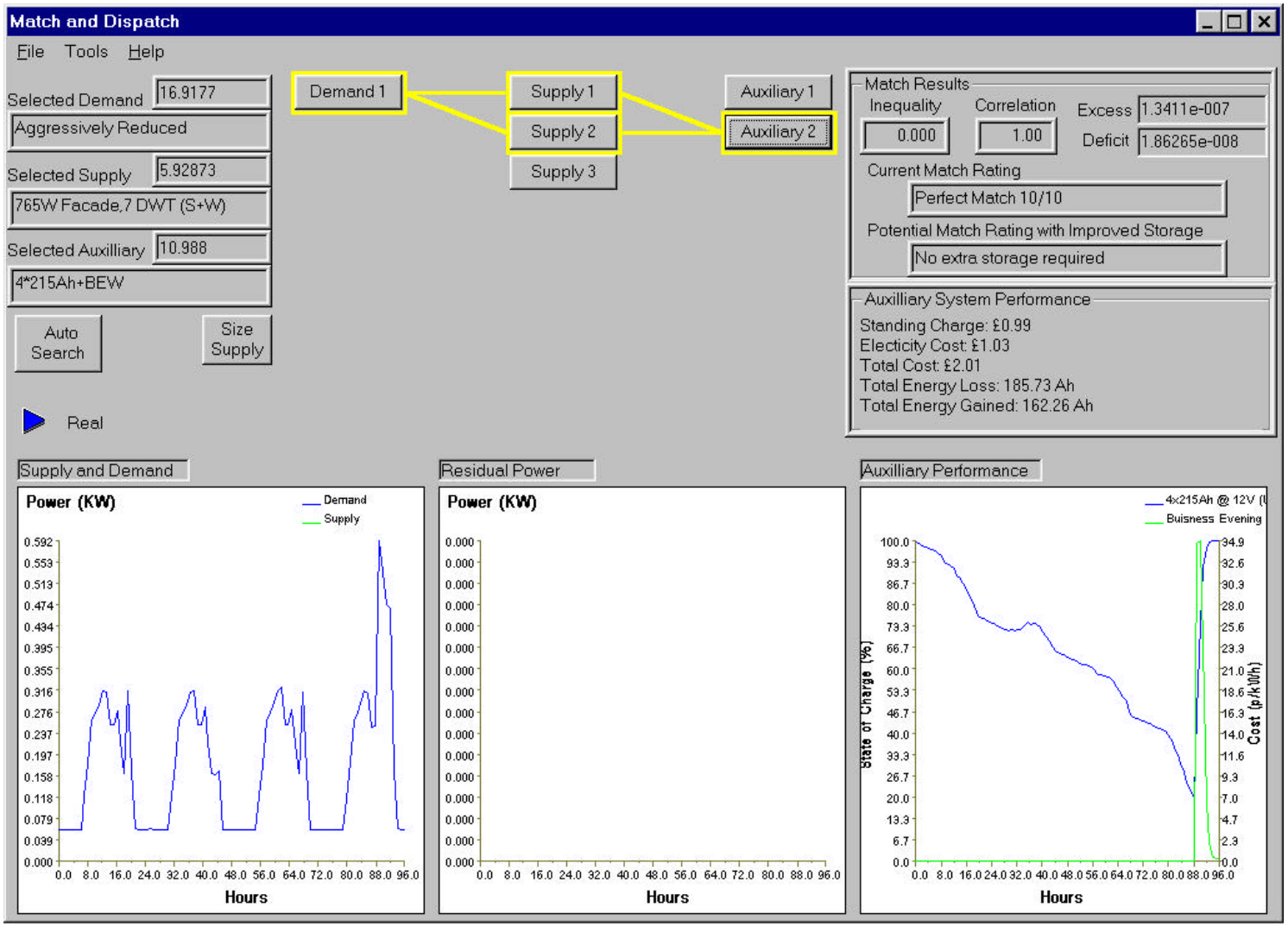

Figure 9.10: Seasonal performance of lower capacity RE supply option with higher battery storage capacity

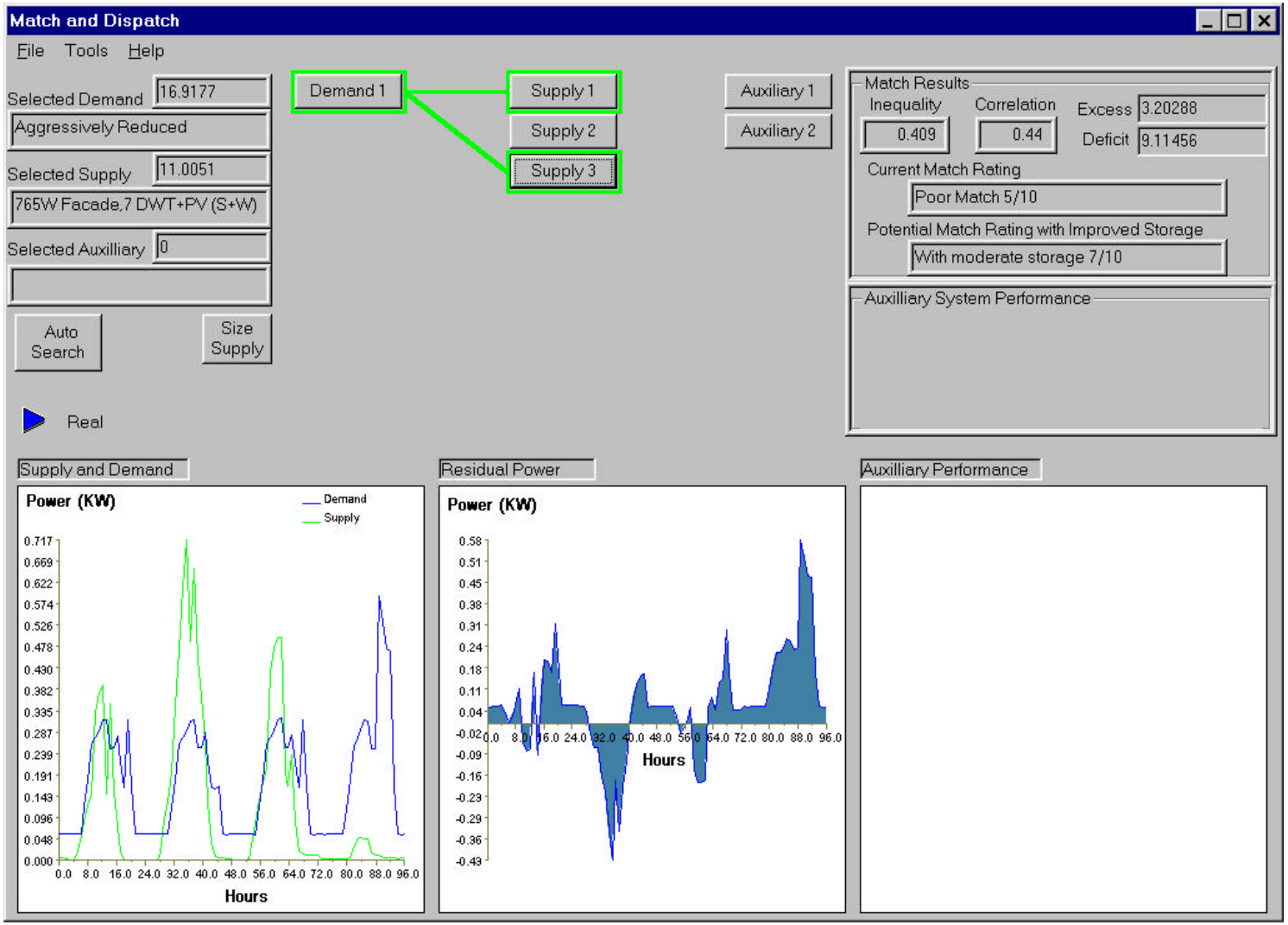

Figure 9.11: Seasonal performance of higher capacity RE supply option

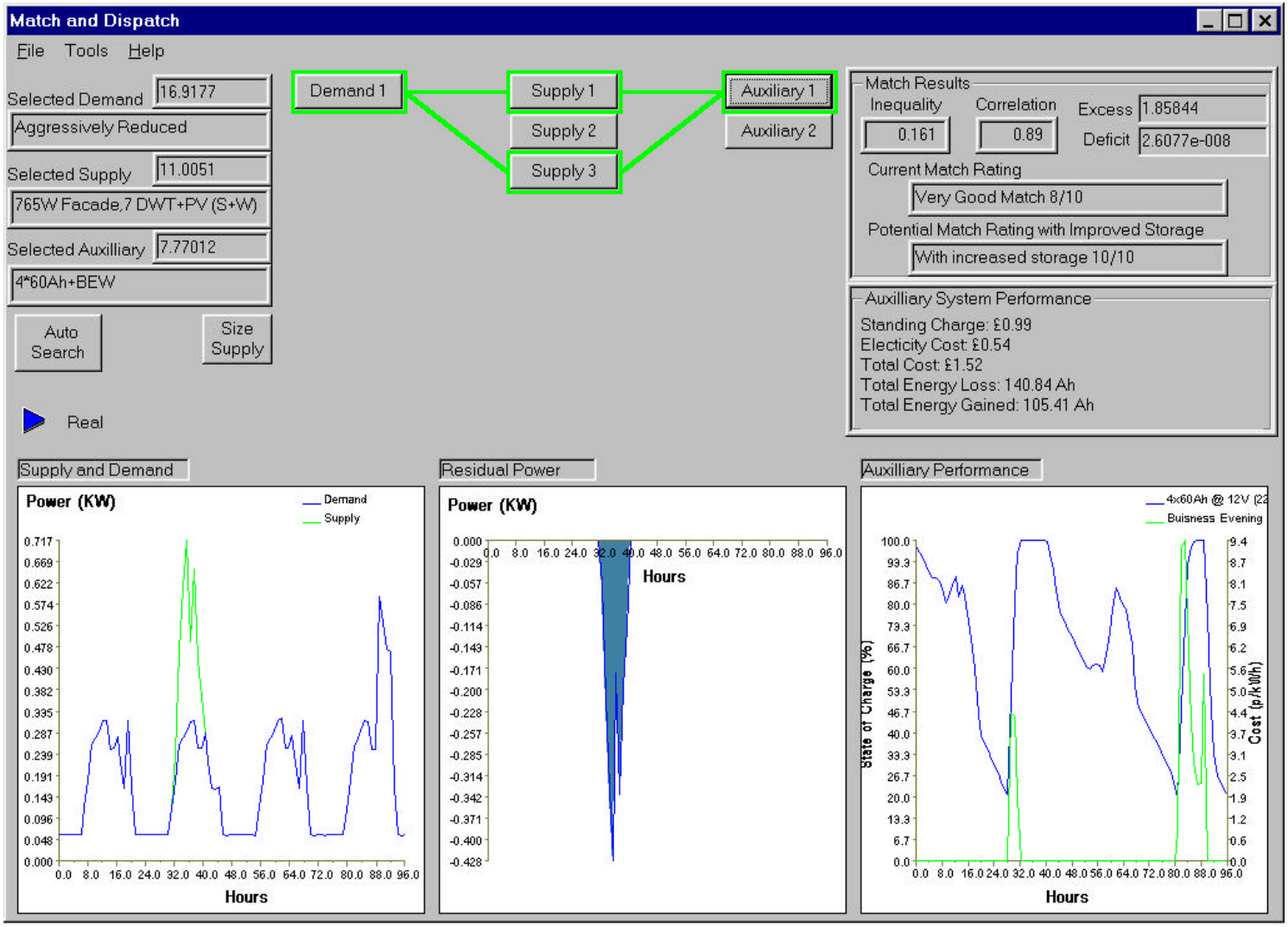

Figure 9.12: Seasonal performance of higher capacity RE supply option with lower battery storage capacity

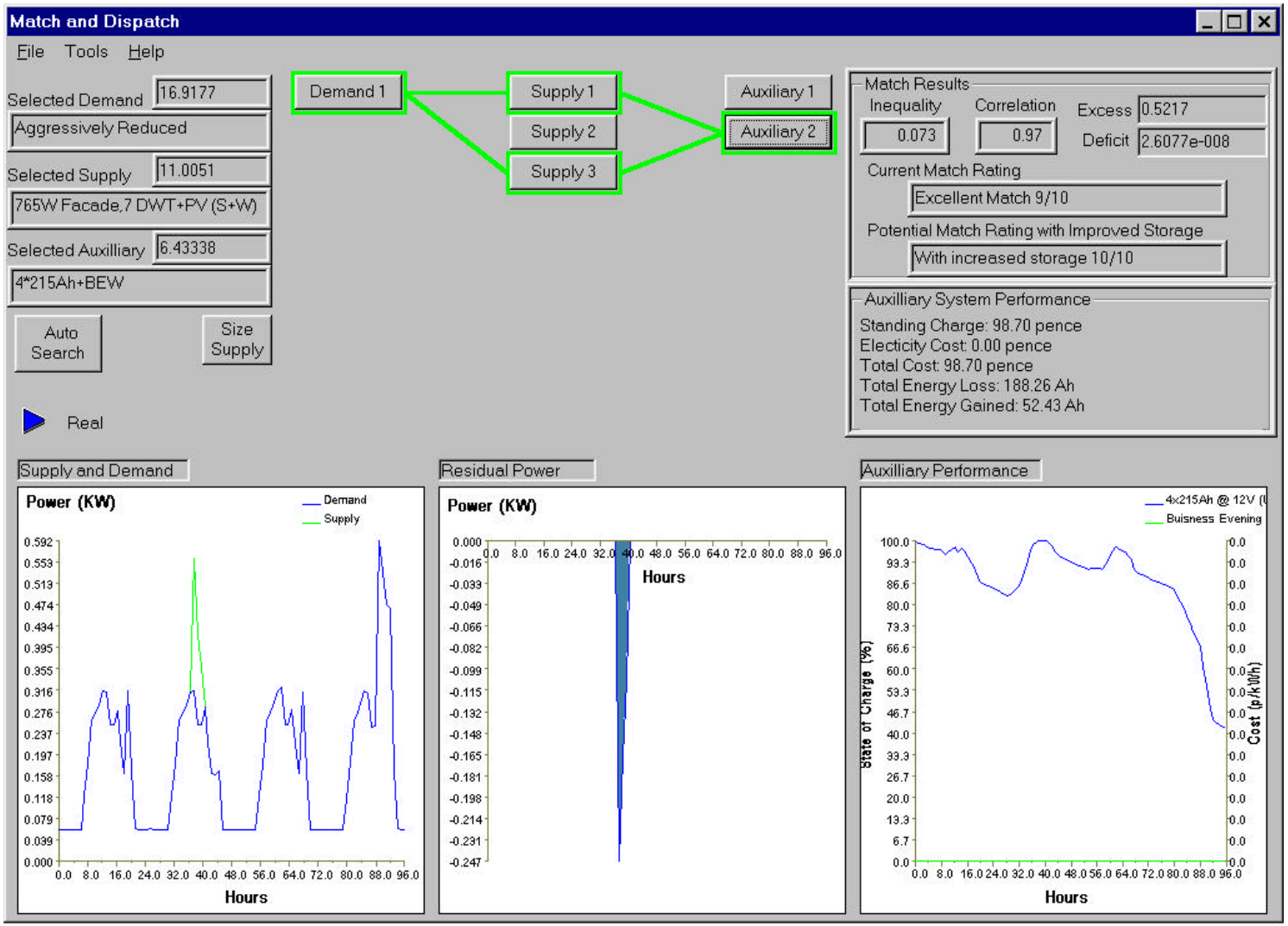

Figure 9.13: Seasonal performance of higher capacity RE supply option with higher battery storage capacity

9.1.3 Detailed Design Stage

The MERIT analysis involved three matching phases. The initial phase demonstrated that typical high power demands, are not conducive to renewable energy deployment where capture areas are limited, as is often the case with urban-type buildings. Thus for renewables to make a notable contribution, there is a necessity to reduce demands by adopting both energy efficient technologies and energy management measures. Having assumed a low demand scenario, the second phase examined the possible combinations of RE technologies best suited to the lighthouse buildings demands. This phase involved an analysis of electrical, thermal and hot water demands. An initial analysis of hot water consumption, and supply through a solar water pre-heat system was performed. The results indicated that, the performance of a flat-plate collector is compromised without regular hot water draw-off from the storage tank. As the requirement for hot water could be extremely variable at this site, a solar water heating system was not justified. A thermal analysis was undertaken involving two PV-hybrid facades and illustrated that although a larger façade was better equipped to meet winder space heating requirements, there was an extreme over production of thermal energy in the summer. The electrical analysis performed coupled the two hybrid facades together with possible roof deployed technologies, and the results illustrated that a better match was achieved when dissimilar technologies were coupled. Deploying single-source technologies together resulted in unbalanced periods of excessive generation and no generation at all. The third phase was therefore focused on the performance of a mixture of wind and solar technologies, and the effects of different capacities of battery storage. The results from the final phase found that by increasing the renewable energy supply, the grid electricity costs could be reduced, however this also increased the energy wastage. Increasing battery capacity reduced the wasted energy component, as well as grid electricity costs, and the battery cycling.

Having identified suitable technologies for the site, a detailed design stage was required to evaluate means of achieving the reduced demand scenario, and to determine the impact of the renewable technologies, particularly the hybrid façade, on internal

environmental conditions such as thermal comfort. MERIT is not capable of assessing the various passive technologies required to realise the required energy reductions, and this appraisal was subsequently carried out using the integrated building simulation approach (Clarke et al., 1996), employing the ESP-r system (Clarke, 1985). The methodology adopted in this appraisal are reported elsewhere (Clarke et al., 2000) and the results showed that the buildings demands could be reduced from a simulated base case demand of 220 kWh/m^2yr to 70 kWh/m^2yr, a 68% reduction. This was achieved through the deployment of advanced glazing systems, energy efficient lighting with daylight control, transparently insulated walls and an occupant responsive convective heating control system. The final technologies selected comprised the ducted wind turbines with PV aerofoils and PV hybrid façade.

9.1.4 Conclusions

Following the detailed design stage, the lighthouse viewing-gallery was retrofitted with the various passive and active technologies identified. The building has been instrumented to monitor climatic conditions, energy consumption, supply system performance, internal environmental conditions and electrical power quality. The final stage of this project will be to test the robustness of the modelling approach through a comparison of simulated predictions and monitored performance.

9.2 Energy Investigation on Community Scale: Dalmarnock Urban Business Park

Glasgow City Council (GCC) is currently initiating an urban regeneration project in the Dalmarnock area, and wish to investigate the deployment of renewable energy and combined heat and power technologies. As this project is in the initial investigative stage, it provides an excellent opportunity for the use of a decision support simulation based design approach in the identification of an alternative energy supply strategy. The council provided data pertaining to building type, and floor area as detailed in Figure 9.10. These data have been used to generate demand profiles to enable MERIT to evaluate a suitable strategy in which to incorporate both renewable technologies and CHP.

9.2.1 Demand Scenario

As none of the buildings currently exist, the required demand profiles have to be generated using appropriate techniques. The previous case study illustrated that a lowest case demand scenario is best suited to renewable integration, and the presented building demands were based on the assumption of the buildings complying with good energy efficiency standards, as recommended by the Best Practice Guides (Energy Efficiency Office, 1996). The demands forecast are building demands only, and neglect any industrial process energy requirements. Using the Best Practice Guides for this class of buildings, the consumption figures were estimated from the building type, and floor area data. Five building types were considered and comprised residential, office, light industrial/commercial, general industrial, and sports/recreational.

Annual Energy Consumption

The residential sector was assigned demands adapted from Ref (Energy Efficiency Office, 1996c), and included energy efficiency savings of 40% on typical thermal demands, and 20% on electrical, with energy demands for cooking neglected. The office component, which may for example include a call centre, was allocated

consumption data based on the definition for a factory-office building (Energy Efficiency Office, 1996a). This type of building is defined as a modern office-like space with little differentiation working and storage areas. Such buildings are characterised by clear internal heights of 4m, often with lower suspended ceilings in office parts, double glazed perimeter windows, ducted warm air heating to 20°C, lighting typically to 500 lux, and some local mechanical ventilation. The usage pattern is based on flexi-time operation, typically with 10 working hours, and 2 cleaning hours per day.

The light industrial, and research and development sites were assigned demands derived from the definition of light manufacturing buildings (Energy Efficiency Office, 1996a). These include light engineering and electronic equipment assembly. Such industrial units include areas for office, storage, and dispatch. The buildings typically have 5m clear internal height, use warm air or radiant heater units to 18°C, and are largely naturally ventilated with occasional local mechanical extraction. Lighting is generally to 300 flux with an average of 10% roof lights. Occupation patterns are based on 1.5 working shifts.

The general industrial sites were assigned demands based on the definition of general manufacturing buildings (Energy Efficiency Office, 1996a). The definition incorporates plastics manufacture, large scale printing, heavy engineering and food processing. Such sites may include mezzanine areas in places, and generally provide 8m clearances to accommodate tall equipment, gantry cranes and local storage racking. They are heated by warm air, radiant or steam heating to 16°C, with ridge or mechanical ventilation to areas of high process heat gain, and illuminated to 200 lux. The demands are based on two-shift operation.

The sports facility demand was based on the demands given for a sports facility without a pool offering some wet facilities (e.g. steam rooms, saunas and whirlpools), and based on 4800 hours of use (Energy Efficiency Office, 1996b).

A summary of the demand consumption figures used in this study is given in Table 9.1. Also provided is the electrical load profiles assigned to each category of building. Figures 9.11 and 9.12 describe a breakdown of the total thermal and electrical demands by sector.

Table 9.1: Summary of demand data derivation

Building Type	Floor Area (m^2)	Units	Thermal Demand per Unit (kWh/year)	Electrical Demand per Unit (kWh/year)	Electrical Profile	DF
Residential 3 Bed	150	41	29550	2113	Domestic Rate 1	2
Residential 1/2 Bed	120	123	13133	1690	Domestic Rate 1	3
Offices A	3000	4	300000	165000	LIT Office	3
Offices B	1700	4	170000	93500	Load Factor 30-40%	4
Light Industry	675	16	60750	20925	Non Domestic Rate 1	4
R&D	3000	3	270000	93000	Load Factor 20-30%	2
GI - A	2750	1	343750	137500	Load Factor >40%	0
GI - B	2250	1	281250	112500	Load Factor 30-40%	0
GI - C	2850	1	356250	142500	Load Factor 20-30%	0
GI - D	1500	1	187500	75000	Non Domestic Rate 1	0
GI - E	2000	1	250000	100000	Load Factor 0-20%	0
GI - F	2300	1	287500	115000	Load Factor 20-30%	0
Sports & Rec	500	1	97150	47850	LIT Hotel Profile	0

Figure 9.14: Proposed building type plan of Dalmarnock

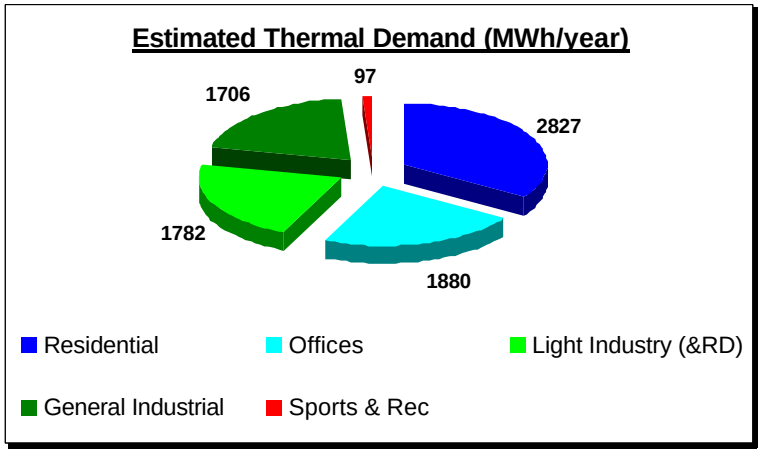

Figure 9.15: Estimated thermal demand for site

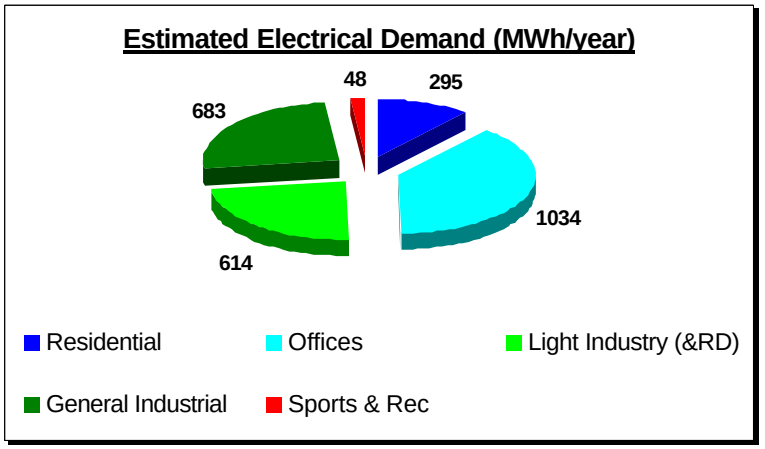

Figure 9.16: Estimated electrical demand for site

Load Profile Derivation

The annual consumption figures for each of the building sectors was used to scale appropriate profiled data. The profiles were derived using the profile designer module of MERIT using the procedure detailed below.

Electrical Demand Profiles

Electricity demand profiles for the UK are defined by the Electricity Association Load Research Group (Allera and Horsburgh, 1998) for five seasons (winter, spring, summer, high summer, autumn, and winter) and 3 day types (weekdays, Saturdays and Sundays). The seasons are defined by the following dates:

- Winter: 10th - 16th January
- Spring: 17th - 23rd May
- Summer: 14th - 20th June
- High summer: 9th - 15th August
- Autumn: 27th September - 3rd October

Table 9.1, describes the profile classes used on each of the building units. Two additional non-UK profiles, obtained from the Lund Institute of Technology (Noren, 1997) were also used. The first for one of the office buildings and the second for the sports centre, which was adapted from the profile defined for a hotel building. The LIT profiles are also defined for weekday and weekend day types with the profiles are characterised by average ambient temperatures as opposed to specific dates. UK climate data was therefore used to evaluate the average daily temperatures, and assign profiles accordingly.

Having defined sets of profiles for specific periods, profiles for the periods in between were developed using interpolation. The annual profiles were subsequently modified to include varying degrees (up to 10%) of random fluctuations, to more accurately portray the unpredictability of energy consumption.

Residential profiles were derived from the UK Domestic Rate 1 profile, which describe domestic properties with non-electrical heating. Non-domestic UK profile classes are defined by average load factors as opposed to building function. As the load factors for the Dalmarnock sites were unknown, an analysis of different profile types was required to enable appropriate profiles to be assigned. Average load factors for a range of profiles taken from the Pacific Gas & Electric Profiles (Pacific Gas and Electric, 1998), together with the LIT and UK profiles were calculated, and are shown in Figure 9.13. This figure illustrates that the load profile classes for all UK non-domestic profiles span a large range of load factors between differing commercial and industrial sites. The average load factors calculated were used to assign profiles to the different building categories. For example, one of the office sites was assigned the profile for load factors 30-40%, as the average load factor for this profile class was closest to the LIT office profile. The other office site was assigned the LIT office profile. The light and general industrial units proposed for the Dalmarnock project were assigned a mixture of the non-domestic profiles to obtain a good cross section of demand profiles scenarios.

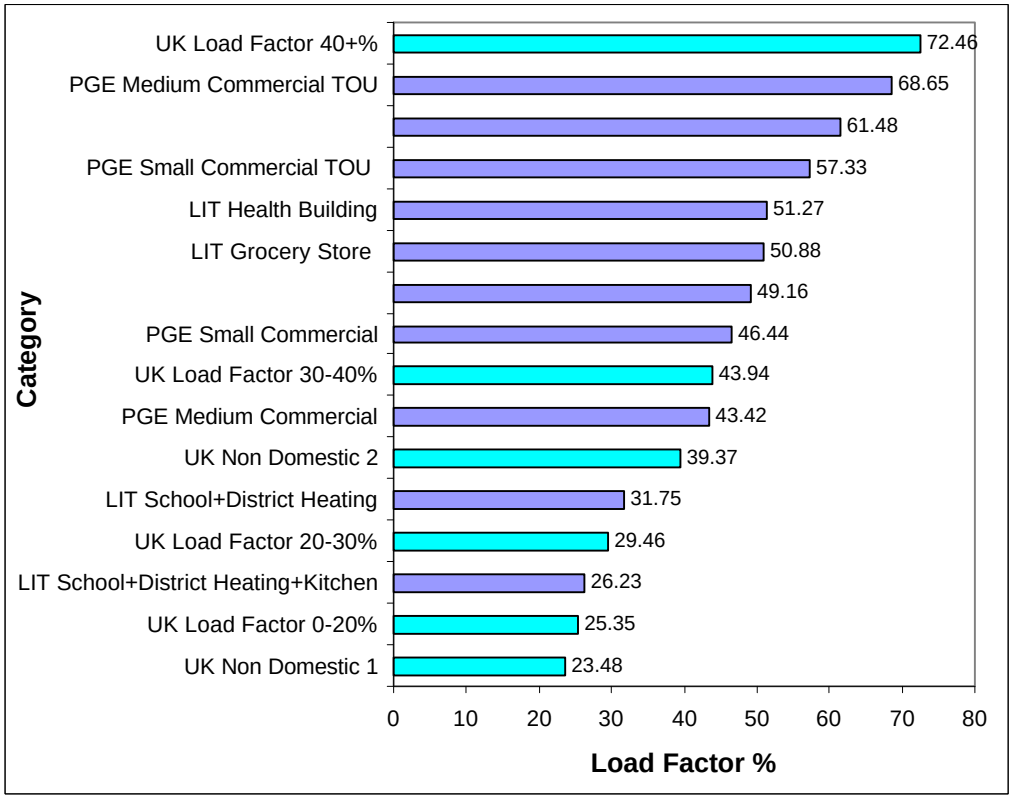

Figure 9.17: Average load factors for a range of non-domestic profiles

Thermal Demand Profiles

Typical thermal demand profiles are currently not available, and the option of obtaining a profile through simulation is inhibited, as the building designs are as yet unknown. Consequently, thermal profiles for each of the building types were derived by estimating occupancy hours, and assigning appropriate heating loads. These heating loads were correlated with ambient temperatures from the UK climate data. Hot water demands were included in the thermal profiles as variability over occupancy hours. The resulting profiles were subsequently scaled to provide the estimated annual consumption figures for each building type.

Resultant Seasonal Demand Profiles

Figures 9.14 through 9.18 describe the thermal and electrical demand profiles for each of the building sectors, with Figure 9.19 describing the total consumption profiles for the proposed development. The profiles indicate typical demands for summer, transitional and winter weeks. Thermal demands are characterised by significant reductions during the summer period, as space heating requirements become negligible, and electrical demands are seen to fluctuate with building occupancy.

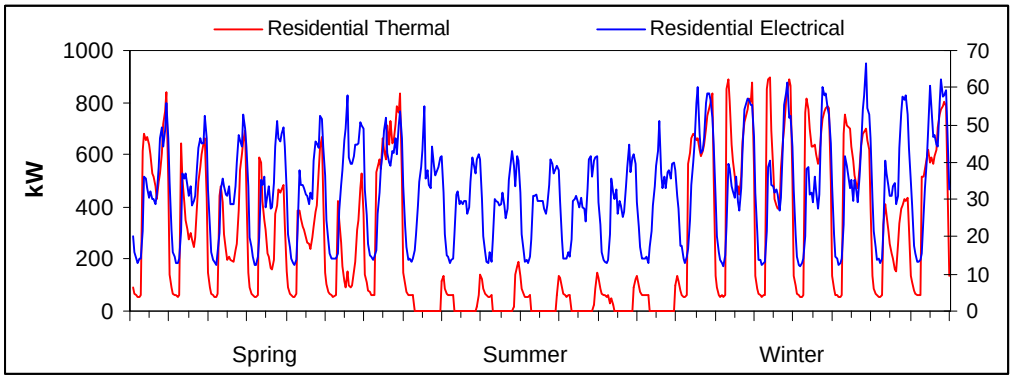

.

Figure 9.18: Typical seasonal residential demands

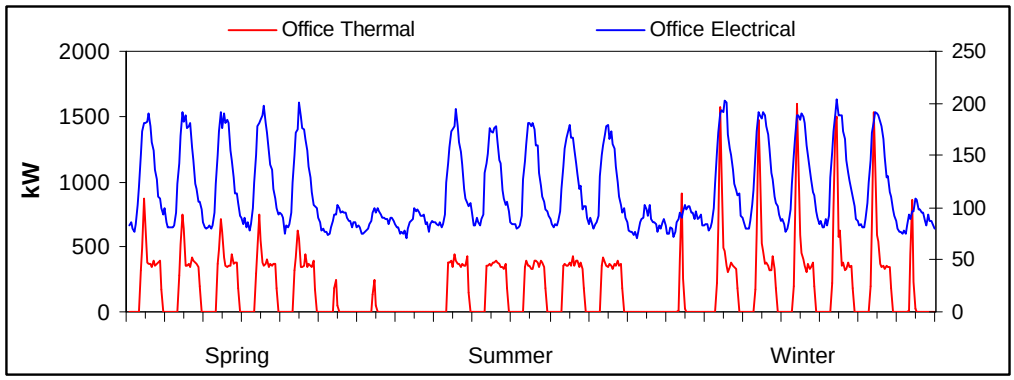

Figure 9.19: Typical seasonal office demands

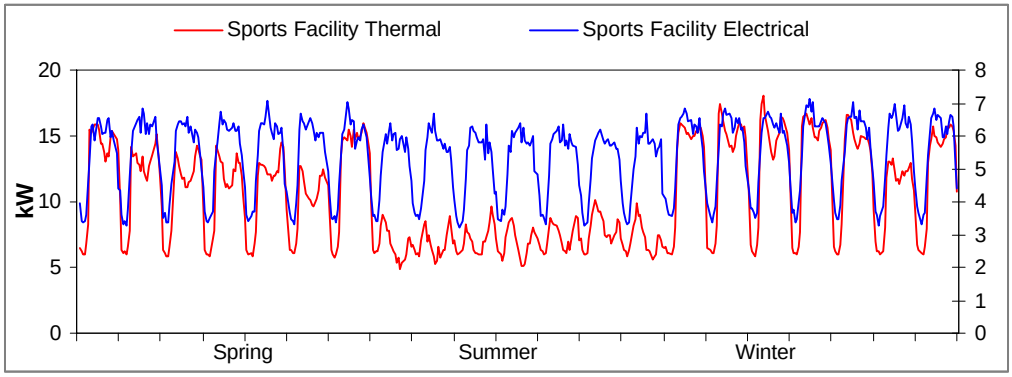

Figure 9.20: Typical seasonal sports facility demands

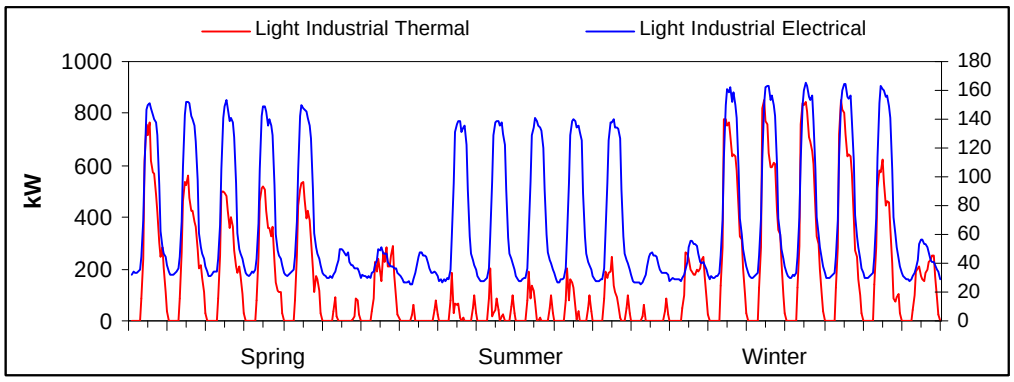

Figure 9.21: Typical seasonal light industrial demands

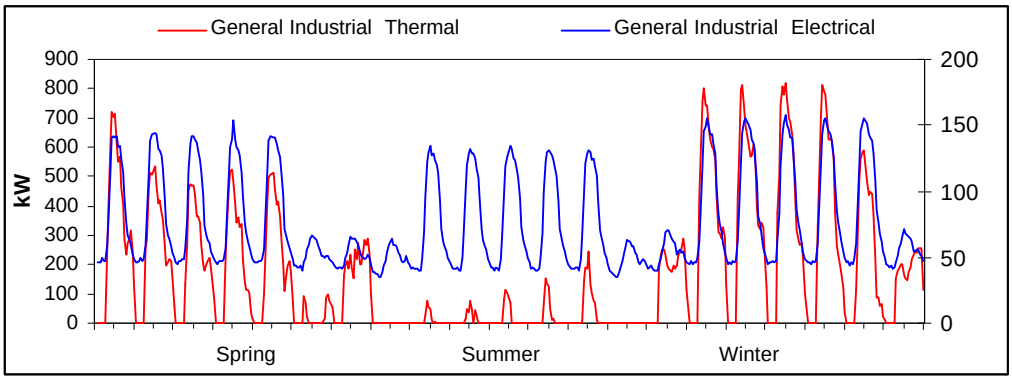

Figure 9.22: Typical seasonal general industrial demands

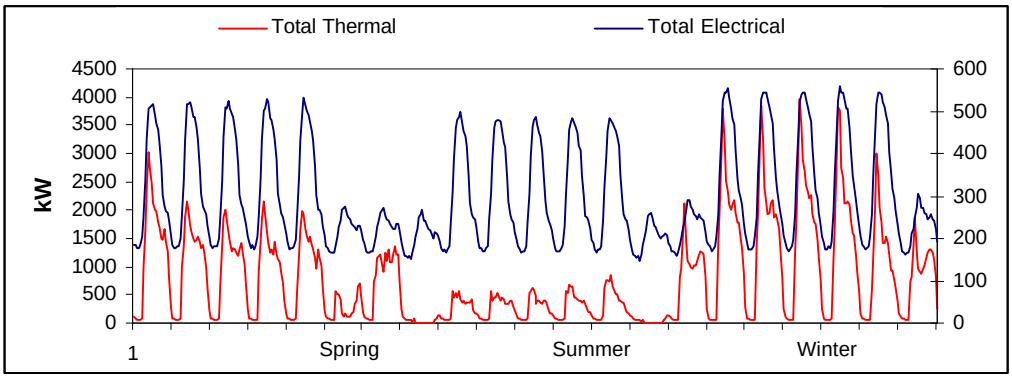

Figure 9.23: Typical seasonal total demands

9.2.2 Supply Scenario

Figures 9.24 and 9.25 illustrate the progressive addition of supply profiles to the thermal demands for typical weeks in all four seasons. Figures 9.26 through 9.28 detail the electrical matches obtained over the incremental addition of RE supplies. The supply profiles were selected through the method described below.

Ideally, the supply technologies should be designed to meet both electrical and thermal demands. As Glasgow City Council expressed a particular interest in CHP, the diesel generator model was modified to include a heat to power ratio of 1.8:1, which indicates heat exchangers are used to extract thermal energy losses from both engine coolant and exhaust system. Additionally, as the life expectancy of CHP is decreased by cyclic operation, the generator was assumed to run continuously to meet base load requirements, with down time for maintenance neglected. Inspection of Figure 9.20 shows that the electrical base load is in the region of 200 kW, and the thermal load around 1.4 MW. Utilising the auto sizing function of MERIT, the optimised performance in satisfying both thermal and electrical loads was achieved using a 325 kW diesel generator, adapted to recover heat loss. Having approximately satisfied the base loads, with an inequality index of 0.647, the next stage in the analysis was to attempt to meet some of the daily variations that are observed in the thermal profiles to improve the match between supply and demand.

As this project is currently in the conceptual phase, and the hot water demand is difficult to forecast, the sizing of individual hot water storage tanks and the prediction of draw-off was not considered to be appropriate. However to obtain an indication of thermal energy gains that can be achieved through the deployment of flat plate collectors, they were modelled assuming a constant inlet temperature of 10°C. The tilt angle optimiser in MERIT was used to determine the angle of tilt resulting in maximum supply over the year, which was found to be 35°. Having configured the collector model accordingly, the auto-sizing utility was again used to determine the optimal number of collectors required as 600. The inequality index of the thermal match is reduced to 0.498, and is a significant improvement to that of CHP deployment alone. The match is not ideal, however: given the level of uncertainty in the demand profiles, it was considered to be satisfactory. Furthermore, the use of any additional solar thermal technology would only increase the excess supply in the summer weeks, without improving the performance in winter weeks significantly.

The Dalmarnock electrical demands met by the CHP system alone is illustrated in Figure 9.26, with an inequality index of 0.34. This match is improved to 0.305 through the deployment of PV, as can be seen in Figure 9.27. The PV modules were optimally positioned at a tilt angle of 35 degrees facing south, with auto-sizing indicating the number of panels required to be 800.

The majority of the demand is met through the use of a large wind turbine. An iterative approach was used to determine the capacity of wind generator required, and identified to be a stall regulated turbine rated at 300 kW, at a hub height of 40m. Including this wind system improved the inequality index to 0.226. Figure 9.28 illustrates the combined RE technologies matched to the demand, some serious excess supply periods can be seen to exist although the profiles are largely well matched. These excess supplies may well be used by industrial process energies, which have not been considered in this analysis. Alternatively the generation of hydrogen could be considered which, could be used to meet some of the winter thermal demands. Again the level of uncertainty involved at this stage of the project implies that any further attempts to improve the match between supply and demand becomes meaningless.

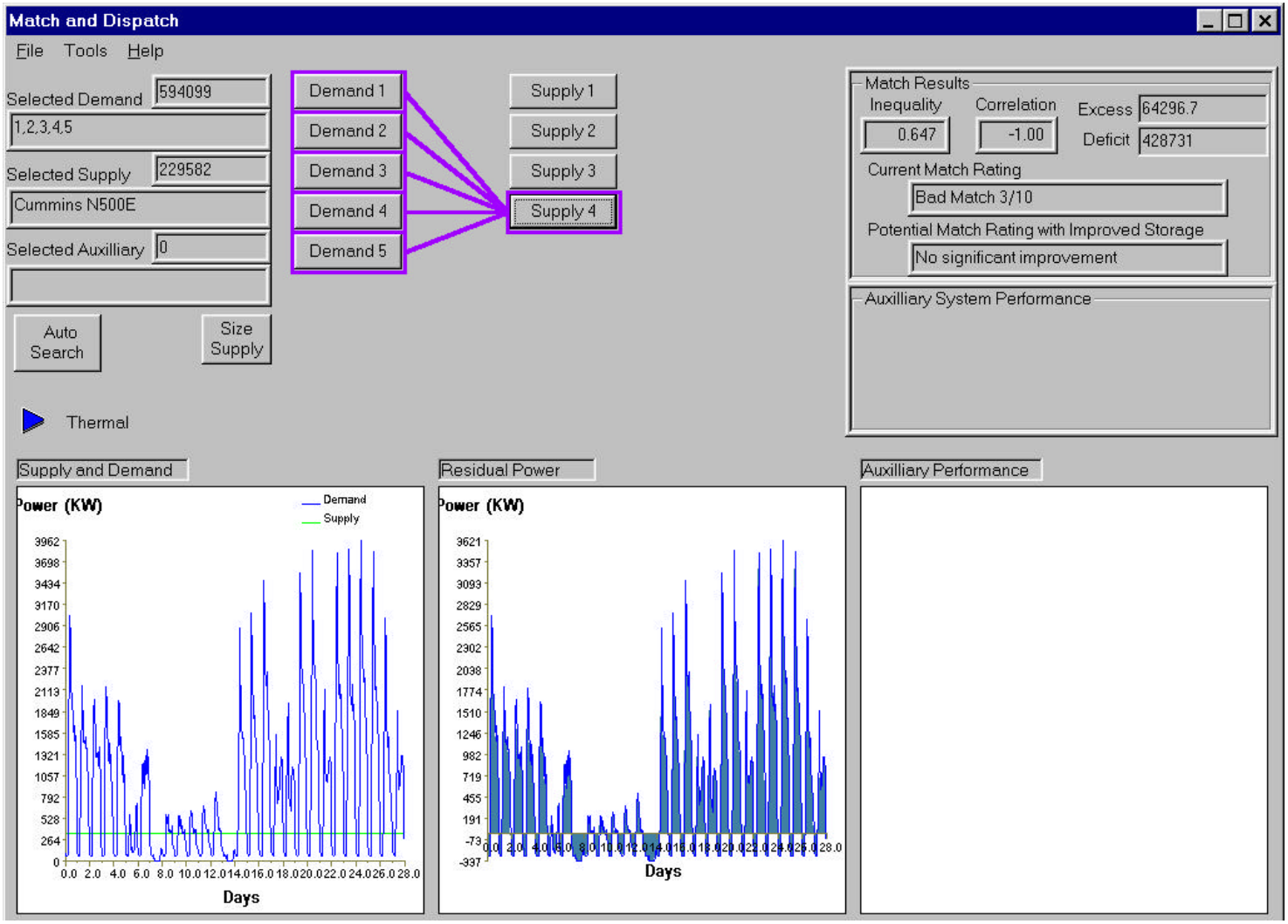

Figure 9.24: Dalmarnock thermal demands met by CHP

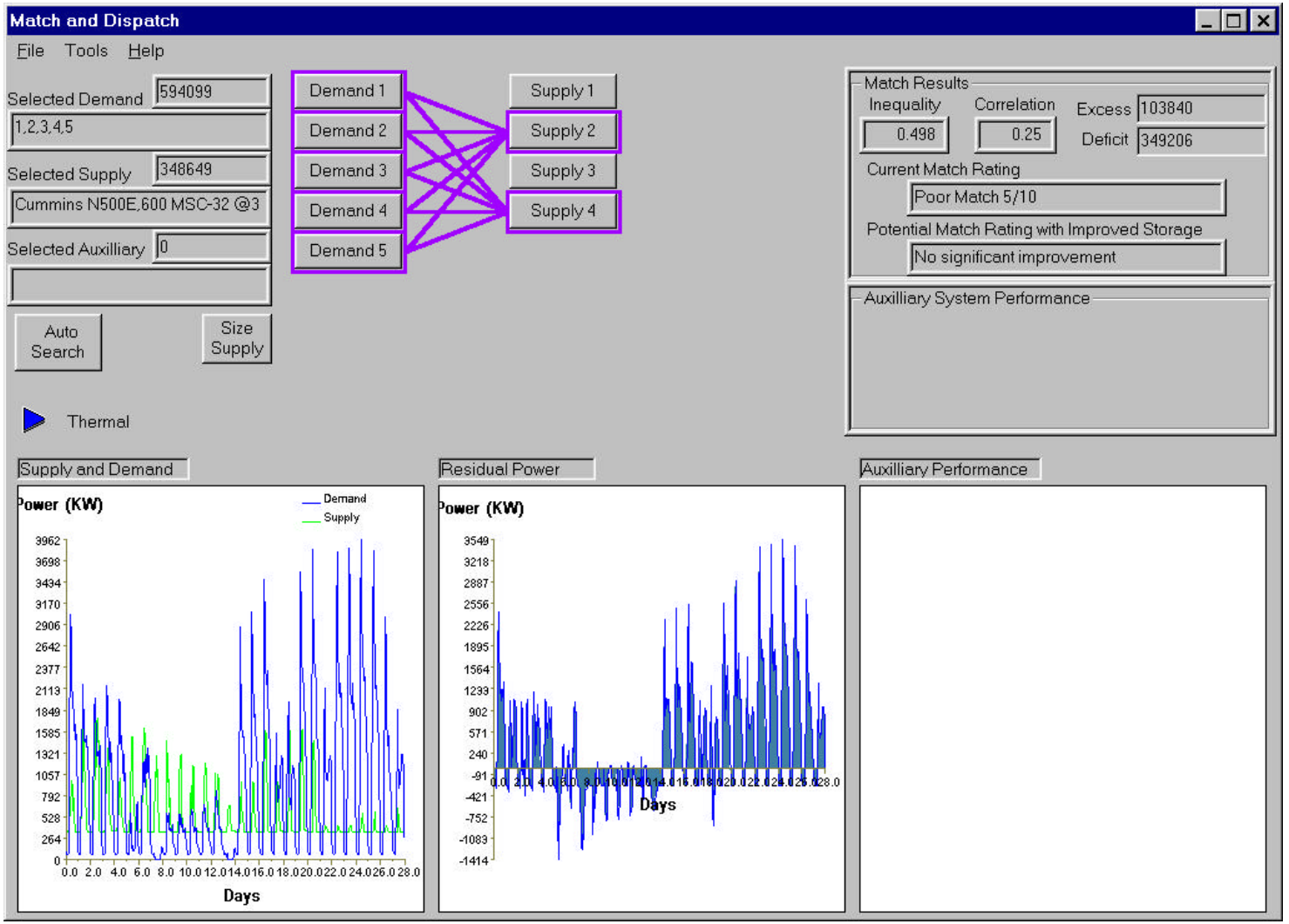

Figure: 9.25: Dalmarnock thermal demands met by CHP and Flat-plate collectors

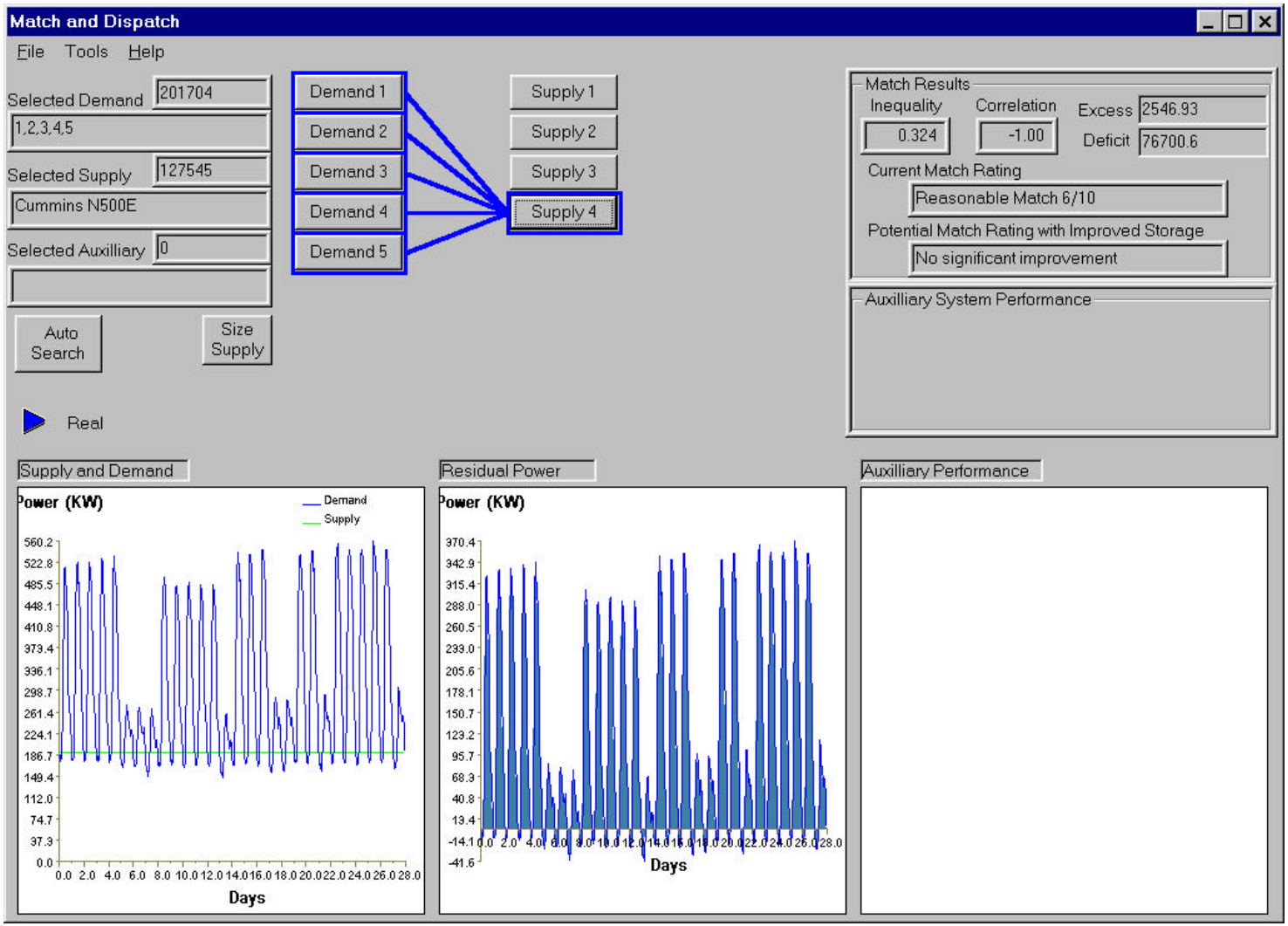

Figure 9.26: Dalmarnock electrical demands met by CHP

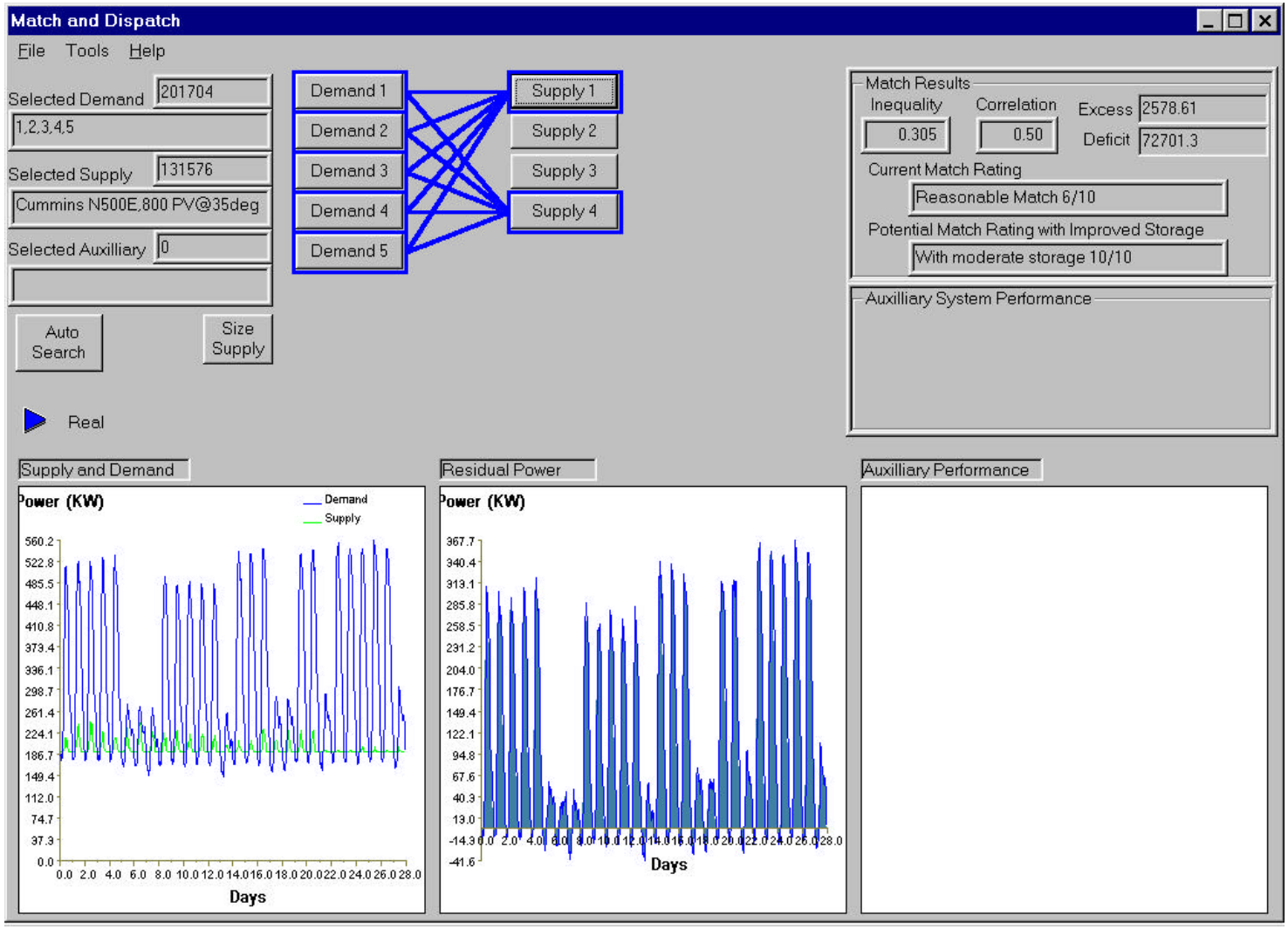

Figure 9.27: Dalmarnock electrical demands met by CHP and PV

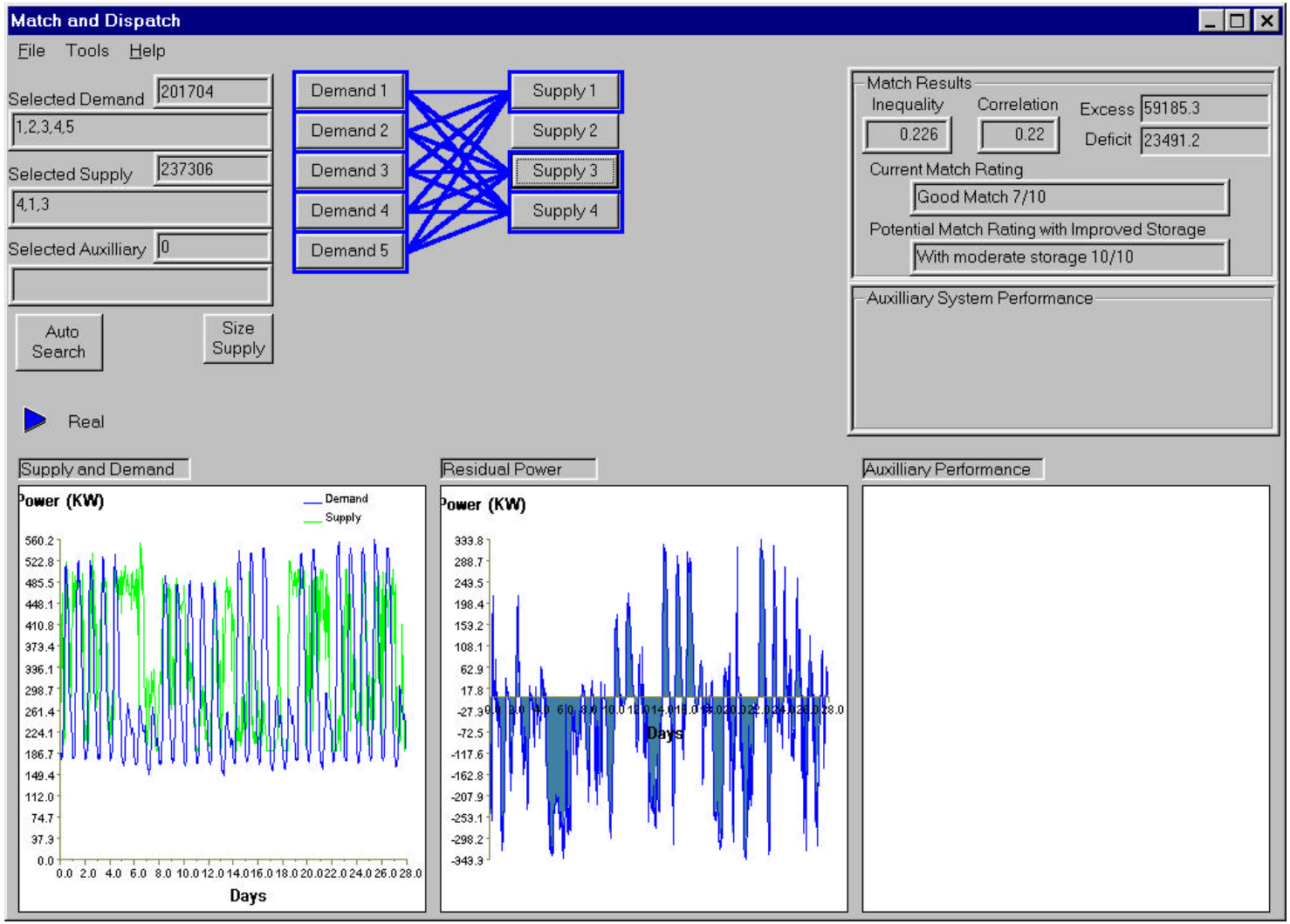

Figure: 9.28: Dalmarnock electrical demands met by CHP, PV and wind turbine

9.2.3 Conclusions

The analysis undertaken for the urban regeneration project provides an example of how MERIT could be applied to a large-scale project involving a variety of building types. Furthermore, it has demonstrated that even when a high degree of uncertainty is involved, the tool can be used to aid the focus of such a project, and to justify further detailed analyses. The analysis demonstrated that a CHP generator could be sized according to base loads, with additional thermal hot water demands being met by flat-plate collector systems. Large wind turbines could subsequently be deployed to meet substantive quantities of electrical demands, and PV deployment could further improve the demand and supply match. Having identified a suitable supply strategy, further work is recommended to undertake a detailed appraisal of building demands, to enable the approach to be refined. As the buildings have not been constructed, an appraisal of energy consumption through the use of building simulation is required. Such simulation could furnish MERIT with detailed demand profiles required to undertake a focused study, to determine component sizing and investigate storage scenarios.

9.3 Summary

MERIT has been applied to two case studies. The first case study provided an example of how the tool could be used on a single building level, and the second demonstrated its use at the larger scale. The tool has been designed to be scale independent, and the case studies presented are in support of this having been achieved. Just as the tool can be applied to a single building or to a composite mixture of buildings, it could conceivably be applied at the mirco-scale to investigate appliance power requirements or at the macro-scale to aid national supply and demand studies. Furthermore, it has been shown that decision making is supported from the initial identification of suitable supply technologies and appropriate demand management requirements, through to individual supply component sizing and positioning optimisation.

9.4 References

1. Allera S V and Horsburgh A G, Load Profiling for Energy Trading and Settlements in the UK Electricity Markets , October 1998, London
2. BS CP 310, Water Supply
3. C.I.B.S. Guide, Section B5
4. Clarke J A , Johnstone C M , Macdonald I A , French P , Gillan S , Glover C ,Patton D , Devlin J and Mann R, The Deployment of Photovoltaic Components within the Lighthouse Building in Glasgow, www.esru.strath.ac.uk, 2000
5. Clarke J A, Energy simulation in building design, Adam Hilger, Bristol and Boston, 1985
6. Clarke J A, Hand J W, Hensen J L H, Johnsen K, Wittchen K, Madsen C and Compagnon R, Integrated Performance Appraisal of Daylight-Europe Case Study Buildings, Proc. 4th European Conference on Solar Energy in Architecture and Urban Planning, Berlin, 1996
7. Clarke J.A., Hensen J.L.M., Johnstone C.M. and McDonald I., On the Use of Simulation in the Design of Embedded Energy Systems, www.esru.strath.ac.uk, 2000
8. Energy Efficiency Office, Department of the Environment, Energy Efficiency in Industrial Buildings and Sites, Best Practice Programme, 1996
9. Energy Efficiency Office, Department of the Environment, Energy Efficiency in Sport and Recreation – A Guide for Owners and Energy Managers, Best Practice Programme, 1996
10. Energy Efficiency Office, Department of the Environment, Energy Efficiency in Dwellings – What can tenants afford?, 1996
11. Engineering Recommendations G5/3, Limits for Harmonics in the United Kingdom Electricity Supply System, Engineering Publications, Electricity Association, UK, 1976

12. Engineering Recommendations G59/1, Recommendations for the Connection of Embedded Generating Plant to the Regional Electricity Companies' Distribution System, Engineering Publications, Electricity Association, UK, 1990
13. McLaughlin R.K., McLean R.C., Bonthron W. J., Heating Services Design, Butterworth & Co. Publishers Ltd, 1981
14. Noren Corfiz, Typical Load shapes for Six Categories of Swedish Commercial Buildings, Lund Institute of Technology, 1997
15. Pacific Gas & Electric, 1998 Static Load Profiles, URL:http://www.pge.com/whats_new/issues/electric_restructuring/profiles/1998.html

Chapter 10: Conclusions and Recommendations

10.1 Review

The principal findings of the work presented can be summarised as follows:

There is a need to consider small-scale renewable energy technology deployment as a means of supporting energy sustainability. These systems are ideally suited to building integration, for which the applications are as vast. Embedding these generation capacities within the distribution network could however adversely affect network stability and power quality, as today's electricity networks were not designed to support embedded generation.

A methodology in which information technology can be utilized to ensure the market penetration of RE technologies has been described. Within this information framework the IT components have been shown to be largely in existence, with the exception of energy matching facilities.

The criteria for effective demand and supply matching are that energy is matched quantitatively and temporally, to ensure RE generation coincides with periods of demand and is significantly substantial to contribute in meeting the demand without requiring grid export. The components required in matching are profiled descriptions of demand and supply.

The primary means for obtaining demand profile data have been reviewed and can be classified as measurement, load profiling and simulation. Measurement results in the most accurate profiled data, at the expense of installing measuring equipment and the time required in obtaining data. Load profiling is the inference of profiles for different customer types. Although this method is fundamentally inaccurate compared with

measurement, it is also significantly less expensive and the research has identified many of the influential variables on demand patterns. Building simulation can be a very accurate means of deriving load profiles and is not limited to the existing building stock, thus enabling the prediction of load patterns for proposed developments. The most significant disadvantage of this method is the specialist knowledge involved in creating accurate building models.

It was concluded that each method could make a valuable contribution in a database environment and the envisaged system was described as aggregated profiling. Removing preferences for particular methods enables the scope of profile information to be extended. The processes of augmentation and fragmentation, both of which enable data sources to be combined, support aggregated profiling. Fragmentation allows profiles to be decomposed into sub-profiles which, describe some individual characteristic of a profile. This can be applied to a single building, resulting in profiles for individual end use technologies or for a grid supply point profile, resulting in individual building type profiles. Augmentation is the inverse of fragmentation and is simply the summation of sub-profiles. Thus allowing a buildings' demand profile to be created based on a number of end-use profiles or a community profile assembled from the building type profiles which constitute the community.

RE supply profiles can also be obtained through measurement, however as the performance of these technologies is source dependent measured data is highly site specific. Moreover, much of the renewable potential is purely potential and can therefor not be measured. For these reasons simulation is a preferential means of obtaining the required data. Mathematical models were derived to predict supply profiles for wind, PV and flat-plate systems. In an attempt to avoid the pitfall of building simulation being limited to specialist knowledge, the fundamental objective in deriving these models was that the model inputs were based on primarily on manufacturers' data. This would ensure that by providing the required data, no apriory knowledge of technical performance was required. The basis of these input

requirements meant that the model also had to be sufficiently generic to allow for the differences in design of current technologies on the market.

The PV model developed is limited to mono and poly crystalline cells. The technique accounts for temporal changes in solar geometry to calculate the angle of incidence of solar radiation on the PV surface. Losses due to reflection are calculated based on a typical layered PV construction. Panel temperatures are evaluated using an energy balance technique, which accounts for the most significant heat transfer mechanisms. An equivalent electric circuit is used to model the electrical characteristics of PV cells, which results in a PV supply profile. The effect of an inverter is included through the approximation of performance curves. The results from the model have been compared with test data and have shown good agreement.

The wind turbine model was derived based on approximating characteristic performance curves. Four wind turbine classes were defined to account for marked differences in performance. These classes are based primarily on differences in power regulation, which can be separated into unregulated, stall regulated and pitch regulated turbines. The final class of turbine defined was the ducted wind device, which is distinctly different from other turbines, due to its directional sensitivity. Each of the models uses relationships between wind speed and power output, established through regression analysis of a range of turbines, to predict the supply profile for given wind conditions. The wind models described account for surrounding surface roughness, turbine height and variations in air density.

The flat-plate collector model developed incorporates the Hottel and Whillier (Hottel and Whillier, 1958) analysis of the collector together with energy balance techniques to account for a variety of storage options.

Matching is the process of identifying supplies whose peaks are coincident with peak consumption periods. Complementary matching ensures renewable supplies make a

notable contribution in meeting a site's consumption and simultaneously benefit the supply network. Mathematical techniques suitable for quantifying the degree of match considering both magnitude and phase between profiles have been identified.

Two search algorithms were developed to automate the process of match optimisation between a number of supply and demand profiles. The first is based on filtering the match results for combinations of supply and demand profiles, to enable the evaluation of the optimal combination. The second is based on spectral analysis, and utilises the Fast Fourier Transform technique to identify coincident trends. The method correlates the relative phases and magnitudes of dominant cycles within profiles. The searching procedures developed can be used to identify either the best overall combination of profiles, the best set of supplies for every individual demand defined or the best set of demands for every individual supply.

Auxiliary supply systems were shown to have a significant impact on match results and models for battery systems and back up generators were developed. Auxiliary system performance is directly related to the residual profile between demand and supply, which dictates when and how the system is operated. For this reason, the use of measured auxiliary performance data can not be used in match analysis and mathematical modelling is required. Again, the objectives for each of the models was that input parameters could readily be obtained from manufacturers specifications.

The model for the prediction of lead-acid battery performance developed incorporates three modes of battery operation, charge, discharge and self-discharge and accounts for some of the effects of operating temperature and electrical configuration.

The diesel generator model assumes the engine operates at a fixed speed (determined by generator characteristics) and power variations at this speed are achieved by varying the torque on the engine. The maximum conditions of torque and power are obtained

from engine performance charts and the model tracks fuel consumption for given periods of operation.

The development of auxiliary models lead to evolution of a potential match metric defined to indicate the potential match possible if an appropriately sized auxiliary system is incorporated. This potential match index was shown to be useful in the identification of supply and demand combinations, which had the potential to greatly benefit from the incorporation of an auxiliary system.

A procedure for tariff analysis was demonstrated, which could be used to quantify the savings resulting from RE deployment and for tariff negotiation. As a variety of tariff structures exist, calculating the cost of electricity consumption, with respect to different tariff options enables tariff optimisation, which could be used to enhance the value of an RE system.

A matching tool was developed which encompassed the theories presented in this thesis. The tool as been designed to allow both large and small scale renewable systems to be investigated. Large-scale systems can be matched to community demand profiles and small-scale to individual demands. The matching process is significantly more important in small-scale investigations, where exported renewable energy can be detrimental to the grid stability and uneconomical for the exporter. Match analysis provides the necessary information for decision makers to incorporate renewable energy in the overall supply portfolio. The program has been targeted at decision-makers, as the successful penetration of renewable technologies, lies with these people. The tool has additional advantages in the fields of load profiling, demand forecasting and demand side management. Where types of supply profiles are well matched to specific demand types, residual profiles can provide further customer classes, in the anticipation of wide spread RE technology deployment. Similarly, if the effects of RE deployment on demands are predictable, demand forecasting will be simplified. Finally, the

identification of technologies which best match certain demands could be very beneficial in demand side management planning.

Essentially the program consists of three definition stages, the analysis conditions, demand profiles and the supply and auxiliary system parameters used in simulating their performance. Analysis conditions, refers to the climatic conditions under which the technologies will be investigated. Incorporated in this is the period and temporal resolution of the investigation.

The ability to define demand profiles is provided through aggregated profiling. Measured or simulated profiles can be imported to enable detailed analysis. Databases of 'standard profiles', which consist of the profiles used in load profiling, provide the means for conducting initial studies of profile types. A facility is provided through which day-type profiled data can be used to create annual profiles through period interpolation. Profiles can be augmented through simply selecting combinations of profiles, enabling the large-scale type investigation.

Similar import facilities are provided in the supply profile specification, whereby profiled data obtained either through measurement or through simulation can be incorporated. The alternative is to simulate the performance of technologies, which are defined by readily available manufacturers' data. The models described for PV, wind and flat-plate technologies are used in the simulation. Auxiliary system performance is dependent on the behaviour of both supply and demand and profiled data can therefore not be imported. As with the supply specification, the information required in simulating performance is based on manufacturers' data.

Having defined profiles of interest, the processes of match assessment and optimisation can be initiated. Profiles can be combined manually, with match statistics and resultant profiles documented. Alternatively, where several profiles have been defined an automated search procedure can be used to find user defined criteria within

combinations. Selection of auxiliary systems results in the simulation of their performance and this as well as their effect on the net residual is documented. The mathematical models developed for battery and generators are used in the simulations. Through selecting a defined tariff, the cost of electricity supply is calculated relative to the tariff selected.

Because of the notable effects of auxiliaries, a further search parameter is incorporated which can evaluate a potential match. This metric is used to indicate the potential match possible if an appropriately sized auxiliary system is incorporated.

MERIT was specifically designed to avoid the well documented problems of other simulation programs of requiring specialist knowledge by basing all input parameters on easily obtained manufacturers data and providing data bases for a range of technologies. Its target audience encompasses a wide range of users including engineers, utilities, private power developers, renewable technology product suppliers, energy consultants, energy managers, architects, researchers, community planners.

The implementation of MERIT was demonstrated via two case studies. The first illustrated its use in single building decision support and the second demonstrated its applicability at the community scale. The case studies verified the tools scale-independence together with its ability to support decision making from the conceptual stages of identifying suitable supply technologies and appropriate demand management requirements, through to the detailed design phase involving component sizing and positioning optimisation.

10.2 Suggestions for Future work

The theories presented in this thesis and their realisation in the prototype software program MERIT, has been an initiatory investigation into supply and demand matching. Work which could further the capability of profile matching and expand on the foundations of MERIT is discussed in the following paragraphs.

10.2.1 Aggregated Demand Profiling

The concept of aggregated profiling encompassed the pooling together of demand data and was supported by augmentation and fragmentation. Augmentation is simply the summing together of different profile types. However, a community profile may consist of several domestic profiles and in reality no two profiles will ever be exact replications of one another. It would be useful therefor to define a number of diversity factors, which could be incorporated into augmentation. The diversity factors could include the number of occupants or occupation patterns for example. Alternatively, diversity factors could be incorporated to account for structural differences in residences such as floor area, glazing area and levels of insulation. The basis of these diversity factors should describe the relationships between certain loads and their driving variables. The derivation of diversity factors and rules for their implementation would be a very useful step towards replicating the reality of grid supply point profiles. The converse of augmentation is fragmentation and has been introduced in this work as the process of fragmenting a profile into its counterpart profiles. This abstraction would be useful in breaking up certain profiles and putting together variations of profiles however, in order for it to be useful rules for identifying the counterpart profiles are required. For example, a domestic electricity profile consists of a number of appliance profiles, lighting profiles and in some cases heating profiles. If rules were developed for the identification of ‘profile signatures’, variations of the domestic profile could be generated by modifying some or all of the counterparts and augmenting them. The variations of counterpart profiles should account for differences in energy efficiency,

which could encompass both a reduced magnitude in the demand or an alternative control mechanism, which may alter the profile. Assuming counterpart profiles could be identified the next step in demand specification could include the development of control algorithms which could 'decide' when non-critical loads are switched in and out. In the future non-critical loads may be operated by the 'smart plug', which could prioritise loads according to supply capacity. The ability to replace certain loads with more energy conscious variations would add a powerful capability to MERIT in its own right, as users would gain a quantified understanding of the effects of energy efficient technologies. Additionally by comparing demand profiles of varying degrees of energy efficiency in combination with specific tariffs, resultant financial savings can be realised.

MERIT has been designed to allow the study of both electrical and thermal profiles, although the work covered in this thesis has primarily focused on the electrical. Thermal profiles are highly building specific and are best obtained through simulation. The inclusion of a software link to a powerful building simulation tool, such as ESP-r containing a database of building types would be extremely useful in furthering thermal matching. Each building type should allow significant parameters to be modified. For example, a base profile could be obtained through the simulation of the basic building type and variations of this profile could be obtained by the substitution of different construction and/or glazing materials.

The provision of a comprehensive variety of demand profiles could result in the increased complexity in specifying a matching investigation and therefore a prioritisation method should be included. This prioritisation is envisaged to be especially useful in the field of energy management where numerous building types require attending. Prioritisation would process a number of specified profiles according to their hierarchical rank, thereby informing the user of the profiles which would most benefit from some form of 'levelling', whether through energy efficiency or through the coupling with a supply technology.

Finally, just as the provision for thermal profile analysis has been included in MERIT, so has the ability to examine reactive power profiles. Investigations into the nature of reactive profiles of building types/appliances would provide a more holistic approach to match analysis, whereby matching a RE supply with a demand could cover both real and reactive profiles as well as the corresponding thermal side.

10.2.2 Supply Profile Simulation

To improve predictions from the PV model a number of additional factors could be incorporated. Firstly, the current model does not account for the effects of shading or dust on the panel surface, which may be useful to include. Additionally, the surroundings will dictate the quantity of reflected radiation incident on a panel's surface, which could be incorporated through the definition of reflection coefficients for different surrounding types. Cloud cover effects components of direct and diffuse radiation and is thus accounted for to some extent. It may however be useful to include atmospheric clearness indices (Brunger and Hooper, 1993), for further accuracy.

A weakness in the current model is that multiple module power output is calculated through summation without accounting for the configuration of the modules. Performance will be effected by the way modules are connected and the user should be able to specify the number of modules connected in series/parallel.

The model is currently limited to the prediction of crystalline silicon modules, for it to be truly generic further work is required to encompass the performance prediction of amorphous silicon cells. The performance characteristics of amorphous are distinctly different from crystalline in that they experience seasonal fluctuations in performance, opposite to that of crystalline modules and initial light degradation effects (Ichikawa et al., 1996). In order to include such effects some form of regression analysis performed on experimental data may be useful. Modelling amorphous cells is thought to require

the mathematical representation of a shunt resistor in parallel with the p-n junction, as illustrated in the equivalent electrical circuit in Figure 5.6. Fry (Fry, 1998) describes a method for determining the value of the shunt resistance, from the slope of the characteristic IV curve, which is often available for amorphous modules.

Since the dc power provided by PV systems is frequently inverted to ac, it is recommended that the inverter model is improved to more accurately predict its effects on performance. Currently inverter performance is included through a characteristic curve, however an approach based on an equivalent electrical circuit would certainly approximate the reality better.

Thermophotovoltaic systems convert the radiant energy produced by fuel combustion directly into electricity by the photovoltaic effect (Catalano, 1996). Since a model for PV cell performance has been developed, this could be extended to incorporate thermophotovoltaic systems, which are capable of converting the energy in the infrared spectrum. Additional models would be required for the burner/emitter and for filter systems, which are used to recycle unused radiation.

Solar concentrator devices too utilise the infrared spectral region to produce electricity (Decher, 1997). The increased power-densities available with such systems require smaller cell areas, which reduce costs. Models could be developed to predict the concentrator optics and thermal effects and this could lead to further development of thermal storage devices, which would give better control of natural solar sources. Stirling engines can be coupled to concentrating solar collectors as another means of power production (Diver, 2000) and the development of a mathematical model for Stirling engines would be a useful addition to the supply model portfolio.

Another model for future incorporation would be that for a fuel cell, which could be used in conjunction with renewables technologies to generate hydrogen. Various mathematical models for fuel cells have been sited in literature (Ahmed et al., 1991),

(Bessette et al., 1995), (Amphlett et al., 1995), (Besset and Wepfer, 1995). The difficulty with each of these methods is that they have been developed to predict the performance of specific fuel cell configurations and are thus not generic in nature. More generic approaches are described by Gardner (Gardner, 1997) and by Decher (Decher, 1997). A model for electrolysers would be required to investigate the quantity of hydrogen, which could be extracted from water during periods of excess renewable production.

The ducted wind turbine model was developed using a limited data set, as the performance data of these devices is collated, the model should be refined. As the equations governing performance are clarified, some simplifying assumptions could be applied to avoid the use of numerous equations for different wind directions and wind speed ranges. Thereafter, by replicating the performance test data, using the collated wind data, the model could be validated. Validation of the models used for the other classes of turbines is required.

No corrections have been included for the non-availability of the wind turbine due to repair and maintenance. This factor could be incorporated by the reduction of power output by a user specified outage percentage, however in terms of correlating supply and demand profiles this approach would not result in a realistic indication of match. Alternatively, the user could specify the frequency and period of ‘down-time’, which could be simulated accordingly.

A number of other renewable technologies are in various stages of development and including their performance modelling would clearly expand the scope of the current tool. Some of the technologies of interest include hydroelectric, wave, geothermal, thermionic and thermoelectric converters.

10.2.3 Auxiliary Performance Simulation

The battery model requires validation through experimental methods. Morgan et al. (Mogan et al., 1997) describe both dynamic and steady-state testing procedures for lead acid batteries, which could be deployed for the validation of the model developed in this work.

Where multiple generator sets are specified to meet a load, a control algorithm is required to determine how the load is shared amongst the parallel generators. Liu et al. (Liu et al., 1993) describe a methodology for modelling N generator sets by the representation of an equivalent machine.

The back-up generator model should be extended to allow the specification of heat recovery systems for the prediction of thermal performance in combined heat and power systems. Kelly (Kelly, 1998) reported a methodology for the modelling of CHP units using a control volume approach. The model is constructed from an engine and generator unit, a cooling water heat exchanger and a gas-air heat exchanger. Energy balances are used in each component to establish thermal characteristics. The heat released from the combustion process is equated to the work done, together with the heat transferred to the combustion cylinder walls and to the exhaust gases. The heat transfer terms are subsequently used in determining the basic energy exchanges in the heat exchangers. The difficulty with this approach is that it utilises empirical heat transfer moduli, which need to be determined through an iterative calibration process tuned to experimental test data. Experimental work could be used to find relations between the moduli values and different CHP configurations to produce a generic model.

The development of a generic approach for predicting the performance of heat exchangers would facilitate the future development of further cogeneration models where a variety of power producing components could be selected. Numerous

technologies can be coupled with heat exchangers for cogeneration including the different combined cycle technologies, fuel cells and geothermal applications.
The development of models for combined heat and power systems could subsequently lead to the inclusion of an algorithm which optimises the CHP systems operational heat to power ratio, for a given set of thermal and electrical loads. Chou and Song (Cho and Song, 1997) proposed a search algorithm, based on the foraging behaviour of ants to solve economic dispatch of CHP systems. If the implementation of such a search technique proved successful it could be extended and used as an alternative search strategy for optimising the match between profiles.

Control Algorithms

Hybrid energy systems comprising diesel generators, battery inverter systems and renewable systems can configured in series, parallel or based on switched operation. Series configurations feed the power produced by the generator and/or renewable source through the battery inverter systems. Although such configurations are easily implemented, they have the disadvantages of being inefficient and requiring a battery capacity substantially larger than the peak load demand, which results in increased expense. Parallel systems allow the generator and/or renewable to supply a portion of the demand directly and charge the battery simultaneously enabling efficient load management and system sizing. Switched systems use power from diesel and/or renewable systems to meet the load during peak times, with any excess used to charge the battery. During low consumption periods the battery system is used, provided the switching device is not based on a time clock but on some for of load sensor, optimisation in performance could again be achieved. The differences in operation could be modelled using control algorithms, which would enable users to gain an understanding of the significance of configuration.

10.2.4 Further Analysis Functionality

The development of MERIT has been a foundation from which a sophisticated matching tool could be developed. A number of recommendations are made in the following paragraphs, which would enhance its analysis capability and therefore broaden its scope for future applications.

Economics

Decision-makers are largely lead by economics and this important factor is yet to be incorporated into the software package. The only economic factor currently included in MERIT is the ability to specify and analyse the effects of different tariff structures on consumption costs. It has been stated that it is economically favourable not to export energy from embedded generation systems to the grid (Markvart and Arnold, 1997). There may of course be exceptions to this rule, so for a thorough economic analysis, a facility should be incorporated to enable the specification of a unit price for exported electricity, similar to the tariff specification.

Each of the supply and auxiliary system specifications should incorporate a capital cost figure, which would include system, installation and maintenance costs and ideally account for life expectancy to enable life-cycle cost analysis. Using life cycle costing to produce an additional chart displaying costs over time would enable the user to 'see' the frequency of cash injection requirements. This chart could be presented together with some accounting metrics such as payback or net present value. Economics fluctuate and a database of costs could quickly become obsolete, it is therefore envisioned that the economic facility would be linked by a software connection to relevant internet sites whose prices are regularly updated.

In addition to capital cost, an economic analysis would need to entail some procedure to account for the avoidance of grid extension/reinforcement costs and for the cost of losses due to transmission.

Environmental Analysis

Environmental impact analysis has been neglected in this work. For a though investigation, the various gas emissions involved in meeting a defined load should be calculated. To do so, would require assumptions about the grid supply plant and the transmission distances to account for the losses. This would require the specification of grid parameters such as the base load plant type, i.e. whether it is made up of fossil-fuel or nuclear fired plant, hydro, wind farms, gas turbines etc. and the transmission distance from the demand site. Additional assumptions could be made regarding the supply mix with respect to time. For example during low periods of consumption the grid supply is made up of base load plant only and at peak consumption times a certain percentage of the grid supply will come from other plant such as gas turbines.

Additionally some new metrics should be incorporated which define life-cycle environmental damage of renewables, incorporating effects of manufacturing and decommissioning.

By including environmental and economical facets, search procedure could be specified accordingly, to find either the most economic topology of supply systems or the least environmentally damaging.

Autosizing

Other facilities, which would enhance the power of MERIT, would be an autosize option, whereby the specification of, for example a single PV module could be matched to a demand and the optimal number of modules would be calculated. Clearly, the autosizing function should also be available for auxiliary systems. With sizing calculation procedures, the ability to search for potential matches could be refined to return a specification of the optimal auxiliary system.

Transport Analysis

MERIT could also be taken a step further to incorporate transport supply and demand. It has been stated that photovoltaics are well suited to light train/tram applications which generally operate on dc current (Energie Edition, 2000) and could be used in ships and boats where their integration onto exposed surfaces would be relatively simple. Prototype Stirling engines and fuel cells are in various stages of development for uses in transport including power for automotive, navel and space applications. The investigation into a 'hydrogen economy' would benefit from the inclusion of transport analysis, as this would support the concept of hydrogen fuelling stations.

10.3 Perspective

A recent article in the Economist (Economist, 2000), described a future made up of 'micro-grids'. The micro-grid network would consist of a varied portfolio of power units, all connected via a "plug and play" microprocessor converter. The information technology behind such a system would clearly be concerned with unit dispatch. In keeping with this vision, a real-time version of MERIT could be monitoring the current demand on the micro-grid and simultaneously switching in and out generators according to optimised supply topology.

In addition to a software link to a building simulation program, an additional connection to an energy management program such as the Entrack-GIS system (Clarke et al., 1996) would be extremely powerful. Such a connection would facilitate a number of user actions in both specifying demand and supply and would facilitate the extension of analysis functionality. In specifying demand, the user is required to define the scaling factor for the consumption pattern, with a link to an energy management program, the user could opt to select a typical consumption figure, for a given building type, in a given geographical region, supplied by the energy management system. In specifying supply, there are practical limitations to the supply systems which can be specified which are not accounted for by MERIT. If a geographical area is specified, the GIS

system could supply information regarding the land value. A land value, incorporating factors such as proximity to dwellings, bird population, scientific/archaeological interest and air traffic/telecommunications could be used to effectively 'ban' certain developments. This 'ban' would switch off the ability to specify certain supply systems (e.g. large scale wind farms) and enable the user to proceed with a realistic analysis, without later finding that the optimised topology of supply could not be realised due to planning restrictions. Furthermore, the link could facilitate the future specification of grid supply metrics, as the GIS system could contain data relating to the geographical supply system composition as well as estimating losses due to transmission.

10.4 References

1. Ahmed S., McPheeters C. and Kumar R., Thermal-Hydraulic Model of a Monolithic Solid Oxide Fuel Cell, J. Electrochem. Soc., Vol. 138, No. 9, pp. 2712-2718, September 1991
2. Amphlett J.C., Baumert R. M., Mann R.F., Peppley B.A. and Roberge P.R., Performance Modelling of the Ballard Mark IV Solid Polymer Electrolyte Fuel Cell, J. Electrochem. Soc., Vol. 142, No.1, pp. 1-8, Jan 1995
3. Bessette N. F., Wepfer W. J. and Winnick J., A Mathematical Model of a Solid Oxide Fuel Cell, J. Electrochem. Soc., Vol. 142, No. 11 pp. 3792-3800, November 1995
4. Bessette N. F., Wepfer W. J., Prediction of Solid Oxide Fuel Cell Power System Performance Through Multi-Level Modelling, Journal of energy Resources Technology, Vol.117, pp. 307-317, December 1995
5. Brunger A. P. and Hooper F. C., Anisotropic Sky Radiance Model Based on Narrow Field View Measurements of Shortwave Radiance, Solar Energy, Vol. 51, No.1, pp. 53-64, 1993
6. Catalano Anthony, Thermophotovoltaics: A new Paradigm for Power Generation, WREC 1996.
7. Chou C. S. and Song Y. H., Ant Colony-Tabu Approach for Combined Heat and Power Economic Dispatch, The Universities Power Engineering Conference (UPEC), pp. 605-608 1997
8. Clark J. A., Evans M. S., Grant A. D., Kelly N., Simulation Tools for the Exploitation of Renewable energy in the Built Environment: The Entrack-GIS system
9. Decher Reiner, Direct Energy Conversion – Fundamentals of Energy Conversion, Oxford University Press, 1997
10. Energie Edition 2000, New Solutions in Energy Supply, Photovoltaic Solar Energy Best Practice Stories, 2000

11. Fry Bryan, Simulation of Grid-Tied Building Integrated Photovoltaic Systems, Msc Thesis, University of Wisconsin-Madison, 1998
12. Gardner F. J., Thermodynamic Processes in Solid Oxide and Other Fuel Cells, Proc. Instn Mech Engrs Vol 211, Part A, pp.367-380, 1997
13. Hottel H. C. and Whillier A., Evaluation of Flat-Plate Collector Performance, Transactions of the Conference on the Use of solar Energy, 2, Part 1, 74, University of Arizona Press, 1958
14. Ichikawa Y., Tanda M. and Sakai H., Analysis of Field Test Data for Amorphous Silicon PV Array, WREC, 1996
15. Kelly Nicolas, Towards a Design Environment for Building-Integrated Energy Systems: The Integration of Electrical Power Flow Modelling with Building Simulation, PhD Thesis Strathclyde University, October 1998
16. Liu W., Ding R. and Wang Z., Intergrated Optimal Control of Speed, Excitation and Load Sharing of Parallel Operating Diesel Generator Sets, IEE 2nd International Conference on Advances in Power System Control, Operation and Management, December 1993, Hong Kong, pp. 142-146
17. Markvart T. and Arnold R. J., Integration of Photo-Voltaic Converters into the Public Electricity Supply Network, The Institution of Electrical Engineers, 1997
18. Morgan T. R., Marshall R. H., Brinkworth B. J., 'Ares' – A refined Simulation Program for the Sizing and Optimization of Autonomous Hybrid Energy Systems, Solar Energy, Vol. 59, No 4-6, pp. 205-215, 1997.
19. Science and Technology: The dawn of Micropower, The Economist, 5th August, 2000

Appendix A: Domestic Energy Categorisation

Table A: U.S. Energy Categories for Domestic Energy Use

Category	**Sub-categories**								
Urban Status	Urban	Central City	Suburban	Rural					
Climate Zone	< 2,000 CDD	> 7,000 HDD	5,500 - 7,000 HDD	4,000 - 5,499 HDD	< 4,000 HDD	> 2,000 CDD & < 4,000 HDD			
Total Number of Rooms	1/ 2	3 - 5	6 - 8	> 9					
Type of Housing Unit	Single-Family	Detached	Attached	Mobile Home	Multi-family 2 - 4 Units	Multi-family > 4 Units			
Heated Floor	< 1,000	1,000 -	2,000 -	> 3,000					

space (square feet)		1,999	2,999						
Ownership of Unit	Owned	Rented	Public Housing	Not Public Housing	Rent Subsidy	No Rent Subsidy			
Year of Construction	1939 or Before	1940 - 1949	1950 - 1959	1960 - 1969	1970 - 1979	1980 - 1984	1985 - 1987	1988 - 1990	1991 - 1993
Family Income ($)	< 5,000	5,000 - 9,999	10,000 - 14,999	15,000 - 19,999	20,000 - 24,999	25,000 - 34,999	35,000 - 49,999	50,000 - 74,999	> 75,000
Below Poverty Line (%)	100	125	150						
Eligible for Federal Assistance	Yes	No							
Category	**Sub-categories**								
Age of	< 25	25 - 34	35 - 44	45 - 59	> 59				

Householder (Years)									
Education of Householder (Years)	< 13	13 - 16	> 16						
Race of Householder	White	Black	Other						
Householder of Hispanic Descent	Yes	No							
Household Size (Persons)	1	2	3	4	5	> 5			

Source

Energy Information Administration/Household Energy Consumption and Expenditures 1993 Source: Energy Information Administration, Office of Energy Markets and End Use, the 1993 Residential Energy Consumption Survey. Consumption and Expenditures 1993, Detailed Tables, Energy End Uses Ranked by Energy Consumption, 1989 File Last Modified: November 24, 1997, URL: http://www.eia.doe.gov/emeu/recs/recs2c.html

Appendix B1: Solar Geometry

Duffie and Beckman (Duffie and Beckman, 1974) describe the various aspects of solar geometry. Figure B.1 illustrates a section of earth in conjunction with a number of angles used to describe the position of the sun relative to a plane on the earth's surface. The angle of incidence of beam radiation, θ, is defined as the angle between the beam and the normal to the plane. This angle is calculated using equation B.1.1, and describes the portion of solar radiation incident on the panel surface. From Equation B.1.1, the angle of incidence is shown to be dependent on number of other angles; latitude; declination; tilt; azimuth, and the hour angle. The latitude is given a sign convention whereby the northern hemisphere is positive. The azimuth angle describes the directional component of the plane, where surfaces facing due south are zero, west facing surfaces are positive and east facing surfaces are negative.

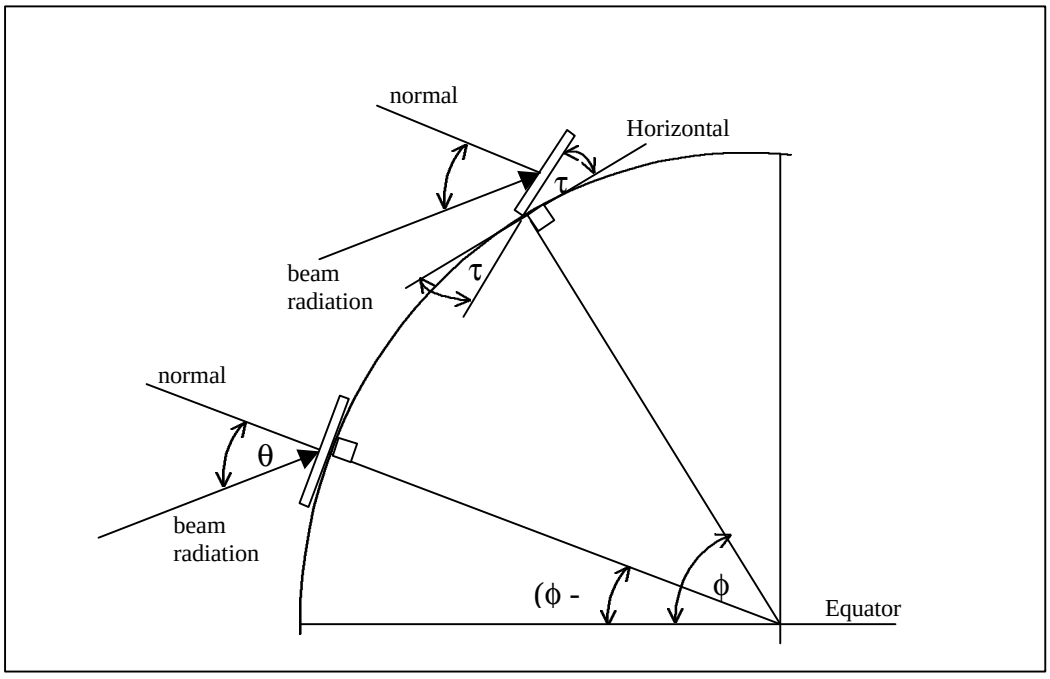

Figure B.1: Section of earth illustrating the definitions for angles τ, θ, ϕ, and (ϕ - τ) (Benford and Block, 1939)

$$\cos(\theta) = \sin(\delta)\cdot\sin(\phi)\cdot\cos(\tau) - \sin(\delta)\cdot\cos(\phi)\cdot\sin(\tau)\cdot\cos(\gamma) + \cos(\delta)\cdot\cos(\phi)\cdot\cos(\tau)\cdot\cos(\omega) + \cos(\delta)\cdot\sin(\phi)\cdot\sin(\tau)\cdot\cos(\gamma)\cos(\omega) + \cos(\delta)\cdot\sin(\tau)\cdot\sin(\gamma)\cdot\sin(\omega)$$

Equation B.1.1

Where δ = angle of declination

ϕ = latitude (north is positive)

τ = angle of tilt (i.e. between the horizontal and the plane of the surface)

γ = azimuth angle (due south is zero)

ω = hour angle

The angle of declination, δ, can be found from the Equation B.1.2 (Cooper, 1969)

$$\delta = 23.45\cdot\sin\left[\frac{360\cdot(284 + n)}{365}\right]$$

Equation B.1.2

Where n = the day of the year

The hour angle, ω, is described by Equation B.1.3 (Duffie and Beckman, 1974)

$$\omega = 180 - 15\cdot t$$

Equation B.1.3

Where t = time of day (hours)

The solar radiation incident on a surface comprises three components, direct, diffuse and reflected.

These are derived using climatic data in conjunction with Equations B.1.4 - B.1.6.

The direct beam component on surface, Q_{direct} is defined by:

$$Q_{direct} = Q_{DN} \cdot \cos(\theta)$$ Equation B.1.4

Where Q_{DN} = Direct normal solar intensity (W/m^2)

θ = Angle of incidence

The diffuse component on surface, $Q_{diffuse}$ is calculated from (Lui and Jordan, 1963):

$$Q_{diffuse} = Q_d \cdot \frac{1 + \cos(\tau)}{2}$$ Equation B.1.5

Where Q_d = Diffuse solar radiation on the horizontal (W/m^2)

τ = Angle of tilt

The reflected component, $Q_{reflected}$ is obtained using (Lui and Jordan, 1963):

$$Q_{reflected} = (Q_{direct} + Q_{diffuse}) \cdot \frac{1 - \cos(\tau) \cdot \rho}{2}$$ Equation B.1.6

Where ρ = value of ground reflectance (no-snow condition ρ=0.2, for snow ρ=0.7)

τ = Angle of tilt

References

1. Benford F. and Block J. E., A Time Analysis of Sunshine, Trans. Am. Illum. Eng. Soc., 34, 200, 1939
2. Cooper P. I., The Absorption of Solar Radiation in Solar Stills, Solar Energy, 12, 3, 1969
3. Duffie, J.A. and Beckman W. A., Solar Energy Thermal Processes, John Wiley & Sons, New York, 1974
4. Liu B. Y. H. and Jordan R. C., Availability of Solar Energy for Flat-Plate Solar Heat Collectors, Low Temperature Engieering Applications for Solar Energy, Am. Soc. of Heat, Ref. and Air Cond. Eng., 1976

Appendix B2: Optical Laws

Fresnel's relationship describes the reflection of non-polarised radiation at the interface of two mediums (Duffie and Beckman, 1974).

$$\rho = \frac{I_r}{I_0} = \frac{1}{2}\cdot\left[\frac{\sin^2(\theta_2-\theta_1)}{\sin^2(\theta_2+\theta_1)} + \frac{\tan^2(\theta_2-\theta_1)}{\tan^2(\theta_2+\theta_1)}\right] \qquad \text{Equation B.2.1}$$

Where ρ = reflection of non-polarised radiation

I_r = Reflected radiation

I_0 = Incident radiation

θ_1 = Angle of Incidence

θ_2 = Angle of refraction

Snell's law governs the relationship between refracted angles and indices of refraction of two mediums (Duffie and Beckman, 1974).

$$\frac{n_1}{n_2} = \frac{\sin(\theta_2)}{\sin(\theta_1)} \qquad \text{Equation B.2.2}$$

Where n_1 = Refractive index of medium 1

n_2 = Refractive index of medium 2

Bouger's law describes the absorption of radiation in a partially transparent medium (Duffie and Beckman, 1974).

$$\tau_a = e^{-KL} = e^{-K \cdot \frac{t}{\cos(\theta)}}$$ Equation B.2.3

Where τ_a = Transmittance considering only absorption

K = Extinction coefficient

L = Path length of the radiation

t = thickness of layer

θ = Angle of light transmitted into layer

References

1. Duffie, J.A. and Beckman W. A., Solar Energy Thermal Processes, John Wiley & Sons, New York, 1974

Appendix B3: Surface and Environment Energy Exchanges

Developments in the field of solar collectors have determined a number of relationships The radiant exchange with the sky is described by Equation B.3.1 (Rogers and Mayhew, 1998)

$$Q_{sky} = \varepsilon \cdot A \cdot VF \cdot \sigma \left(T_{sky}^{4} - T^{4} \right) \qquad \text{Equation B.3.1}$$

Where Q_{sky} = Radiant Exchange with sky

ε = Emissivity of glass

VF = View Factor

σ = Stefan-Boltzmann constant (5.669×10^{-8} W/m^2 K^4)

T_{sky} = Temperature of sky

T = Temperature of Panel

The view factor VF, depends on the angle of tilt, which dictates the portion of the sky exposed to the module, and can be calculated from Equation B.3.2

$$VF = \frac{1}{2} \cdot (1 + \cos(\tau)) \qquad \text{Equation B.3.2}$$

Where τ = Angle of Tilt

The sky temperature can be calculated from a variety of long-wave radiation correlations. The more sophisticated of which account for the degree of cloud cover and the height of clouds. However, as this information is not contained within readily available climate data, a simpler relation was used to evaluate sky temperature. This relationship is described below (Swinbank, 1963).

$$T_{sky} = 0.0552 \cdot T_a^{1.5}$$ Equation B.3.3

Where T_a = Ambient dry bulb temperature (K)

The heat transfer coefficient for an external PV surface, exposed to wind, is calculated using Equation B.16 (McAdams, 1954)

$$h_w = 5.7 + 3.8 \cdot V$$ Equation B.3.4

Where h_w = heat transfer coefficient ($W/m^2°C$)

V = corrected wind speed (m/s)

The wind speed is corrected according to the following conditions (Evans, 1994)
For windward conditions, with wind speeds greater than 2m/s

$$V = 0.25 V_w$$ Equation B.3.5

For windward conditions, with wind speeds less than 2m/s

$$V = 0.5$$ Equation B.3.6

For leeward conditions, with wind speeds greater than 2m/s

$$V = 0.3 + 0.05 V_w$$ Equation B.3.7

Where V_w = actual wind speed (m/s)

References

1. Evans M. S., Plant Modelling and Simulation for Small Renewable Energy Systems. M.Sc. Thesis, University of Strathclyde, September 1994

2. McAdams W. C., Heat Transmission, 3rd Ed., New York, McGraw Hill, 1954

3. Rogers and Mayhew, Engineering Thermodynamics – Work and Heat Transfer 4th Edition, Longman Group Limited 1998

4. Swinbank W. C., Long-wave Radiation From Clear Skies, Quart. J. Roy. Meteorol. Soc., 89, 1963

Appendix B4: Equations used To Determine Convection Coefficients in a PV-Hybrid Air Gap

Table B.1: Equations used to determine properties of dry air at low pressure.

Property	Regression Equation	Units
Kinematic Viscosity	$\nu = \left(1\times 10^{-5}\cdot T^2 + 0.0024\cdot T - 0.1864\right)\cdot 10^{-5}$	$\frac{kg}{ms}$
Dynamic Viscosity	$\mu = \left(-1\times 10^{-6}\cdot T^2 + 0.0076\cdot T - 0.002\right)\cdot 10^{-5}$	$\frac{m}{s}$
Thermal Conductivity	$k = \left(-3\times 10^{-6}\cdot T^2 + 0.0099\cdot T - 0.0234\right)\cdot 10^{-5}$	$\frac{kW}{mK}$
Density	$\rho = 352.58\cdot T^{-0.9998}$	$\frac{kg}{m^3}$
Prandtl number	$Pr = 4\times 10^{-7}\cdot T^2 - 0.0005\cdot T + 0.8186$	NA

Table B.2: Equations used to determine dimentionless parameters.

Geometrical parameter	$L = Gap\_Width$	$D_h = \frac{4\cdot A_c}{P}$	$Lc = \frac{A_s}{P}$
Grashof number	$Gr = \frac{g\cdot\beta\cdot\rho^2\cdot L^2\cdot\theta^2}{\mu^2}$		$Gr_L = \frac{g\cdot\beta\cdot\rho^2\cdot L_c{}^2\cdot\theta^2}{\mu^2}$
Reynolds number		$Re_D = \frac{\rho\cdot U\cdot D_h}{\mu}$	
Nusselt number	$Nu = \frac{H\cdot L}{k}$	$Nu_D = \frac{H\cdot D_h}{k}$	$Nu_L = \frac{H\cdot L_c}{k}$
Rayleigh number			$Ra_L = Gr_L\cdot Pr$

Table B.3: Conditions for use, and Equations Employed for Natural Convection

Condition	Equation
Horizontal $10^5 \le Ra_L < 10^{10}$	$Nu_L = 0.27 \cdot Ra_L^{0.25}$
Vertical	$Nu_L = 0.825 + \frac{0.387 \cdot Ra_L^{\frac{1}{6}}}{\left[1 + \left(\frac{0.492}{Pr}\right)^{0.5625}\right]^{\frac{8}{27}}}$
Vertical $Ra_L \le 10^9$	$Nu_L = 0.68 + \frac{0.67 \cdot Ra_L^{\frac{1}{4}}}{\left[1 + \left(\frac{0.492}{Pr}\right)^{0.5625}\right]^{\frac{4}{9}}}$
Tilted $0.0 \le \theta < 60$ $Gr_L = \frac{g \cdot \cos(\theta) \cdot \beta \cdot \rho^2 \cdot L_c^2 \cdot \theta^2}{\mu^2}$	$Nu_L = 0.825 + \frac{0.387 \cdot Ra_L^{\frac{1}{6}}}{\left[1 + \left(\frac{0.492}{Pr}\right)^{0.5625}\right]^{\frac{8}{27}}}$
Tilted $Ra_L \le 10^9$ $0.0 \le \theta < 60$ $Gr_L = \frac{g \cdot \cos(\theta) \cdot \beta \cdot \rho^2 \cdot L_c^2 \cdot \theta^2}{\mu^2}$	$Nu_L = 0.68 + \frac{0.67 \cdot Ra_L^{\frac{1}{4}}}{\left[1 + \left(\frac{0.492}{Pr}\right)^{0.5625}\right]^{\frac{4}{9}}}$
$Gr > 2 \cdot 10^5$	$Nu = \left[0.069 - 0.020 \cdot \left(\frac{\tau}{90}\right)\right] \cdot (Gr \cdot Pr)^{\frac{1}{3}} \cdot Pr^{0.074}$

Table B.4: Aspect ratios and Corresponding Nusselt numbers for fully developed Laminar Flow Conditions

Fully developed Laminar Flow - Uniform Q $Re_D < 2300$	
$\frac{b}{a} \leq 1.0$	$Nu = 3.61$
$\frac{b}{a} \leq 1.43$	$Nu = 3.73$
$\frac{b}{a} \leq 2.0$	$Nu = 4.12$
$\frac{b}{a} \leq 3.0$	$Nu = 4.79$
$\frac{b}{a} \leq 4.0$	$Nu = 5.33$
$\frac{b}{a} \leq 8.0$	$Nu = 6.49$
$\frac{b}{a} \leq \infty$	$Nu = 8.23$

[b = width, a = depth]

Table B.5: Conditions for Use, and Equations used for Friction Factors in Fully developed Turbulent Flow Regimes

$Re_D \leq 3000$	$f = 0.316 \cdot Re_D^{-0.25}$
$3000 \leq Re_D \leq 5 \cdot 10^6$	$f = \left(0.79 \cdot \ln\left(Re_D\right) - 1.64\right)^{-2}$
$Re_D > 5 \cdot 10^6$	$f = 0.184 \cdot Re_D^{-0.2}$

Table A.6: Conditions for Use, and Equations for Fully developed Turbulent Flow Regimes used in Forced Convection

Condition	Equation
$10^4 < Re_D < 5 \cdot 10^6$ $0.5 < Pr < 2000$	$Nu = \frac{\frac{f}{8} \cdot Re_D \cdot Pr}{1.07 + 12.7 \cdot \left(\frac{f}{8}\right)^{\frac{1}{2}} \cdot \left(Pr^{\frac{2}{3}} - 1\right)}$
$0.5 < Pr < 2000$ $3000 < Re_D < 5 \cdot 10^6$	$Nu = \frac{\frac{f}{8} \cdot \left[\left(Re_D - 100\right) \cdot Pr\right]}{1.0 + 12.7 \cdot \left(\frac{f}{8}\right)^{\frac{1}{2}} \cdot \left(Pr^{\frac{2}{3}} - 1\right)}$
$0.7 < Pr < 160$ $Re_D \geq 10,000$ $\frac{a}{b} \geq 10$ $\Delta T < 10$	$Nu = 0.023 \cdot Re_D^{0.8} \cdot Pr^n$ $T_s > T_m \qquad n = 0.4$ $T_s < T_m \qquad n = 0.3$
$0.7 < Pr < 160,700$ $Re_D \geq 10,000$ $\frac{a}{b} \geq 10$ $\Delta T > 10$	$Nu = 0.027 \cdot Re_D^{0.8} \cdot Pr^{\frac{1}{3}} \cdot \left(\frac{\mu}{\mu_s}\right)^{0.14}$
$\frac{b}{a} \leq 10$	$Nu = 0.0158 \cdot Re^{0.8}$

Source

Incropera, F. P. and DeWitt, D. P., Fundamentals of Heat and Mass Transfer, 4th Edition, John Wiley & Sons, New York, 1996.

Appendix C: Correction of Wind Speed for Specified Turbine Height & Surroundings

Wind speeds are available from meteorological observations, which are generally measured at a height of 10 metres. Hub heights of modern 600 to 1,500 kW wind turbines are typically 40 to 80 metres above ground level. Wind speeds reduce logarithmically as height tends to ground level. The rate of decline increases with surrounding terrain roughness. As a result of this phenomenon wind speeds obtained from meteorological measurements are corrected to account for surrounding terrain and hub height. The procedure described below is employed to correct wind speeds for different hub heights and roughness classes. The roughness classes are shown in Table C.1, with definitions according to the European Wind Atlas (Troen and Petersen, 1991)

Table C.1: Roughness classes of varying surfaces

Surrounding Surface Type	**Roughness Class**
Water Surface	0.0
Open Terrain with Smooth Surface	0.5
Open Agricultural Area with Little Shelter	1.0
Agricultural Land with 1250m of 8m Shelter (approx.)	1.5
Agricultural Land with 500m of 8m Shelter (approx.)	2.0
Agricultural Land with 250m of 8m Shelter (approx.)	2.5
Extremely Well Sheltered Agricultural Land	3.0
Very Rough and Uneven Terrain	3.0
Village / Small Town	3.0

Larger City with Tall Buildings	3.5
Very Large City with Tall Buildings and Skyscrapers	4.0

The wind speed correction methodology is based on two assumptions. Firstly, that there are no obstacles close to (up to 1km) or above the specified hub height of the wind turbine, or the point of meteorological measurement. Secondly, that meteorological wind speeds are obtained in open terrain at 10m (roughness class 0.5).

Data presented by the Wind Energy Reference Manual (Wind Energy Reference Manual, 2000) shows the logarithmic decline of wind speeds, from 100m to 10m for different roughness classes. An example data set presented is shown in Figure C.1. Analysis of each data set identified a relationship between height and wind speed for different roughness classes. This relationship is described mathematically below.

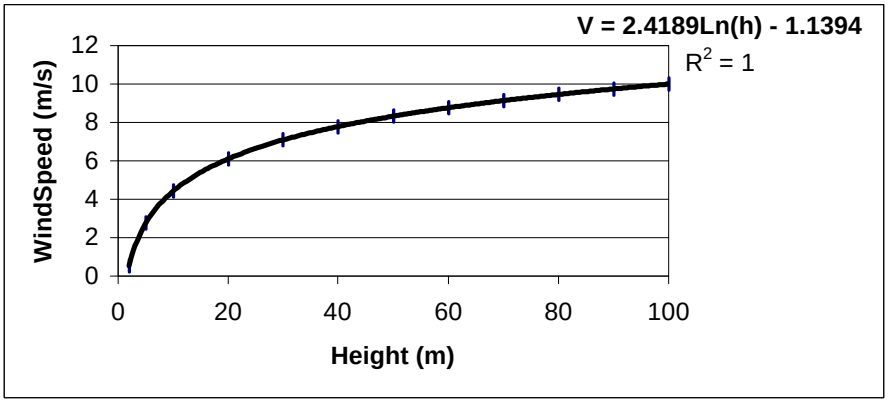

Figure C.1: Example data set presented for roughness class 4.0

Analysis of the data presented showed that the constant a and b could be found from the equations C.2 and C.3

$$V_{w\_corr} = a \cdot \ln(H) + b \qquad \text{Equation C.1}$$

$$a = \frac{V_{100} - V_{10}}{\ln(100) - \ln(10)} \qquad \text{Equation C.2}$$

$$b = V_{10} - a \cdot \ln(10) \qquad \text{Equation C.3}$$

The wind speed at 100m and at 10m will depend on whether the original wind speed was obtained in a similar roughness class, or whether it was obtained from standard meteorological observations (SMO).

For SMO

$$V_{100} = \frac{V_w}{\ln(2.190215)} \qquad \text{Equation C.4}$$

$$V_{10} = \ln(-0.1712 \cdot RC + 2.267) \cdot V100 \qquad \text{Equation C.5}$$

For similar terrain

$$V_{10} = V_w \qquad \text{Equation C.6}$$

$$V_{100} = \frac{V_w}{\ln(-0.1712 \cdot RC + 2.267)} \qquad \text{Equation C.7}$$

References

1. Troen Ib and Petersen Erik Lundtang: European Wind Atlas, Risoe National Laboratory, Risoe, Denmark, 1991, ISBN 87-550-1482-8.
2. Wind Energy Reference Manual Part 1: Wind Energy Concepts URL:http://www.windpower.dk/tour/wres/calculat.html

Appendix D1: Calculations used to Determine Heat Loss Mechanisms in Flat plates

No Covers

With reference to Figure 5.18 (Koo, 1999)

$$Q_{sky} = VF \cdot \varepsilon_p \cdot \sigma \cdot A_p \cdot \left(T_p^4 - T_{sky}^4\right) \quad \text{Equation D.1.1}$$

$$Q_{wind} = h_w \cdot A_p \cdot \left(T_p - T_a\right) \quad \text{Equation D.1.2}$$

$$Q_{back} = \frac{k_b}{t_b} \cdot A_c \cdot \left(T_p - T_a\right) \quad \text{Equation D.1.3}$$

$$Q_{edge} = \frac{k_e}{t_e} \cdot A_e \cdot \left(T_p - T_a\right) \quad \text{Equation D.1.4}$$

Where Q_{sky} = Radiant heat loss to sky

VF = View Factor between plate and sky

ε_p = Emissivity of plate

σ = Stephan Boltzman Constant

A_p = Surface area of plate

T_p = Plate temperature

T_{sky} = Sky temperature

Q_{wind} = Convective heat loss due to wind

h_w = Wind loss coefficient

T_a = Ambient temperature

Q_{back} = Heat loss to back insulation

k_b = thermal conductivity of back insulation

t_b = thickness of back insulation

A_c = Collector area

Q_{edge} = Heat loss to edge insulation

k_e = thermal conductivity of edge insulation

t_e = thickness of edge insulation

A_e = Collector edge area

The equations used in calculating sky temperature, view factor and wind loss coefficient where described in the previous section of this chapter (Section B.3: Surface and Environment Energy Exchanges).

Flat plates with One Cover

With reference to Figure 5.19 (Siegel and Howell, 1992)

$$Q_{1in} = \rho_p \cdot Q_{1out} + \varepsilon_p \cdot \sigma \cdot T_p^4 \qquad \text{Equation D.1.5}$$

$$Q_{2in} = \sigma \cdot T_{sky}^4 \qquad \text{Equation D.1.6}$$

$$Q_{2out} = \tau_c \cdot Q_{1in} + \rho_c \cdot Q_{2in} + \varepsilon_c \cdot \sigma \cdot T_c^4 \qquad \text{Equation D.1.7}$$

$$Q_{1out} = \tau_c \cdot Q_{2in} + \rho_c \cdot Q_{1in} + \varepsilon_c \cdot \sigma \cdot T_c^4 \qquad \text{Equation D.1.8}$$

Where ρ denotes the reflectivity, τ the transmissivity, and ε the Emissivity. The subscripts, p, and c, denote the plate and cover, respectively (Koo, 1999).

$$Q_{p\_c} = h_{p\_c} \cdot A_p \cdot (T_p - T_c) \qquad \text{Equation D.1.9}$$

$$Q_{sky} = VF \cdot \rho_c \cdot \sigma \cdot A_p \cdot \left(T_c^4 - T_{sky}^4\right) \qquad \text{Equation D.1.10}$$

$$Q_{wind} = h_w \cdot A_p \cdot (T_c - T_a) \qquad \text{Equation D.1.11}$$

Where Q_{p_c} is the heat transfer due to natural convection between the plate and cover, and h_{p_c} the natural convection coefficient. The natural convection heat transfer between two parallel plates tilted at an arbitrary angle to the horizon can be calculated by evaluating the following dimensionless parameters; the Nusselt number Nu, the

Rayleigh number Ra, and the Prandtl number Pr. The Rayleigh and Prandtl numbers are given by (Rogers and Mayhew, 1992)

$$Ra = \frac{g \cdot \beta \cdot \Delta T \cdot L^3}{\nu \cdot \alpha} \qquad Pr = \frac{\nu}{\alpha}$$ Equation D.1.12

Where L is the distance between parallel plates, and ΔT is the temperature difference between them. The other parameters are: g the gravitational constant; β the volumetric coefficient of expansion;α the thermal diffusivity; and ν the kinematic viscosity, of air at the mean plate temperature of the parallel plates.

The Nusselt number is calculated according to the following relations for tilt angles from 0 to 75 degrees:
For the isothermal plates Equation D.1.13 is used (Hollands et al., 1976), and for materials with low values of conductivity, and therefor small temperature gradients along the covers Equation D.1.14 is used (Yiqin et al., 1991).

$$Nu = 1 + 1.44 \cdot \left[1 - \frac{1708 \cdot (\sin(1.8 \cdot \beta))^{1.6}}{Ra \cdot \cos(\beta)} \right] \cdot \left(1 - \frac{1708}{Ra \cdot \cos(\beta)} \right) + \left(\frac{Ra \cdot \cos(\beta)}{5830} \right)^{\frac{1}{3}} - 1$$ Equation D.1.13

$$Nu = 1 + 1.44 \cdot \left[1 - \frac{1296 \cdot (\sin(1.8 \cdot \beta))^{1.6}}{Ra \cdot \cos(\beta)} \right] \cdot \left(1 - \frac{1296}{Ra \cdot \cos(\beta)} \right) + \left(\frac{Ra \cdot \cos(\beta)}{5830} \right)^{\frac{1}{3}} - 1$$ Equation D.1.14

.

The natural convection coefficient is calculated from Equation D.1.15.

$$h_c = \frac{Nu}{L} \cdot k$$ Equation D.1.15

Flat plates with Two Covers

With reference to Figure 5.20 (Siegel and Howell, 1992)

$$Q_{1out} = \tau_{c1} \cdot Q_{2in} + \rho_{c1} \cdot Q_{1in} + \varepsilon_{c1} \cdot \sigma \cdot T_{c1}^{4} \quad \text{Equation D.1.16}$$

$$Q_{2out} = \tau_{c1} \cdot Q_{1in} + \rho_{c1} \cdot Q_{2in} + \varepsilon_{c1} \cdot \sigma \cdot T_{c1}^{4} \quad \text{Equation D.1.17}$$

$$Q_{3out} = \tau_{c2} \cdot Q_{4in} + \rho_{c2} \cdot Q_{3in} + \varepsilon_{c2} \cdot \sigma \cdot T_{c2}^{4} \quad \text{Equation D.1.18}$$

$$Q_{4out} = \tau_{c2} \cdot Q_{3in} + \rho_{c2} \cdot Q_{4in} + \varepsilon_{c2} \cdot \sigma \cdot T_{c2}^{4} \quad \text{Equation D.1.19}$$

$$Q_{1in} = \rho_{p} \cdot Q_{1out} + \varepsilon_{p} \cdot \sigma \cdot T_{p}^{4} \quad \text{Equation D.1.20}$$

$$Q_{2in} = Q_{3out} \quad \text{Equation D.1.21}$$

$$Q_{3in} = Q_{2out} \quad \text{Equation D.1.22}$$

$$Q_{4in} = \sigma \cdot T_{sky}^{4} \quad \text{Equation D.1.23}$$

$$Q_{sky} = VF \cdot \rho_{c2} \cdot \sigma \cdot A_{p} \cdot \left(T_{c2}^{4} - T_{sky}^{4} \right) \quad \text{Equation D.1.24}$$

$$Q_{wind} = h_{w} \cdot A_{p} \cdot \left(T_{c2} - T_{a} \right) \quad \text{Equation D.1.25}$$

$$Q_{p\_c1} = h_{p\_c1} \cdot A_{p} \cdot \left(T_{p} - T_{c1} \right) \quad \text{Equation D.1.26}$$

$$Q_{c1\_c2} = h_{c1\_c2} \cdot A_{p} \cdot \left(T_{c1} - T_{c2} \right) \quad \text{Equation D.1.27}$$

Where Q_{p_c1} is the heat transfer due to natural convection between the plate and cover 1, and h_{p_c1} the natural convection coefficient between the plate and the cover. Similarly, Q_{c1_c2} is the heat transfer due to natural convection between cover 1 and cover 2. The natural convection coefficients h_{p_c1} and h_{c1_c2} are calculated as previously described by Equations D.1.12-D.1.15.

References

1. Hollands, K. G. T., Unny, T. E., Raithby, G. D., and Lonicek, L, “Free Convection Heat Transfer Across Inclined Air Layers,” Transactions of ASME Journal of Heat Transfer, Vol. 98, pp. 189, 1976.
2. Koo Jae-Mo,Development of a Flat-plate Solar Collector Design Program, MSc Thesis, University of Wisconsin-Madison, 1999.URL:http://sel.me.wisc.edu/theses/koo99.zip
3. Rogers G. and Mayhew Y., Thermodynamic and Transport Properties of Fluids –SI Units, Basil Blackwell Ltd, 1992
4. Siegel, R. and Howell, J. R., Thermal Radiation Heat Transfer, 3rd Edition, Taylor & Francis, New York, 1992.
5. Yiqin, Y, Hollands, K. G. T., Brunger, A. P., “Measured Top Heat Loss Coefficients for Flat Plate Collectors with Inner Teflon Covers,” Proceedings of the Biennial Congress of the International Solar Energy Society, Denver, Colorado, USA, August 19-23, pp. 1200, 1991.

Appendix D2: Flat plates Performance with Fluid Circulation

Overall Heat Loss Coefficient

The heat loss from a collector to the environment comprises the losses through the cover system, and through the back and edge insulation. Assuming the losses are based on the mean plate temperature T_{pm}, the overall heat loss coefficient U_L is calculated using Equation D.2.1 (Hottel and Whillier, 1958)

$$U_L = U_t + \frac{k_b}{t_b} \cdot \frac{A_c}{A_p} + \frac{k_e}{t_e} \cdot \frac{A_e}{A_p} \qquad \text{Equation D.2.1}$$

Where k_b and k_e are the back and edge thermal conductivities, and t_b and t_e the thicknesses of back and edge insulation. A_c, A_p, and A_e denote the surface areas of the collector, plate and edge, respectively. U_t is the top loss coefficient and will depend on the number of covers incorporated in the collector, the temperatures of those covers, as well as the ambient conditions. The mathematical analysis of each of the cover systems was described previously. Referring to Figures 5.18 through 5.19, for collectors with no cover, one cover and two covers respectively, the top loss coefficients for each system can be described as follows (Hottel and Whillier, 1958):

$$U_{t_0} = \frac{Q_{sky} + Q_{wind}}{T_p - T_a} \qquad \text{Equation D.2.1}$$

$$U_{t_1} = \frac{Q_{1in} - Q_{1out} + Q_{p\_c1}}{T_p - T_a} \qquad \text{Equation D.2.2}$$

$$U_{t_2} = \frac{Q_{1in} - Q_{1out} + Q_{p\_c1}}{T_p - T_a} \qquad \text{Equation D.2.3}$$

Heat Transfer Coefficient to Tubes

The following calculations are used to determine the heat transfer coefficient to the fluid. First the Reynolds number is calculated from Equation D.2.4.

$$Re = \frac{4 \cdot \frac{m}{n}}{\pi \cdot D_i \cdot \mu} \qquad \text{Equation D.2.4}$$

Where m is the mass flow rate (kg/s), N is number of tubes, D_i is the tube inner diameter (m), and μ is the dynamic viscosity (kg/sm) of the fluid at the inlet temperature.

For fully developed turbulent flow inside of tubes (Re>2300), the Nusselt number is obtained from Gnielinsky correlation (Gnielinski, 1976) together with the McAdams relation (MacAdams, 1954), giving:

$$Nu = \frac{\frac{f}{8} \cdot (Re - 1000) \cdot Pr}{1 + 12.7 \cdot \sqrt{\frac{f}{8} \cdot \left(Pr^{\frac{2}{3}} - 1 \right)}} \cdot \left[1 + \left(\frac{D_i}{L} \right)^{0.7} \right] \qquad \text{Equation D.2.5}$$

$$f = (0.079 \cdot \ln(Re) - 1.64)^{-2} \qquad \text{Equation D.2.6}$$

Where L is the tube length, and f, the friction factor for a smooth surface, which is calculated from the Petukhov relation (Petukhov, 1970) given by Equation D.2.6. The Prantle number Pr, is calculated from Equation D.2.7, where μ is the dynamic viscosity (kg/sm), Cp the specific heat (J/kgK),and k the thermal conductivity (W/mK) of the fluid at the inlet temperature (Incropera and DeWitt, 1996).

.

$$Pr = \frac{\mu \cdot Cp}{k}$$ Equation D.2.7

For laminar flow, assuming it is fully developed inside short tubes, with a constant heat flux, is given by (Incropera and DeWitt, 1996).

$$Nu = 4.4 + \frac{0.00172 \cdot \left(Re \cdot Pr \cdot \frac{D_i}{L} \right)^{1.66}}{1 + 0.00281 \cdot \left(Re \cdot Pr \cdot \frac{D_i}{L} \right)^{1.29}}$$ Equation D.2.8

The heat transfer coefficient to the tubes is subsequently determined using Equation D.2.9

$$h_{fi} = \frac{Nu \cdot k}{D_i}$$ Equation D.2.9

Collector Efficiency

The collector efficiency factor is described in Equation D.2.10. For most collector geometries, this equation can be interpreted as the ratio of the heat transfer resistance, from the absorber plate to the ambient air, to that from the fluid to the ambient air (Hottel and Whillier, 1958)

.

$$\eta_c = \frac{\frac{1}{U_L}}{W\cdot\left[\frac{1}{U_L\cdot\left[D_o + F\cdot\left(W - D_o\right)\right]} + \frac{1}{C_b} + \frac{1}{\pi\cdot D_i\cdot h_{fi}}\right]}$$ Equation D.2.10

Where W = Spacing between tubes

D_o= Outer tube diameter

F = Fin efficiency (Equation D.2.11)

C_b = bond conductance (Equation D.2.12)

$$F = \frac{\tanh\left[m\cdot\left(\frac{W - D_o}{2}\right)\right]}{m\cdot\frac{\left(W - D_o\right)}{2}}$$ Equation D.2.11

$$C_b = \frac{k_B\cdot L_B}{t_B}$$ Equation D.2.12

Where k_B is the bond thermal conductivity, t_B the average bond thickness, and L_B the bond length.

Heat Removal Factor

The collector heat removal factor is described by Equation D.2.13 (Hottel and Whillier, 1958).

$$F_R = \frac{m\cdot Cp}{U_L}\cdot\left(1 - \exp\left(\frac{-U_L\cdot\eta_c}{m\cdot Cp}\right)\right.$$ Equation D.2.13

Where m = the mass flow rate per unit area of the collector

Useful Gain

The useful gain from the collector can be calculated as a function of the fluid inlet temperature, and represented by Equation D.2.14 (Hottel and Whillier, 1958).

$$Q_u = A_c \cdot F_R \cdot \left[Q_{rad} - U_L \cdot \left(T_{in} - T_a \right) \right] \qquad \text{Equation D.2.14}$$

Mean Fluid Temperature

As the fluid temperature will increase with increases in displacement across the collector length, the following equation is used to calculate the mean fluid temperature (Hottel and Whillier, 1958).

$$T_{fm} = T_{in} + \frac{Q_u}{A_p \cdot F_R \cdot U_L} \cdot \left(1 - \frac{F_R}{\eta_c} \right) \qquad \text{Equation D.2.15}$$

Mean Plate Temperature

The mean plate temperature will always be greater than the mean fluid temperature due to the heat transfer resistance between the absorbing surface and the fluid. Therefore the mean temperature can be evaluated from the following (Hottel and Whillier, 1958):

$$T_{pm} = T_{fm} + \frac{Q_u}{h_{fi} \cdot \pi \cdot D_i \cdot n \cdot L} \qquad \text{Equation D.2.16}$$

For liquid mediums this temperature difference is usually small, however for an air medium the temperature difference can be significant.

References

1. Gnielinski, V., Int. Chem. Eng., Vol. 16, pp. 357, 1976
2. Hottel H. C. and Whillier A., Evaluation of Flat-Plate Collector Performance, Transactions of the Conference on the Use of solar Energy, 2, Part 1, 74, University of Arizona Press, 1958
3. Incropera, F. P. and DeWitt, D. P., Fundamentals of Heat and Mass Transfer, 4th Edition, John Wiley & Sons, New York, 1996.
4. MacAdams, W. C., Heat Transmission, 3rd Edition, New York, McGraw Hill, 1954.
5. Petukhov, B. S., in T. F. Irvine and J. P. Hartnett eds., advances in Heat Transfer, Vol 6, Academic Press, New York 1970.